University of Nevada, Reno

Oxidative Aging of Binders with High Recycled Asphalt Materials

A thesis submitted in partial fulfillment of the
requirements for the degree of Master of Science in
Civil and Environmental Engineering

by

Sara Pournoman

Dr. Elie Y. Hajj / Thesis Advisor

May, 2017

THE GRADUATE SCHOOL

We recommend that the thesis
prepared under our supervision by

SARA POURNOMAN

Entitled

Oxidative Aging of Binders with High Recycled Asphalt Materials

be accepted in partial fulfillment of the
requirements for the degree of

MASTER OF SCIENCE

Elie Y. Hajj, Ph.D., Advisor

Peter E. Sebaaly, Ph.D., Committee Member

Nathan E. Morian, Ph.D., Committee Member

Sage Hiibel, Ph.D., Graduate School Representative

David W. Zeh, Ph. D., Dean, Graduate School

May, 2017

ABSTRACT

The objectives of this research effort focused on the oxidative aging of binders with high recycled asphalt materials. A coordinated program of forced-draft oven aging experiments was conducted on eleven sorts of binder blends including three different types of base binders from TX, NH, and NV, two different types of recycled material (RAP/RAS), and two different types of recycling agents (RA). Implementing the Fourier-Transform Infrared Spectroscopy (FT-IR) and Dynamic Shear Rheometer (DSR) isothermal frequency sweep tests, the oxidation kinetics and rheological performance were determined for the evaluation materials. Results indicated that the oxidative aging rates were influenced by the aging temperature, duration, base binder type, as well as the utilized asphalt modifier, i.e. recycled materials and RAs. It was also noted that the RAs reduced the overall stiffness in the investigated stages of oxidation. However, differential aging rates and hardening susceptibilities were observed between the RA and RAP/RAS additions to each of the three bases, noting that these differences were not consistent with the type of RAS, i.e. MWAS or TOAS. Additionally, the base binder aging properties due to the addition of the recycled material was highly influenced by the RA dosages within each blend.

Furthermore, the binder blend oxidative aging predictions at binder specific geographical location indicated that using the recycled materials along with the RAs at the optimum dosage, according to the proposed methodology, was able to restore the binder blend properties to the virgin binder.

The influences of the recycled material and RAs on the PG 64-28P base binder were also investigated through the binder PG grading and mortar testing. Consistent directions for the influence of the evaluation materials were observed within both procedures, suggesting the capability of the mortar procedure in characterizing the effects of RAP and RA materials on virgin binder without the use of chemical extraction.

The Uniaxial Thermal Stress and Strain Test (UTSST) was also conducted on the PMFC and RPMLC specimens of the NV field project to investigate the influence of the high recycled material and RAs on the asphalt mixtures. Through consideration of the thermo-viscoelastic properties, marked differences in the binder oxidation were noted between the experimental factors. Typically, decreases in the viscous response of the mixtures as well as increases in both the stiffness and brittle behavior were observed with aging and also inclusion of the recycled material. Although the addition of the RAs to the recycled mixtures indicated some extent of properties restoration, crack initiation and fracture were observed to occur in significantly warmer temperatures compared to the virgin mixture.

DEDICATION

To my parents, my sister, my brothers

and all of my friends,

for all of their love, understanding, and support.

I praise and thank the GOD Almighty for each of them.

AKNOWLEDGEMENTS

I am grateful to my advisor, Dr. Hajj, for his expertise, understanding, patience, generous guidance and support regarding my study over the long term.

I am hugely indebted to Dr. Morian for his guidance and kind advice, for being ever so kind and patient over the duration of this research.

I also extend many thanks to Dr. Sebaaly for all his continued supports and advices during my program study.

Another thanks I would like to say is to my thesis committee member, Dr. Sage Hiibel, for his great support and understanding.

I also would like to extend my appreciation to WRSC lab manager, Murugaiyah Piratheepan, for his extensive assistance during the laboratory experiments.

Last but not least, I would like to thank my colleagues in UNR Pavement Engineering and Science Program, Hadi, Johnny, Mohamed, Dario, Jorge, Lauren, Victor, Farzan, Pratha, JeyaKaran, Sarah, Rami, Elise, Alberto, Daniela, Federico and so on for their help and great friendship. .

TABLE OF CONTENTS

LIST OF TABLES

LIST OF FIGURES

CHAPTER 1 INTRODUCTION

1.1 General Introduction

Conservation of natural resources is gaining more attention these days due to global environmental and economic issues on earth. The asphalt pavement industry has considered implementation of recycled pavements in hot mix asphalt (HMA) since early 1900 due to dramatic increases in the cost of asphalt binders. However, most of states department of transportation (DOTs) in the United States limit the use of recycled material including recycled asphalt pavement (RAP) and recycled asphalt singles (RAS) in asphalt mixtures to less than 30%. This is due to potential concerns with the variability of the recycled materials and the long-term performance of asphalt mixtures that contain these materials.

One of the solutions to mitigate the performance and construction issues while using recycled materials in hot mix asphalt was initiated in early 1970s and 1980s, which considered the use of a recycling agent. Recycling agents are a type of chemical additives that are deemed effective in alleviating the high stiffness of asphalt mixtures with high recycled materials while improving the cracking resistance and workability of the mixtures (Tran et al., 2012; Mogawer, et al. 2013; Im and Zhou, 2014). These ecycling agents are required to be compatible to the base binder, resistant to bleeding, while to at least maintain, if not improve, the mixture resistance to rutting. Guidelines were developed by Epps et al. (1980) and, more recently, Copeland (2011) to ensure the restoration of the binder rheology,

proper production, handling and construction of hot mix asphalt when using the recycled material along with the RAs.

1.2 Objective of the Study

This study was conducted as a part of on-going National Cooperative Highway Research Program (NCHRP) project in an effort to thoroughly investigate and quantify The Effects of Recycling Agents on Asphalt Mixtures with High RAS and RAP Binder Ratios. The primary objective of this research is to evaluate the oxidative aging behavior of the asphalt binders as it is influenced by the high RAP and RAS content and RAs. Since current practice generally limits recycled binder ratios to 0.3 or less, the scope of this research encompasses asphalt binders and mixtures prepared with RAs and RAS, RAP, or combined RAS/RAP at recycled binder ratios between 0.3 and 0.5. The performance of binders and mixtures will be evaluated through elaborated laboratory aging and actual field project, respectively. The result of this study will be utilized as the initial understanding of the capability of the selected RAs at determined dosages to restore the high recycled binder and mixture properties.

1.3 Problem Statement

This effort is focused on quantifying the effect of recycled material and RAs on the oxidative aging characteristics of three different sources of virgin binder by itself and as a part of asphalt mixture when is subjected to controlled isothermal oven aging and Uniaxial Thermal Stress and Strain Test (UTSST), respectively.

First, the binder quantification will stablish the oxidation parameter of the various binder blends to provide a comparison among different types and amounts of base binders, recycled materials, and RAs. Once a foundation has been laid by determining the influence of the various factors, the predicted aging behavior of the binder blends will be determined in their corresponding environment. Finally, the influence of the recycled material and RAs on the low temperature properties of the asphalt mixtures will be also evaluated through a field project conducted in Reno, Nevada.

CHAPTER 2 LITERATURE REVIEW

2.1 Aging of Asphalt Materials

Binders are one of the most common materials used in the pavement industry due to their particular viscoelastic properties. Two rheological parameters are utilized to describe binder behavior at any temperature and loading frequency: stiffness (shear complex modulus [G*] at high and intermediate temperatures or asphalt binder stiffness [S] at low temperatures) and phase angle (δ at high and intermediate temperatures or m value at low temperatures). As a result of oxidative aging, the binder stiffness increases while the phase angle decreases (King et al. 2012).

Figure 2. 1 shows as an example the aging susceptibility of three different binders in a black space diagram: a neat binder, a polymer modified binder with 3% Styrene-Butadiene-Styrene (SBS) referred to as PMA, and a high polymer modified binder with 7.5% SBS referred to as HP (Morian et al. 2015). The neat binder was used as the base for the two polymer modified binders. The three asphalt binders were subjected to long-term aging in forced draft ovens for various combinations of temperatures (50, 60, and 85°C) and aging durations (ranges from 0.5 days up to 240 days). The three evaluated binders start at different locations in Black Space and each binder has a different rate of aging from the lower right of the diagram to the upper left. The figure also shows a damage zone where the brittle rheological behavior causes onset and significant cracking as defined by the Glover-Rowe (G-R) parameter of 180 and 600 kPa, respectively. The G-R parameter is a result of the relationship between G* and δ from the dynamic shear rheometer (DSR) test

that has been traditionally conducted at 15°C. The aforementioned cracking thresholds for the G-R parameter (i.e., 180 and 600 kPa) are to correlate to ductility values of 5 cm and 3 cm that were reported by Kandhal (1977), respectively. It was originally defined by Ruan et al. (2003) before it was reformulated for more practical use by Rowe (2011) in a discussion by Anderson et al. (2011) as the Glover-Rowe (G-R) parameter, or $G'/(\eta'/G')/\delta = G^* \cdot (\cos\delta)^2/(\sin\delta)$, where all rheological properties are referenced at 0.005 rad/s and 15°C.

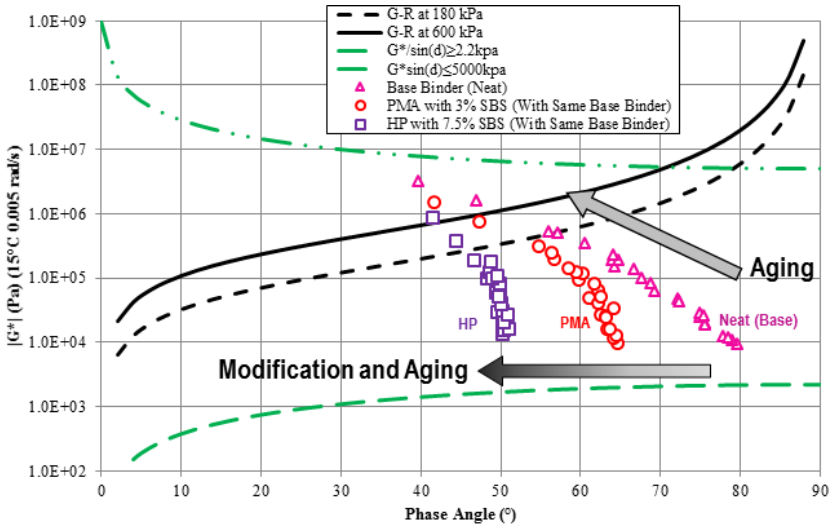

Figure 2. 1. Binder Rheology Due to Aging

Each data point plotted in Figure 2. 1 represents a specific asphalt binder aging condition (i.e., combination of temperature and aging duration). It is anticipated that the lower the G* and the lower the δ, the less susceptible a binder is to long-term aging. In addition, the steeper the slope between G* and δ, the less susceptible the binder is to long-term aging. In other words, a steep curve located closer to the left side of the chart indicates lower susceptibility to long-term aging. The data presented in Figure 2. 1 show that the HP modified asphalt binder is the least susceptible to long-term aging, followed by the PMA

binder, while the neat asphalt binder is the most susceptible to long-term aging. Furthermore, the data show that the neat asphalt binder was the first binder to reach the G-R cracking criterion of 600 kPa after about 170 days of oven aging while the PMA and HP modified asphalt binders lasted, respectively, for about 190 and 230 days before reaching the same failure criterion.

Recently, a new binder parameter called $\Delta T_{c,}$ has been introduced for evaluating age related cracking potential. It is defined as the numerical difference between the low continuous grade temperature determined from the Bending Beam Rheometer (BBR) stiffness criteria (the temperature T_S where stiffness, S, equals 300 MPa) and the low continuous grade temperature determined from the BBR m-value (the temperature T_m where m equals 0.300).The ΔT_c was first proposed by Anderson in 2011 to measure the ductility loss of aged asphalt binder as part of a study examining relationships between asphalt binder properties and non-load related cracking (the study focused on finding a parameter to explain block cracking in airport pavements). . A negative value of ΔT_c (T_S-T_m) indicates the controlling role of the relaxation properties of the binder at low temperature, i.e. m-controlled. Anderson et al. (6) verified the satisfactory correlation of ΔT_c with ductility and G-R in several laboratory and field investigations. They also proposed that a value of -2.5°C and -5°C for ΔT_c would correlate to the same cracking thresholds discussed in G-R parameter, i.e., onset and significant cracking, respectively.

From the construction point of view, oxidation stiffens the binders in asphalt mixtures during refining, production, construction, and in-service, i.e., changing the molecular structure of the binder through chemical reactions with oxygen. This phenomenon reduces the binder phase angle and its stress relief capability. In fact, through the chemical reactions,

the oxygen atoms add to aliphatic carbon atoms attached to aromatic rings to form functional groups called carbonyls and water via extraction of hydrogen atoms. As a result, the ketones and organic acids are produced which are highly polar with strong associations through Van der Waals forces with other active polar sites in the binder. Suh reactions increase the apparent molecular weight and associated increase in stiffness and are known as the predominant cause of binder embrittlement due to aging.

2.2 Recycling of Asphalt Materials

Among many types of recycled materials that are routinely used in asphalt mixtures in the United States, the RAP material are the most often ones used in the asphalt industry. The use of RAS in asphalt mixture has recently received more attention since this type of material contains larger amounts of binder, usually 20 - 30 percent binder by total weight (Zhou et al. 2012). The two main types of RAS that can be recycled in asphalt pavements are Tear-off Asphalt Shingles (TOAS) and Manufactural Waste Asphalt Shingles (MWAS), which are shingles removed during re-roofing or roof removal projects and waste during the manufacturing process, respectively. It should be noted that MWAS has traditionally been preferred over TOAS for several reasons including better known composition of MWAS, fewer contaminants, lower amounts of deleterious or harmful material in such as wood, nails, and asbestos, and the stiffer binder in TOAS compared to MWAS due to in-service exposure of the roof to the environment (Zhou et al. 2012).

Several studies have shown that asphalt mixtures containing 10 to 30 percent of RAP content, which is commonly used in US asphalt industry, perform as well as virgin asphalt mixtures. While State DOTs and contractors are continually looking for incorporating

greater amounts of recycled materials into asphalt mixtures, higher RAP content mixtures (i.e., 30 percent and higher) have indicated an increase in rutting resistance along with a decrease in cracking resistance (Shah et al. 2007; Li et al. 2008; Hajj et al. 2009; West et al. 2009; Hussain and Yanjun 2012; Valdés et al. 2011; Mogawer et al. 2012; Mogawer, Austerman, et al. 2013; West and Marasteanu 2013).

Recently, the use of RAS has received more attention in the asphalt paving industry since this type of material contains larger amounts of binder, usually 20 to 30 percent binder by total weight (Zhou et al. 2012). It is noteworthy to mention that the MWAS have been preferred over TOAS for several reasons including fewer contaminants by the deleterious or harmful material in such as wood, nails, and asbestos, more stiffened asphalt in TOAS.

2.3 Degree of Blending Between Virgin and Aged Binders

The current standard specification for Superpave volumetric mix design, AASHTO M323, considers the assumption of full blending between the virgin and aged binders during asphalt mixture production resulting in a homogenous blend. However, the actual degree of blending in most cases is partial (Coffey et al. 2013; Kriz et al. 2014), and no available standard method currently exists to determine the exact degree of blending.

In an effort to better explain the level of blending between the virgin and recycled material, Kriz et al. (2014) proposed four possible scenarios of virgin-aged binder contact quality (due to mechanical mixing) and blending (due to diffusion) in mixtures, shown in Figure 2. 2. These scenarios imply the complex process of the blending between the virgin and aged binder. On the other hand, a step-by-step blending protocol method based on binder master curves was suggested by Booshehrian et al. (2013). The binder master curves were

shifted using the Christensen-Anderson model and further utilized to determine the degree of blending of different RAP plant-produced mixtures containing multiple RAP contents lower than 40 percent. The results indicated an overall good degree of blending for the evaluated mixtures.

In another study on the mixtures containing 25 percent RAP material, the impact of degree of blending on the recycled mixtures was evaluated by Coffey et al. (2013). A negligible effect was detected on the mixtures' fatigue and rutting performance when the degree of blending exceeded 85 percent (calculated based on a previous study of similar mixtures). They concluded that when the degree of blending is high or the percentage of RAP in a mixture is 25 percent or less, the full blending assumption will be cost-effective without compromising pavement performance.

In summary, limited studies were conducted to quantify and assess the impact of the degree of blending between virgin and recycled binders. Additional comprehensive investigations are required to evaluate the degree of blending and its influence on pavement performance for mixtures with RAP, RAS or combination of RAP and RAS at high Recycled Binder Ratios (RBR).

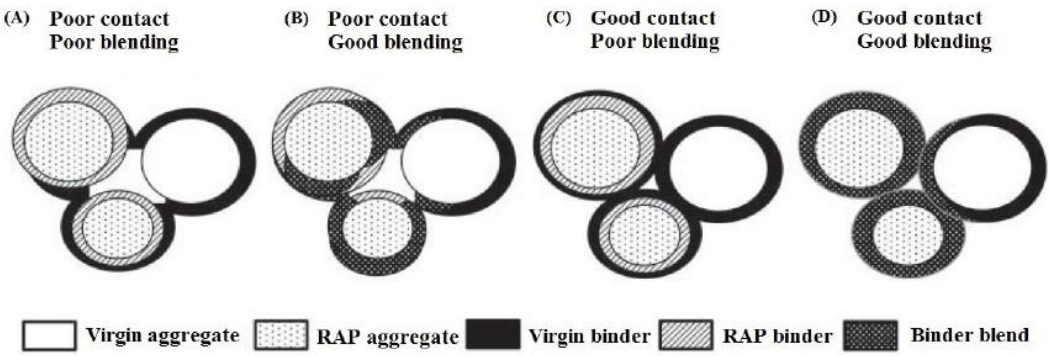

Figure 2. 2. RAP-Virgin Binder Contact and Blending (Kriz et al. 2014)

2.4 Restoring and Characterizing Binder Rheology with Recycling Agents

According to the Asphalt Institute (1986) definitions, recycling agent is an organic material with chemical and physical characteristics selected to restore aged asphalt to desired specifications. The various types of recycling agents (RA) that are currently commercially available, according to NCAT (2014a), are listed in Table 2. 1.

Rostler and co-workers at Witco/Golden Bear (Rostler and White 1959; Kari et al. 1980) have been conducted several investigations on RAs. The main purposes for adding RAs to asphalt mixtures with recycled materials include: (a) restore the aged binder by decreasing the stiffness for construction purposes and mixture performance in the field; (b) restore the recycled mixture in terms of durability or resistance to cracking by increasing the phase angle of the binder; (c) provide sufficient additional binder to coat the recycled and virgin aggregates; and (d) provide sufficient additional binder to satisfy mix design requirements (Kandhal and Mallick 1997; Epps et al. 1980; Newcomb et al. 1984; Newcomb and Epps 1981).

Table 2. 1. Recycling Agents Categories and Types (NCAT 2014a)

Category	Types	Description
Paraffinic Oils	Waste Engine Oil (WEO) Waste Engine Oil Bottoms (WEOB) Valero VP 165 Storbit	Refined used lubricating oils
Aromatic Extracts	Hydrolene Reclamite Cyclogen L ValAro 130A	Refined crude oil products with polar aromatic oil components
Napthenic Oils	SonneWarmix RJ™ Ergon HyPrene	Engineered hydrocarbons for asphalt modification
Triglycerides and Fatty Acids	Waste Vegetable Oil Waste Vegetable Grease Brown Grease Oleic Acid	Derived from vegetable oils
Tall Oils	Sylvaroad™ RP1000 Hydrogreen	Paper industry by-products Same chemical family as liquid antistrip agents and emulsifiers

With the intention of characterizing RAs in terms of their physical and chemical properties, Kari et al. (1980) published an early specification for RAs combining selected properties presented in Table 2. 2 . The work was based on the characterization of 33 type of RAs along with their blends with aged binders. The specification was developed by establishing thresholds that would allow selecting the RA and blend that best restored the aged asphalt. Noncompliance with the specification threshold does not necessarily indicate a poor blend, while compliance also does not imply complete blending and full restoration of the aged binder.

In a comprehensive effort, Shen et al. (2005) evaluated the effect of RAs on crumb rubber modified (CRM) binders. The properties of the RAs in terms of viscosity, specific gravity, flash point, volatility, RTFO, and saturates were analyzed. Other properties were also

investigated by several researchers (Yu et al. (2014), Lin et al. (2014), Yu et al. 2014, Asli et al. 2012) as presented in Table 2. 2 according to Kari et al. (1980).

Table 2. 2. Tests Used for the Proposed Specification

Functional Reason	Test Evaluated
Grade Designation and product consistency	Viscosity @ 60°C, cSt Viscosity @ 135°C, cSt
Handling and shipping	Flash point Fire point
Volatility	Rolling thin film (RTF-C), Oven weight change Smoke point ASTM D 1160 distillation
Compatibility and solvency	Saturates, weight percent Aniline and mixed-aniline point Refractive index Compositional analysis
Durability	Viscosity ratio
Accounting	Specific gravity 60/60 F

2.5 Effect of RAs on Binders with High RBRs

The addition of the recycled materials including RAP and RAS to the virgin binders in asphalt mixtures is expected to increase the high and low temperature grades of the blended binder. However, a RA can mitigate the stiffening effect of the aged binder by reducing the PG of the blended binder (Shen and Ohne 2002; Shen, Amirkhanian, and Miller 2007; Tran et al. 2012; Mogawer, Booshehrian, et al. 2013; Zaumanis et al. 2014a).

Although the true softening procedure is not fully understood, several investigations have been conducted on RA's working mechanism. In general, the working mechanism depends on the uniform dispersion of the RA within the mixture as well as the diffusion of the RA into the aged binder, as Tran et al. (2012) has established.

The dispersion is mixing caused by physical processes that is a function of the mixing time, and significantly affect the RA efficiency in the asphalt mixtures. The mechanical mixing at the plant is usually adequate to achieve uniform dispersion of the RA within the recycled mixture, however in some cases the aged binder tends to quickly absorb any hydrocarbon-type liquid before that liquid (i.e., the RA) is uniformly distributed throughout the mixture (by the diffusion mechanism) (Lee et al. 1983).

Diffusion is the process where a constituent move from a higher concentration to a lower concentration. The method of adding the RA into the recycled materials influence its diffusion efficiency, meaning that the RA is better diffused when is added to the recycled material before combining them with virgin binder and aggregate. However, in practice, the RA is typically added to the virgin binder, and subsequently the blend is added to the mix of virgin aggregate and the recycled materials (Tran et al. 2012).

2.6 RA Type and Dosage

As investigated by several researchers, not all types of RAs have a similar influence on the chemical and physical properties of an aged binder (Little et al. 1981; Lin et al. 2011; Mogawer, Booshehrian, et al. 2013; Zaumanis et al. 2014b). In selecting a RA for a specific binder, it is crucial to determine the best type and composition of the RA that provide the highest restoration level. However, it is almost impossible to state which type of RA is best for a particular binder without testing the impact of the RA on the properties of the specific aged binder including but not limiting to compatibility and temperature susceptibility (Zaumanis et al. 2014a, Epps and Holmgreen, 1980; Holmgreen et al. 1982, O’ Sullivan 2011, Holmgreen et al. 1982).

However, the most important aspect when determining the appropriate RA dosage is its influence on binder PG restoration as well as the field performance. While low dosages are not able to restore the recycled binder blend to that of the virgin binder, using high dosages of RAs will soften the aged binders, which is beneficial for cracking resistance. However, it should be noted that high dosages negatively affect the mixture resistance to permanent deformation. Therefore, the dosage should be carefully optimized in this range.

Typically, the dosage of the RAs is recommended by the manufacturers based on historical experiences. However, they should not be kept constant due to the particular effect of the binder and aggregate type, source, to name but a few. Currently, although no standard method is available, several efforts have been conducted to select an optimum binder dosage considering the blending charts based on the viscosity and/or penetration as well as the changes in PG due to the addition of RAs (Little et al. 1981; Zaumanis et al. 2013; Zaumanis et al. 2014b; Yan et al. 2014, Shen and Ohne 2002; Shen, Amirkhanian, and Miller 2007; Tran et al. 2012; Zaumanis et al. 2014a).

The minimum RA dosage is defined as the dosage to ensure sufficient fatigue resistance, while the maximum dosage is the one to ensure enough rutting resistance. However, determining the optimum dosage to meet both of the aforementioned concerns while considering the cost aspect of it has been the state of interest in some research studies (Zaumanis et al. 2014a).

In a comprehensive approach for determining the RA dosage, Shen and Ohne (2002) considered the performance-related properties of the aged binder at the three temperature requirements specified by the Superpave binder system. Blends of aged binder and RA at

different dosages were tested using DSR and BBR testing at three aging conditions including original, RTFO, and RTFO + PAV. Results indicated a significant non-linear reduction in the G*/sin(δ) and a linear increase in the G*.sin(δ) upon the addition of the RA. Similarly, on the low temperature side, the observation of the BBR results showed that the stiffness at low temperature decreased linearly, while the m-value increased linearly with an increase in the RA dosage.

Employing a similar approach, Tran et al. (2012) used the lowest dosage that met the PG requirement as an optimum dosage. However, they observed a linear decrease in both critical low and high temperature grades contrary to Shen and Ohne (2002) results.

In summary, additional research is needed to properly define the RA effect on restored aged binder rheology and the RA dosage optimization procedure in asphalt mixtures with recycling materials.

2.7 Degree of Binder Aging

The degree of aging of the recycled blend is one of the most influential factors that controls and finally judges the efficiency of a sample RA in restoring the properties of the aged binders. Shen and Ohne (2002) found the addition of a particular RA to a highly-aged binder decreases the G*/sin(δ) more quickly than for a less aged binder. Similar trend has been also observed for low-temperature properties. Table 2. 3 represents a summary of the comprehensive literature review conducted in the NCHRP 09-58 project on the effect of RAs on aged binders.

Table 2. 3. Previous Research on the Effect of RAs on the Stiffness of Recycled Asphalt Mixtures

Authors	Main Findings
Shen and Ohne (2002)	Properties at high temperature ▪ The incorporation of the RA dropped the high-temperature grade in a nonlinear relationship, where the rate of decline in G*/sinδ was more rapid at lower contents (0-6%) than higher contents (6-14%) ▪ Although the different implemented binder sources have the same penetration, the effect of adding the RA differed a little for the parameter G*/sinδ, indicating that the source of the aged plays a role here. Properties at low temperature: ▪ The incorporation of the RA decreased the low- temperature grade in a quite linear relationship. ▪ The extent of the stiffness decrease or m-value increase (in RBR test) was greater in the harder-aged asphalt than the less one.
Shen, Amirkhanian, and Miller (2007)	▪ The incorporation of RAs decreases the high- and low-temperature parameters in a linear relationship. ▪ Using test results and extrapolating the linear equation of RA dosage and PG parameters, the optimum dosage was determined.
Tran et al. (2012)	▪ A linear correlation between the RA dosage and the critical high and low temperatures of the RAP and RAS binders was observed. ▪ The continuous grade of RAP binder (at 0% RAP) was 141.7-10.5. The addition of the RA dropped this PG to 120.1-22.8 and 96.9-32.5 for 10% and 20%, respectively. ▪ RA dosage of 12% by the total weight of recycled binders was selected as optimum dosage based on the critical low-temperature criteria.
Mogawer, Booshehrian, et al. (2013)	▪ The incorporation of 35% RAP and 5% RAS binders into the virgin binder altered the continuous PG from 60.9-31.1 to 74.2-25.2, and the addition of the RAs dropped this PG to 68.4-27.5, 68.9-26.5, and 69.1-26.2 for different RAs.
Zaumanis et al. (2014a)	▪ The incorporation of RAs decreases the high- and low-temperature parameters in an almost linear relationship for most types of RAs. ▪ The incorporation of RAs decreases the intermediate-temperature parameter, but the relationship is not linear with RA dosage. ▪ From penetration test results, RAs can reduce the penetration of aged binders to the target level of virgin binder's penetration. However, organic oils require lower dosage to provide the same effect as petroleum products.

2.8 Summary of the Chapter

This chapter provides results of the literature review of the efforts came from diverse viewpoints with specific objectives. Topics covered in this chapter focuses on aging and recycling of asphalt materials, restoring and characterizing binder rheology with RAs, and the influence of RAs on binders with high RBRs.

CHAPTER 3 RESEARCH METHODOLOGY

An in-depth investigation of the oxidative aging of the asphalt binders requires the application of multiple research methodologies along with consideration of specific conditions depending upon the corresponding materials is being evaluated. This chapter is intended to present the methodologies utilized for asphalt binder and mixture characterization throughout this effort. The main concepts and test methods will be discussed in detail to allow the following chapters to focus on the results analysis and interpretation.

3.1 Asphalt Binder Characterization Procedures

A significant amount of effort was expended in this study to characterize the oxidation properties of the various evaluated asphalt binder blends. As such, the aging stages of the binders will be quantified with Fourier-Transform Infrared Spectroscopy, FT-IR, following by stiffness and relaxation characterization properties including G* and phase angle, respectively. Additional information regarding the utilized tools and software have been explored in the following sections with detailed analyses and results presented in subsequent chapters.

3.1.1 Performance Grading

As the primary step of the asphalt binder characterization, the performance grade of the blends was determined in accordance with AASHTO M320 (AASHTO, 2015). The Dynamic Shear Rheometer (DSR) and Binder Beam Rheometer (BBR) test methodologies were utilized to determine the high and low temperature continuous grades for the material

being evaluated. The following sections will provide a brief description of both test methodologies as describes in the respective AASHTO standards.

3.1.1.1 Bending Beam Rheometer

The AASHTO T 313 covers the determination of the flexural creep stiffness of asphalt binders by means of a bending beam rheometer. In this effort, the material has been aged through Rolling Thin Film Oven aging and Pressure Aging Vessel according to AASHTO T 240 and AASHTO R 28, respectively, to simulate the short and long-term aging condition of the material in the actual field performance. In the next step, the evaluated long-term aged binder blends were poured in the bending beam rheometer molds to measures the midpoint deflection of the simply supported beam of asphalt binder subjected to a constant load of 980 ± 50 mN for 240 seconds applied to the midpoint of the beam. The maximum bending stress and strain at the midpoint of the beam is calculated from the dimensions of the beam, the span length, the deflection of the beam and the load applied to the beam for loading times of 8, 15, 30, 60, 120, and 240 s. Subsequently, the stiffness of the beam for the loading times specified above is calculated by dividing the maximum stress by the maximum strain. At the end, the software provides the user with calculated stiffness and the slop of the logarithm of stiffness versus logarithm of time curve in 60th second of testing named m-value. This test is required to be conducted in at least two different temperature to enable a linear relationship between the stiffness and m-value with the testing temperature. The temperatures at which the 300 MPa stiffness and m-value of 0.3 are met will be subtracted by 10°C due to the time-temperature superposition, reported as the S-controlled and m-controlled continuous low-temperature grades, respectively. The

maximum of the two aforementioned temperatures is also reported as the low temperature continuous grade.

3.1.1.2 Dynamic Shear Rheometer

The AASHTO T 315 test method covers the determination of the dynamic shear modulus (G*) and phase angle (δ) of asphalt binder when tested in dynamic (oscillatory) shear using parallel plate test geometry. The method is intended to determine the linear viscoelastic properties of unaged or aged asphalt binders in accordance with AASHTO T 240 and AASHTO R 28 as required for specification testing described in AASHTO M 320.

In this effort, test specimens were prepared as 1 mm thick by 25 mm in diameter for unaged and RTFO aged binders or 2 mm thick by 8 mm in diameter for PAV aged binders and formed between parallel metal plates. One of the parallel plates is oscillated with respect to the other at 10 rad/sec strain controlled mode so that the measurements stay in the linear viscoelastic behavior region. The final high and intermediate continuous PG grades were determined utilizing the resulting parameters combining G* and δ for each binder blend at corresponding aging level in accordance with the criteria specified in AASHTO M 320.

3.1.2 Fourier-Transform Infrared Spectroscopy Test

Fourier-Transform Infrared Spectroscopy is a widely-used technique to identify the material composition by identification of certain molecules or functional groups and the concentration of those within a sample, here binder sample (Smith, 2011). The fundamental theory of infrared spectroscopy is that infrared radiation passes into the material, meanwhile some fractions of the radiation is absorbed, and the remaining radiation is transmitted to the material or reflected by the material surface. Consideration of the specific

absorbed and reflected wavelength, the chemical components of the tested specimen can be recognized. Detailed information regarding the FT-IR theoretical background can be find elsewhere (Morian, 2014; Zhu, 2015).

3.1.2.1 FT-IR Measuring and Sample Preparation Techniques

In basic terms, there are two primary categories of FT-IR sample preparation and measurement technique. The first method called transmission testing involves with directly passing an IR beam through the investigated sample before being read by any detector. The tested sample in the transmission method is required to either be mixed with a transparent powder, contained within an IR transparent cell, or made thin enough that the IR energy may pass completely through it. The most common material being used as a powder or cell is potassium bromide (KBr) which, as a drawback, will readily absorb moisture from the atmosphere and could potentially dissolve. The other method is generally known as reflectance testing, where the IR beam is reflected or bounced off of the specimen surface then measured by the detector. One of the common types reflectance measurements is known as attenuated total reflectance (ATR) in which the measurement is conducted by passing the IR beam through a crystal of high refractive index on to the surface of the sample with a lower index. To avoid adding further variability to the experiment by using the hydroscopic KBr, ATR spectrum of Nicolet 6700 manufactured by Thermo Scientific Inc. was used in this study to get the infrared absorption spectrum with binder samples with an ATR attachment.

As described, the ATR measuring technique was selected to conduct the FT-IR spectroscopy on the binder samples. Several sample preparation methods have been tried

during this study to come up with a unique methodology applicable to all the various binder blends being evaluated. The finalized step-by-step methodology with the Nicolet 6700 located in the University of Nevada, Reno can be summarized as the following:

1. Heat up 2 oz of the binder at 300°C for 5 minutes.
    a. The time-temperature superposition concept is applicable for special conditions to avoid burning binders in high temperatures.
    b. The heating temperature and duration can be increased or decreased based on the evaluated binder stiffness.
2. Fully blend the heated binder sample.
3. Let the binder cool down for one minute to avoid damaging the crystal with heated binder.
4. Use a sharp tool to pick a small amount of binder and place it on the FT-IR crystal.
5. Cover the binder with a plastic glove to avoid asphalt binder sticking to device, and apply a slight pressure to fully cover the crystal with the binder, then remove the glove to avoid any contamination of the sample spectra.
6. Collect the FT-IR spectra
7. Repeat step 3 to 6 for 2 more times to collect a total of 9 spectra.
8. Clean the binder with Ethanol and wait for the ethanol to evaporate at least one minute before starting next measurement.

Upon collecting at least three measurements and three replicates per each measurement, the average of at least 2 measurements were used to determine the average carbonyl area (CA) which is indicator of oxygen absorption into the binder by quantifying the growth of

the carbonyl and functional groups. The value of CA was determined by considering a baseline defined as the absorption level at 1,524 and 1,820 cm^{-1}. This value of CA was determined as the area in arbitrary units, integrated between the average absorption spectra and the determined baseline from 1,650 to 1,820 cm^{-1} wavenumbers and the magnitude of the growth in CA in each aging level compared to the un-aged level was utilized as an indication of aging, i.e. CAg. Figure 3. 1 demonstrates the FT-IR spectra and the CA area for 40hr PAV aged 64-28 binder in the specified range of wavenumbers. In addition, an example of replicate selection for the same binder is shown in Table 3. 1.

Figure 3. 1. FT-IR Spectrum for 64-28 Example Binder

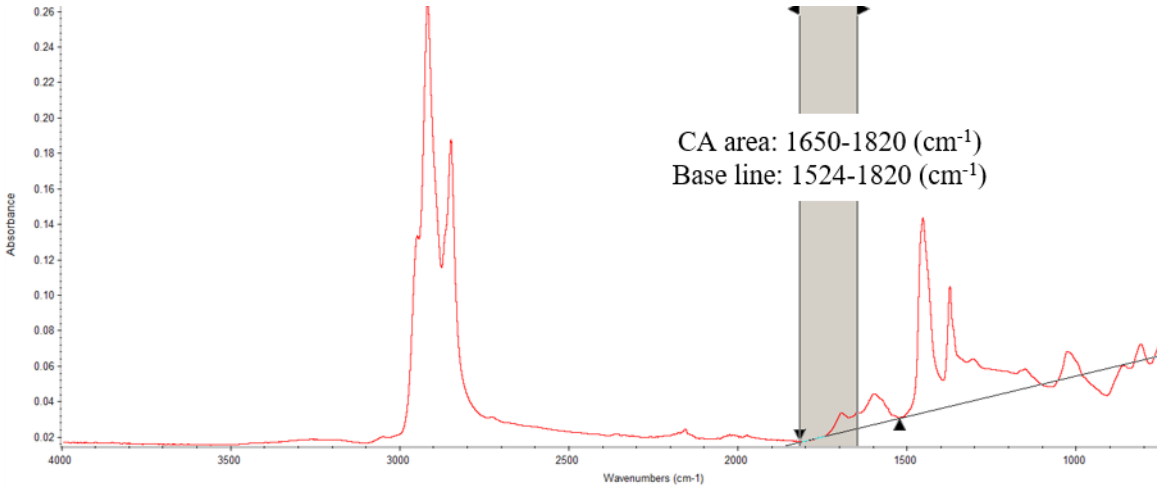

Table 3. 1. FT-IR Measurement for 64-28 Example Binder

	Measurement			Average Measurement	Selected Replicates	Overall Average
	1	2	3			
Replicate 1	0.554	0.542	0.537	0.544	✓	0.551
Replicate 2	0.331	0.348	0.331	0.337	x	
Replicate 3	0.553	0.558	0.559	0.557	✓	

3.1.3 DSR Frequency Sweep Test

As previously described the DSR test in accordance with AASHTO T 315 were conducted at a specific frequency to determine the high and intermediate continuous PG grade of the evaluated binders. Also, similar test was utilized to test the binders over multiple frequencies as well as temperatures while keeping the strain at a low value of 1 percent for all testing to stay in the linear viscoelastic region. The varied test condition in terms of temperature and frequency are indicated in Table 3. 2. It should be noted that not all the binders were evaluated at all the temperatures and frequencies. Detailed information will be provided in Chapter 4.

Table 3. 2. DSR Frequency Sweep Test Conditions

DSR Test Temperature (°C)	Parallel Plate Diameter (mm)	Gap Setting (mm)	Tested Frequencies (rad/s)
60, 64, 70	25	1	0.001 to 100
60, 70, 80	25	1	
85, 95, 100	25	0.5	
46, 34, 22	8	2	
15, 10, 4	8	2	

3.1.4 Shear Modulus Master Curves

Asphalt binder shear modulus master curve is an indication of the relationship between the binder stiffness and reduced frequency in a referenced temperature that has been developed from frequency sweep tests in multiple temperature. Noting that not a strict standard exists for binder master curve construction, in this effort a rheological software package, Rhea software version 1.2.9, was utilized perform the initial shifting of the complex shear modulus master curves to the referenced temperature (Rhea, 2011). Inside the software, the frequency sweep measured data will be fit into a smooth master curve utilizing methods of "free shifting". Subsequently, the fit of the master curve will also be determined through

the Christensen-Anderson-Sharrock (CAS) or prony series master curve forms. The corresponding shifting is then fit to the shift functions according to using Arrhenius, Williams-Landel-Ferry (WLF), and Kealble functional forms according to the time-temperature superposition principle. The term "free shifting" indicates that the master curve data are shifted to the master curve without a predefined shape function, which is then fit to the equation forms, i.e. master curve and shift function, as described. From a true rheological measurement standpoint, this method, i.e. free shifting, is more desirable rather than shifting the data to fit a particular master curve function and a corresponding shift function. Further detail information can be found elsewhere (Morian, 2014; Zhu, 2015). Example outputs of the Rhea are presented in Figure 3. 2 through Figure 3. 7.

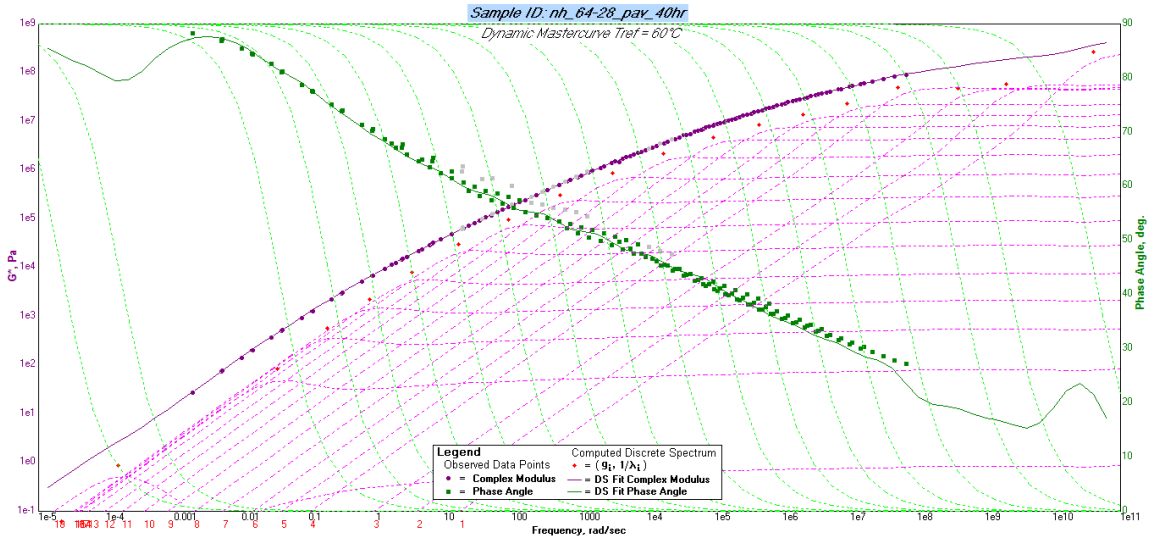

Figure 3. 2. Example of Rhea Output, Binder Master Curve

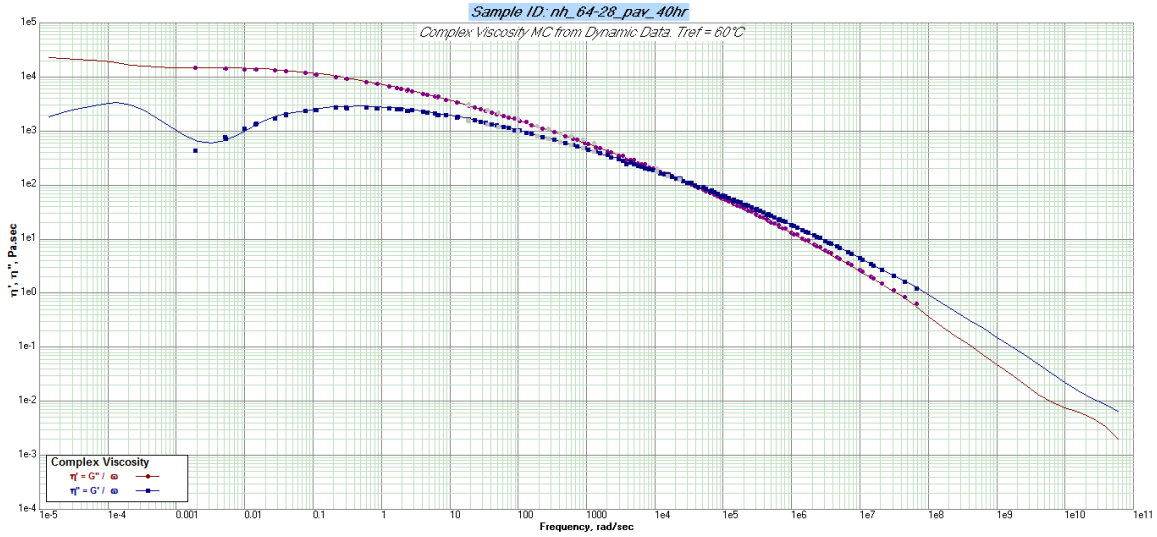

Figure 3. 3. Example of Rhea Output, Low Shear Viscosity

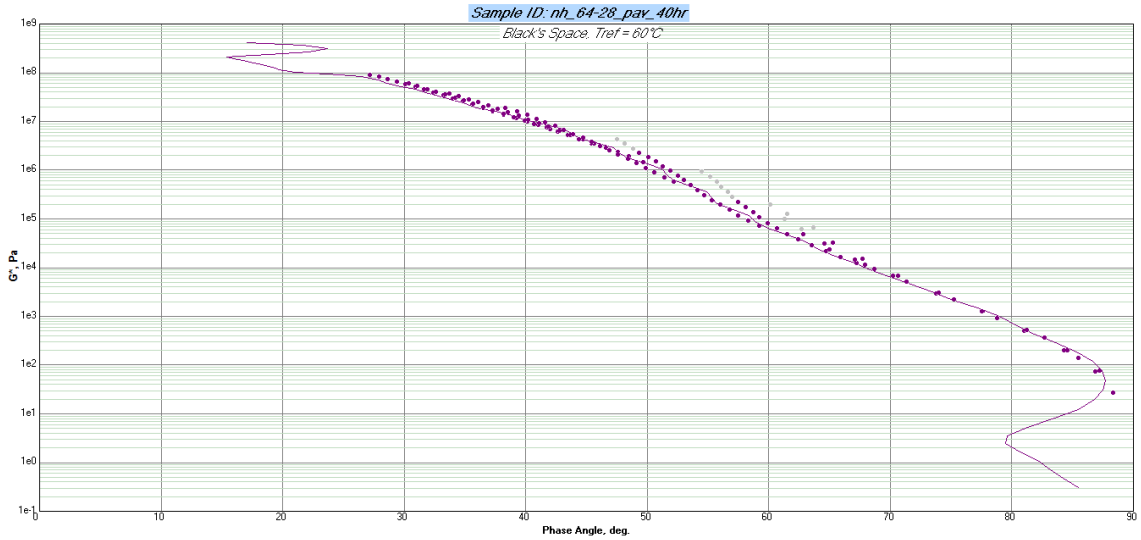

Figure 3. 4. Example of Rhea Output, Black Space Diagram

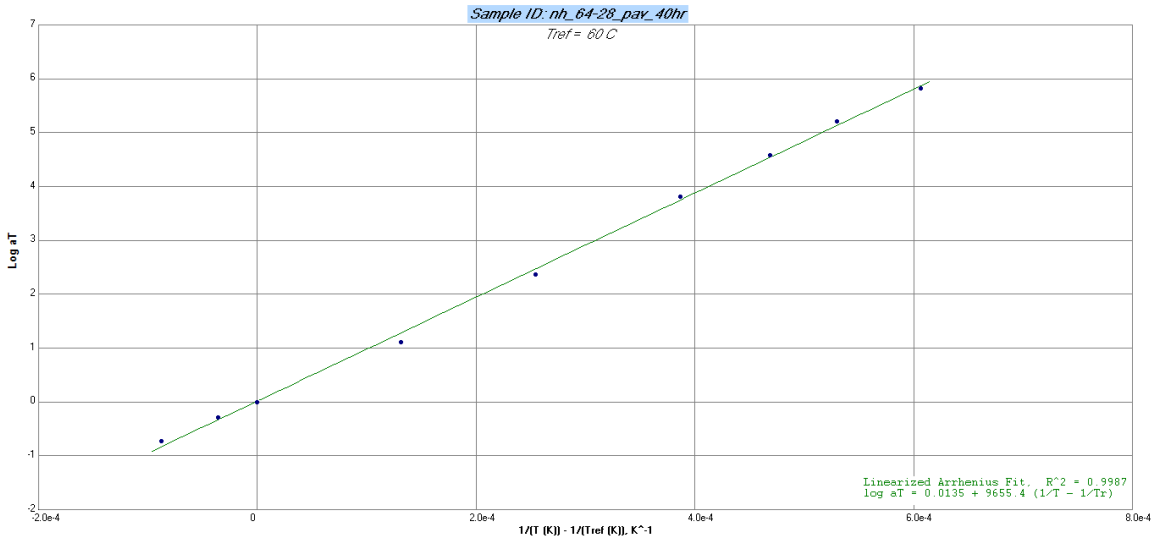

Figure 3. 5. Example of Rhea Output, Arrhenius Function Shift Factors

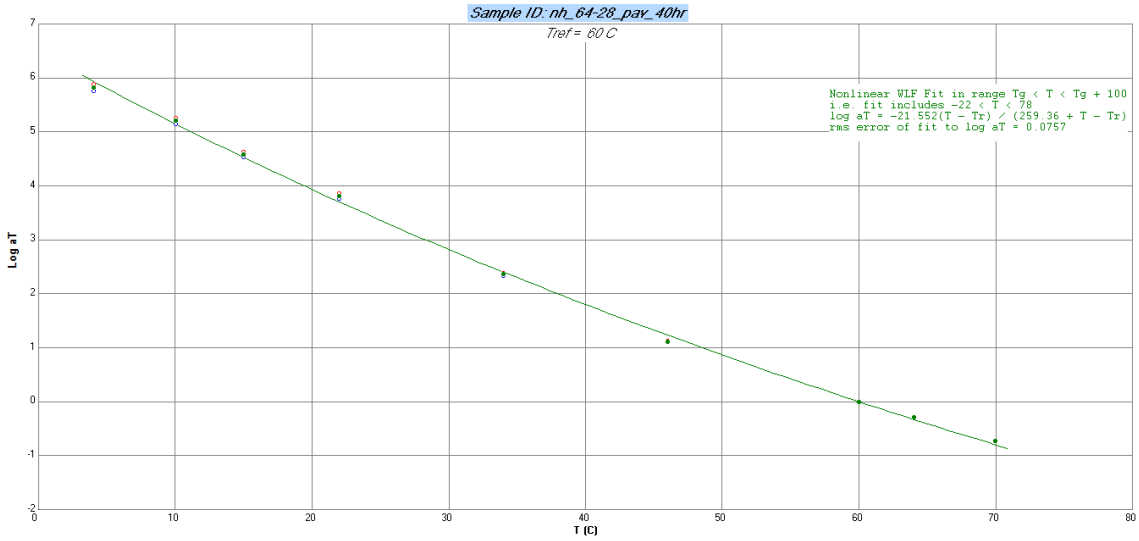

Figure 3. 6. Example of Rhea Output, WLF Function Shift Factors

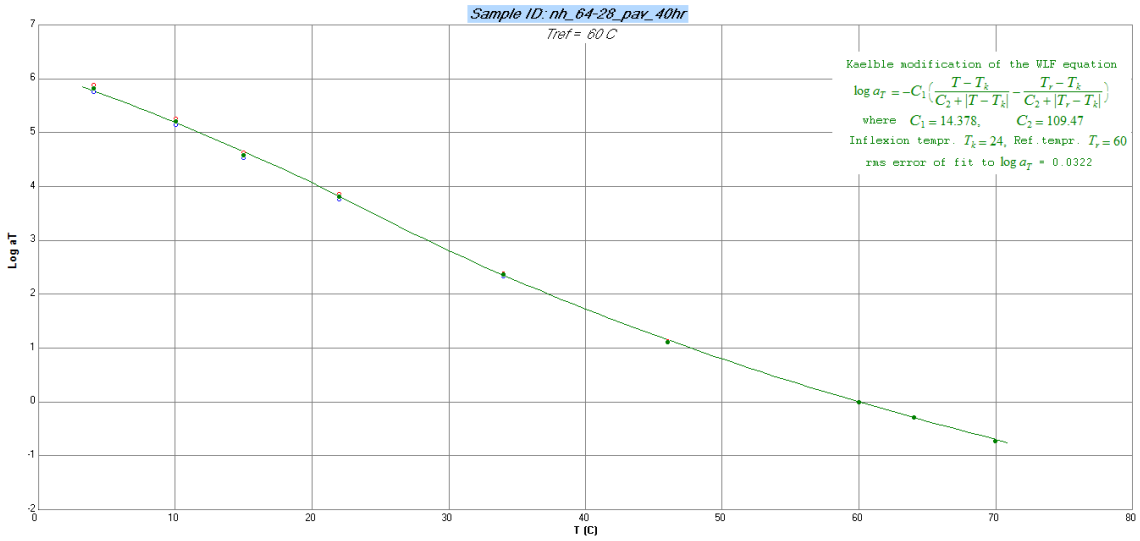

Figure 3. 7. Example of Rhea Output, Kaelble Function Shift Factors

3.1.5 Glover-Rowe Parameter (G-R)

The Glover-Rowe (G-R) parameter was originally defined by Glover et al. (2005) as the DSR function (G'/(η'/G')) and reformulated for greater practical use by Rowe (2011) in a discussion of Anderson et al. (2011) as the G-R parameter:

$$\text{G-R} = G'/(\eta'/G')/\delta = G^*(\cos\delta)^2/\sin\delta \qquad \text{Equation 3. 1}$$

Where,

G* : Complex dynamic shear modulus;

G' : Storage or elastic shear modulus;

η' : Storage dynamic viscosity; η'=G''/ ω;

δ : Phase angle;

All rheological properties are referenced to 0.005 rad/s and 15°C.

These measures have been shown to correlate well with ductility and thus cracking resistance as well as binder oxidation levels (Ruan et al., 2003). The G-R parameter

captures both rheological parameters needed to characterize binder viscoelastic behavior: stiffness (G* at high and intermediate temperatures) and phase angle (δ at high and intermediate temperatures).

However, there have also been limitations observed with the G-R parameter measured in the DSR at intermediate temperatures, particularly when correlations were attempted with modified binders (Glover et al., 2005). Traditionally, the DSRFn is reported as a single point measurement at 15°C and a frequency of 0.005 rad/s (Ruan et al., 2003) as is the corresponding G-R parameter (Rowe, 2011). It has been proposed that the original DSRFn correlation to ductility measures (Kandhal, 1977) were based upon the Pennsylvania climate using a PG 58-28 binder and thus have inherent assumptions. It has been proposed that the original DSRFn and the subsequent G-R evaluation temperature of 15°C can appropriately be considered as either a constant offset of 43°C from the low temperature PG grade (King et al., 2012; King, 2013) or as the midpoint of the PG binder grade (King, 2013). Both interpretations yield the original 15°C evaluation temperature for the climate and materials used in the early development of the DSRFn and G-R parameters, but will necessitate temperature adjustment for many of the modified binders as well as binders not matching the original PG 58-28 grade. Further investigations have been conducted by other researchers to evaluate the concept of equal stiffness through climate specific or material specific temperatures at which the G-R parameter is evaluated. (Hajj et al., 2016; Morian et al., 2017)

3.1.6 Black Space Diagram

Black space diagram is an indication of the, G*, versus phase angle, δ, at a particular temperature and frequency as shown in Figure 3. 8. The specific temperature and frequency is selected similar to those of the traditional Glover-Rowe parameter, i.e. 15°C and 0.005 rad/s, respectively. Each point in the black space diagram represents an aging state and further aging moving the binder rheologically from the lower right to the upper left of the diagram by increasing G* and decreasing δ. The figure also shows a damage zone where cracking likely begins due to brittle rheological behavior defined by G-R parameter between 180, onset of cracking, and 600 kPa, significant cracking, that correlates to low ductility values of 5 to 3 cm, respectively. These limits were previously related to surface raveling and cracking by Kandhal (1977).

Figure 3. 8. Black Space of Glover-Rowe Parameter at 15°C for PG 64-28 Base Binder

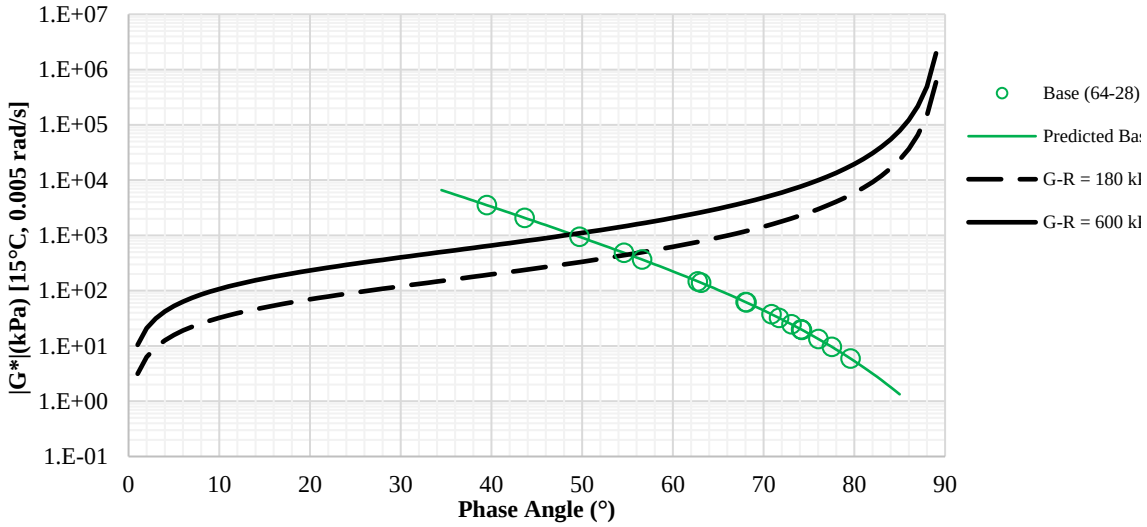

3.1.7 Low Shear Viscosity (LSV)

Zero shear viscosity (ZSV) is an important rheological indicator of asphalt binder to represent the capability of asphalt mix to resist the shear deformation at high temperatures as well as the rutting resistant properties of asphalt binders. However, zero shear viscosity is a theoretical concept and there is no practical methodology to test the asphalt binder at zero shear rate directly. As a result, the low shear viscosity (LSV) at 60°C and 0.001 rad/s was utilized instead of the ZSV. To determine LSV, the complex viscosity (G*) is plotted as a function of testing frequency. This plot creates a clear plateau in complex viscosity with lower frequencies as presented in Figure 3. 3. The definition of LSV is essentially when the response is purely viscous, i.e. the elastic response is very small, but not exactly zero. More details can be found elsewhere (Morian, 2014).

3.2 Mortar Testing

The mortar terminology is allocated to the blend of the binder and R100 aggregate, i.e. passing sieve #50 and retained on sieve #100. Mortar testing is performed based on the draft standard procedure (AASHTO T-XXX-12) intending to provide an estimate of original binder performance grade change rate when it is blended with recycled material. It also eliminates the hazardous and time-consuming chemical extraction and recovery process as well as the associated issues with the solvent remaining in the recovered binder. As described in the draft standard, three samples including one virgin binder and two void-less mortar samples with identical gradation and identical total binder content are prepared. One of the mortar samples contains a percentage of recycled binder (referred to as RAP mortar or RAS mortar) while the other one is made of only the virgin

binder (referred to as aggregate mortar); thus, any difference in properties between the mortar samples is attributed to the percentage of recycled binder used in the mortar sample. The three samples are tested at low, intermediate and high critical Superpave temperatures according to the standard performance grading procedure. The rate of the grade changes due to the addition of the recycled binder in the mortar samples are then calculated for each critical temperature allowing for the estimation of true PG at desired recycled percentages. Figure 3. 9 to Figure 3. 11 demonstrate the results of the mortar test procedure for the PG 64-28P baser binder for the three critical temperatures. Comprehensive analysis are provided in Chapter 7.

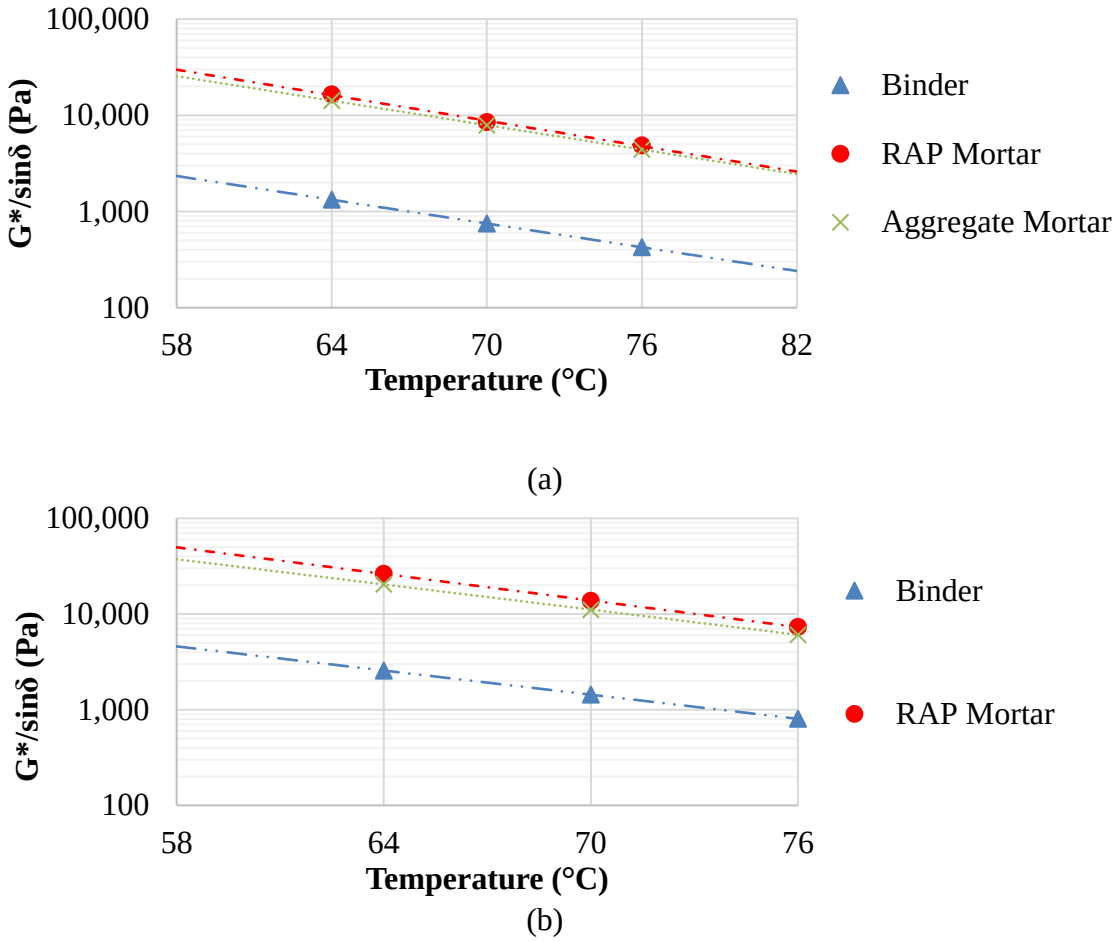

Figure 3. 9. High Temperature Properties for PG 64-28P (a) Original (b) RTFO

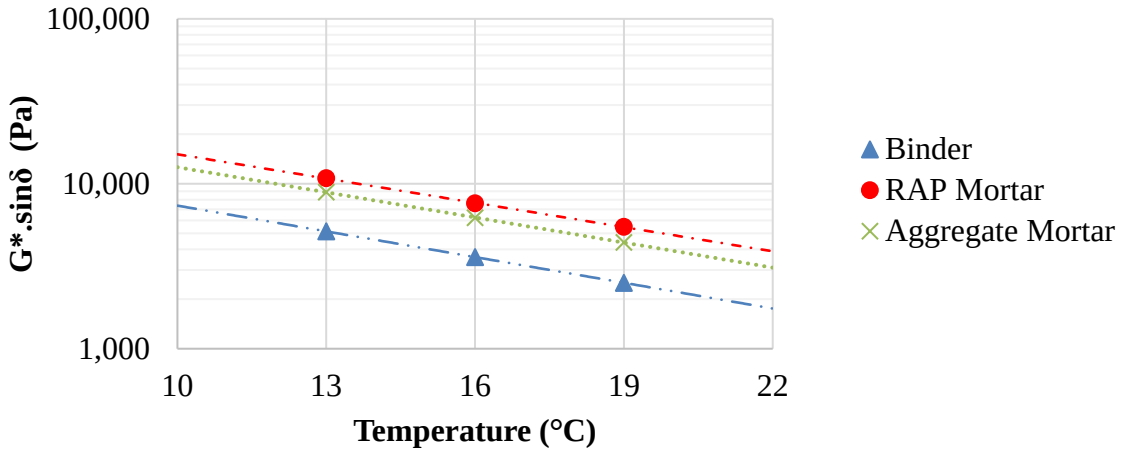

Figure 3. 10. Intermediate Temperature Properties for PG 64-28P

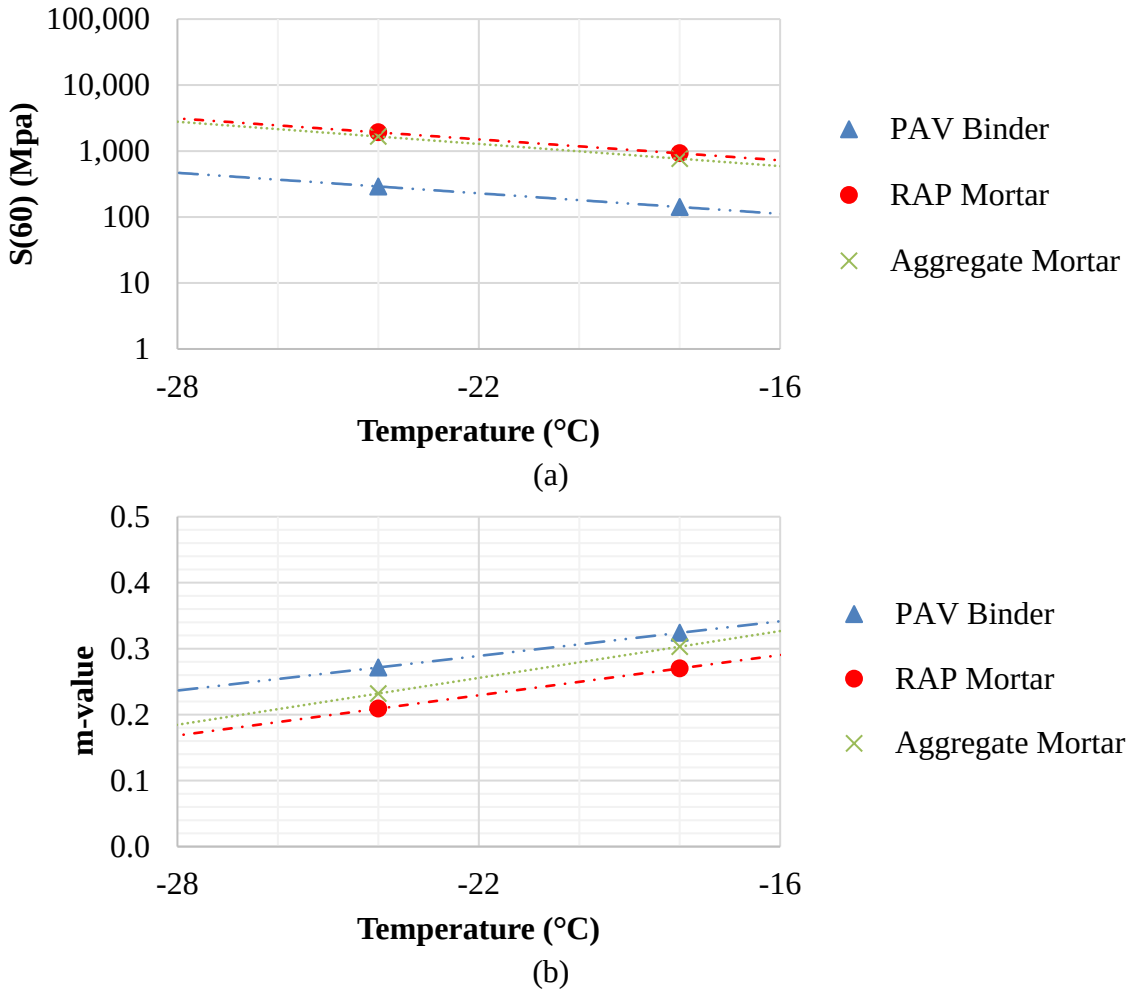

Figure 3. 11. Low Temperature Properties for PG 64-28P (a) Stiffness (b) m-value

3.3 Binder Extraction and Recovery Test

As a primary step in characterizing the recycled binder blends, the AASHTO T164 standard procedure is employed to extract the recycled binder from recycled material following with the recycled binder recovery according to ASTM D5404. It should be noted that the extraction solvent utilized in this study was not the same as the recommended solvent in the AASHTO standard, i.e., trichloroethylene. In fact, trichloroethylene had been noted to stiffen the rheology of binders even upon full recovery of the solvent. This was proved by several different tests including DSR, FT-IR and Gel Permeation Chromatography, done by Glover at the Texas A&M University (Morian, 2014).

As a summary of the effort, approximately, 1,000 g of the RAP material was subjected to a chemical solvent blend including 85% of Toluene and 15% of Ethanol for at least 5 times to extract all the recycled binder from the RAP material. In parallel, the recovery procedure was conducted on the solution of the extracted recycled binder and solvent to remove the solvent form the binder. In this procedure, the solution is distilled by partially immersing the rotating in a heated oil bath while the solution is subjected to a partial vacuum and a flow of nitrogen gas. Also, an extra step was added to the standard recovery procedure to make sure all the solvents are distilled from the solution. In practice, when no more solvent was distilled from the solution, the remaining material in the container was exposed to theoretically zero vacuum pressure and 65mmHg Nitrogen pressure for 2 hours. Then, as the final step, the container was placed in an oven to gather the remaining binder, subjected to testing as required.

3.4 Optimum RA Dosage Selection

For specific combinations of various base binder and recycled binder from RAP/RAS, recycling agents might be utilized to restore the binder blend properties to that of a preselected target binder. In practice, low RA dosages will fail to provide the mixture with sufficient fatigue and thermal cracking resistance. Conversely, high RA dosages will be costly and potentially detrimental to the rutting performance of the mixture, especially during its early life. Therefore, determining an optimum dosage to meet both of the aforementioned concerns as well as cost issues has been the state of interest in several research studies (Shen and Ohne 2002; Shen, Amirkhanian, and Miller 2007; Tran et al. 2012; Zaumanis et al. 2014a, high-temperature PG grade; Zaumanis et al. 2014a). These approaches include using binder blending charts based on viscosity and/or penetration or employing the PG system by evaluating the changes in the binder PG due to the addition of an RA. However, no standard method is currently available for RA dosage selection.

The most recent methodology for optimum RA dosage selection is presented in NCHRP 09-58 2nd Interim Report (Epps et al., 2016). This methodology evaluates the binder PG results of the intended binder blend at multiple RA dosages, and then provides recommendations regarding the RA optimum dosage with respect to the PG high and low restoration. The last updated version of the step-by-step RA optimum dosage selection methodology based on the efforts conducted in the on-going NCHRP 09-58 project is as follows:

- Plot original high temperature continuous PG grade (PGH), RTFO PGH, S-controlled low temperature continuous PG grade (PGL), and m-controlled PGL values versus RA dosage,
- Establish linear regression equations for each value versus RA dosage,
- Select initial RA dosage rate in 0.5% increments to restore target binder PGL using the limiting (warmer) PGL regression line,
- Check PGH at initial RA dosage versus target binder PGH using limiting (colder) PGH regression line,
- If required, increase/decrease RA dosage in 0.5% increments to meet target binder PGH while maintaining target binder PGL.

According to the proposed methodology, a comprehensive example of the RA dosage selection procedure for the 64-28P base binder blended with 30% NV RAP binder ratio and a pre-determined aromatic extract named A2 is presented in Table 3. 3 and Figure 3. 12. Subsequent results and discussions are provided in Chapter 7.

Table 3. 3. Binder PG Grade Results

Binder Blend	RA Type	RA Dosage (%)	High-Temperature Continuous PG Grade (°C)		Intermediate-Temperature Continuous PG Grade (°C)	Low-Temperature Continuous PG Grade (°C)		ΔTc	Final Continuous Grade
			Original	RTFO		S-controlled	m-controlled		
Base (64-28P)		0.0	67	65.6	13.4	-34.3	-30.7	-3.6	65.6-30.7
Recycled w/A2 (64-28P / 0.30 NV RAP)	A2	1.5	72.5	70.6	17.5	-31.6	-29.2	-2.4	70.6-29.2
		2.0	71.9	68.7	16.9	-32.2	-29.8	-2.4	68.7-29.8

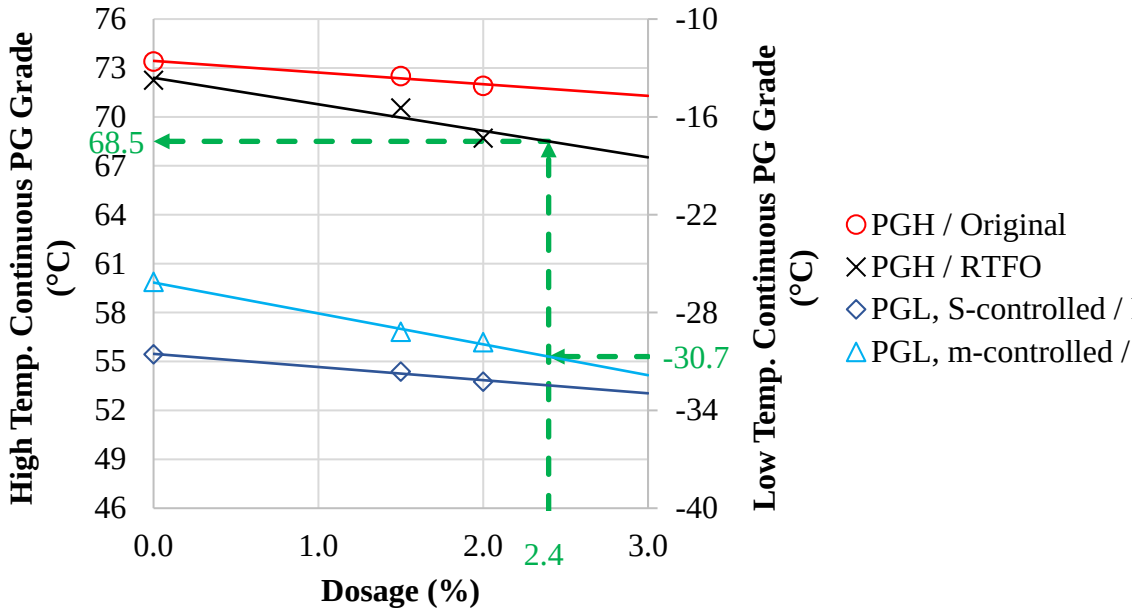

Figure 3. 12. RA Dosage selection for Recycled w/A2 (64-28P / 0.30 NV RAP) in NV Field Project

3.5 Binder Aging Kinetic Parameters

Several efforts have been conducted in the asphalt industry to investigate the binder aging behavior through several oxidation models that are summarized elsewhere (Morian, 2014). In this study, the Texas A&M methodology that has been developed under the direction of Dr. Charles J. Glover and his research team is utilized to characterize the CA growth as a function of aging duration. The FT-IR spectroscopy has been employed to measure the binder oxidation level in this specific methodology. As previously described, the CA measurements are computed, from the OMNIC software, as the area, in arbitrary units, between the absorption spectrum and the magnitude of the absorption at 1,524 to 1,820 cm^{-1} as the baseline and between the wave number of 1,650 and 1,820 cm^{-1}. As the next step, the oxidation measures in each aging temperature are plotted as a function of aging duration. Figure 3. 13 presents an example of the oxidation plot for the PG 64-22 binder utilized in

this study. Each single point on the figure is the average of at least two FT-IR measurements, noting that each measurement is the average of three replicates. Historically, two separate constant oxidation rates are observed within each binder named as fast and constant oxidation rate, k_f and k_c, respectively. The Arrhenius relationship as a function of the inverse of the aging temperature and the gas constant R, Equation 3.2, is then utilized to formulize the oxidation rates separately.

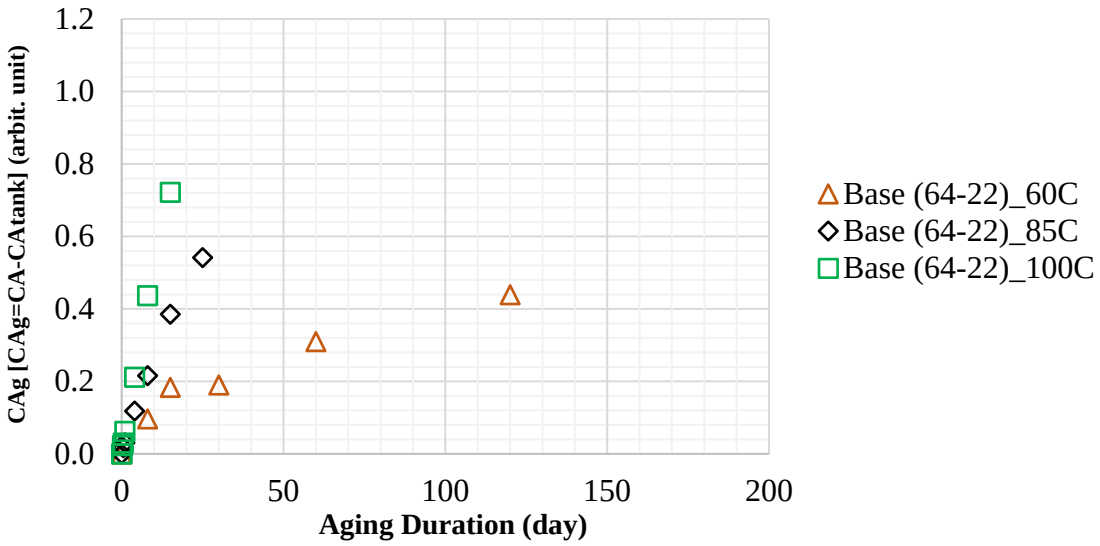

Figure 3. 13. Example of Oxidation Kinetic Measurements

$$r_{CA} = AP^{\alpha}e^{-E_a/RT} \qquad \textbf{Equation 3. 2}$$

Where:

r_{CA}: rate of carbonyl area, CA, growth, either k_f or k_c;

A: pre-exponential factor;

P: absolute oxygen pressure during oxidation, atm;

α: reaction order with respect to oxidation pressure;

E_a: activation energy, J/mol;

R: ideal gas constant, 8.3144621 L/mol.°K;

T: temperature, °K.

Finally, the two oxidation rates can be combined into one relationship describing CA as a function of aging time and duration, presented in Equation 3.3:

$$\mathbf{CA_g = M * \left(1 - e^{-k_f t}\right) + k_c t} \qquad \textbf{Equation 3. 3}$$

Where:

CAg: carbonyl area growth ($CA-CA_0$);

CA: carbonyl area;

CA_0: original or tank CA measurement;

M: initial jump, magnitude of fast rate reaction in terms of CAg;

k_f: fast rate of CA growth;

k_c: slow or constant rate of CA growth;

t: time, days.

As an example of the application of Equation 3.3 is shown in Figure 3. 14, clearly representing the fast and constant oxidation phases as well as the predicted aging path over three different temperatures and multiple aging durations for PG 64-22 base binder.

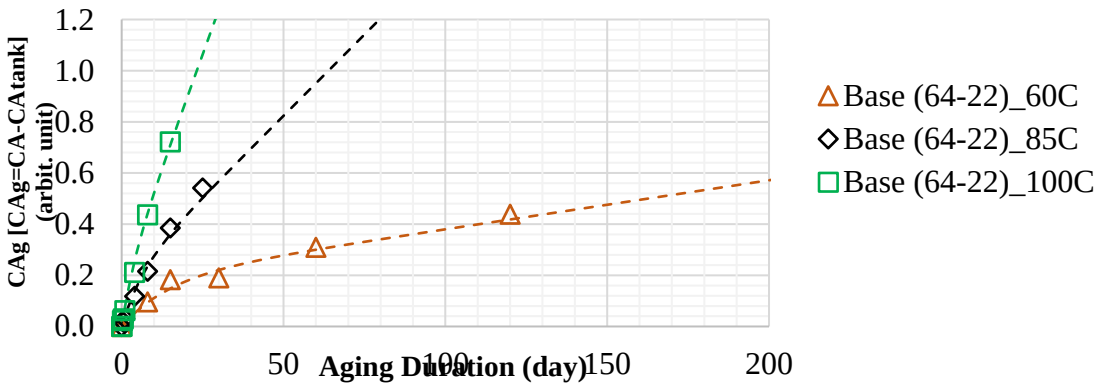

Figure 3. 14. Example of Fast and Constant Oxidation Kinetic Measurements and Predicted Aging Path

3.6 Binder Hardening Susceptibility

One of the most significant parameters in characterizing the binder oxidation properties is hardening susceptibility (HS) which originally relates the binder stiffness with aging. Historically, the LSV and CA from the FT-IR measurements were utilized as an indication of the binder stiffness and aging, respectively. The corresponding HS is a linear relationship between the LSV and CA mathematically defined by Equation 3.4.

$$\ln \eta_0^* = HS * CA + m \qquad \textbf{Equation 3. 4}$$

Where:

η_0^*: low shear viscosity of the asphalt binder;

HS: hardening susceptibility, slope of relationship;

CA: carbonyl area, arbitrary units - unit less;

m: intercept of $\log \eta_0^*$ and CA relationship.

In this study, the HS relationships were also determined with respect to G-R parameter as a binder stiffness parameter. However, in this case, not all the HS relationships were verified to have a linear relationship (especially in the case of a polymer-modified binder). Similar to the two phase kinetic relationships described previously, two separate fast and constant HS rates were also noticed in the G-R hardening susceptibility plots; therefore, a non-linear, two phase equation was developed to mathematically formulize the relationship between the G-R parameter and CA. Equation 3.5 represent the most recent update of the equation. Also, Figure 3. 15 indicates the binder HS measures and predictions for PG 64-28 with both the linear and non-linear equations, in which the latter equation seems to represent a more robust fit.

$$\ln(G-R) = M\left(1 - e^{-k'_f CA_g}\right) + k'_c CA_g + \ln(G-R)_0 \qquad \textbf{Equation 3. 5}$$

Where:

G-R: Glover-Row parameter (kPa) @ 15°C and 0.005 rad/sec

$G\text{-}R_0$: Initial Glover-Row parameter (kPa) @ 15°C and 0.005 rad/sec

CA_g: Carbonyl area growth;

k'_f: fast rate of G-R growth

k'_c: constant rate of G-R growth

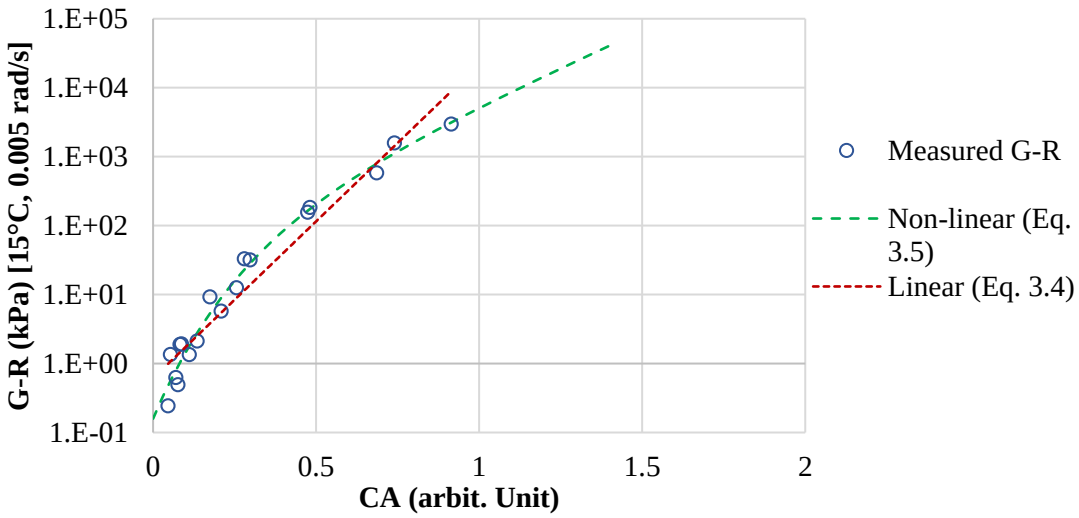

Figure 3. 15. Hardening Susceptibility of the PG 64-28 Base Binder for G-R Parameter

3.7 Mixture Testing

The UTSST methodology was utilized in this study to evaluate the low temperature characteristics and performance of the asphalt mixtures. This test investigates the thermo-viscoelastic (i.e., stiffness-temperature relationship) and fracture properties of asphalt as well as their stiffness-temperature relationship. As a result, a stage of comparison will be

provided among the mixtures with various modifications and additives including recycled material and recycling agents, as presented in several recently conducted studies (Menching et al., 2014, Alavi et al. 2013, Morian 2014).

3.7.1 UTSST

Uniaxial Thermal Stress and Strain Test (UTSST) has recently been developed through enhancement of the traditional Thermal Stress Restrained Speciemn Test (TSRST) setup that measures thermal stress build-up under a constant cooling rate in a restrained prismatic mixture specimen until fracture. The UTSST test allows reliable and repeatable measurements of thermal stress and strain from restrained and unrestrained asphalt mixture specimens resulting in Thermo Visco-Elastic Properties (TVEP) determination. In this study, the UTSST specimens were obtained from Superpave gyratory compacted (SGC) specimens of the reheated plant mixed laboratory compacted or field cores with a lift thickness of at least 65 mm. More detailed information regarding the test setup and sample fabrication can be found in the literature (Alavi *et al.*, 2013, Hajj *et al.*, 2013).

Figure 3. 16 presents the layout of the UTSST apparatus. The restrained and unrestrained specimens were subjected to a cooling rate of 10°C/hr starting from an initial temperature of 20°C, to measure the thermal stress and strain, respectively. Detailed information regarding the effect of cooling rate on UTSST results can be found in literature (Alavi and Hajj, 2014). In this effort, a minimum of two replicates for the restrained specimen were tested for the evaluated mixture, noting that the same unrestrained specimen was tested twice, once for each of the corresponding retrained specimen replicate tests, to obtain the corresponding thermal strain.

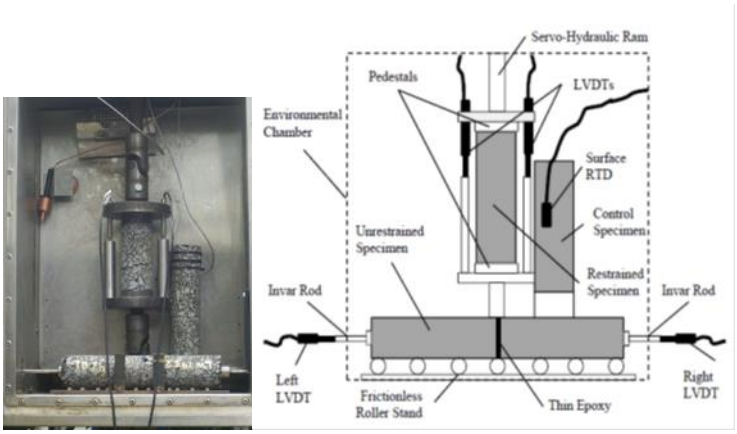

Figure 3. 16. Uniaxial Thermal Stress and Strain Test (UTSST) Setup

The developed stiffness-temperature curve relationship and thermal build-up stress curve (Figure 3. 17a, Figure 3. 17b) indicate five typical stages of material behavior. A brief description for these behaviors is described in the following. Further information regarding the thermo-viscoelastic properties and the stiffness-temperature relationship can be found in the literature (Alavi *et al.*, 2013; Hajj *et al.*, 2013; Morian, *et al*, 2014; Alavi and Hajj, 2014; Menching *et al.*, 2014, Alavi, *et al.*, 2015).

Viscous softening: At this stage, the UTSST modulus of the asphalt mixture increases rapidly, mostly in a linear fashion, with decreasing temperature. The point of viscous flow can be identified as the temperature at which the second derivative of the UTSST modulus with respect to temperature reaches zero on the warmer temperature side.

Viscous-glassy transition: At this stage, the glassy properties of the material become more dominant over the viscous properties. The transition stage can be detected as the point at which the second derivative of the UTSST modulus with respect to temperature reaches a maximum.

Glassy hardening: At this stage, the behavior of the asphalt material is almost completely glassy. The glassy hardening stage can be identified as the point at which the second derivative of UTSST modulus with respect to temperature reaches zero on the colder temperature side.

Crack initiation: At this stage, micro cracking occurs in the specimen due to the induced thermal stresses when the material behavior is glassy or brittle. This stage is identified as the maximum value of the UTSST modulus as seen in Figure 3. 17b. An instantaneous decrease in the calculated UTSST modulus reveals that the asphalt mixture specimen is no longer uniform as a result of initiation of micro cracks in the specimen, i.e. discontinuities with in the cross section of the specimen.

Fracture: At this stage, the asphalt mixture specimen breaks due to the propagation of micro cracks as a result of the induced thermal stresses as depicted in Figure 3. 17. It should be noted that other researchers have also observed that mixture failures in the TSRST do not always exhibit clear brittle fracture (Pucci et al., 2004). They observed a reduction in the slope of thermal stress curve prior to ultimate fracture. This behavior was referred to as the initiation of micro cracks.

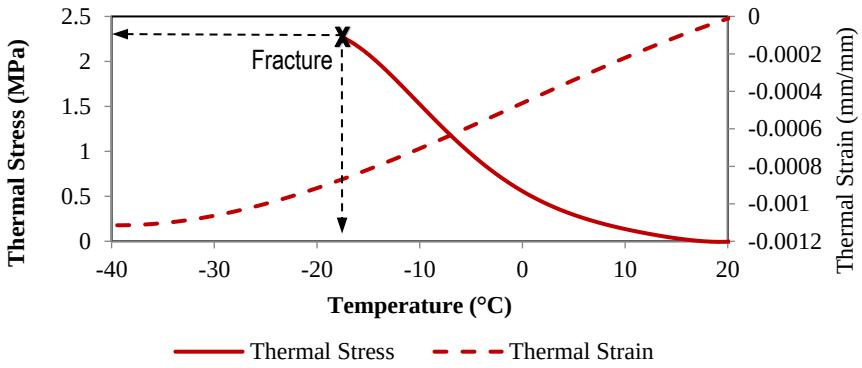

(a)

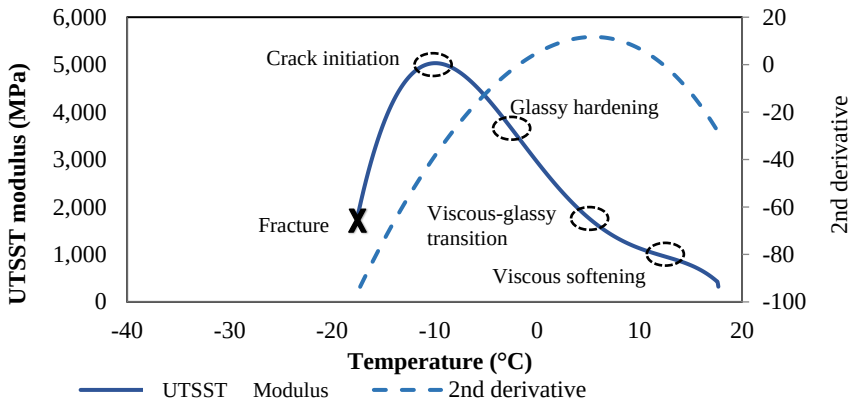

(b)

Figure 3. 17. (a) Measured Thermal Stress and Strain; (b) Calculated UTSST Modulus and Associated Characteristic Stages

Detailed information regarding the thermo-viscoelastic properties calculation can be found in ASTM 2016.

3.7.1.1 Coefficients of Thermal Contraction

As an additional thermo-volumetric property of the asphalt mixtures, the thermal contraction strain of the unrestrained specimen caused by constant cooling rate was fitted with the proposed model presented in Equation 5.1 (Bahia, 1991). The solver function for the Microsoft Excel was utilized to solve the equation for the unknown parameters.

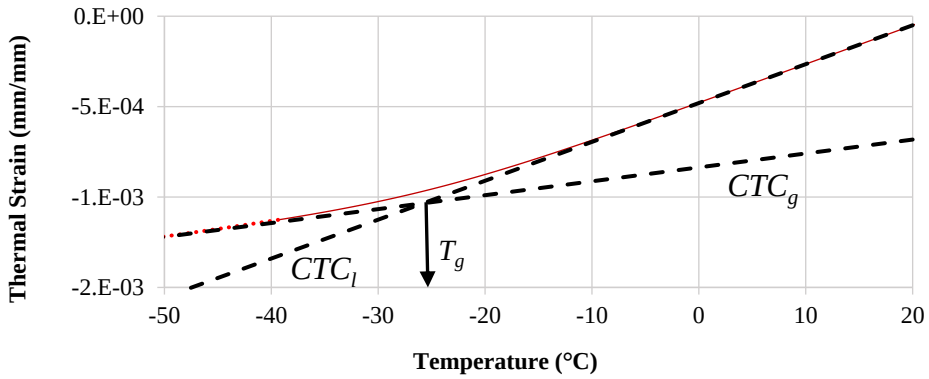

Figure 3. 18. Determination of Thermo-Volumetric Properties From Thermal Strain Measurements

$$\varepsilon_{th} = \frac{\Delta l}{l_0} = C + CTC_g(T - T_g) + ln\left\{\left[1 + e^{\frac{(T-T_g)}{R}}\right]^{R(CTC_l - CTC_g)}\right\} \quad \textbf{Equation 5. 1}$$

Where:

$\frac{\Delta l}{l_0}$: relative change of length or thermal strain;

C: fitted intercept;

CTC_l: liquid coefficients of thermal contraction;

CTC_g: the glassy coefficients of thermal contraction;

T_g: glass transition temperature (determined by the intersection of the two linear portions of the curve with respect to the CTC_g and CTC_l, i.e., above andbelow T_g);

R: the parameter representing the curvature between the two linear asymptotes;

ε_{th}: thermal strain

T: temperature (°C).

3.7.1.2 UTSST Resistance Index

Additional investigations of the UTSST measures have recently been developed to evaluate the cracking resistance of a particular asphalt mixture through a single parameter. This resistance index value, identified as CRI_{UTSST}, is determined through calculations of the measured thermal stress and thermal strain plots presented in Figure 3. 19.

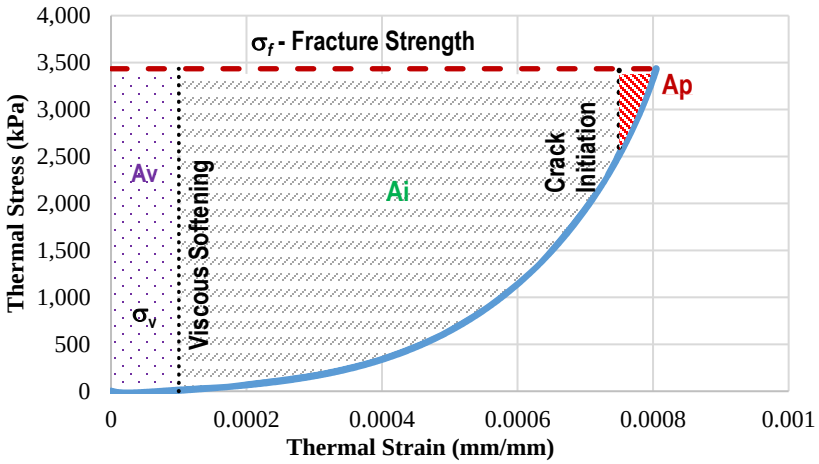

Figure 3. 19. Thermal Stress and Strain Plots Indicating CRI_{UTSST} Parameters

The CRI_{UTSST}, formulated by Equation 5.2, combines specific aspects of the thermal stress and strain relationships with the thermo-viscoelastic property regions to present an overall understanding of the mixture behavior.

$$\mathbf{CRI_{UTSST}} = \frac{\mathbf{A_v + A_i}\left(\mathbf{1 + \frac{A_v}{A_v + A_i} + \frac{A_p}{A_p + A_i}}\right)}{\left(\mathbf{\sigma_{GT}}/\mathbf{\sigma_F}\right)} \qquad \textbf{Equation 5. 2}$$

Where:

CRI_{UTSST}: UTSST cracking resistance index

A_v: area of viscous behavior, i.e. area of stress-strain to viscous softening

A_i: area of crack initiation, i.e. area of stress-strain from viscous softening to crack initiation

A_p: area of crack propagation, i.e. area of stress-strain from crack initiation to ultimate fracture

σ_{GT}: thermal stress at glassy transition

σ_F: thermal stress at fracture

In this configuration, the larger values of the CRI_{UTSST} denotes increased levels of thermal cracking resistance. For example, a given mixture with a limited resistance to crack propagation, i.e. low A_p, may still show higher levels of CRI_{UTSST}, if the mixture has a high level of crack initiation resistance, i.e. A_i. Similarly, the cracking resistance of a mixture would increase with larger measured fracture stress, σ_f. However, the overall resistance would be reduced by an elevated stress level at the glassy transition stage, σ_{GT}.

CHAPTER 4 AGING EXPERIMENTAL PLAN AND SCOPE

This study covers the laboratory binder aging as well as the UTSST mixture testing portion of the NCHRP 09-58 entitled with "The Effects of Recycling Agents on Asphalt Mixtures with High RAS and RAP Binder Ratios", a collaborative effort among the Texas A&M University, the University of New Hampshire and the University of Nevada, Reno. The overall objectives of this project are to evaluate rejuvenating agents (RA) effectiveness in mixtures with high Recycled Asphalt Shingles (RAS), Recycled Asphalt Pavements (RAP), or combined RAS/RAP binder ratios through laboratory testing and field projects. Noting 0.3 as a common upper limit for the recycled binder ratio (RBR) without changing the virgin asphalt binder grade in a given mixture, the scope of the NCHRP 09-58 encompasses higher RBR values between 0.3 and 0.5. Under this project, the performance of the binders and mixtures containing high RBRs will be monitored with and without various RAs at determined dosages in both laboratory and field experiments, permitting the extended observation of the theoretical and actual material performances. NCHRP 09-58 is still on-going and the final report is expected to be published in 2018. As previously mentioned, this study embodies only the binder aging laboratory testing and related results as well as the UTSST mixture testing conducted at the University of Nevada, Reno.

4.1 Material

In the binder aging portion of NCHRP 09-58 project, several binder blends have been used to investigate the impact of various recycled materials from different sources as well as

several rejuvenating agent types. Three binder sources from Texas, New Hampshire and Nevada have been blended with TX recycled materials and two different rejuvenating agents (RA), generally described in Table 4. 1. Detailed information regarding the nomenclatures of the binder blends tested at the University of Nevada, Reno are presented in Table 4. 2. Table 4. 2depicts the three different types of recycled materials, namely RAP, manufactured waste asphalt shingles (MWAS), and tear-off recycled asphalt shingles (TOAS) along with the respective blended compositions. Both of the recycled binder ratio (RBR) numbers and the RA dosages for the binder blends have been selected by the Texas A&M University research team through the NCHRP 09-58 project.

Table 4. 1. Binder Aging Rejuvenating Agents Properties

Category	Description	Name	ID
Aromatic Extracts	Refined crude oil products with polar aromatic oil components	Hydrogreen	A1
Tall Oil	Same chemical family as liquid antistrip agents and emulsifiers	Hydrolene	T1

As defined in Table 4. 2, the RAs have been categorized as either OPT or FLD; the OPT is an abbreviation for optimum denoting the dosage of the RA that is able to restore the base binder PG grades; and the FLD designation indicates the dosage used in the field project if it were not the determined OPT value. It is also noteworthy to mention that there are two different methods for using the RAs in recycled materials, either by binder replacement or by addition. Binder replacement means that the RA selected dosage, 0.3 for instance, is calculated by weight of the base binder or the mixture, then the same amount of base binder will be removed from the binder blend and will be replaced by the calculated

amount of RA. Addition, however, indicates that the RA will be added as a percentage to the binder blend without replacement. All the RAs in Table 4. 2 are used as a replacement. A comprehensive list of related definitions have been provided in Chapter 3. It should be mentioned that the RBR determination for recycled materials and dosage selection for RAs have been conducted in the Texas A&M University.

Table 4. 2. Binder Blend Identification and Aging Experimental Plan

Binder ID	Base Binder Type	RAP (RBR)	RAS (RBR)	RA	Dosage by Replacement (%)	Forced-draft Oven Aging Temperature (°C)			PAV Aging
						60	85	100	100
Base (64-22)	TX PG64-22	—	—	—	—	1, 4, 8, 15, 30, 60, 100, 120, 160 days	0.5, 1, 4, 8, 15, 25, 40 days	0.08, 0.25, 0.5, 1, 4, 8, 15 days	RTFO, 20, 40, 60 hrs
Base w/T1 @ TX FLD[1] (64-22 / 2.65%)		—	—	T1	2.65				
Recycled w/T1 @ TX FLD (64-22 / 2.65% / 0.25 TX RAP, 0.25 TX MWAS)		TX (0.10)	TX MWAS (0.20)	T1	2.65				—
Base (64-28)	NH PG64-28	—	—	—	—	1, 4, 8, 15, 30, 60, 100 days	1, 4, 8, 15, 25, 40 days	0.08, 0.25, 1, 4, 8, 15 days	RTFO, 20, 40, 60 hrs
Base w/T1 @ TX FLD (64-28 / 2.65%)		—	—	T1	2.65				
Base w/A1 (64-28 / 6%)		—	—	A1	6				—
Recycled w/T1 @ OPT[2] (64-28 / 12.5% / 0.25 TX RAP, 0.25 TX TOAS)		TX (0.25)	TX TOAS (0.25)	T1	12.5				
Recycled w/A1 @ OPT (64-28 / 6% / 0.40 TX RAP)		TX (0.40)	—	A1	6				
Base (64-28P)	NV PG64-28P	—	—	—	—	4, 8, 15, 30, 60, 100 days	1, 4, 8, 15, 25, 40 days	0.08, 0.25, 1, 4, 8, 15 days	RTFO, 20, 40, 60 hrs
Base w/T1 @ TX FLD (64-28P / 2.65%)		—	—	T1	2.65				
Recycled w/T1 @ OPT (64-28P / 11% / 0.25 TX RAP, 0.25 TX TOAS)		TX (0.25)	TX TOAS (0.25)	T1	11				

[1] at Texas Field dosage, [2] at Optimum dosage

4.2 Forced-Draft Oven Aging

The binder blends defined in the experimental plan in were exposed to free atmospheric air at multiple aging temperatures and durations, shown in Table 4. 2. Accordingly, 1 mm thick asphalt binder films covering 140 mm diameter pressure aging vessel (PAV) pans were utilized to age the binders in specialized forced-draft ovens with stringently controlled temperature variation under free-atmospheric air and pressure.

4.3 Accelerated Aging

In addition to the forced-draft oven aging, a secondary aging protocol was also undertaken with the selected binders from the NCHRP 09-58 stablished experimental plan presented in Table 4. 2. It included short-term aged rolling thin film oven (RTFO), and 20 hour pressure aging vessel (PAV) aging regimes as outlined in AASHTO M320. Furthermore, prolonged PAV aging was extended to include 40 and 60 hour durations to obtain additional oxidation levels.

The main objective of utilizing two aging protocols, forced-draft oven aging and accelerated aging was to evaluate the appropriateness of the much reduced time durations required for the aging practices established for the PG binder grading outline in AASHTO M320.

4.4 Aging Experiments

The aging experiments were conducted through two binder tests including dynamic shear rheometer (DSR) testing at multiple temperatures as well as Fourier Transform Infrared

(FT-IR) Spectroscopy. The test methodologies are vastly discussed in Chapter 3. A brief explanation regarding the test conditions are summarized in the following sections.

4.4.1 Binder Grading

As the primary step in the binder characterization, all the binder blends in the two aging methodologies were graded according to the established procedures for PG binder grading AASHTO M320, standard specification for performance graded asphalt binder. Rather than the typical high, intermediate and low temperature continuous grades, an additional parameter, ΔTc, was also determined as the difference in the continuous PG grade of the binders based upon the respective limits of 300 MPa stiffness (S) and 0.30 m-value. The current version of the ΔT_c parameter subtracts the stiffness or S-controlled temperature from that of m-controlling temperature. Thus, a positive value of ΔT_c indicates a grade that is stiffness controlled, while a negative value represents an m-controlled condition.

4.4.2 Dynamic Shear Rheometer (DSR) Frequency Sweep Test

The DSR test was conducted on each specific binder samples after aging at corresponding temperature and duration. In general, each binder sample was tested at three different temperature ranges including high, intermediate and low noting that high temperature testing range varied through the different base binders. Table 4. 3 represents a summary of the test conditions applied to each respective binder blend during the DSR measurements.

4.4.3 Fourier Transform Infrared (FT-IR) Spectroscopy

The chemical characterization of the binder composition was identified through the identification of certain functional groups investigated through FT-IR measurements using

an attenuated total reflectance (ATR) attachment as detailed elsewhere (Woo et al., 2008; Alavi, 2014) for each specific binder as a function of aging temperature and duration. A minimum of three replicate FT-IR spectra measurements were used to determine the average carbonyl areas (CA), which is an indicator of oxygen absorption into the binder by quantifying the growth of the carbonyl functional groups. The value of CA was determined by considering a baseline defined as the absorption level at 1,820 and 1,524 cm^{-1}. This value of CA was determined as the area in arbitrary units, integrated between the average absorption spectra and the determined baseline from 1,650 to 1,820 cm^{-1}. Detailed information regarding the FT-IR measurements has been descripted in Chapter 3.

Table 4. 3. Dynamic Shear Conditions

Binder ID	DSR Temperatures (°C)				
	High Temperature Range (°C)			Intermediate Temperature Range (°C)	Low Temperature Range (°C)
	60-64-70	60-70-80	85-95-100	46-34-22	15-10-4
Base (64-22)	X			X	X
Base w/T1 @ TX FLD (64-22 / 2.65%)	X			X	X
Recycled w/T1 @ TX FLD (64-22 / 2.65% / 0.25 TX RAP, 0.25 TX MWAS)	X			X	X
Base (64-28)		X		X	X
Base w/T1 @ TX FLD (64-28 / 2.65%)		X		X	X
Base w/A1 (64-28 / 6%)	X			X	X
Recycled w/T1 @ OPT (64-28 / 12.5% / 0.25 TX RAP, 0.25 TX TOAS)	X			X	X
Recycled w/A1 @ OPT (64-28 / 6% / 0.40 TX RAP)	X			X	X
Base (64-28P)			X	X	X
Base w/T1 @ TX FLD (64-28P / 2.65%)			X	X	X
Recycled w/T1 @ OPT (64-28P / 11% / 0.25 TX RAP, 0.25 TX TOAS)			X	X	X

4.5 Summary of Binder Laboratory Testing

Figure 4. 1 depicts an abbreviated demonstration of the binder aging method and testing in this study. Starting from the top, the recycled binders were obtained through extraction and recovery from the determined recycled materials at Texas A&M University. The aging process started at the University of Nevada, Reno upon receiving the recycled binders by blending them with the corresponding base binders according to the matrix shown in Table 4. 2. The binder blends evaluation then continued to the oven aging in each respective temperatures and durations described in Table 4. 2. At last, the aged binders were taken out of the ovens at each specific duration and subjected to FT-IR and rheological measurements. Results are discussed in detail in Chapter 5.

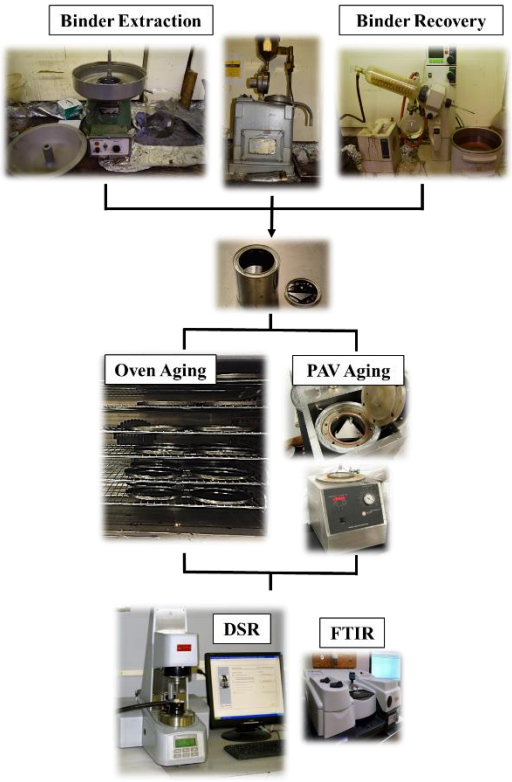

Figure 4. 1 Flowchart of Binder Ag

CHAPTER 5 AGING TEST RESULTS AND DATA ANALYSIS

The test methodologies of Chapter 3 have been applied to the materials defined in Chapter 4 through the described experimental plan in Chapter 4. The main objective of this chapter is to present the aging characteristics of the various pre-determined binder blends and, as a result, provide an evaluation of the impact of the recycled materials and recycling agents utilized in this study.

The pre-defined binder blends were exposed to forced-draft oven aging and PAV aging protocols with multiple temperatures and durations completed through the two experiments. First, the Fourier-transform infrared (FT-IR) spectroscopy data is used to stablish the level of the oxidation within each binder at a specific aging time and temperature; second, the dynamic shear rheometer (DSR) presented the binder samples rheological frequency sweep measurements to develop the dynamic shear modulus (G*) master curves and rheological parameters. Ultimately, the results of the first and second steps were combined establishing the hardening susceptibility (HS) of the binder blends. The two methods of laboratory aging, i.e. forced draft oven aging and PAV aging, have been compared at the end to investigate the potential difference between these aging methods outcomes.

5.1 Forced Draft Oven Aging

This section discusses the results of the forced-draft oven aging for the various binder blends with respect to the FT-IR and DSR measurements. Three different base binders from TX, NH and NV were blended with various recycled materials and/or recycling agents

proceeding with aging over multiple temperatures and durations. After the corresponding aging time, the binder samples were subjected to FT-IR and DSR tests to measure the oxidation level and kinetic parameters, respectively. Table 5. 1 shows the summary of the forced-draft oven aging experimental plan that has been previously described in Chapter 4.

5.1.1 Oxidation Kinetics

The oxidation levels of the binder blends were quantified through the determination of the carbonyl area (CA) from the FT-IR measurements. According to the experimental plan described in Chapter 4, all the binder samples at their respective aging temperatures and durations were tested using the Nicolet 6700 infrared spectrometer supplied by Thermo Fisher Scientific Inc. at the University of Nevada, Reno. For the sake of accuracy, a minimum of three replicates were measured for each binder sample to provide at least two close measurements. The value of CA was determined by considering a baseline defined as the absorption level at 1,820 and 1,524 cm^{-1}. This value of CA was determined as the area in arbitrary units, integrated between the average absorption spectra and the determined baseline from 1,650 to 1,820 cm^{-1}. The procedure then continued with averaging at least two of the closest measurements within each sample and utilizing the result number into the oxidation models that have been described previously in Chapter 3. The CA raw data measurement for each specific binder sample is presented in Appendix B.

Table 5. 1. Binder Blend Utilized in Forced Draft Aging

Binder ID		Forced-draft Oven Aging (day)		
		Temperature (°C)		
		60	**85**	**100**
TX	Base (64-22)	1, 4, 8, 15, 30, 60, 100, 120, 160	0.5, 1, 4, 8, 15, 25, 40	0.083, 0.25, 0.5, 1, 4, 8, 15
	Base w/T1 @ TX FLD (64-22 / 2.65%)			
	Recycled w/T1 @ TX FLD (64-22 / 2.65% / 0.25 TX RAP, 0.25 TX MWAS)			
NH	Base (64-28)	1, 4, 8, 15, 30, 60, 100	1, 4, 8, 15, 25, 40	0.083, 0.25, 1, 4, 8, 15
	Base w/T1 @ TX FLD (64-28 / 2.65%)			
	Base w/A1 (64-28 / 6%)			
	Recycled w/T1 @ OPT (64-28 / 12.5% / 0.25 TX RAP, 0.25 TX TOAS)			
	Recycled w/A1 @ OPT (64-28 / 6% / 0.40 TX RAP)			
NV	Base (64-28P)	4, 8, 15, 30, 60, 100	1, 4, 8, 15, 25, 40	0.083, 0.25, 1, 4, 8, 15
	Base w/T1 @ TX FLD (64-28P / 2.65%)			
	Recycled w/T1 @ OPT (64-28P / 11% / 0.25 TX RAP, 0.25 TX TOAS)			

In this study, the main focus of the FT-IR measurements was on the growth of the CA measures rather than considering the individual measurement outright. The carbonyl growth, CAg, is represented as the difference between the measured CA at a given aging condition and the original CA measurement of the asphalt binder otherwise known as CA_{Tank}. The justification of this modification is to provide a comparison mode among the various binder blends containing different components. The addition of the highly oxidized binders in the recycled materials greatly increased the CA of the corresponding recycled

binder blend compared to the base binder. As shown is Figure 5. 1. a, a significant rise in the CA measurements can be observed due to the addition of 0.5 RBR along with T1 to the 64-28P base binder. However, normalizing the CA measurements with respect to the CA_{Tank} permits the capture of the effect of aging within each binder blend without involving the initial effect of the additive components, namely the recycled materials. The normalized aging paths in 85°C aging temperature for the two aforementioned binder blends is represented in Figure 5. 1. b.

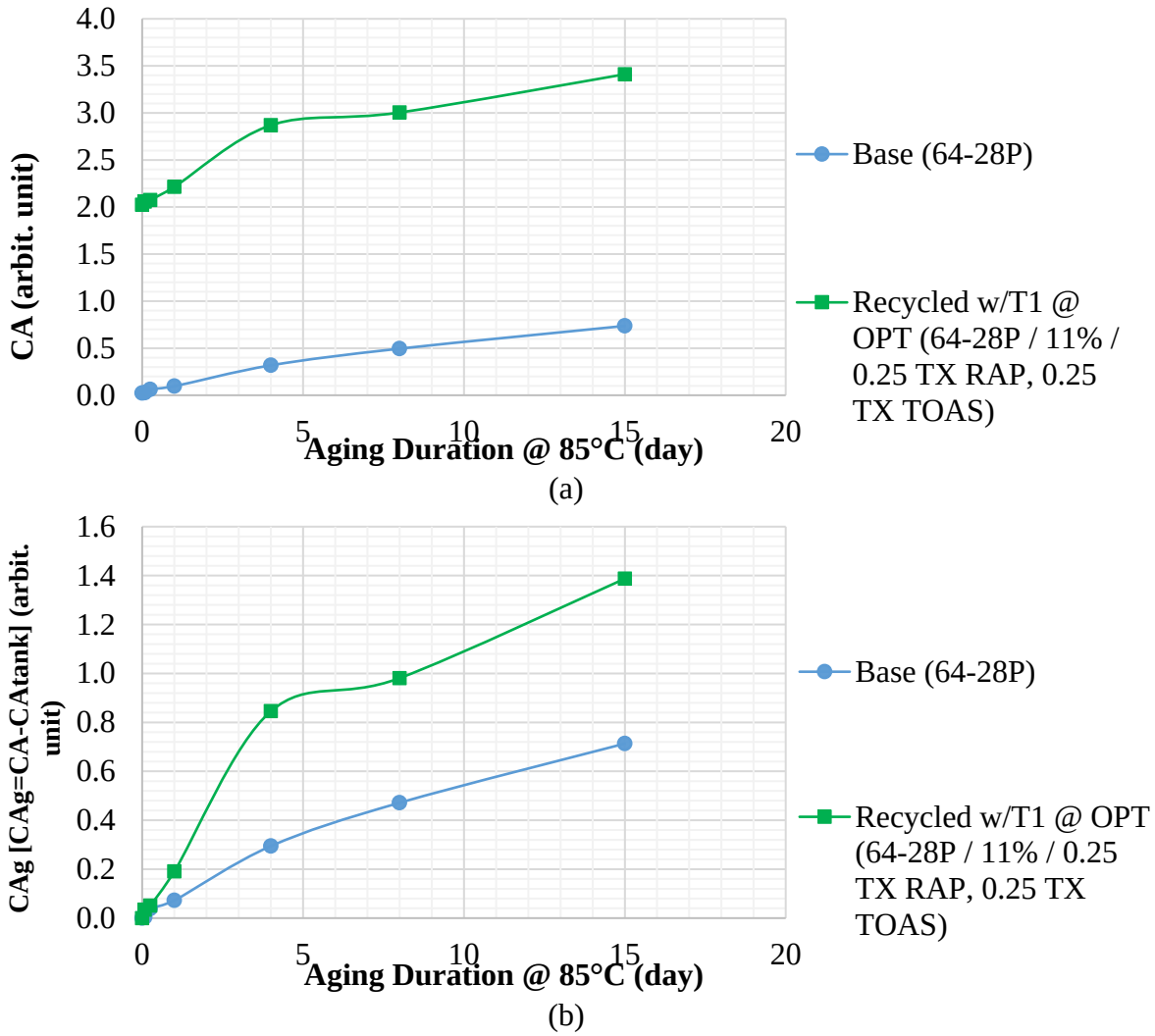

Figure 5. 1. Aging Path in Comparison in 64-28P Base Binder Blends (a) Based on CA (b) Based on CAg

The primary step for evaluating oxidation rate is through FT-IR measurements of carbonyl formation at each aging temperature over the respective series of durations. The oxidation model parameters were then determined by fitting these plots at each oxidation temperature to the kinetic model presented by Equation 5.1.

$$\mathbf{CA_g = M * \left(1 - e^{-k_f t}\right) + k_c t} \qquad \textbf{Equation 5. 3}$$

where,

CAg: carbonyl area growth ($CA-CA_0$);

CA: carbonyl area;

CA_0: original or tank CA measurement;

M: initial jump, magnitude of fast rate reaction in terms of CAg;

k_f: fast rate of CA growth;

k_c: slow or constant rate of CA growth;

t: time, days.

Figure 5. 2 through Figure 5. 4 show example plots of the PG 64-22 base binder blends. In these plots, the CAg measurements and predicted curves resulted from the kinetic prediction model are indicated by single symbol and dashed lines, respectively. The CAg is highly dependent upon the aging temperature with separate fast and constant oxidation rates is observed within each temperature path. Similar plots for other binder blends are provided in Appendix B.

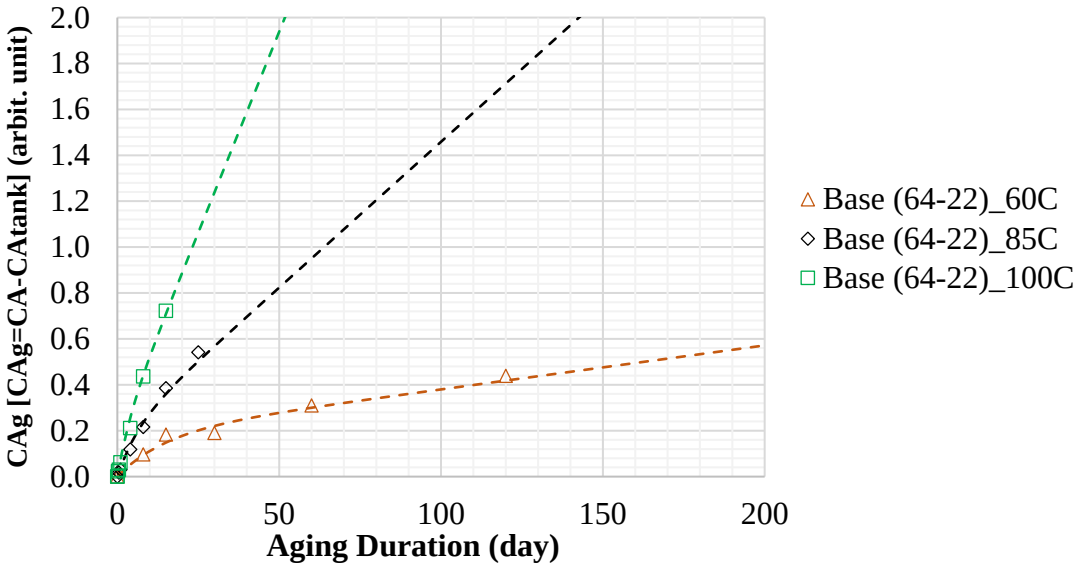

Figure 5. 2. Oxidation of Base PG 64-22 after 60, 85, and 100°C Oven Aging

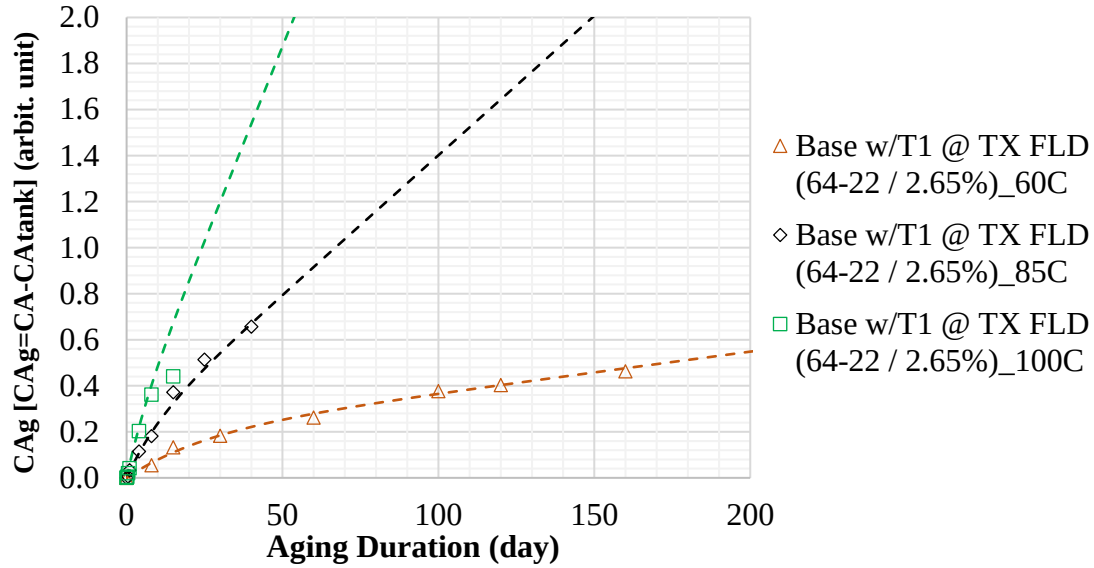

Figure 5. 3. Oxidation of Base PG 64-22 w/T1 @ TX FLD after 60, 85, and 100°C Oven Aging

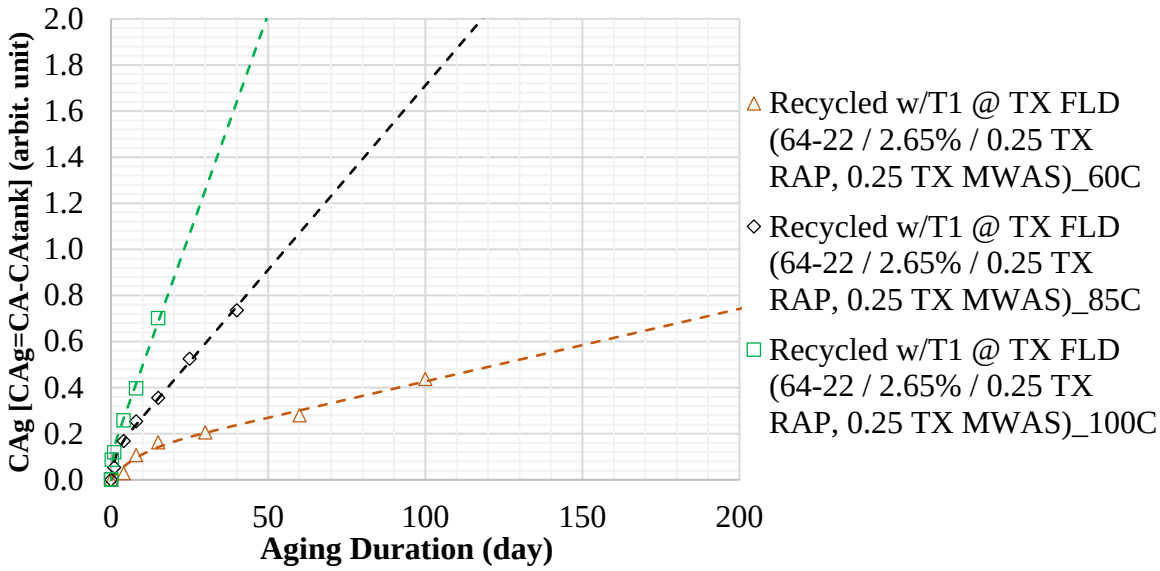

Figure 5. 4. Oxidation of Recycled w/T1 @ TX FLD (Base 64-22) after 60, 85, and 100°C Oven Aging

Additionally, as observed the duration of the fast rate is getting much shorter than the constant rate as the temperature increases; this phenomenon is consistent with the chemistry principle-Arrhenius Reaction Function previously discussed in Chapter 3 and Equation 5.2. The oxidation kinetics parameters are the fast and constant oxidation rates, k_f and k_c, respectively, and are commonly represented by the Arrhenius relationship as a function of the inverse of the aging temperature and the gas constant R, as shown below:

$$\mathbf{r_{CA} = AP^{\alpha} e^{-E_a/RT}} \qquad \textbf{Equation 5. 4}$$

Where,

r_{CA}: rate of carbonyl area growth (CAg), either k_f or k_c;

A: pre-exponential factor;

P: absolute oxygen pressure during oxidation, atm;

α: reaction order with respect to oxidation pressure;

E_a: activation energy, kJ/mol;

R: ideal gas constant, 8.3144621 L/mol.°K;

T: temperature, °K

Considering this study was conducted in Reno, the value of α and P were selected as 0.27 and 0.164 (atm), respectively. The focus of the current study will be based upon the oxidation rates (k_c and k_f) as a function of the inverse of the aging temperature multiplied by the gas constant R, 1/RT, as represented in Figure 5. 5 through Figure 5. 7. These parameters can be considered as a direct indication of the rate of the long-term oxidation rate, e.g. units of CAg/day. Obviously, the higher the temperature the lower the 1/RT value. The AP^{α} and E_a terms from Equation 5.2 for the oxidation rates, both kf and kc, were fitted in Equation 5.1 and determined through a solver function in Excel software.

Detailed comparisons regarding the influences of addition of recycled material and/or RAs within each base binder blends are made in this section; it will be followed by an overall comparison through the summary table of the kinetic parameter values presented in Table 5. 2 for all the binder blends used in this study.

Observations of Figure 5. 5. a indicated that the addition of T1 to the 64-22 base binder did not change the rate of oxidation noticeably at each of the respective aging temperatures, i.e., 60, 85, and 100°C corresponding to the 1/RT values of 0.36, 0.34 and 0.32, respectively. However, the addition of 0.50 RBR of recycled material including 0.25 RAP and 0.25 MWAS along with 2.65% of T1 to the blend of base 64-22 and T1 RA increased the constant rate of oxidation to a higher value. It should be noted that the 2.65% is not the optimum dosage of the discussed binder blend; the optimum dosage refers to a dosage that is able to restore the recycled binder blend PG grades to those of the base binder. In addition,

the temperature dependency of the recycled blend, i.e., the slope of the oxidation rate versus 1/RT known as E_{af} or activation energy, was found to be lower than the other two binders.

Similar comparisons can be also made for the fast oxidation rate, k_f, within the various base binder blends. As shown in Figure 5. 5. b the addition of the T1 to the 64-22 base binder slightly reduced the value of the k_f over the aging temperature range; however, no change in the temperature susceptibility, or the slope, was observed. In contrast, the recycled blend indicated a significant increase in both of the oxidation rates magnitude and temperature susceptibility compared to the other binder blends.

The aforementioned variations in oxidation rates magnitudes and temperature susceptibilities are summarized in Table 5. 2. In overall, not a constant trend was captured among all the kinetic parameters by the addition of the recycled materials or/and T1 RA except a pronounced increase in the oxidation rate values, k_f and k_c, due to the addition of the 0.50 RBR recycled material along with 2.65% of T1.

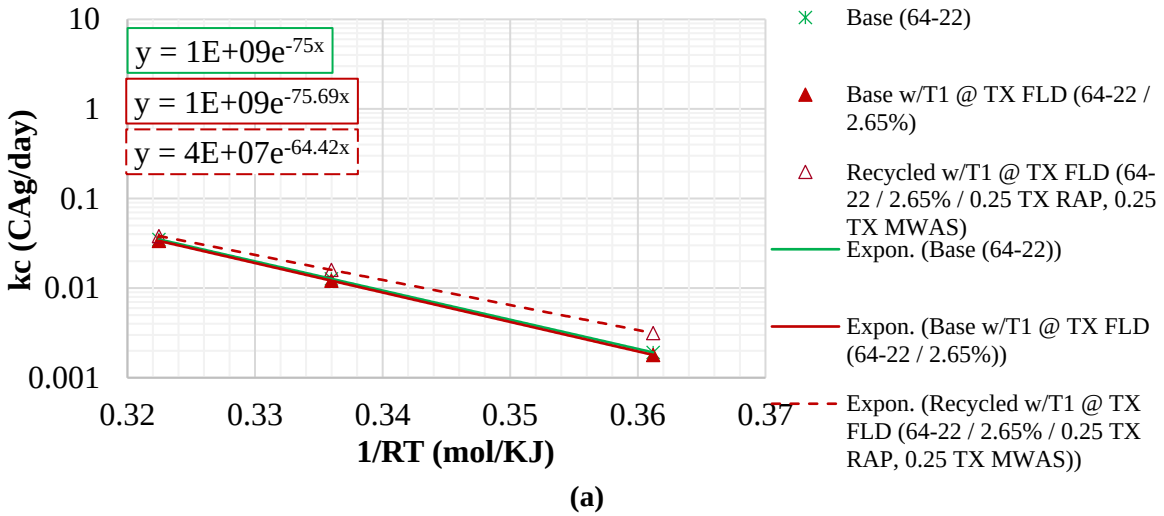

(a)

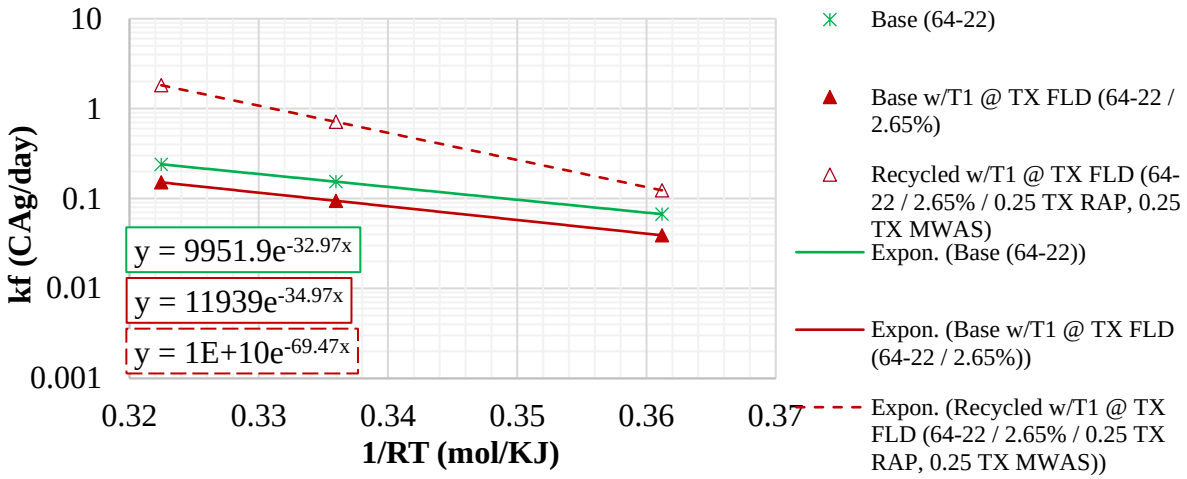

(b)

Figure 5. 5. Oxidation Kinetic rates for 64-22 Base Binder Blends

(a) Fast Rate, (b) Constant Rate

Figure 5. 6. a represents the constant rate oxidation measures of the five binder blends containing the 64-28 base binder. At the first glance, all the binder blends, except the recycled blend with T1, show analogous trends in terms of the constant rate oxidation with a slight change in temperature dependency (especially in the recycled blend with A1). Similar to previous observations in 64-22 recycled binder blend, the recycled blend, containing 0.25 RAP, 0.25 TOAS binder ratio and T1 at 12.5, seems to have a relatively different value of kc compared to the base binder. However, contrary to the 64-22 recycled blend, here the magnitude of the kc of the recycled blend with T1 was lower than that of the base binder. It should be noted that the recycled blend with T1 had the optimum dosage rate (i.e., 12.5%) which is significantly higher than the field dosage rate of 2.65% that was used with the 64-22 base binder blends. Additionally, the constant oxidation rate of the recycled blend with A1, containing 0.4 RBR of RAP materials, did not show significant

changes relative to the base binder with and without A1 although having the optimum dosage rate (i.e. 6%).

In the same way, Figure 5. 6. b shows the fast oxidation rate of the 64-28 base binder blends. It is observed that the magnitude of the k_f did not change significantly for the blends free of the recycled materials; on the other hand, the one containing the 0.40 RBR of RAP materials and A1 at optimum dosages of 6% indicated an obvious reduction in the fast rate values compared to the base binder and the blend with A1 only. This reduction was further pronounced with the addition of both RAP and TOAS materials as a total of 0.5 RBR and 12.5% of T1 which is the optimum dosage.

It is noteworthy to mention that the addition of either recycled materials or RAs at the corresponding RBRs and dosages, respectively, did increase the temperature susceptibility of the blends compared to the 64-28 base binder in both constant and fast oxidation rates. The recycled blend with A1 and the recycled blend with T1 had the highest temperature susceptibilities among all the 64-28 binder blends in constant and fast rates, respectively. Summary of the kinetic parameter are presented in Table 5. 2.

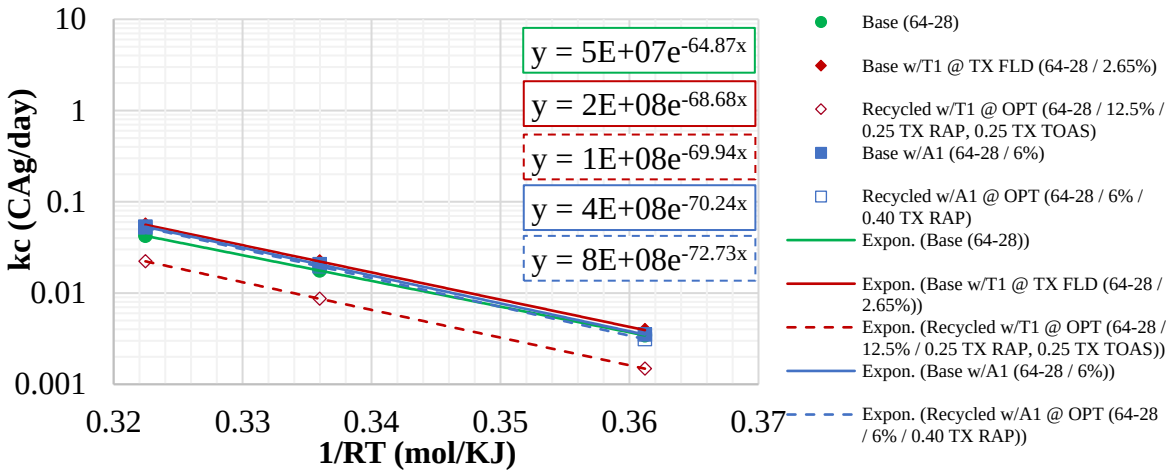

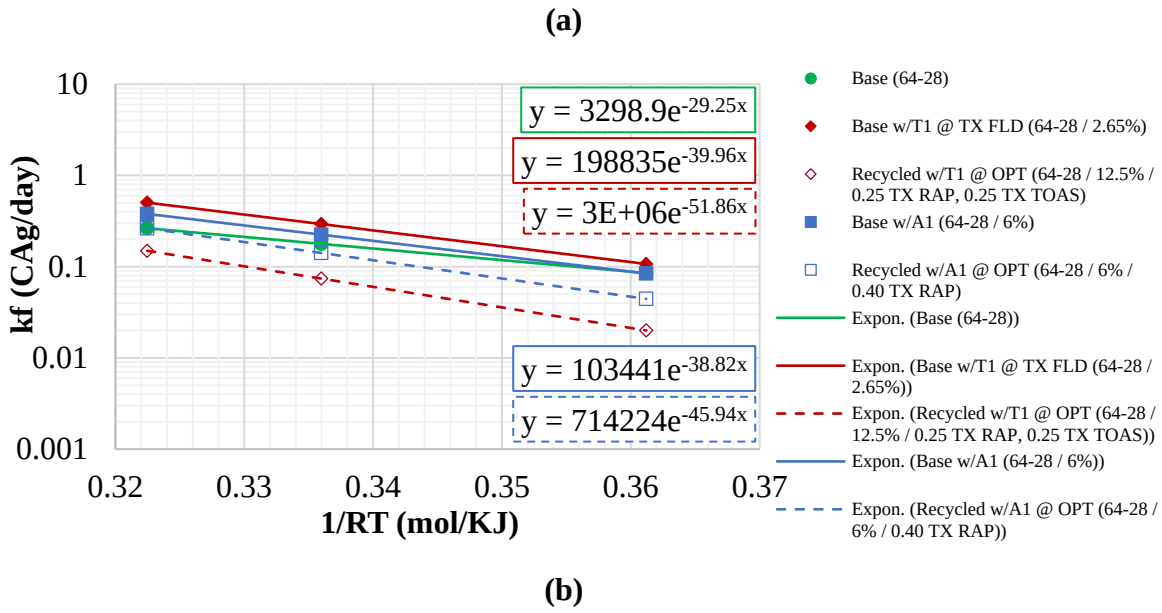

Figure 5. 6. Oxidation Kinetic rates for 64-28 Base Binder Blends (a) Fast Rate, (b) Constant Rate

Observations of the 64-28P binder blends presented in Figure 5. 7. a indicates that the addition of the T1 at the field dosage rate (i.e., 2.65%) to the NV polymer-modified binder, i.e. 64-28P, led to a modest reduction in the rate of oxidation at each of the respective aging temperatures. Figure 5. 7. a also demonstrates the decreased rate of oxidation for the recycled blend with T1 at optimum dosage compared to the base binder, but the blend with only T1 at the smaller field dosage was quite similar to that of this recycled blend. It is also noted that the temperature dependency of the aging rates, i.e., the Ea or exponential term, are slightly different from each other in this data set. Specific to the constant-rate reactions, the base binder with recycled and T1 provides the highest slope or Ea, followed by the base with only T1 and then the base binder.

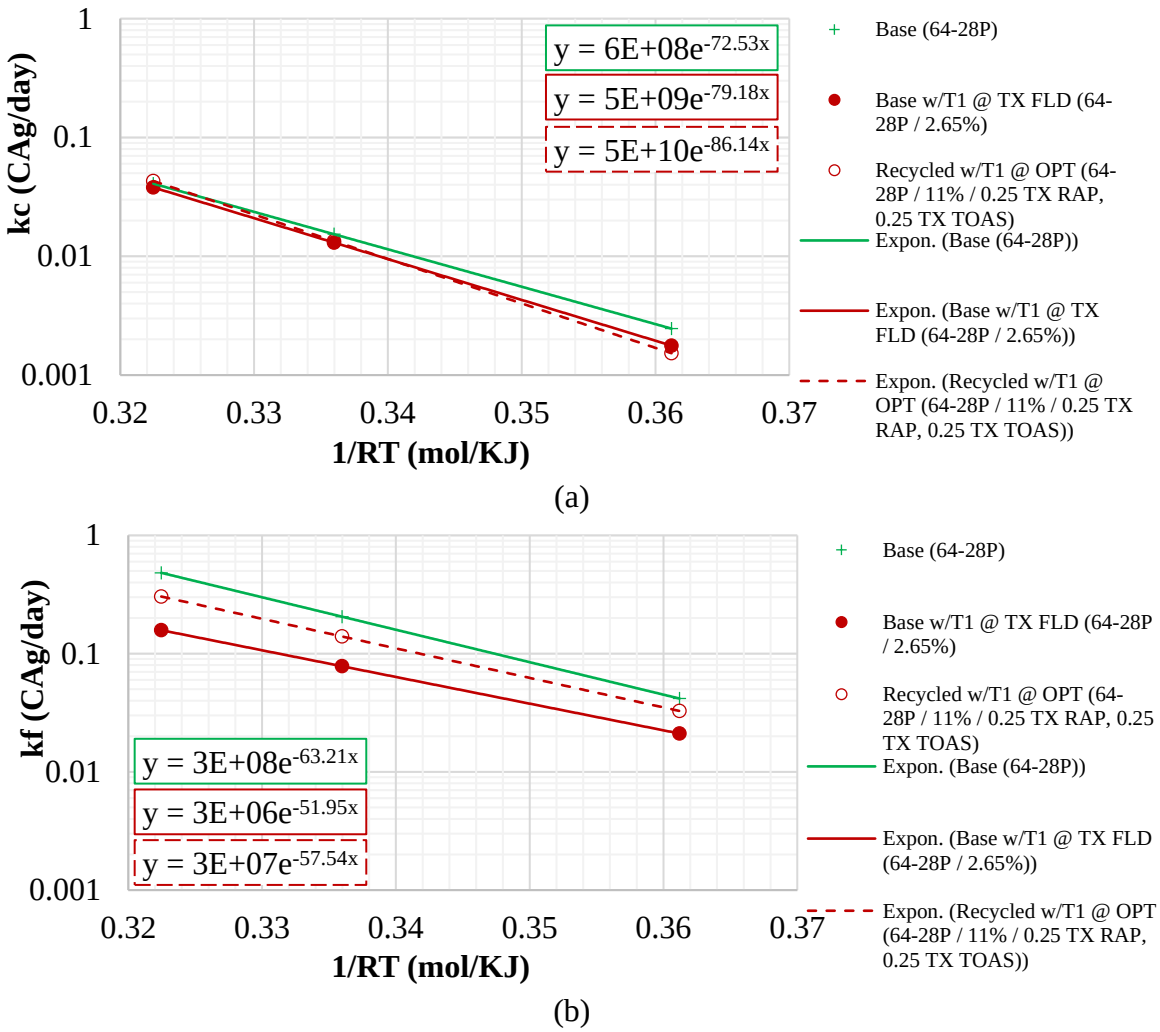

Figure 5. 7. Oxidation Kinetic rates for 64-28P Base Binder Blends (a) Fast Rate, (b) Constant Rate

For the sake of clarity, the kinetic parameters for all the binder blend are summarized in Table 5. 2. General observations from Table 5. 2 are provided in the following:

- The addition of T1 in 2.65% dosage to the base binder did not follow a specific trend in any of the kinetic parameters. For 64-22 and 64-28P bases binders, the addition of T1 reduced the fast oxidation rate, kf, while the 64-28 base binder showed an increase in kf due to the addition of the T1. These observations were also supported by activation energy, E_a, which is an indication of temperature

susceptibility, and pre-exponential terms, especially in 64-28 and 64-28P base binders. Similar trend was also observed in the constant oxidation rate, kc; however, it should be noted that the difference in the kc terms between the base binder and T1 blend within all the three base binders was significantly lower in comparison with kf; it suggests that the T1 at 2.65% dosage was too low to be able to make a noticeable change in the long-term aging properties of the base binders; this conclusion is supported by considering the kinetic parameters in the Base w/A1 (64-28 / 6%) blend. The addition of the A1 to the 64-28 base binder at 6% dosage significantly increased the oxidation rates compared to the base binder and Base w/T1 blend. In other words, noting the higher dosage of A1, i.e. 6%, the difference in the long-term aging properties of the Base w/A1 blend compared to the base binder is relatively more substantial than the Base w/T1 blend.

- The base binder aging properties due to the addition of the recycled material was highly influenced by the RA dosages within each blend. In 64-22 base binder, the addition of 2.65 % of T1 was not apparently able to alleviate the recycled blend kinetic parameters to that of the base binder in either the fast nor constant oxidation rates. However, the 0.50 RBR, including 0.25 RASBR and 0.25 RASBR, recycled blends in 64-28 and 64-28P base binders containing T1 at optimum dosages showed a relatively lower oxidation rates compared to their base binders; it was also observed in the 0.40 RAPBR recycled blend of 64-28 base binder contain A1 at optimum dosage. These findings again highlight the importance and effect of the dosage selection on the binder aging behavior.

Table 5. 2. Summary of Fitted Relationships for Asphalt Binder Kinetics

	Binder Blend	Fast Oxidation Rate						Constant Oxidation Rate					
		E_a (kJol.mol^{-1}.°K^{-1})	Pre-exponential Factor, AP$^{\alpha}$	A[1]	kf Temperature (°C)			E_a (kJol.mol^{-1}.°K^{-1})	Pre-exponential Factor, AP$^{\alpha}$	A[1]	kc Temperature (°C)		
					60	85	100				60	85	100
TX	Base (64-22)	33	1.000E+04	1.629E+04	0.067	0.154	0.240	75	1.129E+09	1.840E+09	0.002	0.013	0.035
	Base w/T1 @ TX FLD (64-22 / 2.65%)	35	1.200E+04	1.955E+04	0.039	0.094	0.151	76	1.357E+09	2.211E+09	0.002	0.012	0.034
	Recycled w/T1 @ TX FLD (64-22 / 2.65% / 0.25 TX RAP, 0.25 TX MWAS)	70	9.859E+09	1.606E+10	0.123	0.712	1.820	64	4.049E+07	6.597E+07	0.003	0.016	0.038
NH	Base (64-28)	29	3.313E+03	5.398E+03	0.085	0.178	0.264	65	5.189E+07	8.454E+07	0.003	0.018	0.042
	Base w/T1 @ TX FLD (64-28 / 2.65%)	40	2.000E+05	3.259E+05	0.107	0.293	0.503	69	2.354E+08	3.836E+08	0.004	0.022	0.056
	Recycled w/T1 @ OPT (64-28 / 12.5% / 0.25 TX RAP, 0.25 TX TOAS)	52	2.748E+06	4.477E+06	0.020	0.074	0.149	70	1.400E+08	2.281E+08	0.001	0.009	0.022
	Base w/A1 (64-28 / 6%)	39	1.040E+05	1.695E+05	0.084	0.224	0.379	70	3.700E+08	6.028E+08	0.004	0.021	0.053
	Recycled w/A1 @ OPT (64-28 / 6% / 0.40 TX RAP)	46	7.190E+05	1.172E+06	0.044	0.141	0.263	73	8.101E+08	1.320E+09	0.003	0.020	0.052
NV	Base (64-28P)	63	3.464E+08	5.644E+08	0.042	0.205	0.482	73	5.931E+08	9.663E+08	0.002	0.015	0.041
	Base w/T1 @ TX FLD (64-28P / 2.65%)	52	3.000E+06	4.888E+06	0.021	0.078	0.158	79	4.709E+09	7.672E+09	0.002	0.013	0.038
	Recycled w/T1 @ OPT (64-28P / 11% / 0.25 TX RAP, 0.25 TX TOAS)	58	3.498E+07	5.700E+07	0.033	0.140	0.304	86	5.045E+10	8.219E+10	0.002	0.013	0.043

[1]Noting that in these studies, α=0.27 and P = 0.164 atm in Reno, A is founded specifically.

Additional investigations were conducted exploring the relationship between the kinetic parameters of the binder blends in fast and constant oxidation rate. As a result, Figure 5. 8 and Figure 5. 9 demonstrate a comparison between the pre-exponential factor and the calculated activation energies between all the investigated binder blends. General observation shows the change in magnitude from 10^7 to 10^{11} and for the constant oxidation rate which was reduced into 103 to 1010 for the fast oxidation rate. A much reduced but similar order of magnitude from 60 to 90 and 30 to 80 were also depicted in the activation energy for the constant and fast oxidation rates, respectively. These similar trends suggest a relationship between the pre-exponential term and activation energy as plotted in Figure 5. 10. The existence of the relationship between kinetic parameters was previously observed by Glover and Cui (2013) and Morian (2014).

Therefore, the plot of the pre-exponential factor versus the activation energy from the constant oxidation rate parameters is prepared in Figure 5. 10. The linear trend line equation in the logarithmic scale of the pre-exponential factor suggests similar values to what had been observed by Glover and Gui (2013) and Morian (2014). As stated by Morian (2014) regarding the Glover and Gui research, “in fact, their reported data which spanned over a 17-year time period, 1996 through 2013, reported nearly the same relationship with a pre-exponential factor of 0.0266 and the exponent of 0.3347”. Table 5. 3 represents the constant oxidation kinetic parameters relationship, i.e. pre-exponential factor as function of activation energy, reported by other researchers along with the one determined in the current study. It should be noted that the definition of the CA calculation method implemented by aforementioned researches is slightly different from the current study. That might be responsible for the difference between the values presented in Table 5. 3.

Table 5. 3. Trend line Components in the Constant Rate Kinetic Relationship

Researcher(s)	Pre-exponential Factor	Exponent
Glover and Gui (2013)	0.0266	0.3347
Morian (2014)	0.0204	0.3392
Current Study	0.0455	0.3206

Although currently, no practical methodology exists for using this relationship, these findings might be a starting point for modification in the oxidation rate calculation equations, as Morian (2014) recommended. Currently, the constant rate pre-exponential factor and activation energy are calculated simultaneously using the solver tool in Excel software. Further investigations are required to evaluate the possibility of the modifying the calculation methodology, as Morian endorsed "to determine the activation energy term from some other evaluation tool, maybe some correlation with Arrhenius shift factors may provide additional information, but at this point in the overall research effort, such relationships have not been developed or thoroughly analyzed".

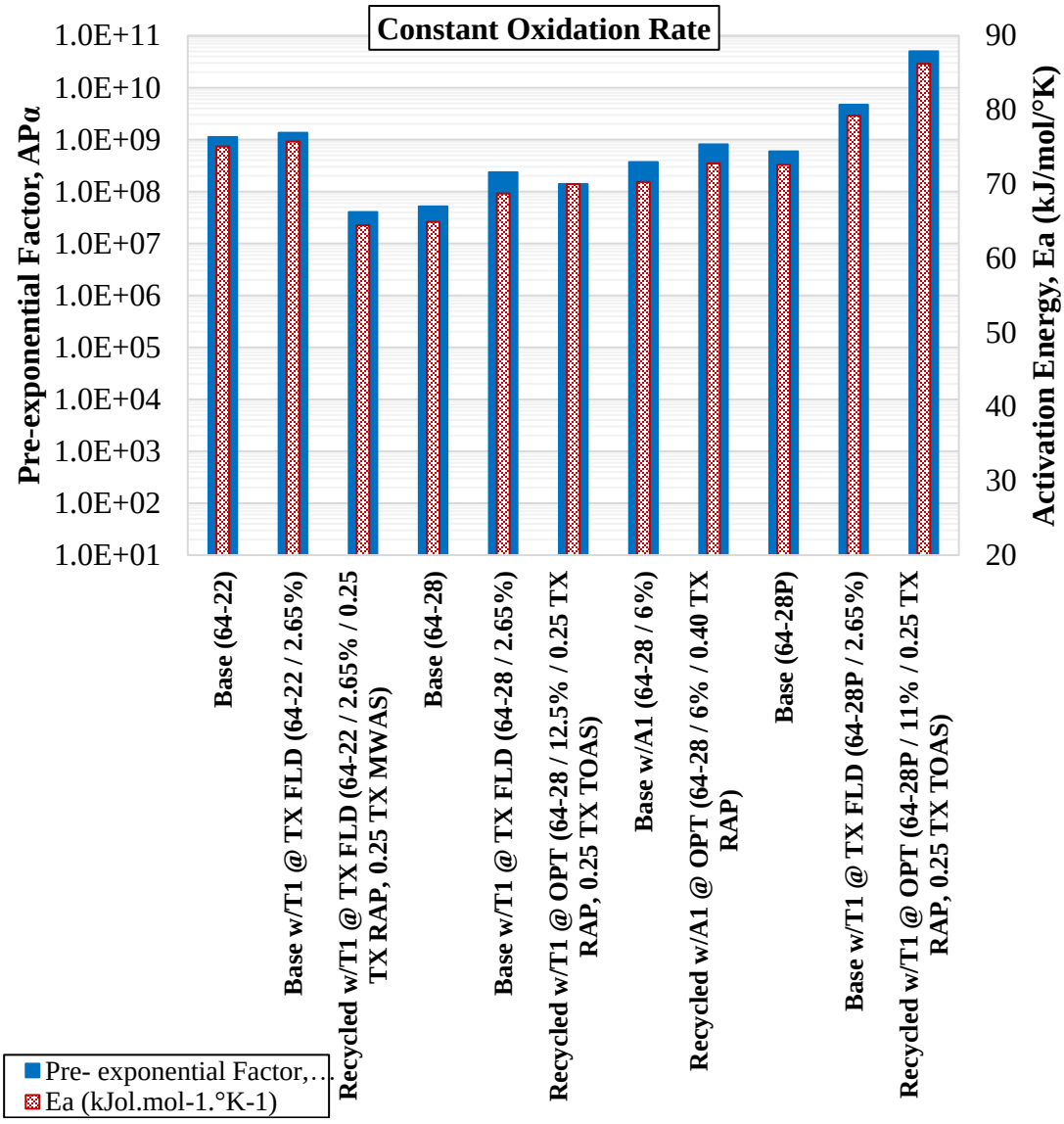

Figure 5. 8. Constant Rate Binder Kinetic Parameters

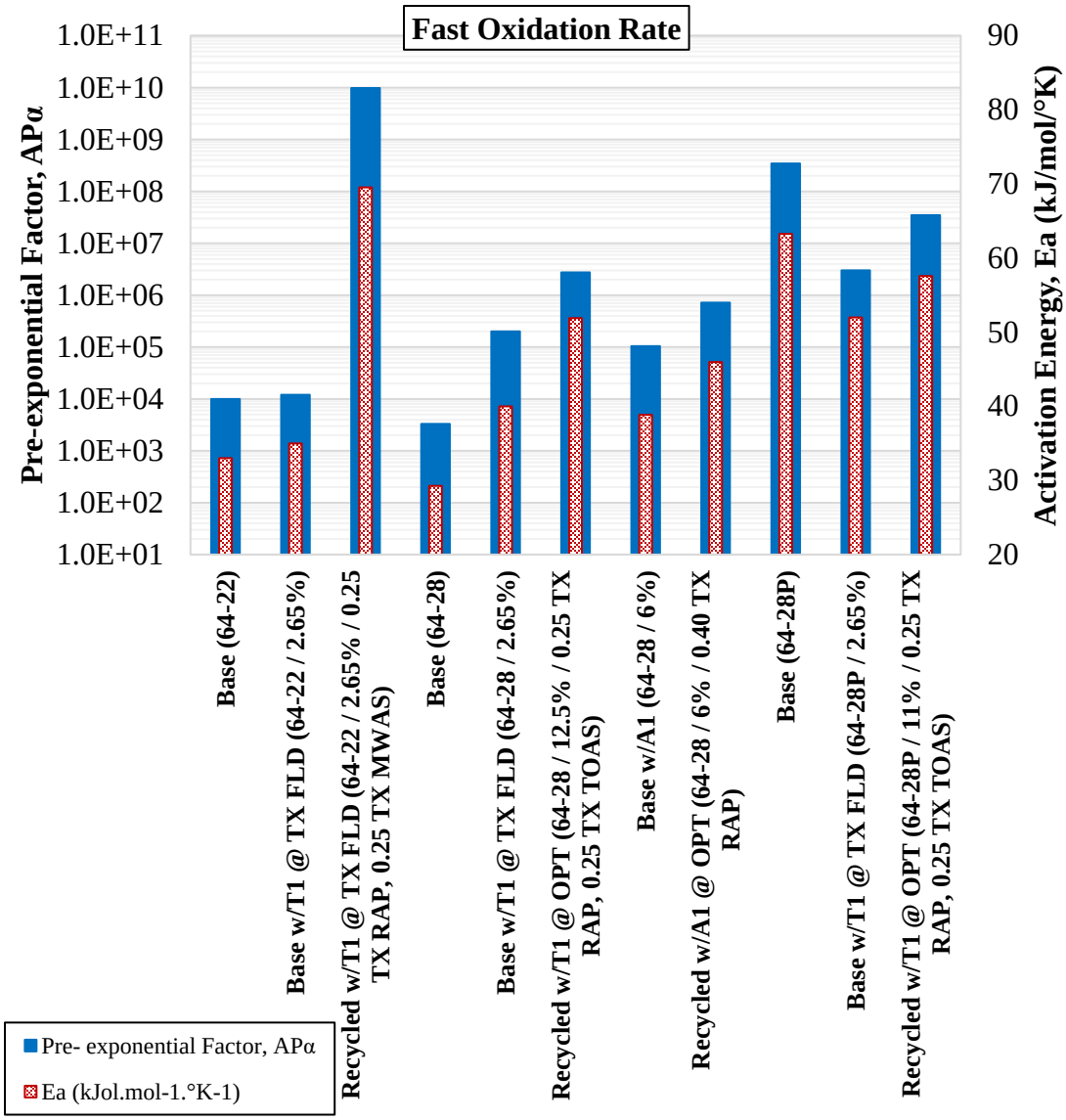

Figure 5. 9. Fast Rate Binder Kinetic Parameters

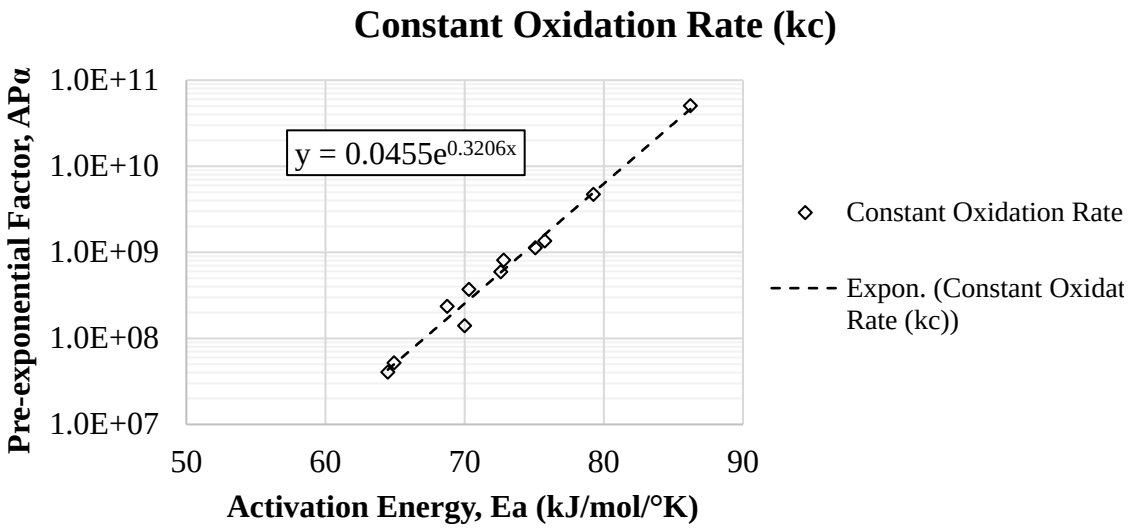

Figure 5. 10. Constant Rate Binder Kinetics Relationship for All the Binder Blends

5.1.2 Black Space Diagram

Additional analysis of the effects of oxidation on rheology has been completed at each of the respective aging temperatures and durations through DSR measurements and determination of the full dynamic shear modulus (G*) master curve as defined in Chapter 3. Figure 5. 11 through Figure 5. 13 present the Black Space diagram of all the binder blends within each base binder in the experimental plan described in Chapter 4. Black Space diagram, a plot of shear modulus (G*) as a function of phase angle (δ), indicates that with aging the binder blends progress from the lower right hand corner of the diagram toward the upper left corner; in other words, an increase in stiffness (G*) and a loss of phase angle (δ) that indicates the loss of flexibility and increased brittleness. It should be noted that the measurements of the binders considered are specific to the testing conditions of 0.005 rad/s at 15°C to maintain consistency with the original DSRFn traditionally reported. However, some modifications to the black space effective temperature has been

recently suggested to make the results more binder specific; detailed information regarding the original DSRFn and the corresponding modifications are provided in Figure 5. 1. Furthermore, the Glover-Rowe (G-R) parameter at the established limit of 180 and modified limit of 600 kPa are presented in the Black Space diagrams parallels to the 5 and 3 cm ductility, indicating onset and significant cracking limits, respectively. Detailed information regarding the effects of RAs and recycled materials within each of the binder blends in this study are provided in the following.

Initial observations of the Black Space diagram Figure 5. 11 through Figure 5. 13 indicate the expected outcome. The younger or lesser aged binders initially starting in the lower right corner of the diagram and progress toward the upper left corner with increased aging. This migration across the plots indicate the loss of flexibility and increased brittleness in the binder blends. The overall aging characteristics seem to be predominantly influenced by the base binder.

For the PG 64-22 base binder, Figure 5. 11. a and b, there is a distinct increase in the flexibility noted by the addition of either T1 to the base binder, as depicted by the substantial shift to the lower right corner of the Black Space diagram. Besides, the addition of the recycled materials also indicated a substantial reduction in the flexibility noting both an increase in stiffness (G*) and a reduction in δ for a given oxidation state despite the addition of RA. This loss in ductility extends past that of each respective base binder for the lesser aged conditions. This finding suggests differences in the aging rate of the blended materials, at least so far as the rheological properties of the Black space indicate.

In addition, considering the different blends of the PG 64-22 base binder indicated fairly similar paths in the base binder with and without T1. However, this should not be misinterpreted to indicate that the aged properties or more specifically the rate of progression are the same with the blended materials. As previously mentioned, the range or distances travelled across the Black Space diagram are substantially different between the base and blended materials. While the addition of both the recycled material and RA, the path is slightly different from the base binder path. When the Black Space diagram is summarized without the data points in Figure 5. 11. b, the relationship between the blended materials becomes clearer: the addition of the RA to the base binder resulting in a slight reduction in the binder stiffness but also a shift to the right, or increased phase angle for a similar stiffness.

With all the aforementioned observations taken into account, the addition of the T1 at 2.65 % dosage along with the recycled materials in 0.50 RBR to the PG 64-22 base binder was not able to restore the binder blend properties. It was not unexpected since the 2.65% is not considered the optimum dosage for the recycled blend.

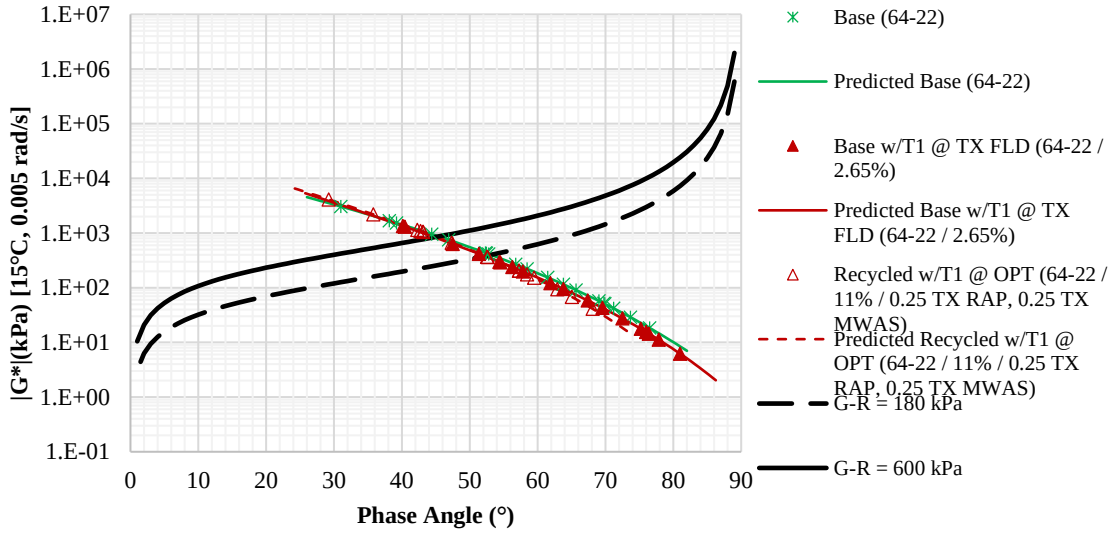

(a)

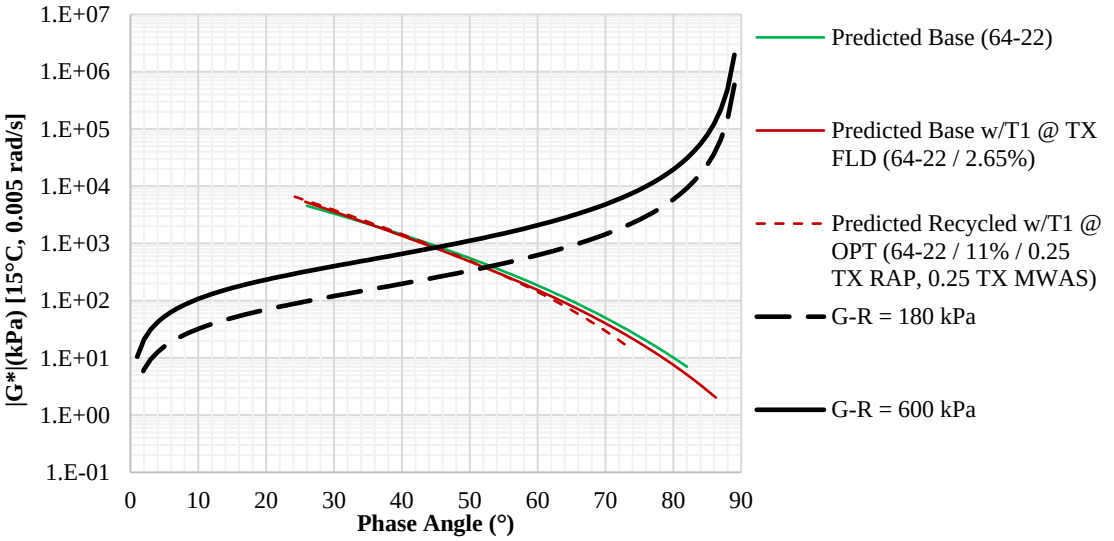

(b)

Figure 5. 11. Black Space of Glover-Rowe Parameter at 15°C for PG 64-22 Base Binder (a) Completed (b) Summarized

Conducting similar comparisons is PG 64-28 binder blends depicted in Figure 5. 12. a and b, there is some decrease in stiffness and increase in phase angle with the addition of T1 to the base binder, but the addition of recycled materials in the recycled blend that also includes T1 reversed this softening, and, also, significantly decreased the phase angle (δ) by at least 9° leading to increased brittleness. For the recycled blend, the path across the

Black Space diagram for the same aging temperatures and durations also extends further (along the x-axis) than that of the base binder or the base binder with T1, which is more obvious in the summarized Black Space diagram without the data points (Figure 5. 12. b). For this particular recycled blend, the high 0.5 TX RBR including 0.25 TX RASBR is likely causing the aging path to deviate from that of the base binder.

The 64-28 base binder with 6% of A1 has an overall likewise behavior to the blend with T1 only; a clear decrease in stiffness and increase in phase angle can be observed in the A1 blend compared to the base binder. However, the reduction in the stiffness is more pronounced in base w/A1 blend in comparison with the base w/T1 blend, which might be related to the relatively higher dosage of A1. Observations of the PG 64-28 recycled blend including 0.40 TX RBR and A1 at optimum dosage indicated a high decrease in the phase angle by at least 6° compared to the PG 64-28 base binder as well as an increase in the stiffness especially at the first levels of aging. However, the addition of either A1 or both A1 and 0.40 RBR to the base 64-28 binder were still observed to follow the base binder path.

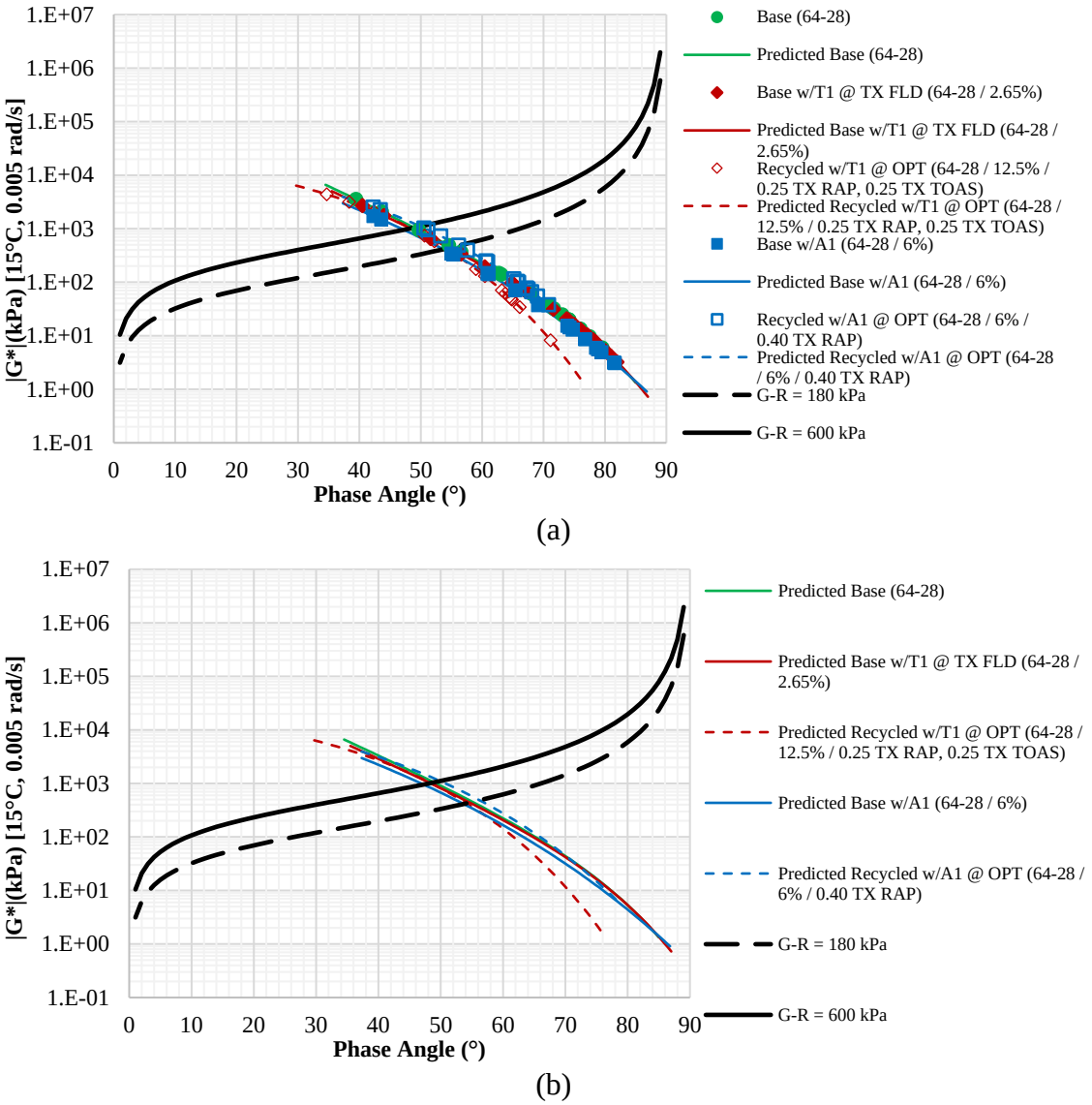

Figure 5. 12. Black Space of Glover-Rowe Parameter at 15°C for PG 64-28 Base Binder (a) Completed (b) Summarized

Figure 5. 13 demonstrates the aging path through the Black Space diagram for PG 64-28P binder blends. As previously observed with the other binder blends, all the PG 64-28P binder blends migrated from the lower right to the upper left of the diagram getting more brittle and stiff during the aging path. However, a distinct curvature is apparent within the PG 64-28P binder blends suggesting a kind of fast and constant aging paths in the Black

Space diagram, similar to the oxidation rates, i.e. k_f and k_c. The fast rate covers the initial aging durations in which a small increase in the phase angle value is accompanied by a significant increase the stiffness. While the same rise in the phase angle value in the constant rate area still stiffens the blend but not as much as the fast rate. However, further investigations including more binder blends are required to exactly determine the margin between the fast and constant rate.

Contrary to the previous observations, the addition of T1 did not significantly improve the phase angle in the PG 64-28P base binder. This might be related to the internal interaction happening between the polymer components of the PG 64-28P base binder with T1. Besides, the amount of T1, i.e. 2.65%, might be too low to change the aging behavior of the polymer modified PG 64-28P base binder. On the other hand, the PG64-28P binder blend containing both TX recycled material and T1 at a relatively high optimum dosage, decreased the phase angle by almost 5°C along with a relatively significant increase in the stiffness. Furthermore, the aging path can change significantly with the addition of TX TOAS to binder. In general agreement, the aging paths of the PG 64-28P base binder with and without T1 are similar. When the Black space diagram is summarized without the data points in Figure 5. 13, the relationship between the blended materials becomes clearer. For this particular blend, the high RBR (0.50) caused the recycled blend to deviate from the base binder path.

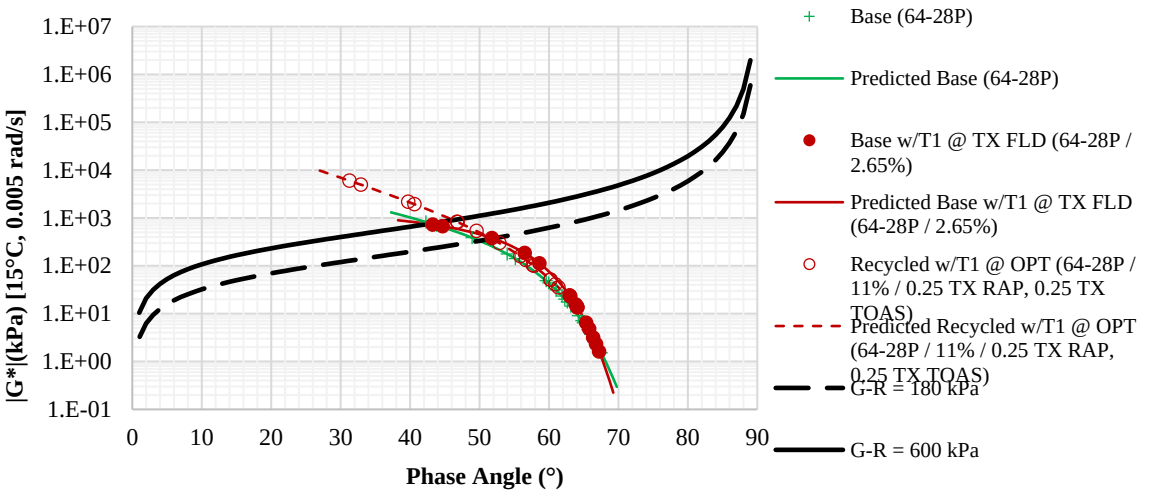

(a)

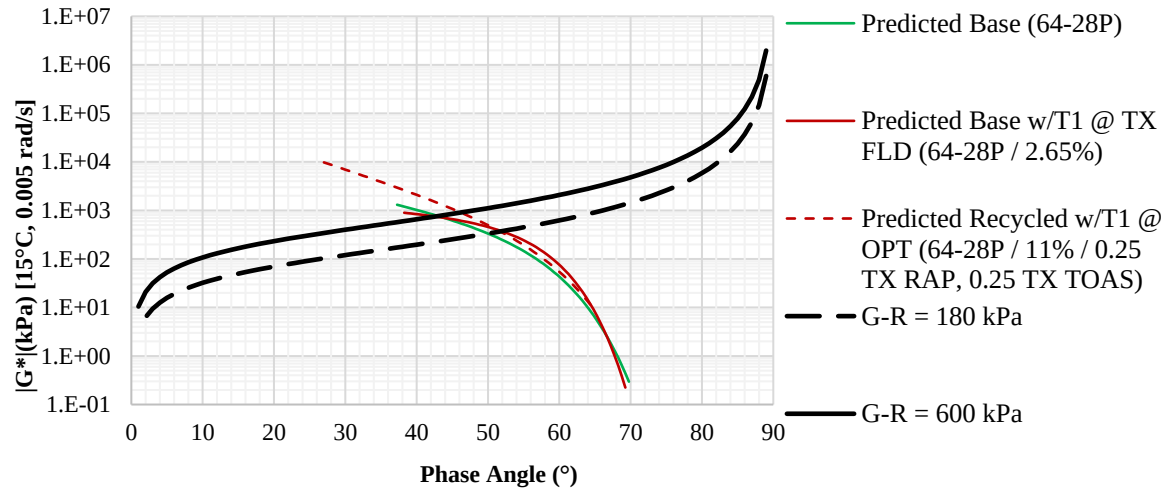

(b)

Figure 5. 13. Black Space of Glover-Rowe Parameter at 15°C for PG 64-28P Base Binder (a) Completed (b) Summarized

By comparing the range of the G* values between the unaged and highly aged binders, the two datasets for PG 64-22 and PG 64-28 base binders can be considered fairly similar, e.g. between the base PG 64-22 and PG 64-28. However, the observed phase angle indicates a substantial change with the PG 64-28 and corresponding blends. Specifically, the binders containing the PG 64-22 binder initially begin with phase angle in the range of about 70 to 80 degrees. At the most aged condition, those binders indicate δ values of nearly 30° for

all three respective binder blends. Conversely, the PG 64-28 and corresponding blends initially exhibit phase angles two degrees higher, but end up over 40° after the same age conditioning. This retention in δ highlights the perceived benefit of utilizing the softer base PG 64-28 binder with recycled materials. Similar investigations in PG 64-28P binder blends led to a pronounced difference between this modified base binder and the other two base binders and their corresponding blends. The difference is highlighted with a comparatively low phase angle along with a reduced stiffness in the PG 64-28P base binder. On the other hand, it should be mentioned that although the phase angle in PG 64-28P base binder showed higher values at the initial aging durations compared to the other base binders, it was retained in the values not higher than 40° for the measured data points. These phenomena might be attributable to the polymer modification which previously observed with researchers to lessen the deteriorative oxidative aging hardening effects as well as improving elastic behavior. (Woo et al, 2007a, 2007b; Airey, 2003; McDaniel and Bahia, 2003; Sebaaly et al. 2002, Lu and Isacsson, 1999; Glover et al., 2005, Zhu, 2015). As another influence of the polymer modification, the PG 64-28P binder blends were observed not to migrate to the upper right of the Black Space diagram as much as the two other base binders. In other words, at the same aging duration and temperature in the constant rate area, the polymer modified blends indicated a lower stiffness as well as a lower phase angle compared to the PG 64-22 and PG 64-28 binder blends. In addition, the PG 64-28P binder blends were observed to have higher capability to retain the phase angle or elastic behavior before reaching to the G-R parameter thresholds, i.e. onset and significant cracking. This was also observed previously by Glover et al., 2005.

Considering fairly similar paths for the three base binders with and without RA, this suggests that the overall behavior is heavily influenced by the base binder. However, this should not be misinterpreted to indicate that the aged properties or more specifically the evolution or rate of progression are the same with the blended materials. Specifically, the range or distances travelled across the Black Space diagram are substantially different between the base and blended materials.

It was further noted that the addition of the TX RAP and TX MWAS did not substantially alter the black space aging path of 64-22 base binder with T1. Likewise, the PG 64-28 recycled blend including TX RAP and A1 was still observed to follow the base binder path. In contrast, the addition of the TX RAP and TX TOAS materials and T1 at the optimum dosage to the PG 64-28 and PG 64-28P base binders was observed to deviate aging path from that of the base and T1 blends in both cases. In general, it was summarized that the differences in the base binders and the type of RAS potentially let to the difference in the interaction of all the blended materials, resulting in the overall difference in aging behavior.

5.1.3 Hardening Susceptibility Results – Glover-Rowe Parameter (G-R)

Utilizing the DSR and FT-IR test results along with the Glover-Rowe parameter methodology presented in Chapter 3, Figure 5. 14 through Figure 5. 16 depicts the G-R parameters as a function of CAg for the binder blends with the additions of the recycled materials and RAs over multiple aging temperatures, identified as the Hardening Susceptibility (HS). The HS readily permits the direct comparison of the stiffening effect and subsequent loss of flexibility in the materials as they age. With the binders in this study, there are generally two rates of aging namely fast and constant, similar to what have

been introduced in the aging kinetic parameters. The fast rate indicates the initial stages of oxidative aging in which the stiffening and loss of flexibility, i.e. increase in G-R parameter value, occurs relatively quickly represented by a high slope in the HS. Following the fast rate, a decrease in the oxidative aging rate is generally observed in the HS recognized as constant rate. Constant rate suggests a slower progress in aging although the G-R value is still increasing.

It should be mentioned that the final version of the carbonyl area (CA) was to be calculated as the area, in arbitrary units, between the IR absorption spectrum and the magnitude of the absorption at 1524 to 1820 cm-1 used as a baseline. This area was integrated from 1650 to 1820 cm-1 wavenumber. To normalize the CA values on relative terms, the carbonyl growth (i.e., CAg) was calculated by subtracting the CA at the un-aged level (i.e., CA_{Tank}) from the measured CA at each of the aging levels.

Based on Figure 5. 14, it is evident that the addition of the RA to the PG 64-22 base binder increased the flexibility of the binder based on lower G-R values at a given CAg during the early stages of the aging process. However, after a certain level of oxidation, the PG 64-22 binder modified with T1 eventually resulted in higher G-R levels, indicating increased embrittlement relative to the PG 64-22 base binder due to aging of the RA. The addition of RAP and MWAS material increased the stiffening level as well as reduced the flexibility of the blend as indicated by the higher G-R level. Further, the RA at the evaluated dosage did not seem to be effective in restoring the rheological properties at least at the early stages of aging. However, as the aging progressed, the T1 in the blend containing both RAP and MWAS retained more flexibility and eventually resulted in the lowest G-R parameter

below that of either the base or base and T1 blends. It should be noted that the highest variability in the data analysis was realized with the RAS blend, which may be related to the limited binder availability from RAS. These issues make direct interpretation of the results less than intuitive. Therefore, this data will be combined with the kinetics measures specific to these binders in the aging predictions presented subsequently.

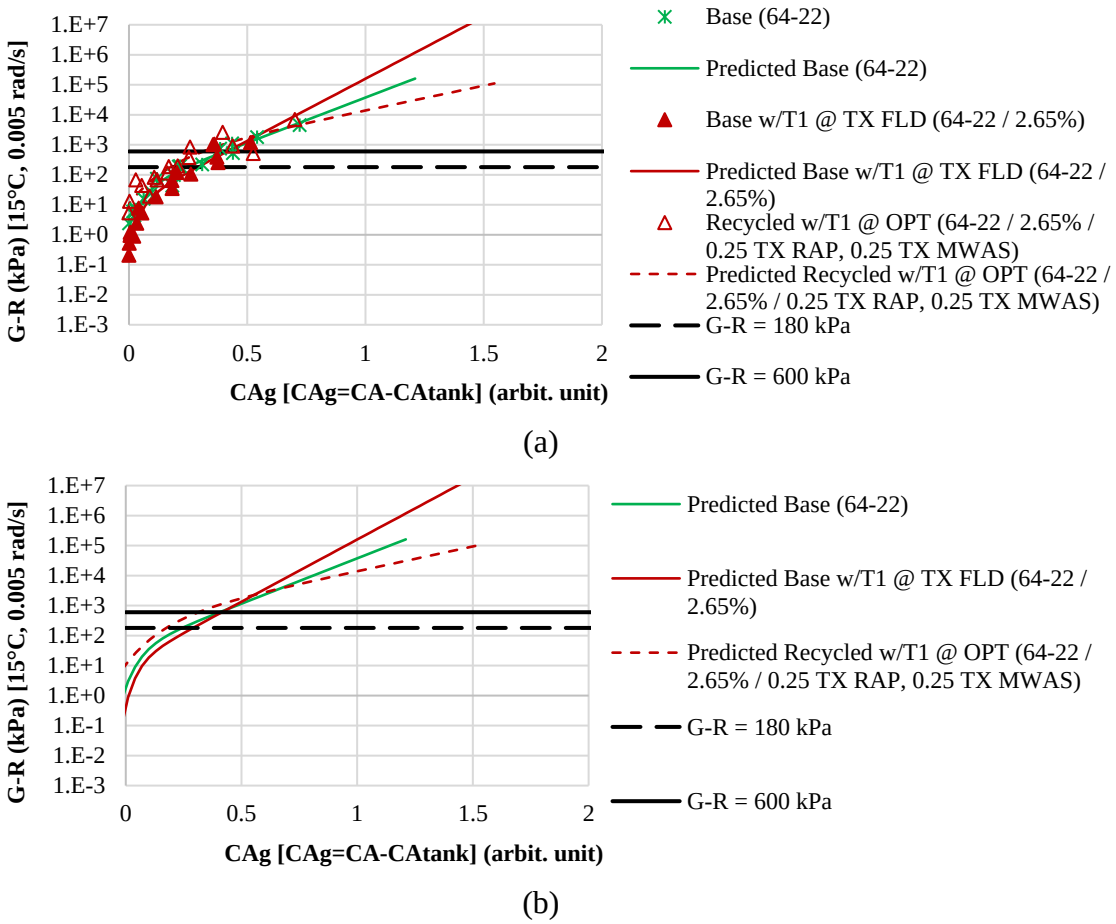

Figure 5. 14. Hardening Susceptibility – G-R Parameter at 15°C for PG 64-22 Base Binder in Forced Draft Oven Aging (a) Complete (b) Summarized

Similar comparisons of the G-R parameter as a function of CAg for the PG 64-28 base binder and respective blends are depicted in Figure 5. 15. It is evident that the addition of the RA to the PG 64-28 base binder increases the flexibility of the binder resulting in lower G-R values at a given CAg. In contrast to the results for the PG 64-22 base binder, the HS

(slope) was relatively unchanged by the addition of the T1 and thus this RA at the evaluated dosage was not as effective in restoring the rheology over the long-term. Similar to the PG 64-22 base binder, the addition of the RAP and RAS materials with T1 significantly increased the brittleness of the blend, and likewise reduced the HS compared to the base. In a similar comparison, the A1 had a similar influence on the PG 64-28 base binder. However, when combined with the RAP and RAS additions, the HS with the A1 was significantly reduced as compared to the T1 blends with either base binder. Again, it should be noted that the highest variability in the data analysis was realized with the TOAS blend that can highlight the arguable assumption of full or complete blending in the recycled binder blends.

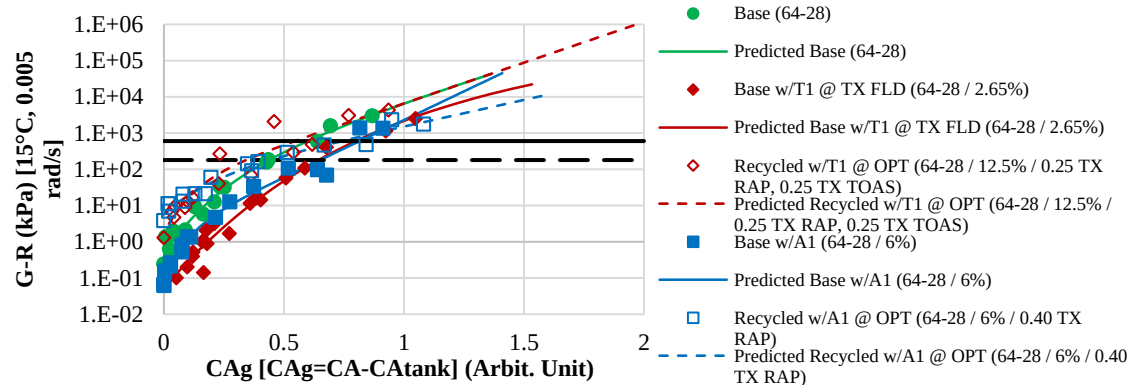

(a)

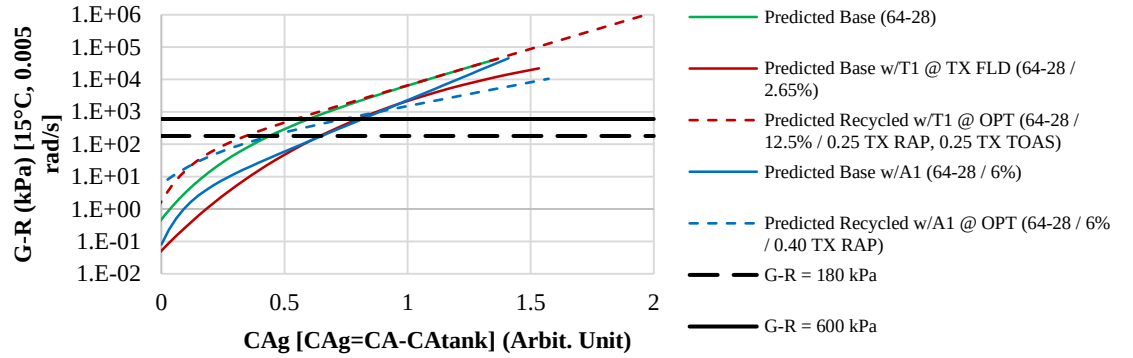

(b)

Figure 5. 15. Hardening Susceptibility – G-R Parameter at 15°C for PG 64-28 Base Binder in Forced Draft Oven Aging (a) Complete (b) Summarized

Additional considerations for the PG 64-28P binder blends are presented in Figure 5. 16. From these comparisons, it is evident that the addition of the T1 RA to the PG 64-28P base binder increases the flexibility of the binder only slightly, resulting in lower G-R values at a given CAg. However, the HS of the two are more similar for this base binder as compared to the other two base binders. When considering the addition of the RAP and TOAS materials with the T1 RA, a similar response to the initial PG 64-22 binder blends was noted. In this case, the initial reduction in flexibility observed at higher levels of G-R was eventually overcome by the reduced HS with the recycled blend. After some level of aging, the G-R values of the recycled blends were lower than those for either the base binder or the blend with only T1 RA. This might suggest that the selected optimum dosage was able to restore the aging properties of the recycled blend to some extent and prevent it from higher levels of stiffening and losing the flexibility.

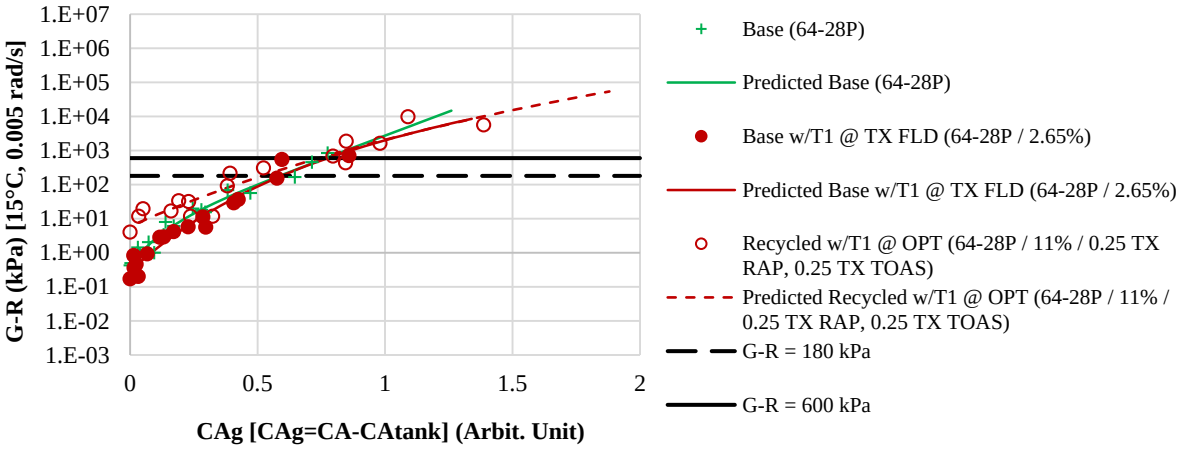

(a)

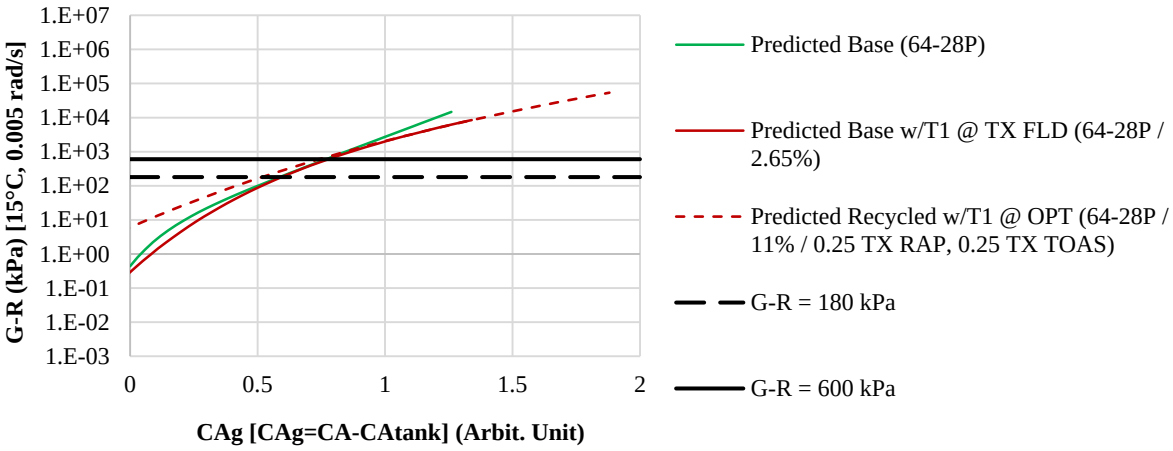

(b)

Figure 5. 16. Hardening Susceptibility – G-R Parameter at 15°C for PG 64-28P Base Binder in Forced Draft Oven Aging (a) Complete (b) Summarized

As an interim summary of the HS relationships, it was noted that both RAs reduced the overall stiffness in the initial stages of oxidation. However, differential aging rates or HS were observed between the RA and RAP/RAS additions to each of the three base binders. Note that these differences were not consistent with the type of RAS, i.e. MWAS or TOAS. It suggests that there are differences in the influences or interactions of the component materials that very well may exhibit behavior of unknown magnitude and direction. Further the complex interactions taking place appear to be very difficult to predict without actual material blending and testing being conducted. These differential findings make it difficult to make generalizing statements regarding the influence of any particular component or type, e.g. RAS, RA etc. Additionally, the G-R parameter was determined at the standard temperature of 15°C for these comparisons.

5.1.4 Hardening Susceptibility Results – Low Shear Viscosity (LSV)

The referenced methodology described in Chapter 3 has been utilized to prepare another type of HS results based upon the low shear viscosity at 60°C and 0.001 rad/sec as a function of aging, again represented as carbonyl area growth (CAg). General observations of Figure 5. 17 through Figure 5. 19 indicated apparent similarities between HS plots conducted with G-R parameter that have been discussed in detail in previous section. However, it should be noted that, unlike to the G-R HS plots, a linear regression through the data points in semi-log LSV HS plots seemed to more closely represent the aging path with a minor exception in PG 64-28P binder blends. Similar to what have been observed with G-R HS plots in the previous section, a two-staged, i.e. fast and constant aging rates, regression might be more reasonable to be fitted through the aging path in LSV plots for PG 64-28P. However, since the slopes and interceptions of the LSV HS plots are required to be used as inputs in CA prediction model that will be discussed in Chapter 6, a linear regression in a semi-log plot was considered for all the binder blend. It should be noted that the oxidation prediction models uses the HS relationship based upon the low-shear viscosity (LSV) due to developed correlations between LSV and the oxygen diffusivity of asphalt binders. For the purpose of completeness, those relationships have also been provided. To avoid repetition, a summary of the observations of Figure 5. 17 through Figure 5. 19 is presented as follows:

Beginning with the PG 64-22 binder blends represented in Figure 5. 17, the addition of the T1 clearly decreased the binder viscosity compared to the base binder at the fixed conditions of 60°C and 0.001 rad/sec, suggesting a softer binder at least at the initial levels

of aging. However, as the aging progressed the stiffening as a result of oxidative aging seemed to overcome the T1 softening effect and increased the low shear viscosity for the T1 blend at the same level of aging.

The addition of the recycled material with T1 at 2.65% to the PG 64-22 base binder highlighted the stiffening effect of the TX RAP and TX MWAS. As expected, the recycled blend represented a significant continuous increase in the viscosity compared to the base and T1 blend. This might suggest the rutting resistance improvement of the recycled pavement when considering the binder aspect only.

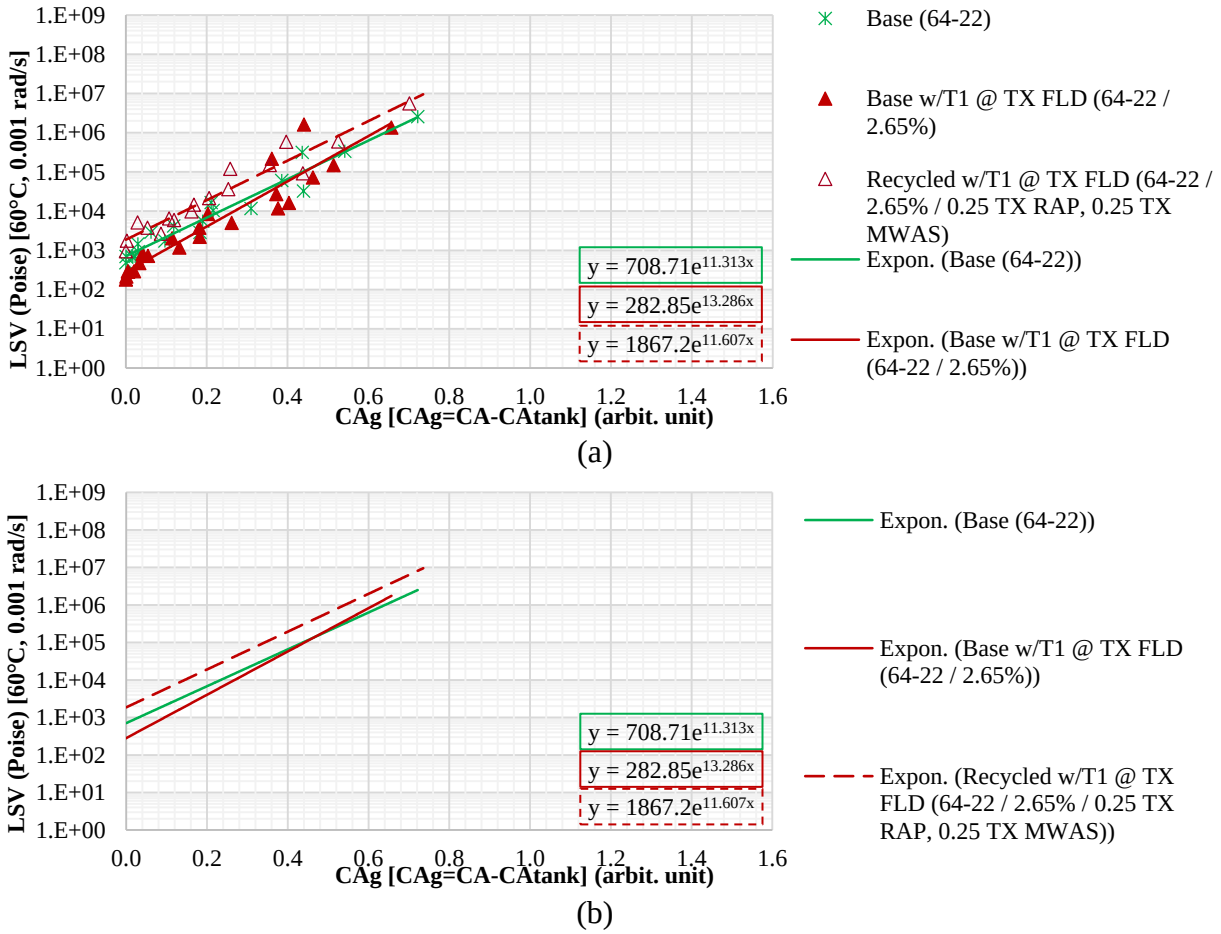

Figure 5. 17. Hardening Susceptibility – LSV at 60°C for PG 64-22 Base Binder

(a) Complete (b) Summarized

Observations of Figure 5. 18 highlighted the softening influence of the RAs, either T1 or A1, on the PG 64-28 base binder viscosity with a more pronounced decrease in LSV with T1 although at a lower dosage value. However, the softening effect of T1 and A1 seemed to become equal at the higher aging levels.

Further, the addition of the recycled material, either TX RAP only or TX RAP and TX TOAS combination, indicated a significant increase in the viscosity of the binder blends with a slightly higher increase in the latter recycled blend. However, noting that the A1 and T1 were used at the optimum dosages in the recycled blends, the initial stiffening seemed to be alleviated at the higher aging levels. As presented, although the viscosity measurements for the recycled blends started with higher values at the initial aging steps, which is completely expected, the HS, i.e. slope of the fitted line, had a lower value compared to that of the base binder, suggesting a slower CAg progression within the recycled blends. It could be concluded that the addition of the recycled material to the base binder along with the relatively high dosages of RAs especially with T1, decreased the portion of the base binder in the blend. With a lower amount of the base binder, the aging progressed slower than the base binder resulting lower stiffness increases at the higher levels of aging.

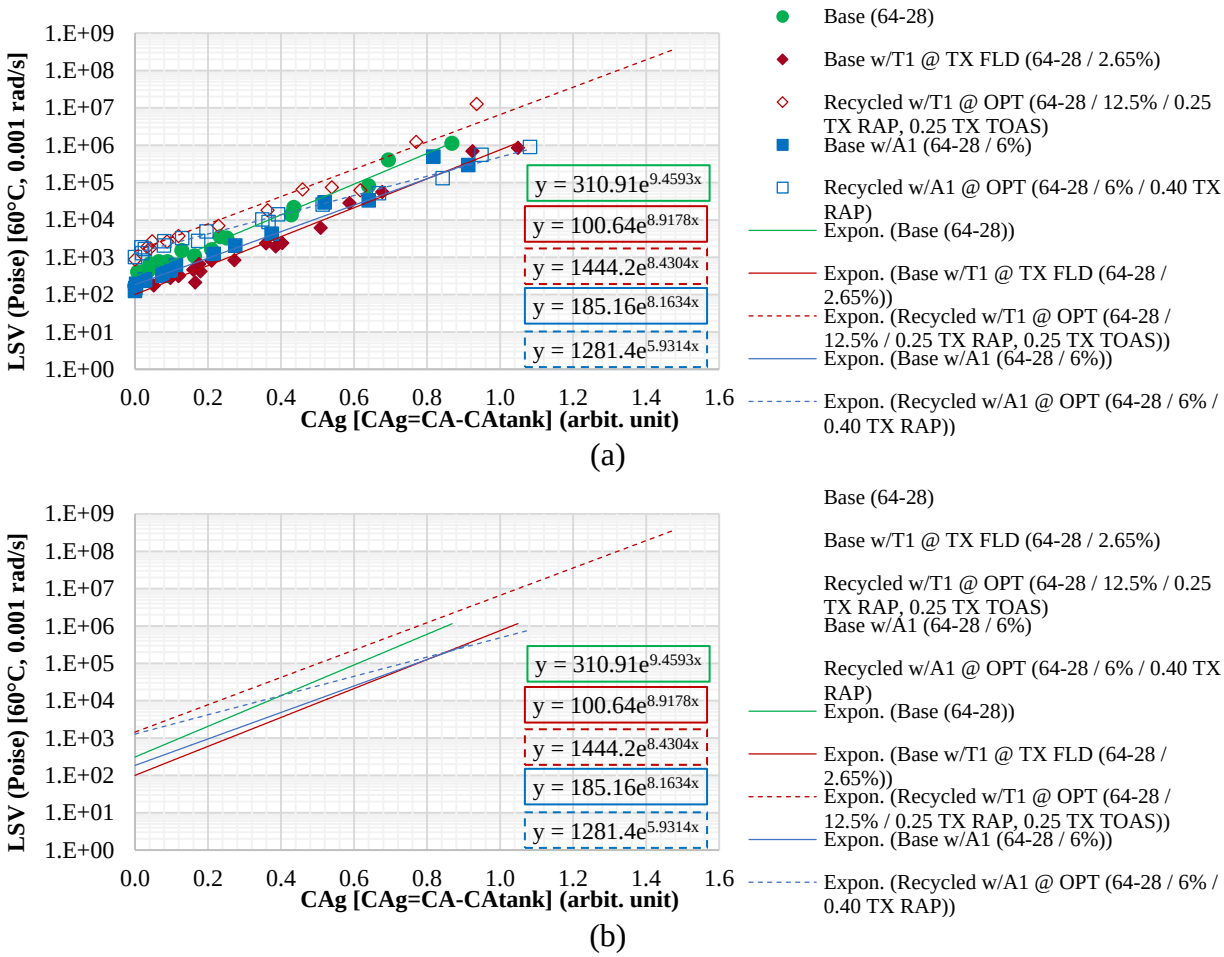

Figure 5. 18. Hardening Susceptibility – LSV at 60°C for PG 64-28 Base Binder (a) Complete (b) Summarized

As previously mentioned, although the linear regression in the semi-log plot might not be the ideal fit for the PG 64-28P binder blends presented in Figure 5. 19, it still follows the overall trend of aging path, thus providing a stage of the comparison with the three different blends. The addition of T1 at 2.65% to the base binder seemed to have a slight reduction in the stiffness at the initial steps of aging following with a slight increase in the stiffness at the higher CAg values. On the other hand, with the addition of the recycled material and T1 at the optimum dosage, the summary plot showed a slight increase in the viscosity, however, a closer consideration of the data points underrated that slight increase, indicating

a restoration to the base binder viscosity. This potentially might stem from a relatively high optimum dosage of T1 along with the polymer modification effects which eventually allowed the recycled blend to have a similar slope in LSV HS to the base binder.

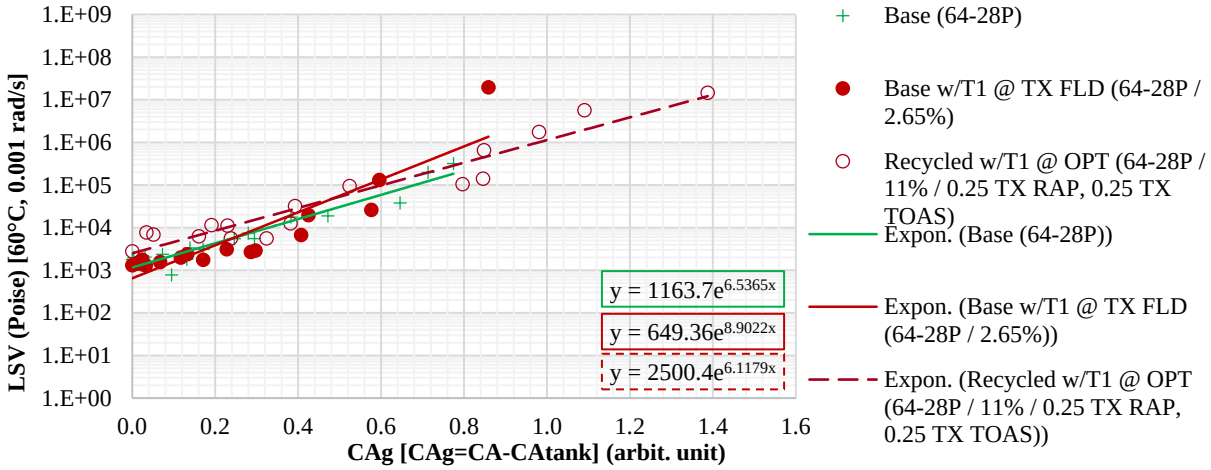

(a)

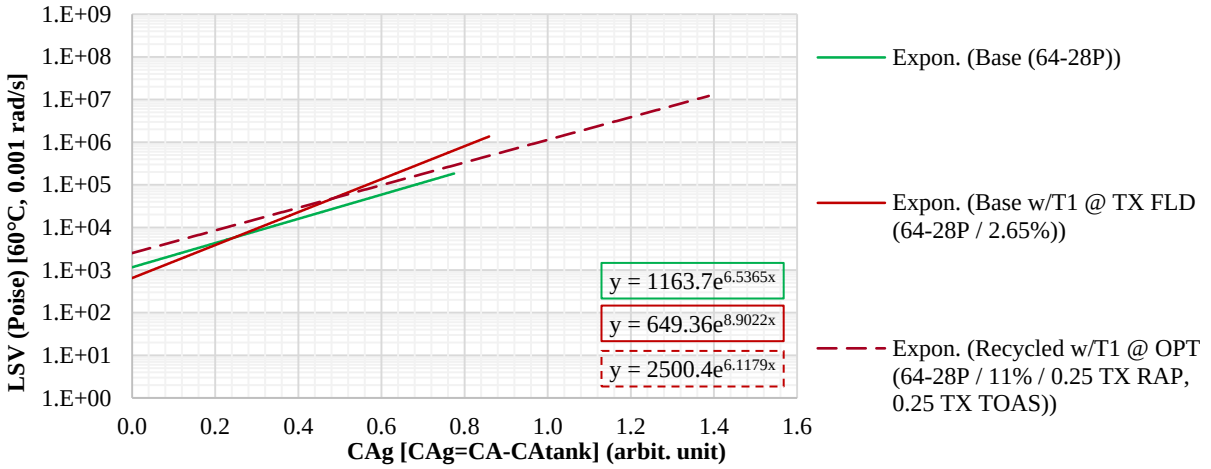

(b)

Figure 5. 19. Hardening Susceptibility – LSV at 60°C for PG 64-28P Base Binder (a) Complete (b) Summarized

5.1.5 Crossover Temperature Results

Crossover modulus is defined as the shear modulus at phase angle of 45°, where the viscous modulus (G") and elastic modulus (G') curves cross each other. The crossover modulus at fixed temperatures have periodically been utilized as an aging indicator for various

applications (Morian, 2014; Zhu, 2015). A slight modification of that methodology has recently been considered by The Texas A&M University as a tool to confirm the optimized RA dosage selection methodology proposed in the NCHRP 09-58 project (Epps et al., 2017). Further details will be discussed in Chapter 6. This effort has been exploring the use of crossover temperature, which represents the temperature of the crossover modulus, i.e. phase angle of 45°, at a test frequency of 10 rad/s. To provide more insight on the effect of aging on this parameter, G-R plots as a function of the crossover temperature have been prepared for the evaluated binder blends in the current study in Figure 5. 20 through Figure 5. 22.

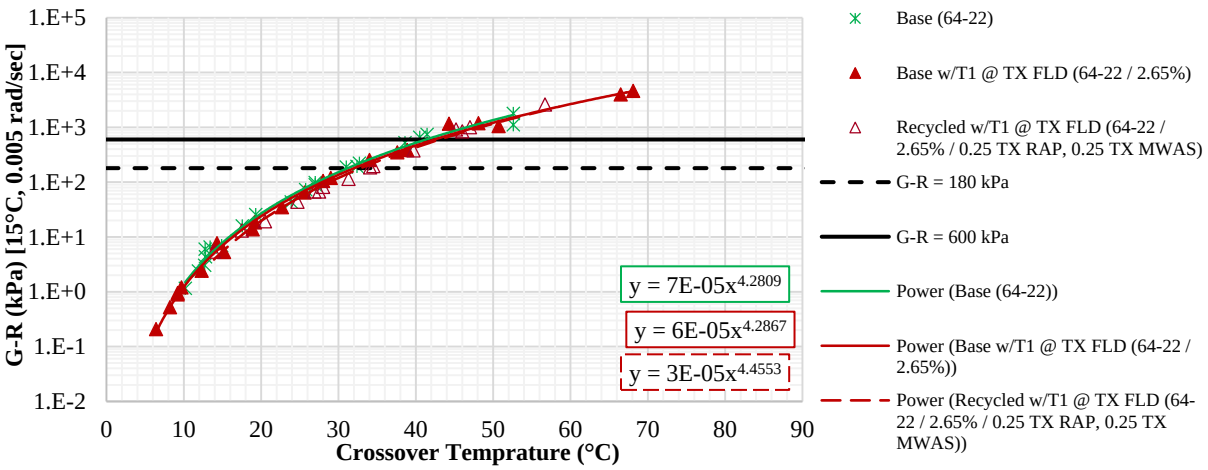

Figure 5. 20. Correlation of the G-R with Crossover Temperature for the PG 64-22 Binder Blends

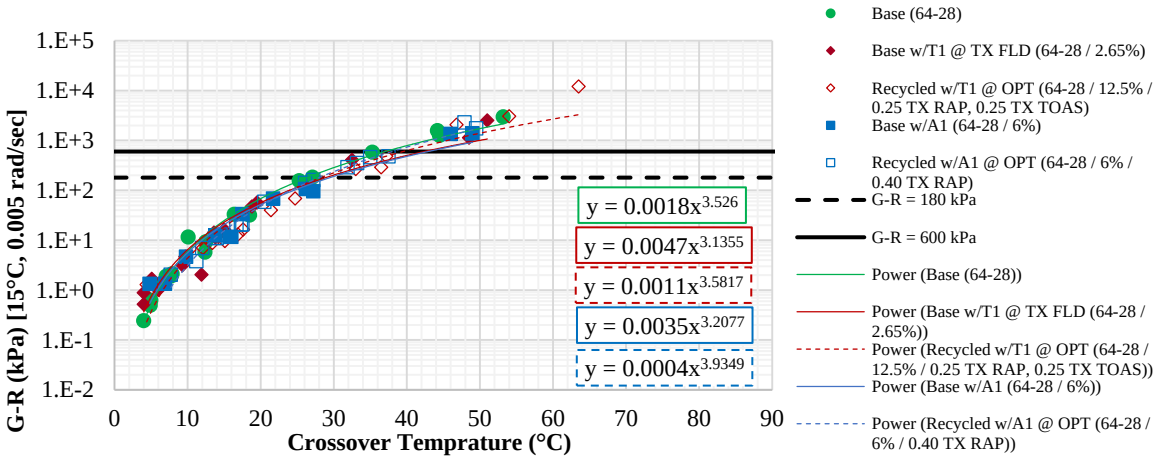

Figure 5. 21. Correlation of the G-R with Crossover Temperature for the PG 64-28 Binder Blends

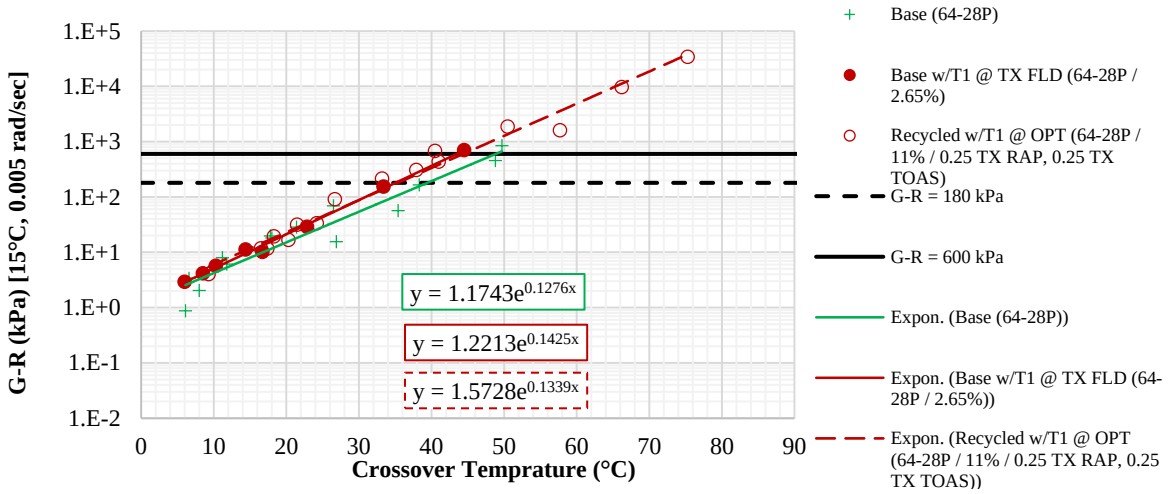

Figure 5. 22. Correlation of the G-R with Crossover Temperature for the PG 64-28P Binder Blends

To begin, Figure 5. 20 clearly showed a certain correlation between the G-R parameter and crossover temperature for all the three different binder blends with PG 64-22 base binder. The addition of the T1 at 2.65% did not change the overall shape of the curve compared to the base binder; however, the T1 shifted the curve to the lower left, which defines lower temperatures and G-R parameters at the first stages of the aging. On the other hand, the

addition of the recycled material along with the T1 shifts the curve to the upper right where the binder has a higher crossover temperature and G-R parameter.

It should be noted that some of the less aged binder samples could not be presented in this plot due to having a lower crossover temperature than the lowest temperature used in the DSR frequency sweep temperature regime, i.e. 4°C. This issue was highlighted even more in Figure 5. 21 for the PG 64-28 binder blends where more data points had been removed inasmuch as the reduction of the crossover temperature and G-R parameters could not be represented. However, similar to what have been observed in the PG 64-22 recycled blend, the addition of the recycled materials, either RAP or RAS, along with the T1 or A1 to the PG 64-28 base binder, shifted the recycled blends curves to the upper right while keeping the overall shape of the curve similar to the base binder.

Figure 5. 22 represents the G-R parameter versus crossover temperature for the PG 64-28P binder blends where a significant number of the lesser-aged binder samples from all three different blends could not be determined, again due to having a lower crossover temperature than 4°C. In this case, it significantly changed the shape of the curves to have more linear shape, acknowledging the exclusion of the lesser aged material range. However, the true points of interest hover around the G-R limits, which were determined and presented in the figure.

Texas A&M University research team also proposed two threshold values of 32 and 45°C for the crossover temperature corresponding to the onset and significant G-R cracking thresholds of 180 and 600 kPa, respectively. These values were supported with the PG 64-22 binder blends; however, the PG 64-28 binder blends seemed to have slightly lower

crossover temperature thresholds for the respective G-R limits. The base 64-28P binder blends indicated slightly different ranges than the proposed 32 and 45°C proposed thresholds.

In general, additional evaluation efforts in laboratory and field are required considering the influence of various base binders and additives whether RAs, or recycled materials such as RAP, RAS, or other modifying agents which may be added to asphalt binders, to explore the potential benefits of this newly proposed limit in crossover temperatures.

5.1.6 Statistical Analysis

The linear regression analysis was utilized in this study to compare the HS within each base binder. However, the curvilinear HS from G-R would take more careful consideration with elaborated non-linear statistical evaluation; therefore, the HS from the LSV were utilized for such statistical analysis. In other words, the slopes and intercepts of the linear fits in the binder blends semi-logarithmic plots of LSV versus CAg, Figure 5. 17 to Figure 5. 19, were compared to that of the corresponding base binder. The idea behind such analysis is to investigate if the addition of the recycled material and/or RAs could change the aging path of the base binder. The response functions utilized in this effort and the related methodology has been discussed in detail elsewhere (Morian, 2014; The Minitab Blog). As a brief description, a simple linear regression model was evaluated on the binder blends within each base binder in Minitab, and the corresponding p-values were utilized to evaluate the level of significance in the difference between the intercept of the various blends to their respective base binder. Also, interaction terms were introduced as the multiplication of the binder category and the respective CAg to determine whether the

slope of the HS differs from that of the base binder. Consequent p-values of the interaction terms and intercepts indicated whether the null hypothesis of the equal slopes and intercepts need to be rejected. Table 5. 4 represents the concluded p-values.

Table 5. 4. Statistical Significance of the various binder blends on LSV with CAg

Binder ID		Intercept		Slope	
		Regression P-values	Statistical Significance Compared to Base Binder	Regression P-values	Statistical Significance Compared to Base Binder
TX	Base w/T1 @ TX FLD (64-22 / 2.65%)	0.057	NS[1]	0.119	NS
	Recycled w/T1 @ TX FLD (64-22 / 2.65% / 0.25 TX RAP, 0.25 TX MWAS)	0.000	SH[2]	0.771	NS
NH	Base w/T1 @ TX FLD (64-28 / 2.65%)	0.000	SL[3]	0.215	NS
	Recycled w/T1 @ OPT (64-28 / 12.5% / 0.25 TX RAP, 0.25 TX TOAS)	0.000	SH	0.218	NS
	Base w/A1 (64-28 / 6%)	0.000	SL	0.056	NS
	Recycled w/A1 @ OPT (64-28 / 6% / 0.40 TX RAP)	0.050	SH	0.000	SL
NV	Base w/T1 @ TX FLD (64-28P / 2.65%)	0.976	NS	0.041	SH
	Recycled w/T1 @ OPT (64-28P / 11% / 0.25 TX RAP, 0.25 TX TOAS)	0.007	SH	0.055	NS

[1]Statistically non-significant
[2]Statistically significantly higher
[3]Statistically significantly lower

Statistical considerations of the various binder blends from Table 5. 4 indicate that the addition of the RA only did not generally change the slope of the HS plots of the binder blends except for the PG 64-28P base binder with T1. However, a closer look into the Figure 5. 19 suggests the necessity of further measurements due to the abrupt jump of the last data point in the corresponding binder blend. Additional measurements are recommended to confirm the validity of this measurement before making a clear exception between the overall behavior of the base binder with RAs for PG 64-28P.

The addition of the recycled material along with the RAs at various dosages, either optimum or non-optimum, showed a non-significant deviation from the base binder aging path except for the PG 64-28 base binder with 0.4 RAPBR and an optimum dosage of A1. The HS of this particular binder blend from Figure 5. 18 seemed to significantly be reduced as confirmed with the statistical analysis.

The intercepts of the HS plots indicated a significant difference with respective base binders due to the addition of the RAs and/or recycled material in almost all the cases. This could be expected from the previous observations, i.e. the change in the chemical properties and as a result the change in the viscosity of the binder blends.

It should be noted that the conducted statistical significance determinations cannot be completely confirmed with the limited range of measurements in the current study. They might be subjected to variation with the additional aging durations and temperature. Therefore, additional measurement and in-depth analysis are highly recommended before making any final conclusions on the aging behavior of the various binder blends.

5.2 Accelerated Aging

A secondary aging protocol was utilized with selected binder blends from the experimental plan to evaluate the appropriateness of the simulated long-term aging through the forced-draft oven aging at multiple durations and temperatures. In this regard, in addition to the standard short and long-term aging procedures outlined in AASHTO M320, i.e. rolling thin film oven aging and 20-hour pressure aging vessel (PAV) aging, respectively, prolonged PAV aging was extended to 40 and 60 hour durations to attain higher oxidation levels. The PAV aged binder blends were then evaluated with the DSR testing at multiple temperatures

as well as FT-IR testing to determine the rheological parameters and oxidative aging level, respectively. Table 5. 5 describes the binder blends selected for the PAV aging and corresponding binder grading results. As observed, no recycled blends were included in the PAV aging experimental blends. Since a substantial degree of variability was noticed with the recycled blends evaluation, they were intentionally avoided in this procedure in order not to add more uncertainty to the evaluation rather than the aging methodology.

Table 5. 5. Binder Blend Utilized in Accelerated Aging

	Binder Blend	High-Temperature Continuous PG Grade (°C)	Low-Temperature Continuous PG Grade (°C)		ΔTc
			S-controlled	m-controlled	
TX	Base (64-22)	67.3	-30.0	-25.5	-4.5
	Base w/T1[1] @ TX FLD	62.9	-31.1	-26.9	-4.2
NH	Base (64-28)	66.0	-28.8	-30.1	1.3
	Base w/T1 @ TX FLD	62.6	-31.2	-32.5	1.3
NV	Base (64-28P)	65.6	-34.1	-32.4	-1.7
	Base w/T1 @ TX FLD	68.2	-35.7	-34.6	-1.0

[1]T1 added as 2.65% by binder replacement

5.2.1 Hardening Susceptibility Results – Glover-Rowe Parameter (G-R)

Figure 5. 23 presents the HS of the selected binders following accelerated aging protocols. As described in Table 5. 5, the accelerated aging path encompassed five data points for each specific binder blend including original, RTFO aged, 20, 40 and 60 hours of PAV aging, noting that utilizing the CAg, the first data point representing RTFO condition would be zero for all the blends.

Similar statements from the forced draft oven aging observations upon the addition of T1 to the base binder are also valid in the accelerated aging results. In nearly all cases, with the addition of T1, the initial stiffness level was measurably reduced for the each of the

binder blends as indicated by the lower G-R values. This reduction in the G-R parameter was observed to be a combination of the reduction in stiffness but also the increase in flexibility, i.e. increased phase angle for a given level of CAg. However, the difference was not consistent for all three base binders, supporting the potential requirement for material specific evaluations when any external component is added to the base binder as noted in the longer durations aging evaluation. Similarly, the phase angle was not consistently impacted in binder blends upon the addition of the T1.

As observed in Figure 5. 23. a and b, the PG 64-22 binder was substantially softened by the T1, and the influence was retained over the total duration of the aging conditions.

Considering the PG 64-28P binder blends in accelerated aging conditions from Figure 5. 23. c, a relatively similar aging path was observed between the base binder and the base with T1. Noting the apparent softening influence of RA with the lower values of G-R in the base w/T1 blend, the two base binders indicated a noticeable deviation starting at 60 hours of aging. Acknowledging the higher aging rate of the PG 64-28P base binder compared to the other based binders, the unknown interaction between the T1 and polymer might be the reason of that significant reduction in the aging rate after 60 hours PAV aging in the blend with T1. However, further investigations are required to insure the accuracy of the fitting line before any final conclusions.

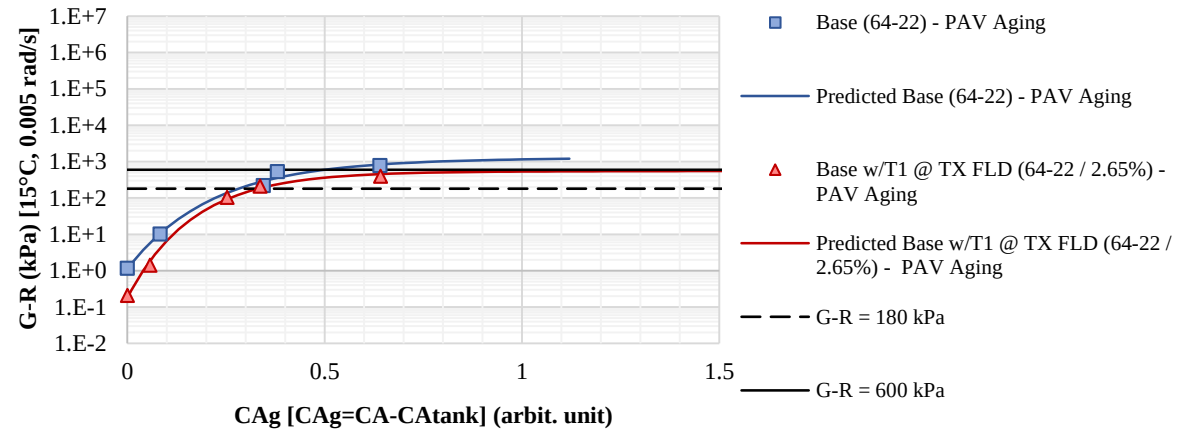

(a)

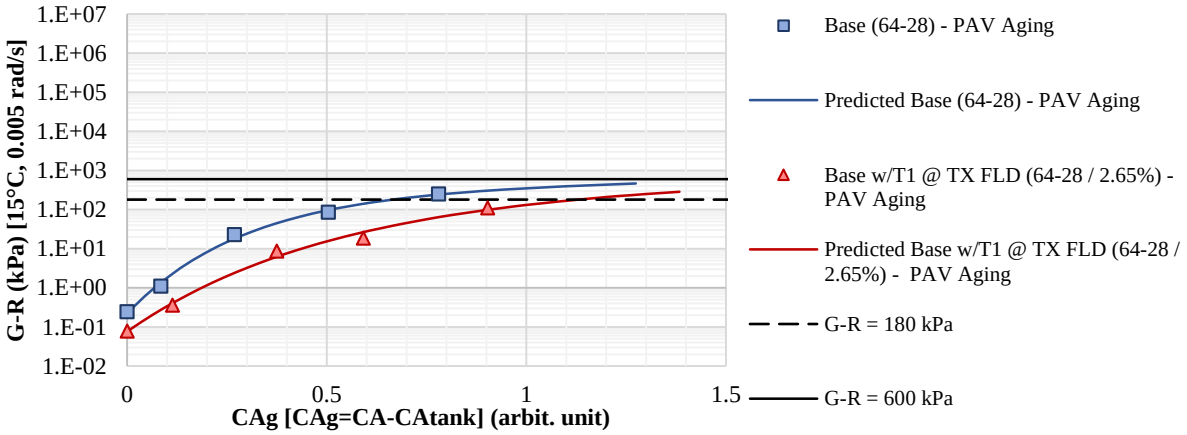

(b)

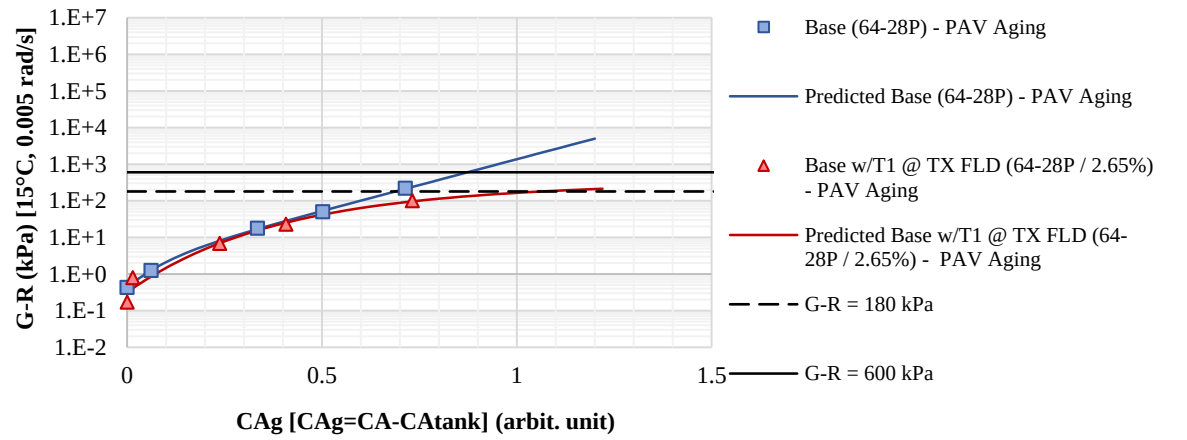

(c)

Figure 5. 23. Hardening Susceptibility – G-R Parameter at 15°C in Accelerated Aging

(a) PG 64-22 (b) PG 64-28 (c) PG 64-28P

5.2.2 Cracking Potential Determination

Generally, the focus of the oxidative aging studies is not limited to evaluation of the binders as a function of aging, i.e. HS. Rather, the intent is to identify the progression of the physical characteristics of the material toward some limiting condition, most likely some performance related measurement to correlate with field distress predictions. Accordingly, this section will evaluate the cracking potential of the PAV aged binders through two of the cracking indicators previously discussed, namely the G-R parameter and ΔTc.

As a reminder, the G-R parameter utilizes relatively small quantities of binder at each respective aging duration as well as a reasonably short time frame to conduct the testing. Conversely, reliable determination of ΔTc values typically require bending beam rheometer (BBR) measures including operator and material dependent variability. With that in mind, the objective at hand is to identify if each of these testing protocol or evaluation methodology would logically recognize potential cracking issues with a subject binder. In other words, the intent is to determine if a reasonable correlation can be established that would permit the identification of critical limits of cracking potential characteristics as a function of PAV aging for the binders evaluated in this study, given the relatively larger quantity of binder produced in shorter time durations with the PAV aging process.

Figure 5. 24 presents the G-R parameter as well as the ΔTc of the PAV aged binder blends of Table 5. 1, both as a function of the PAV aging duration. Also, the cracking limits corresponding to each of the cracking indicators are provided to investigate the influence of the accelerated aging on cracking susceptibility of each corresponding binder blend.

Recall from the background information in Chapter 4, a damage zone of onset cracking followed by significant cracking were proposed by Kandhal (8) where cracking likely begins and progresses due to brittle rheological behavior defined by low ductility values of 5cm to 3cm, respectively. Correspondingly, the G-R parameter values of 180 and 600kPa have been calculated. Also, Anderson et al. (6) suggested -2.5°C and -5°C as the correlation of ΔT_c to the same cracking limits discussed in G-R parameter, i.e. 180 and 600kPa, respectively.

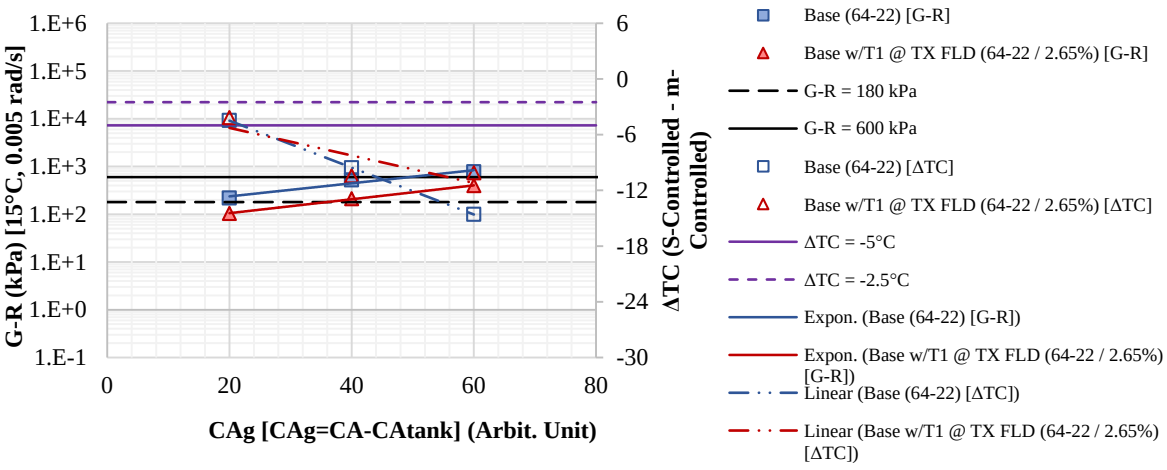

(a)

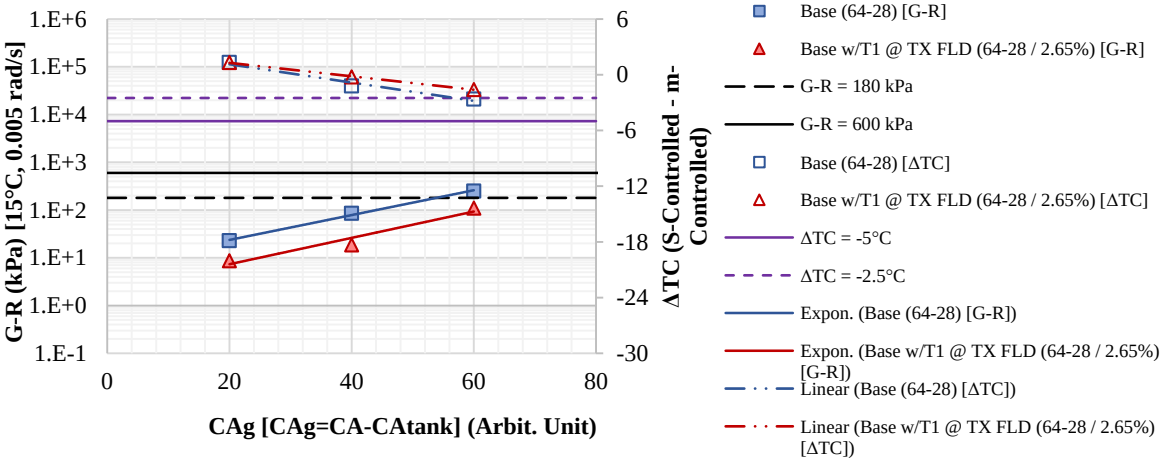

(b)

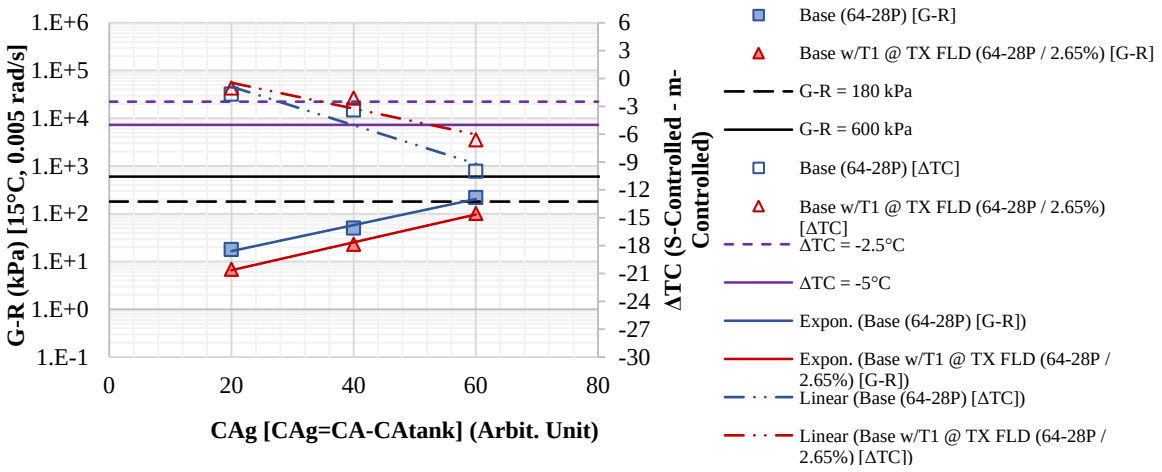

(c)

Figure 5. 24. Cracking Indicator Results with PAV Aging in (a) PG 64-22 (b) PG 64-28 (c) PG 64-28P

All the binder blends presented in Figure 5. 24 were observed to follow a log-linear trend as a function of PAV aging duration with the G-R parameter and a linear relationship with ΔTc. In other words, the longer the binder was subjected to PAV aging, the G-R parameter and ΔTc expectedly showed higher and lower values, respectively. As previously mentioned, the G-R parameter were evaluated at constant temperature of 15°C and constant frequency of 0.005 rad/s while the actual evaluation temperature utilized in the determination of ΔTc varies according to the material stiffness and relaxation behavior at low temperatures. Acknowledging the higher variability with the ΔTc result in all the blends, the G-R values showed a consistent offset from the base binder upon the addition of T1, while in case of ΔTc, the T1 blends were observed to deviate from the base binder as the aging progressed. However, the amount of deviation was not consistent through the various base binders, implying the binder specific influence of T1 on the low temperature characteristics of the base binder.

Further exploration of Figure 5. 24, yielded in Figure 5. 25 representing the correlations between the PAV durations at which the limits of ΔTc and G-R have been reached. As evidence from the results of the figure, a strong correlation between the two cracking indicators was not identifiable with any of the two cracking limits for the evaluated binder blends. However, this was not an unexpected finding; as previously mentioned, the G-R and ΔTc were measuring the binder properties at two different states of intermediate and high temperature, respectively. In the other word, the physical characteristics of the asphalt binder being evaluated in these parameters are dissimilar enough to not show a reasonable correlation, even for a relatively small subset of binder with fairly similar PG grades. This does not reduce the value of either parameter, nor the benefits of cracking parameter evaluations. It merely indicates that the two measurement techniques observe different characteristics of the subject binders, and thus present a more comprehensive evaluation when both systems are utilized.

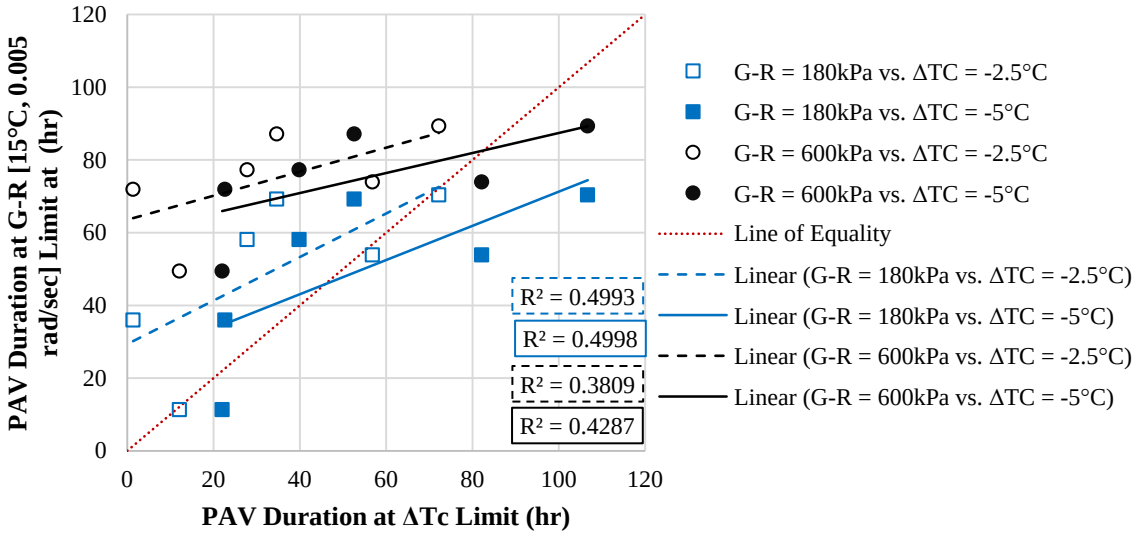

Figure 5. 25. Correlation between Cracking Indicators

As previously mentioned, the current practice of G-R parameter evaluation focuses on the typical fixed temperature and frequency of 15°C and 0.005 rad/sec, respectively. However, there have been limitations observed with the G-R parameter measured in the DSR at intermediate temperatures, particularly when correlations were attempted with modified binders (Hajj et al., 2016). Given that the original DSRFn correlation to ductility measures have inherent assumptions since it was based upon the Pennsylvania climate using a PG 58-28 binder (Hajj et al., 2016; King, 2015), several researchers suggested consideration of G-R parameter at other temperatures specific to the particular binder being evaluated. The idea behind the temperature modification is to provide a binder specific temperature at which all the binder blends indicate an approximate equal stiffness so that a more robust comparison can be made among various binder blends. Subsequently, two different methodologies were recommended for the alternative temperature selection. The first, employed a constant 43°C offset from the continuous low temperature PG grade named PG.low+43°C. The second, identified the midpoint of the continuous high and low temperature PG grades as an approximation for making the comparisons at more comparable stiffness values.

As an example of the application of temperature modification in G-R parameter, Figure 5. 26 present the required PAV time duration for each of the respective binders to reach the G-R cracking limits, noting that the G-R parameter is evaluated at three different temperatures namely: traditional, 15°C, PG.mid and PG.low+43 as presented in Table 5. 6. Observations of the Figure 5. 26. a suggested that the PAV duration to reach the G-R limit of 180kPa, corresponding to onset cracking, at PG.mid was relatively longer compared to the other evaluation temperatures irrespective of the T1 addition. The same binders

however, yielded quite variable results when viewed in the 15°C and PG.low+43°C testing condition. Similar findings were also applicable to the PAV aging time results indicated in Figure 5. 26. b. In general, it is suggested to be beneficial to further investigate the G-R parameter for future studies to evaluate those critical limits with respect to field performance at the more representative temperatures, particularly with modified asphalt binders (Hajj et al., 2016). By similar reasoning, verification of the methodology should also be sought for unmodified asphalt binders whose PG grade does not correspond to the original PG58-28 binder grade and climate, which were originally correlated to the 15°C testing state through ductility measures.

Table 5. 6. Temperature Modification Experimental Plan

Binder ID	Modification	Continuous PG Grade			PG.mid	PG.low + 43
		High	S-contr.	m-contr.		
64-22	None	67.3	-30.0	-25.5	21	21
64-22 w/T1	2.65% T1[a]	62.9	-31.1	-26.9		
64-28	None	66.0	-28.8	-30.1	18	15
64-28 w/T1	2.65% T1[a]	62.6	-31.2	-32.5		
64-28P	SBS	65.6	-34.1	-32.4	18	15
64-28P w/T1	SBS + 2.65% T1[a]	68.2	-35.7	-34.6		

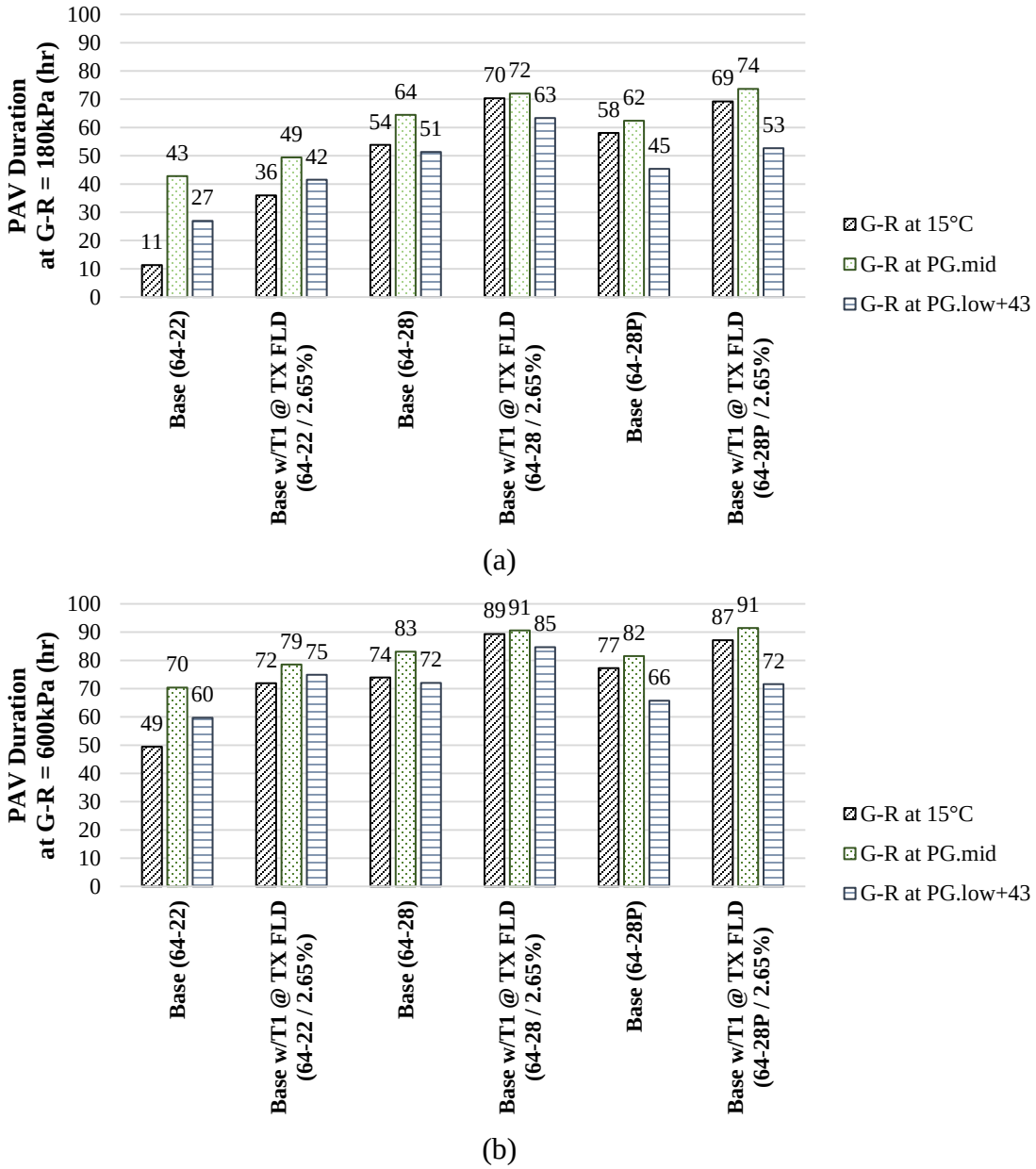

Figure 5. 26. Estimation of PAV Duration to Reach G-R Cracking Limits at (a) G-R = 180kPa (b) G-R = 600kPa

Investigating the influence of the binder type in the PAV aging durations from both Figure 5. 26, it can be concluded that the two PG 64-28 binders, unmodified and polymer modified, are fairly similar, with benefits noted in both due to the addition of the T1 additive. Further, the majority of the measures on the PG 64-22 binder indicated a reduced resistance to

cracking over the represented aging conditions, i.e. PAV duration. However, consideration of the difference between the PAV duration to reach each of the cracking limits, i.e. subtraction of PAV durations at G-R = 600 and 180kPa indicated Figure 5. 27, the PG 64-22 seemed to have a longer crack propagation duration before reaching to sever cracking zone. In other words, after reaching the crack initiation zone at G-R = 180kPa, the flexibility was reduced with a lower rate in the PG 64-22 binder in comparison with the other two binders. Such a discrepancy between the observations of the binder behaviors within this limited sets of evaluated binders highlights the essence of further investigation on the actual in-place pavement mixture specimens to properly understand what happens in reality rather than just binder evaluations conducted in the laboratory.

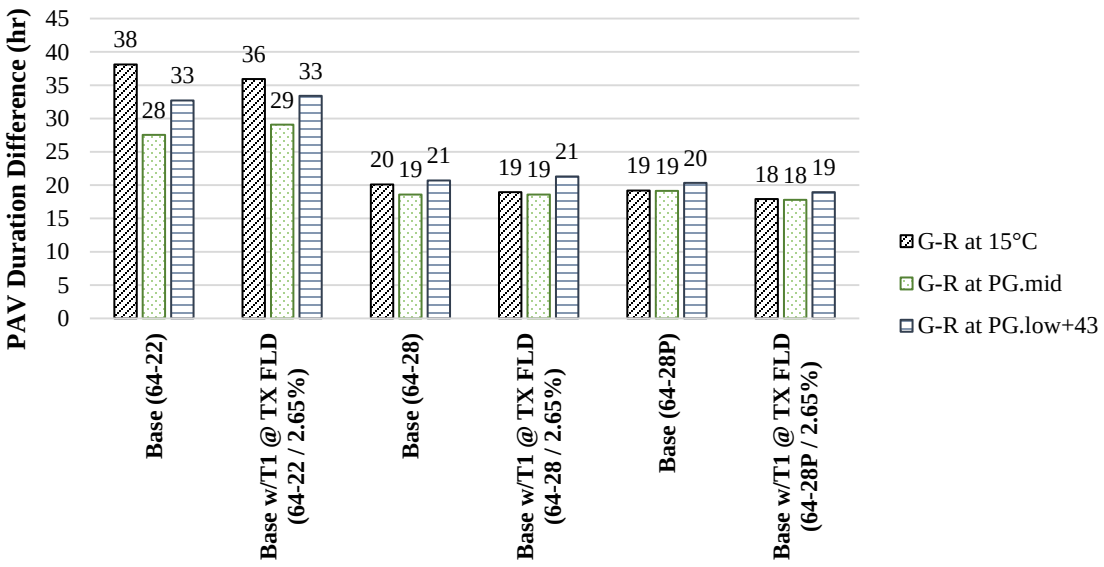

Figure 5. 27. Estimation of PAV Duration to Reach G-R Limit at G-R=180kPa and G-R=600kPa

To continue the overall cracking resistance of the respective binders, Figure 5. 28 is referenced to observe the thermal cracking indications as a result of the ΔTc measures, again represented as PAV duration to the -2.5 and -5°C limits. From this viewpoint, the

reduction in the time-dependent resistance to thermal cracking with the PG 64-22 binder is dramatically evident. By similar measure, the increased benefits of the aging resistance coupled with the more compatible binder is realized in the longer durations required of the PG 64-28 binder.

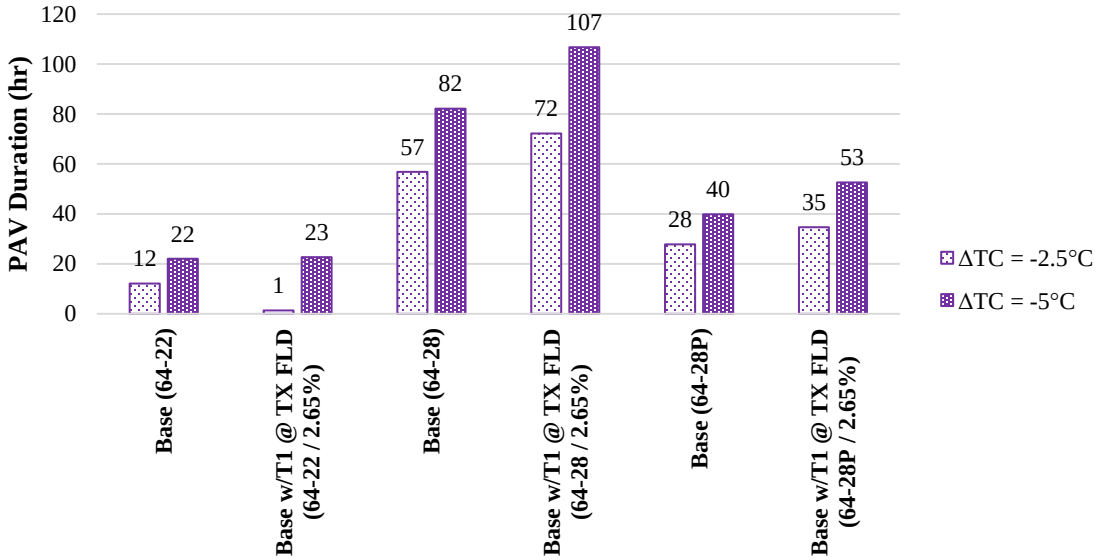

Figure 5. 28. Estimation of PAV Duration to Reach ΔTc Limit at ΔTc = -2.5°C and ΔTc = -5°C

Therefore, as a general summary of the available evaluation techniques, the reduced cracking resistance of the PG 64-22 binder was noted in the G-R comparison and seconded by the ΔTc measures. The similarities observed between the 64-28 and 64-28P binders in the G-R evaluation were further differentiated by the low-temperature considerations of PAV duration. By this simplified consideration, a basic understanding of the cracking resistance of the evaluated binders can be assessed. However, as previously mentioned, this simple comparison does not propose to be accurate or robust aging evaluation of the tested binders. A more comprehensive evaluation would legitimately include variations in the in-service environment, as well as more robust considerations of the aging rates and

subsequent rheological characteristics of the binders as a function of aging. This simple example was intended to highlight the potential usage of the available measurement techniques, despite the lack of reasonable correlation between the methodologies.

5.3 Comparison of Forced Draft Oven Aging and Accelerated Aging

The objective of this specific section is to compare the two aging protocols utilized in this study, i.e. forced draft oven aging and accelerated aging, to decipher if commonly utilized aging protocols yield the same fundamental material characteristics within each base binder blends. In other words, the HS results presented in Figure 5. 29 through Figure 5. 31, permits the evaluation of whether the aging process of asphalt binder is a unique process in spite of the varied aging conditions that influence the aging history of the binder including temperature, pressure, and time.

Specific to the PG 64-22 and PG 64-28 results presented in Figure 5. 29 and Figure 5. 30, the more time consuming but lower temperature aging protocol, i.e. forced draft oven aging, typically yields higher HS slopes than the higher-pressure PAV results especially at the higher oxidation levels. Although all the four aging paths reach the onset cracking limit, i.e. G-R = 180 kPa, at relatively similar oxidation level, the noted higher HS in the forced draft oven aging caused the corresponding paths not to go appreciably further before reaching to the significant cracking limit. Recalling that the pan aging conditions include 60, 85, and 100°C temperatures it can be observed that the 100°C PAV aging temperature was common between the two aging methods. Despite this similarity, the HS is still notably different between the two aging protocols highlighting the influence of additional air pressure and difference in binder film thickness between the two procedures.

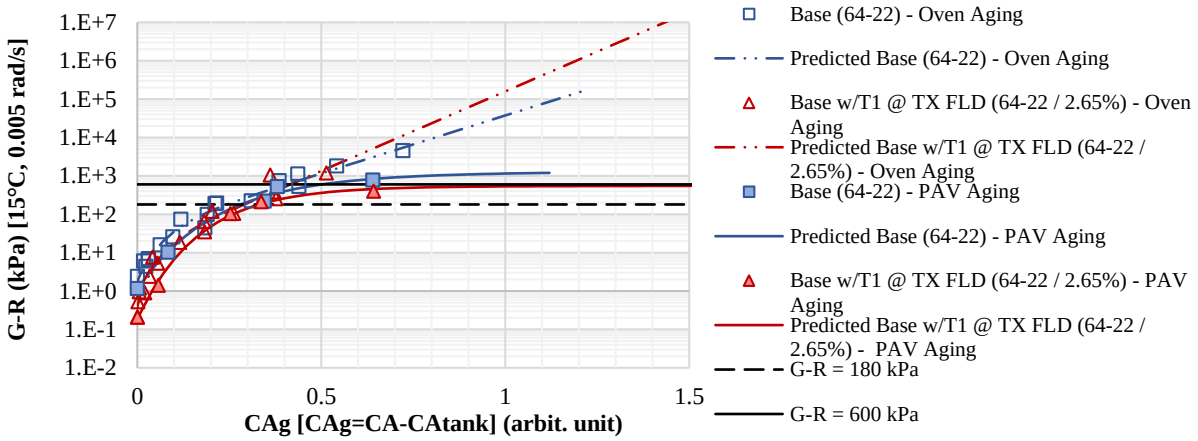

(a)

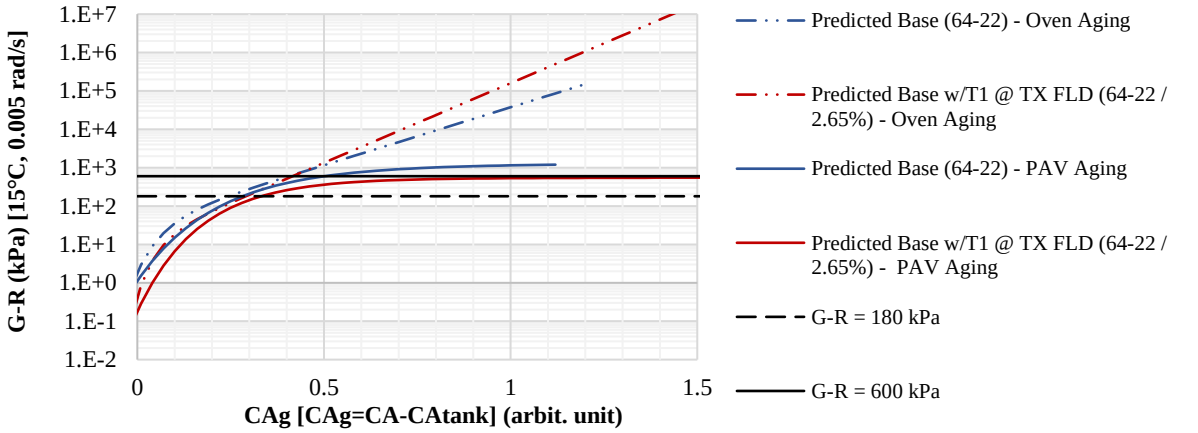

(b)

Figure 5. 29. Comparison of HS in G-R Parameter at 15°C between Forced Draft Aging and Accelerated Aging protocols for PG 64-22
(a) Completed (b) Summarized

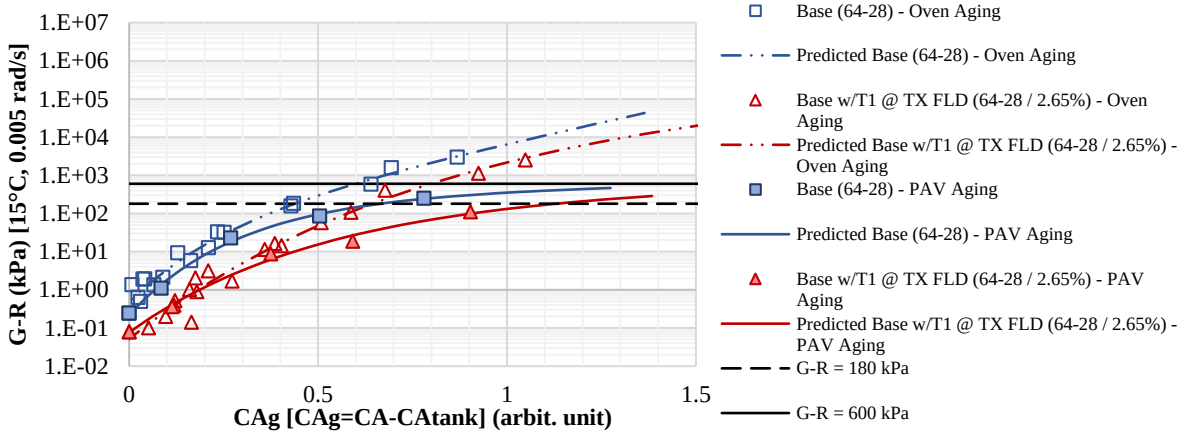

(a)

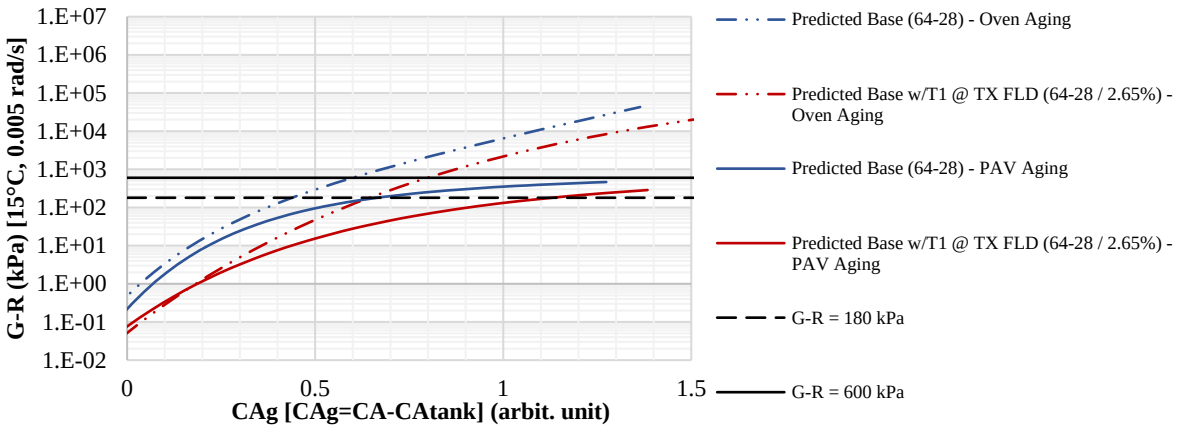

(b)

Figure 5. 30. Comparison of HS in G-R Parameter at 15°C between Forced Draft Aging and Accelerated Aging protocols for PG 64-28 (a) Completed (b) Summarized

Consideration of the SBS modified 64-28P binder found in Figure 5. 31 indicated that the HS relationship was considerably less dependent upon the two aging protocols with the base binder. Although a fairly consistent HS relationship over the range of evaluated aging levels was observed with the base binder, the addition of T1 cause the two aging protocols to noticeably deviate from each other. Similar to the other base binders, the required CA growth to reach the cracking limits were fairly similar in the two protocols except for the T1 blend in the accelerated aging. Such an obvious deviation in this blend might be an indication of hidden interactions between T1 and the binder components particularly SBS.

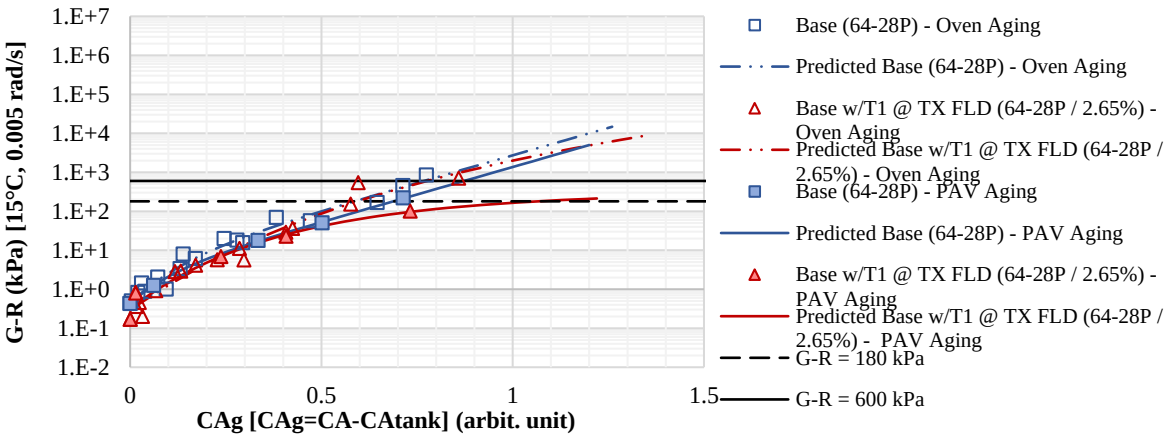

(a)

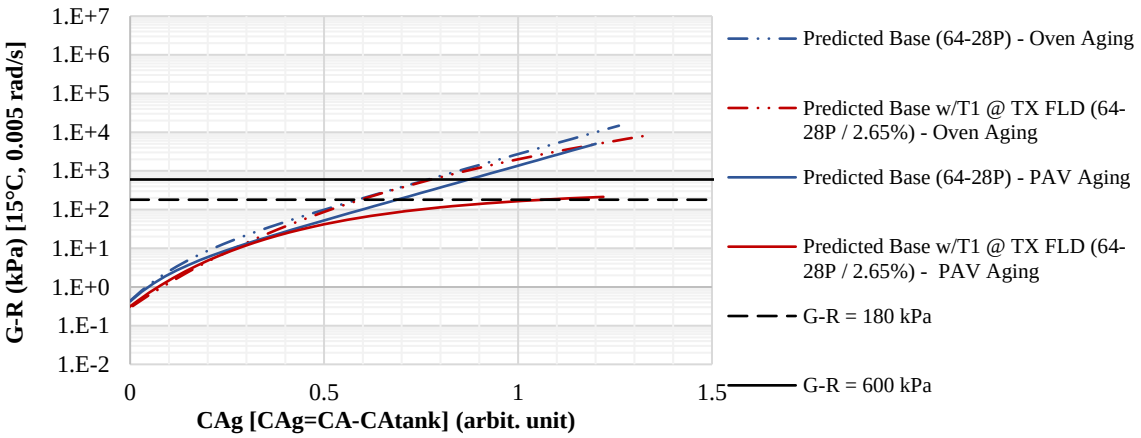

(b)

Figure 5. 31. Comparison of HS in G-R Parameter at 15°C between Forced Draft Aging and Accelerated Aging protocols for PG 64-22 (a) Completed (b) Summarized

In addition, general observations of the HS plots at the first three points, indicating the HS in original, short-term aged (RTFO), and long-term aged oxidation level, showed that the two aging protocols were representing relatively similar results. This observation might suggest a decent correlation between the forced draft oven aging protocol with the short and long-term aging procedures currently outlined in the AASHTO M320 with the specific binders utilized in this study. However, acknowledging the temptation toward utilizing higher temperatures and pressure during laboratory oxidation studies to reduce the required aging durations, caution must be taken in the selection of PAV aging protocol in which the

aging pressure and temperature substantially deviates from pavement sections in actual field condition. In this case, careful evaluations are highly recommended to monitor the oxidation progress and corresponding aging products. While a full evaluation of the particular attributes of differing aging protocols is outside the scope of this study, proper attention should be paid to the aging temperatures, aging durations, oxidation pressures, as well as the quantity of asphalt binder being aged. The quantity of material is specific to the film thickness or mass of binder that the oxygen must diffuse through to age an asphalt binder within a study, which definitely affect the aging progress.

5.4 Summary of the Chapter

This chapter mainly focuses on the analysis of the oxidation kinetics and rheological performance resulting from the FT-IR test and the DSR isothermal frequency sweep test. The kinetic results indicate that the oxidative aging rate are influenced by the aging temperature, duration, base binder type, and the utilized asphalt modifier, i.e. recycled materials and RAs.

For the rheological performance analysis, the master curve was created by shifting the isothermal frequency sweep data within the aid of the software RHEA (Rhea, 2011). Then the rheological parameters, i.e. G*, phase angle, LSV, G-R (at 15°C and 0.005 rad/sec) were implemented along with the CA measurements to provide the HS plots for evaluating the oxidative aging and the different modifier's effect. From both aging protocols, i.e. forced draft oven aging and accelerated aging, it was concluded that both RAs reduced the overall stiffness in the investigated stages of oxidation. However, differential aging rates or HS were observed between the RA and RAP/RAS additions to each of the three base

binders from the forced-draft oven aging. In fact, the base binder aging properties due to the addition of the recycled material was highly influenced by the RA dosages within each blend. This finding highlights the importance and effect of the dosage selection on the binder aging behavior. Further, the noted differences were not consistent with the type of RAS, i.e. MWAS or TOAS. In general, the differences in the base binders and the type of RAS potentially let to the difference in the interaction of all the blended materials, resulting in the overall difference in aging behavior.

Additionally, multiple linear regression analysis was conducted on the LSV HS plots to explore the significance of variation of the modified binder blends aging path to that of the corresponding base binders. The results indicated that the addition of the RA only did not generally change the slope of the HS plots. Also, a non-significant deviation from the base binder aging path were observed upon the addition of the recycled materials except for one of the binder blends. Therefore, additional investigations were recommended to confirm the validity of the statistical analysis measurement before making a clear differentiation between the overall behaviors of the base binder with the modified-blends.

General observations of the HS plots showed that the two aging protocols were representing relatively similar results. However, caution must be taken in the selection of PAV aging protocol in which the aging pressure and temperature substantially deviates from actual field condition.

Additionally, the evaluation of the cracking potential of the PAV aged binders through ΔTc and G-R parameter did not indicate a strong correlation between the these cracking indicators, due to the different states of material evaluation at intermediate and low

temperature, noting the constant temperature of 15°C and constant frequency of 0.005 rad/s for the G-R parameter. Further, the required PAV time duration for each of the respective binders to reach the G-R cracking limits were investigated at modified temperatures of 15°C, PG.mid and PG.low+43. The results yielded to some levels of discrepancy between the observations of the binder behaviors, highlighting the necessity of further investigation on the actual in-place pavement mixture specimens to properly understand what happens in reality rather than just binder evaluations.

CHAPTER 6 OXIDATION PREDICTION

The binder blend aging predictions or oxidation modeling evaluation has been introduced to evaluate the combined influence of both oxidation kinetics and rheological changes on the binder characteristics with age. This effort partially stems from the highly material-specific influence of multiple components observed through the various modes of laboratory testing. In a general sense, the oxidation predictions are made through combined kinetics and hardening susceptibility (HS) models driven by temperature estimation modeling within a given pavement section at a given geographic location. A general description of each aspect is provided below; however, more detailed explanations of the models are best viewed in the respective literature.

6.1 Temperature Profile Prediction

Accurate pavement temperatures data at various depths of the AC surface layer and over time are required to estimate the oxidation level of the asphalt binder. An improved model has been developed and employed to predict pavement temperatures at various depths of pavement (up to 3 meters below the surface) and over time. The development of the proposed model was mainly benefited from the efforts conducted at Texas A&M University (Han et al. 2011) and Arizona State University (Gui et al. 2007). The proposed model requires hourly air temperature, solar radiation, wind speed, and thermal diffusivity properties of the pavement layer materials (i.e., conductivity, density and heat capacity), as well as monthly variable pavement surface radiation properties (i.e., albedo, emissivity and absorption coefficients) to perform the calculation. In this particular study, the hourly

air temperature and wind speed data were obtained from the Enhanced Integrated Climatic Model (EICM) database while the synchronized solar radiation data were gathered from the national solar radiation database (NSRD). Additional advancements of the prediction methodology resulted in numerical calculations of the proposed heat transfer model are completed using finite control volume method (FCVM) in a fully implicit scheme (Alavi, 2014). The improved time-dependent surface boundary condition accounts for a variation in the surface radiation properties, allowing for a better simulation of heat transfer mechanism in the pavement and thus more realistic predictions of pavement temperatures. The discontinuity in the thermal diffusivity properties of the various pavement layers can be handled unconditionally with FCVM by assigning specific thermal diffusivity properties to each control volume. The bottom boundary condition in this model is defined independent of the pavement location by assuming a constant heat flux instead of a constant temperature boundary condition. Furthermore, the numerical solution of the model in implicit time scheme results in a significant reduction in the required time of calculation. The model was validated for different LTPP sections, located in Kingman, Arizona, and Great Falls, Montana. Details of the model components, calculation approach and validation results are available in a separate literature by Alavi et al. (2014). Currently, the research team at the University of Nevada, Reno, has optimized this model and developed a stand-alone calculation tool called Temperature Estimate Model for Pavement Structure (TEMPS) (http://www.arc.unr.edu/Software.html#TEMPS). A general schematic of the inputs has been provided in Figure 6. 1. Additionally, Figure 6. 2 presents an example of predicted hourly pavement temperatures for one year of analysis (i.e., June 2014 to May 2015) at various depths in the AC surface layer for the NV field project location.

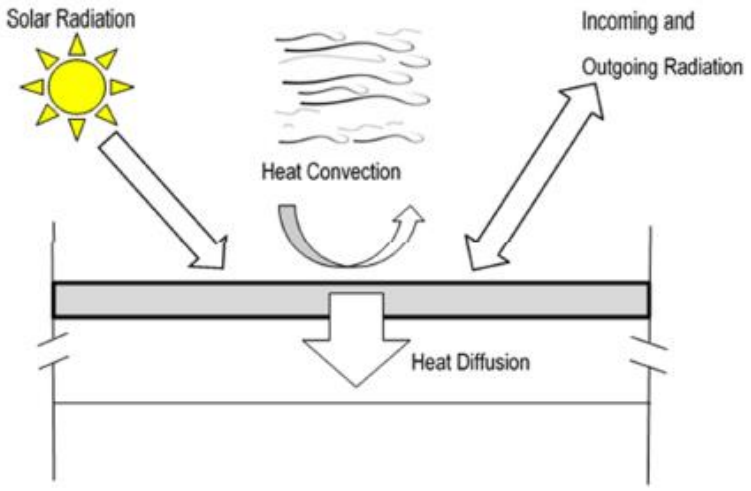

Figure 6. 1. Heat Transfer Model of Pavement and Surrounding Environment

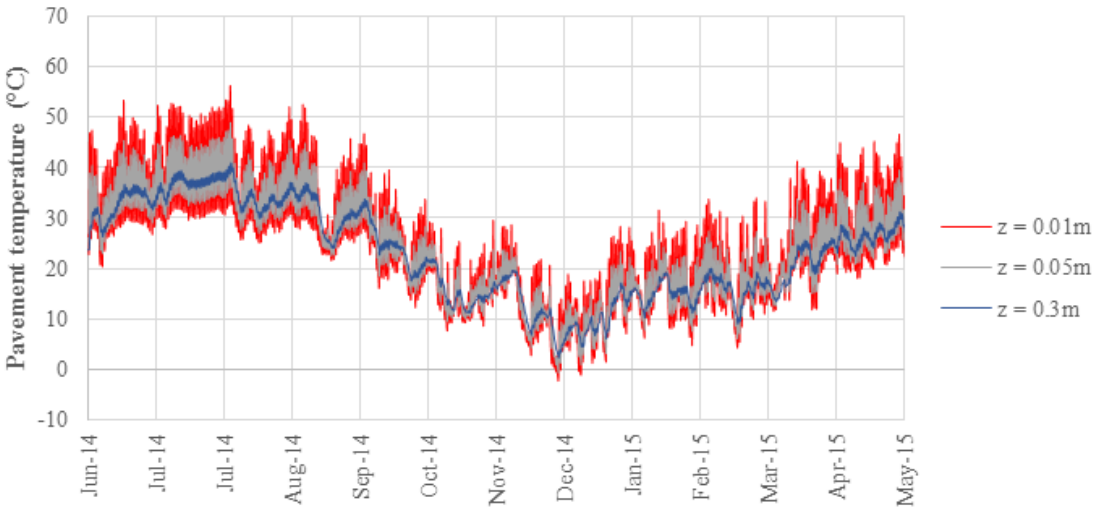

Figure 6. 2. Predicted Pavement Temperature at Various Depths of Asphalt Mixture Surface Layer in Reno, NV Environment

6.2 Oxidative Aging (Carbonyl Area) Prediction

The evolution of oxidation represented as carbonyl area (CA) with time for the asphalt binder at a specific depth in the pavement was predicted using a diffusion-based oxidative aging model, which were developed at the Texas A&M University (Han et al. 2013). The inputs for the aging model are as follows:

- Predicted hourly pavement temperatures at the selected depth in the asphalt concrete layer, e.i. utilizing TEMPS output.
- Asphalt binder aging kinetics (E_a and A) and hardening parameters (HS and m).
- Asphalt binder initial carbonyl at the beginning of constant-rate aging.
- Average representative air void radius and effective aging distance (e.g., asphalt binder film).

In summary, the CA values at various sub-layers in the asphalt binder film are predicted by knowing the oxygen partial pressure at these sub-layers and the oxidative aging kinetics of the asphalt binder. The oxygen partial pressures are estimated from a numerical solution of a partial differential equation with age-dependent diffusivity. The oxygen diffusivity of the binder correlates well with the low shear viscosity (LSV) of the binder. The age-dependent diffusivity is defined by relating the asphalt binder LSV to the hardening susceptibility properties (HS and m) of the binder. Details of the aging model can be found in the respective literature (Han et al. 2013, Alavi 2014). The aging model can be simplified if the gradient of oxygen pressure into the pavement depth is neglected, i.e. full oxygen availability throughout the pavement structure. In this case, the model only requires pavement temperature profile, asphalt binder kinetic parameters (E_a and A) and CA_{tank}. Numerical computation of the aging model is also performed using finite control volume method (FCVM) in implicit time scheme. Oxidative aging kinetics and hardening parameters of the model can be determined through measurements of CA and low shear viscosity (LSV) of the asphalt binder after being aged at various combinations of time and

temperature. The CA of the asphalt binder is measured by Fourier Transform Infrared (FT-IR) Spectroscopy, and the LSV is determined from the complex modulus, which is measured using the Dynamic Shear Rheometer (DSR). A general outline of the overall process is provided in Figure 6. 5.

The use of this procedure permits the relative comparison of the evaluated binder blends in terms of an estimated time to reach any physical measurement that can be correlated back to the oxidation level, e.g. CA level. In this particular case, it is of interest to identify the expected field aging specific to the two predefined G-R limits (i.e., 180 kPa and 600 kPa), which was discussed in Chapter 5, as a function of time in-service at a given environment. Note that, while these are hypothetical aging simulations utilizing measured chemical and rheological binder properties at a particular environmental condition; they are valuable comparisons to be made between respective binder blends.

6.2.1 Determining Oxidative Aging (Carbonyl Area) Prediction Model Inputs

To determine the inputs for the CA prediction model, the hourly pavement temperature profile was determined at the pre-selected depth of 0.01m utilizing the TEMPS software discussed in the previous section. As the next step, the oxidative aging kinetics including the activation energy (E_a) and pre-exponential factor (AP^{α}) were determined for all the binder blends at each respective aging temperature through the correlation between the CA values and the aging durations; the process is widely discussed in Chapter 5 and results are provided in Appendix B.

The HS plots of the G-R parameter as a function of carbonyl area growth were previously discussed in detail in Chapter 5. However, a different format of the HS plots is originally

employed in the TX CA prediction model which is the relationship between the binder low shear viscosity (LSV) at 60°C and the corresponding CA over the range of the aging temperatures and durations due to the dependency of the oxygen diffusion model upon the level of LSV as a sub calculation of the overall oxidation prediction model. The HS plots for the three base binders and their respective blends are provided in Appendix B, and Figure 6. 3 shows an example of those for PG 64-28 binder blends. Generally, an exponential correlation was found between the LSV and CA, and expectedly, the higher the level of aging, the higher the low shear viscosity. Detail information regarding HS plots interpretations can be found in Chapter 5. Subsequently, the slopes (HS) and intercepts (m) of the plots were determined for each respective binder blend as the second series of inputs in the CA prediction model (Table 6. 1).

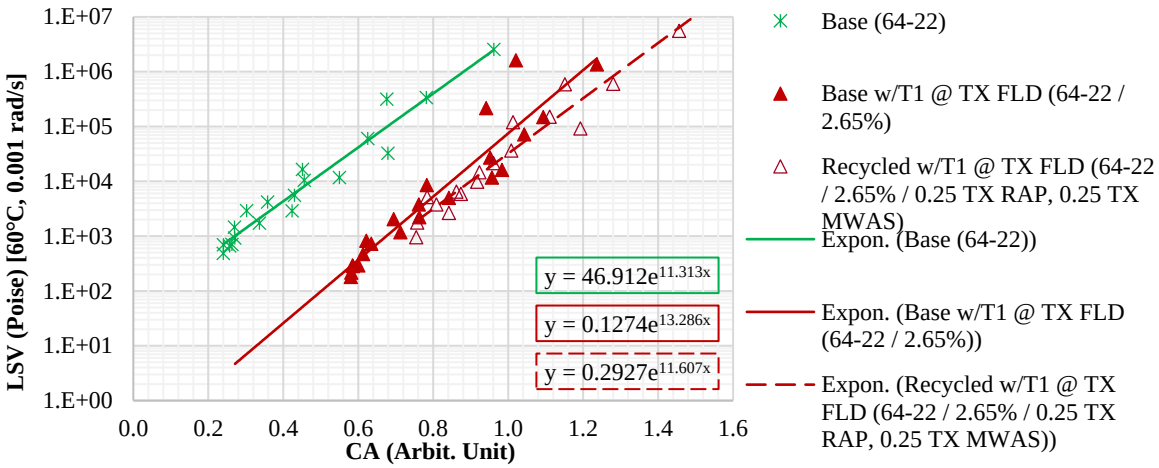

Figure 6. 3. Low Shear Viscosity (LSV) at 60°C for PG 64-22 Base Binder

Regarding the third input for the CA prediction model, i.e. asphalt binder initial carbonyl at the beginning of constant-rate aging, it should be mentioned that utilized CA prediction model uses the original asphalt binder CA, i.e. CA_{tank}, as an input value. However, in this

study, it was considered more appropriate to conduct the CA prediction from the approximate aging level of the plant-produced material, i.e. short-term aging. Therefore, the CA prediction has been conducted upon the RTFO-aged binder as the CA prediction starting point (CA_{RTFO}).

As the last input, the average representative air void radius and effective aging distance (e.g., asphalt binder film) was assumed to be 0.65 and 1, respectively based on a research by Han (2011) using X-ray CT technique and image processing. The values used in this study are within the range of observed values for a typical asphalt mixture.

In summary, details of all inputs for the utilized binders from the experimental plan discussed in Chapter 4, are shown in Table 6. 1, noting that the temperature dependent values of k_c are not an input to the oxidative aging prediction but are combined into the oxidation kinetics, e.g. Ea and pre-exponential factor, but are mentioned here for later investigations in this chapter.

Table 6. 1. Oxidative Aging Model Parameters for The Evaluated Asphalt Binders

	Binder ID	E_a [1] (kJol.mol^{-1}. °K^{-1})	Pre-exponential Factor[2], AP^{α}	HS [3] (1/CA)	m [4] (ln(poise))	CA_{RTFO} [5] (arbit. unit)	k_c Temperature (°C)		
							60	85	100
TX	Base (64-22)	75	1.129E+09	11.31	46.91	0.323	0.002	0.013	0.035
	Base w/T1 @ TX FLD (64-22 / 2.65%)	76	1.357E+09	13.28	0.12	0.637	0.002	0.012	0.034
	Recycled w/T1 @ TX FLD (64-22 / 2.65% / 0.25 TX RAP, 0.25 TX MWAS)	64	4.049E+07	11.61	0.29	0.857	0.003	0.016	0.038
NH	Base (64-28)	65	5.189E+07	9.46	201.22	0.131	0.003	0.018	0.042
	Base w/T1 @ TX FLD (64-28 / 2.65%)	69	2.354E+08	8.92	6.55	0.420	0.004	0.022	0.056

	Recycled w/T1 @ OPT (64-28 / 12.5% / 0.25 TX RAP, 0.25 TX TOAS)	70	1.400E+08	8.43	1.00e-05	2.446	0.001	0.009	0.022
	Base w/A1 (64-28 / 6%)	70	3.700E+08	8.16	123.22	0.107	0.004	0.021	0.053
	Recycled w/A1 @ OPT (64-28 / 6% / 0.40 TX RAP)	73	8.101E+08	5.93	75.43	0.679	0.003	0.020	0.052
NV	Base (64-28P)	73	5.931E+08	6.53	997.61	0.067	0.002	0.015	0.041
	Base w/T1 @ TX FLD (64-28P / 2.65%)	79	4.709E+09	8.90	22.91	0.383	0.002	0.013	0.038
	Recycled w/T1 @ OPT (64-28P / 11% / 0.25 TX RAP, 0.25 TX TOAS)	86	5.045E+10	6.12	0.01	2.112	0.002	0.013	0.043

[1] E_a: Activation energy
[2] AP^{α}: Pre-exponential factor
[3] HS: Hardening susceptibility
[4] m: hardening function constant
[5] CA_{RTFO}: the CA after RTFO aging

6.2.2 Modeling of the Pan-Aged Binder Oxidation

The oxidative aging growth of the pan-aged binder blends can be simulated through the TX CA prediction model described in the previous section. The thickness of the binder film in the PAV pans were prepared at 1 mm and the atmospheric oxygen pressure was approximated to be 0.198 at the University of Nevada, Reno laboratory. Using the CA prediction model (Han 2013, Alavi 2014) with the corresponding inputs discussed in the previous section, the CA values were predicted for all the experimental binder blends. The summary outputs of CAg predictions for the Base 64-28P blended binders over the 18-year analysis period and at 0.01 m below the surface in Reno, NV location is provided in Figure 6. 4. Also, an example of the complete output is presented in Appendix C.

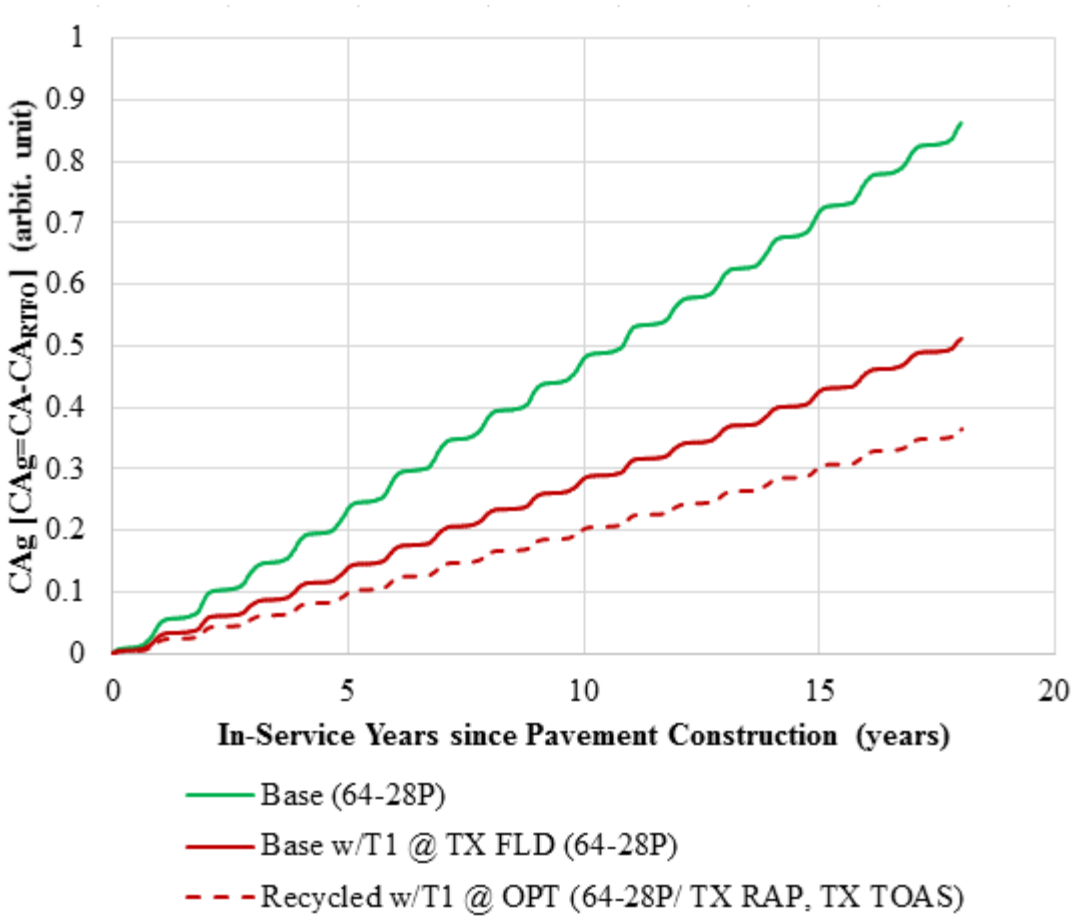

Figure 6. 4. Carbonyl Area Prediction in Asphalt Mixture Surface Layer for Base 64-28P Binder Blends in Reno, NV Environment

6.3 Pavement Life Prediction

Utilizing the CA predictions from all three of the base binder blends in the aging experimental plan resulted in the estimated time to reach the two G-R limits (i.e., 180 kPa and 600 kPa) as a function of time in-service at field experiment. A general outline of the overall process has been provided in the Figure 6. 5. As observed, the process started with conducting the hardening susceptibly plots based on the DSR and FT-IR test result on the pan-aged binder blends, which was widely discussed in Chapter 5. Then, the CA level corresponding to G-R values of 180 and 600 labeled as $CA_{G\text{-}R=180}$, $CA_{G\text{-}R=600}$, respectively,

were determined for each binder blend from the respective trend line. In the next step, the simulated time to reach that CA level was determined following the oxidation prediction model. The oxidation model was derived through inputs of the temperature profile history using the previously discussed inputs namely solar radiation, albedo, emissivity, and absorption coefficients through the TEMPS software. The Texas Oxidation Aging Model were then fed with TEMPS output along with the other inputs presented in Table 6. 1. It should be noted that the temperature profile prediction for each of the three different base binders, i.e. TX 64-22, NH 64-28, and NV 64-28P were conducted at their particular environments, i.e. TX (Tyler), NH (Durham) and NV (Reno), respectively. The concept being explored by such a differentiation was to simulate the binder aging behaviors in the actual environment that they often experience in practice. Eventually, the Texas Oxidation Aging Model outputs were combined with the $CA_{G\text{-}R=180}$ and $CA_{G\text{-}R=600}$ to determine the respective time required to reach the G-R cracking thresholds in an asphalt pavement constructed in the actual selected environment conditions.

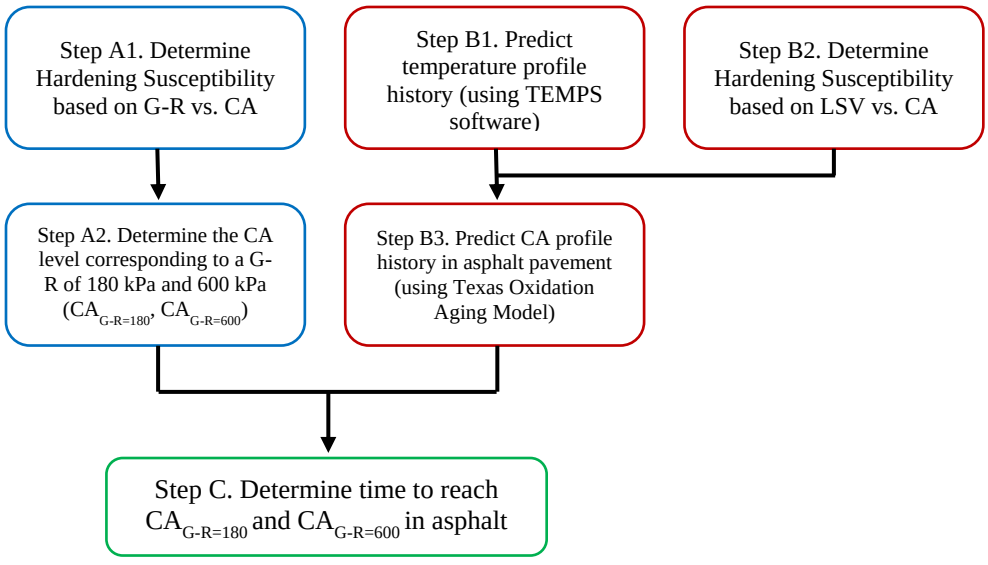

Figure 6. 5. Outline of G-R Parameter Thresholds from Simulated Field Aging

Consequently, Figure 6. 6 through Figure 6. 8 provide a materials specific comparison of the respective binder blends to help decipher the overall influence of the oxidation kinetics and HS relationships noted previously to identify the simulated time to reach the G-R limits for the onset of cracking (i.e., 180 kPa) and significant cracking (i.e., 600 kPa). Observations of the three figures and consequential interpretation of the determined values highlight the complex nature of the potential interactions taking place between the different components in these blended binder systems.

Considering the blended binders containing the PG 64-22 as base shown in Figure 6. 6, there is a systematic influence of the added components. The addition of the T1 at 2.65% dosage rate softens the blend and restores some of the flexibility in the blend, exhibited by longer durations to meet the respective G-R thresholds. Additions of the TX RAP and TX MWAS components resulted in a drastic reduction in the softening effect of the T1. This reduction has resulted a reduction in the simulated duration to G-R limits to a duration shorter than that of the base, acknowledging the fact that all G-R parameters were determined at the standard 15°C. It should be noted that the 2.65% dosage was not the optimum dosage, and this might be a reasonable justification for the reduced in-service years of the recycled blend.

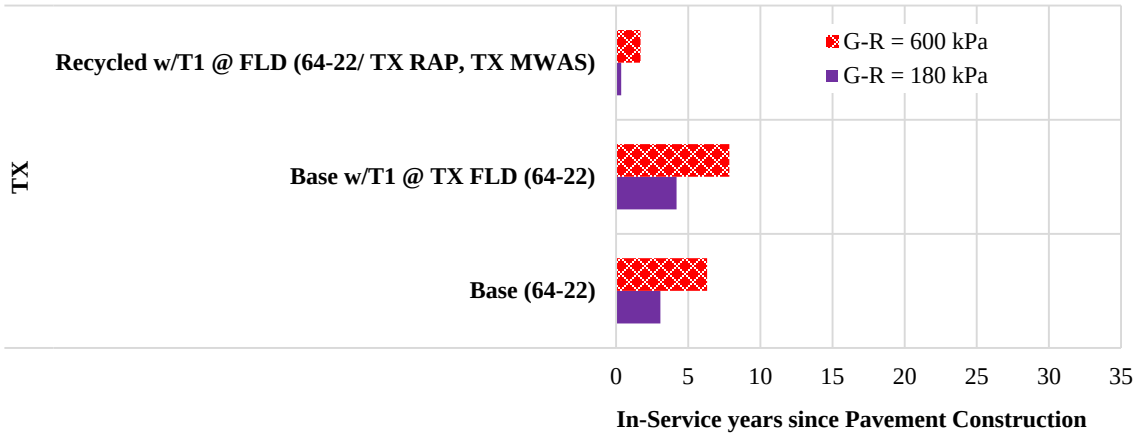

Figure 6. 6. Simulated Time to Reach G-R=180 and G-R=600 in Asphalt Pavement for PG 64-22 Binder Blends (in Reno, NV Environment)

Considering the PG 64-28P blended binders in Figure 6. 7 resulted in similar findings for the respective influences of the various components. The exception noted with this polymer-modified blend was found to be the onset of cracking limit of 180 kPa for the recycled blend was observed at a time interval similar to the base PG 64-28P binder, while the significant cracking limit of 600 kPa was simulated to occur substantially after the base binder. Numerically, this is understood to be the result of the slightly lower oxidation rate or k_c factor combined with the lower HS or flatter slope noted with the recycled binders (can be observed from Table 6. 1), while acknowledging the differences between the field and Optimum dosage rates, i.e. 2.65 and 12.5% by binder replacement, respectively. Physiochemical considerations suggest the potential reduction in the oxidation rate and HS terms may be the initial indication of oxygen diffusion limiting conditions in the laboratory measures as opposed to the assumed oxidation reaction controlled assumptions of the experimental design. A potential explanation for this occurrence is suggested that perhaps with this particular blend of recycled materials, T1, and polymer loading, the oxidation of

the binder may be hindered by some or all of these additional components. Whether this limitation is a simple function of increasing concentrations of non-binder components or the creation of a longer more tortuous oxidation path for oxygen molecules to diffuse through is not fully understood. Inherent to the model prediction is the understanding that the oxygen diffusion rate is inversely dependent upon the binder stiffness, numerically represented by the low shear viscosity (LSV) input relationships. The actual extent of these influences is particularly unknown at this point stemming from the relatively limited understanding of the true degree of blending or remnant heterogeneity remaining within a plant produced mixture. This becomes potentially significant when recalling that these simulations are driven by fully blended binder inputs derived in the lab, although the true homogeneity of the RAS containing blends has also been brought into question.

Nonetheless, the data in Figure 6. 7 show that a similar or better performance for the recycled blend relative to the base binder can be obtained with the optimum dosage of T1.

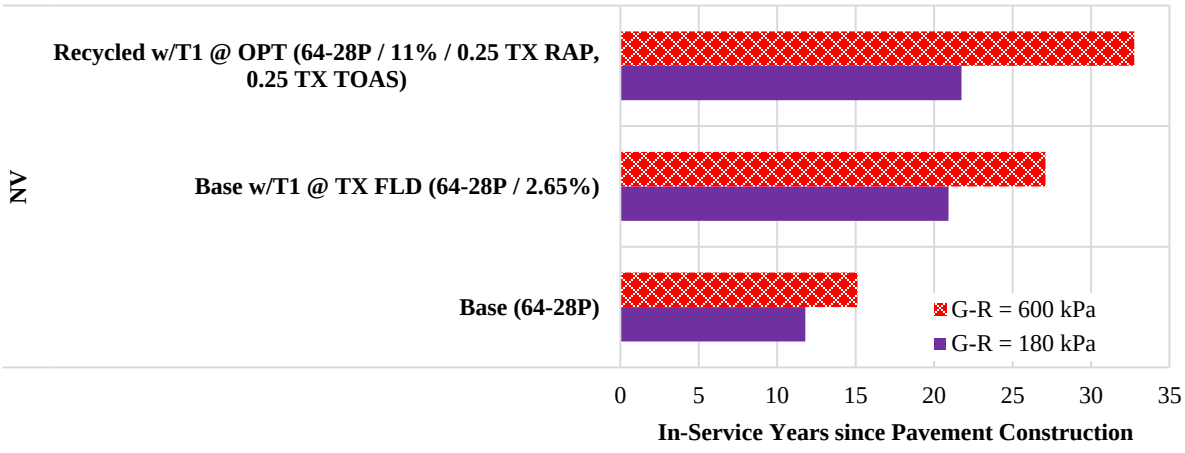

Figure 6. 7. Simulated Time to Reach G-R=180 and G-R=600 in Asphalt Pavement for PG 64-28P Binder Blends (in Reno, NV Environment)

A nearly identical discussion of the PG 64-28 base binder presented in Figure 6. 8 with the A1 RA and RAP material would also be appropriate. An increase in the time to reach the G-R limits was observed when either T1 (at non-optimum dosage) or A1 (at optimum dosage) was added to the PG 64-28 base binder. The addition of recycled materials to this base binder with T1 at optimum dosage resulted in an increase in the time to reach the G-R limits; thus, demonstrating the efficiency of the T1 when used at the optimum dosage. The addition of recycled materials to this base binder with the A1 resulted in similar behavior to that of the base binder with only A1 at the same dosage. Considerations of the diffusion limitation potential becomes even more prominent with the PG 64-28 and the respective blends containing the T1. In this case, both the k_c and HS terms of the recycled blend were lower than for the base with only T1 or even the PG 64-28 base binder. Both of which combined to simulate a much slower oxidation and thus longer time duration to the G-R limits. It is also important to note the differences in the dosages between the blend of the PG 64-28 base binder and T1 only (i.e., at the field dosage of 2.65%) compared to the optimum T1 dosage of 12.5% when TX RAP and TX TOAS were included. Despite the similarities in the dosage of the T1 as well as the TOAS in both the PG 64-28 and PG 64-28P blends, the influence of those components was not consistent.

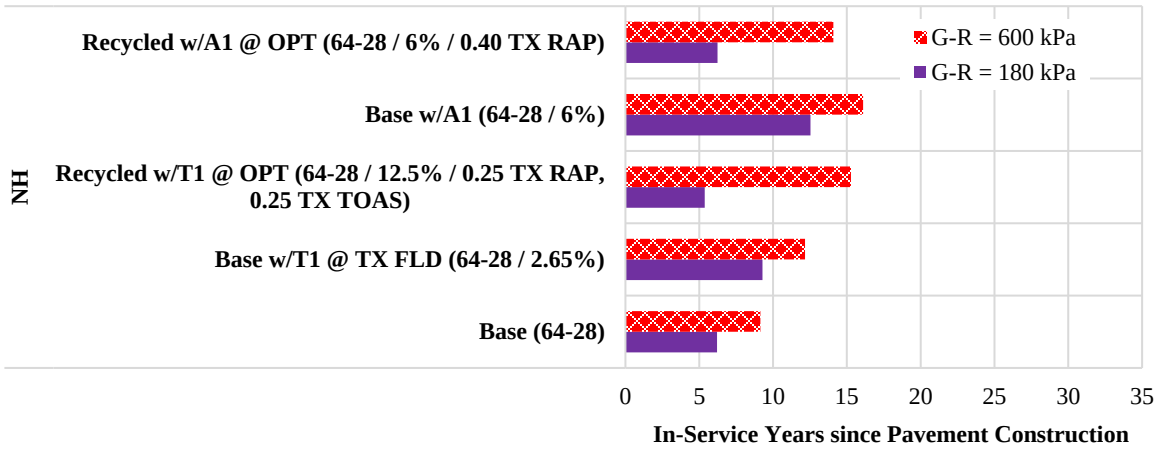

Figure 6. 8. Simulated Time to Reach G-R=180 and G-R=600 in Asphalt Pavement for PG 64-28 Binder Blends (in Reno, NV Environment)

For the sake of a relative comparison, Figure 6. 9 demonstrates the simulated in-service years since pavement construction to reach the onset and significant cracking limits of G-R = 180kPa and 600kPa, respectively. Logically, all the binders took longer simulated in-service years to reach the significant cracking level compared to the onset level. In addition, the effect of the recycling agents and recycled materials can readily be observed from Figure 6. 9, noting the base binders are signified with hollow markers as the point of reference within each binder type. The binder blends with recycling agents and without any recycled material are shown with solid, while the ones with both modifications are represented by hatched markers. The blends with recycling agents only (solid markers) showed a clear increase in the predicted life, or delay in the onset of cracking, compared to the base binder (hollow markers). Thus, both recycling agents, T1 and A1, had a beneficial effect on the base binder life time. With the larger the dosages resulting in more substantial benefits of the recycling agent, pointing to the PG 64-28 blend with A1 at 6% dosage rate. However, this consistent trend does not continue with the inclusion of the

recycled material, which tends to counteract the RA as expected. The simulated oxidative aging predictions generally provide the following conclusions:

- The addition of the recycled material at the 2.65% dosage to the PG 64-22 base binder significantly reduced the predicted in-service year. In the other words, the 2.65 % was not a high enough dosage to be able to restore the binder properties including 0.30 RBR (0.20 RBR of TX RAP and 0.10 RBR of TX MWAS).
- There are two recycled blends with the PG 64-28 base binder; the recycled blend with an optimum dosage of 12.5% and 0.50 RBR (0.25 TX RAP and 0.25 TX TOAS) nearly presented a restoration to the base binder in the onset cracking and even an improvement in significant cracking limits. Similarly, the recycled blend with A1 at the optimum dosage of 6% and 0.40 RAPBR represents a slightly better restoration to the base binder. These two observations imply that using the RAs at the optimum dosage can potentially have a positive influence on restoring the binder properties.
- The 64-28P recycled blend contained 0.50 RBR including 0.25 of RAP and 0.25 of TOAS at 11% (optimum) of T1. The optimum dosage of the T1 along with the high RBR ratio of 0.5 not only restores the binder blend life prediction to the base PG 64-28P, but also improves it for almost 6 years.

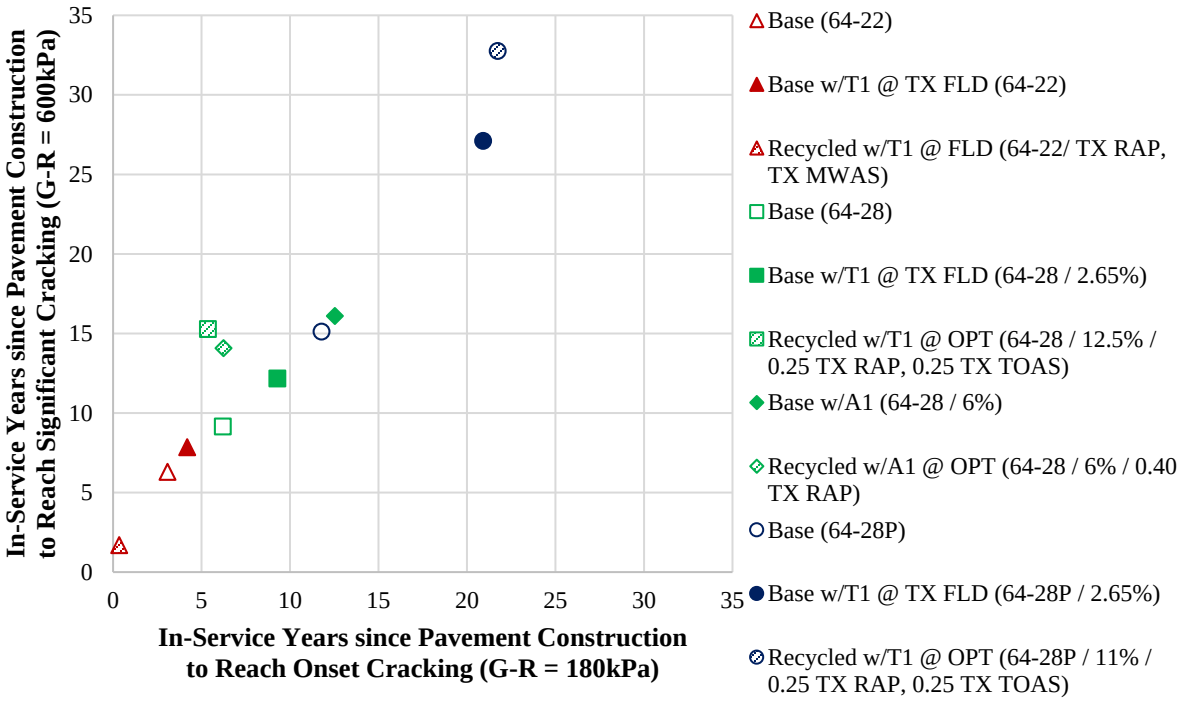

Figure 6. 9. Overall Comparison of the In-Service Years to Reach the G-R Threshold, Including All Binder Blends at Binder Specific Locations

Additionally, for the sake of comparison, the in-service years to reach the G-R thresholds for PG 64-22 and PG 64-28 binder blends were also predicted in Reno, Nevada environment. The overall direction of the results in Figure 6. 10 were observed to be similar to the discussed condition in which base binder specific location were implemented for the binder blends. However, the PG 64-22 and PG 64-28 binder blends showed a reduction in the pavement life due to the change in the location, implying a better performance of the binder blends in the binder specific locations. It is noteworthy to emphasize all the G-R parameters were calculated as constant temperature of 15°C and constant frequency of 0.005 rad/sec.

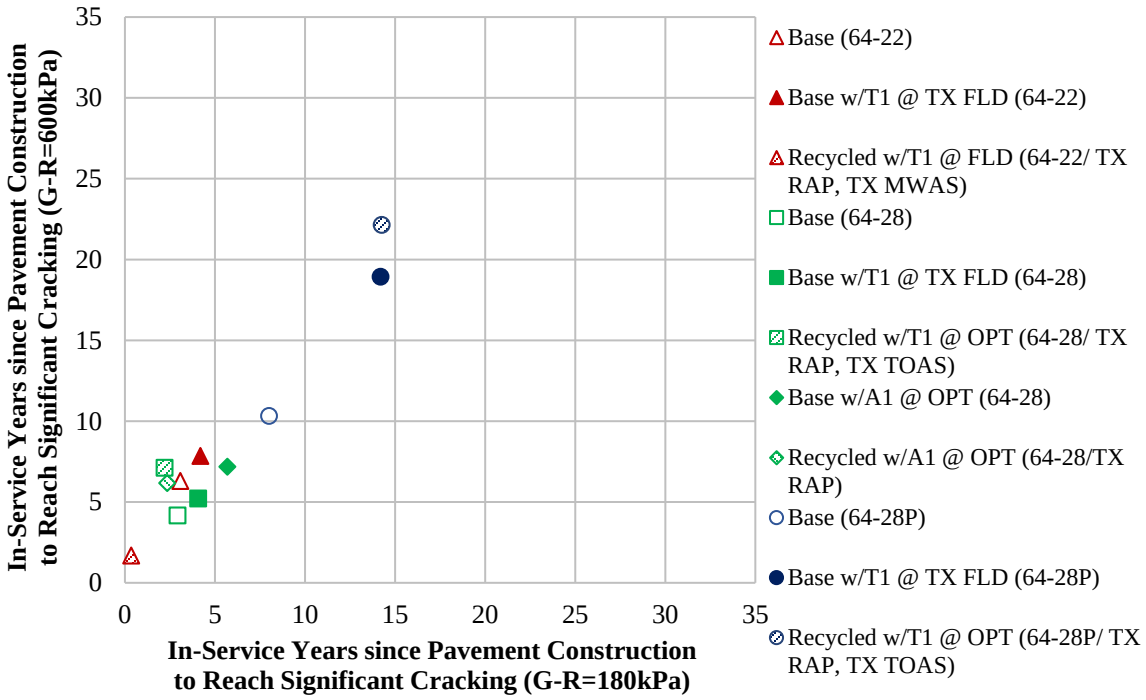

Figure 6. 10. Overall Comparison of the In-Service Years to Reach the G-R Threshold, Including All Binder Blends at Reno, NV Environment

Acknowledging the differences in crude source and realistic discrepancies in the geographic location of usage with each binder, make side-by-side comparisons potentially limited while they still add to the comprehension of the overall evaluation technique. The resulting time simulations of the base binders culminate in the influence of the determined k_c rates combined with the relative differences in the HS relationships. Specifically, it should be noted that there was a minor reduction in the k_c terms of the PG 64-28P binder relative to the other two base binders (particularly at the lower temperatures, i.e. higher 1/RT values). Similar k_c terms for the PG 64-28 and PG 64-22 base binders yielded modest G-R duration simulations when compounded by the minor discrepancies noted in the HS between the two. These conditions were further exemplified by the lower HS for the PG

64-28P base binder resulting in the longest simulated G-R limit durations of the three base binders.

In summary, the binder blend oxidative aging predictions were helpful in identifying the influence of RA at the respective dosages and recycled material on the cracking potential of the various evaluated binders at a given geographical location. The results indicate that using the recycled materials along with the recycling agents at the optimum dosage, though not always at the field dosage, was able to restore the binder blend properties to the virgin binder. Thus confirming on the RA dosage selection methodology proposed under this study, which in general showed the need for a significantly higher optimum RA dosage to restore the PG of the base binder when compared to the low dosage used in the field for the example field projects.

6.4 Summary of the Chapter

This chapter focuses on the binder blend aging predictions conducted through combined kinetics and hardening susceptibility (HS) models driven by temperature estimation modeling (using TEMPS) within the binder specific geographic locations, i.e. TX, NH, and NV. The use of this procedure permits the relative comparison of the evaluated binder blends in terms of an estimated time to reach the two predefined G-R limits (i.e., 180 kPa and 600 kPa) as a function of time in-service at their corresponding environments.

Overall, both recycling agents, T1 and A1, showed a beneficial effect on the base binder life; the larger the dosage results in a more substantial benefit of the recycling agent. However, this consistent trend did not continue with the inclusion of the recycled material, which tends to counteract the RAs as could be expected. The results indicated that using

the recycled materials along with the recycling agents at the optimum dosage was able to restore the binder blend properties to the virgin binder. Thus, confirming on the RA dosage selection methodology proposed in Chapter 3, which in general showed the need for a significantly higher optimum RA dosages to restore the PG of the base binder when compared to the low dosage used in the field.

CHAPTER 7 NEVADA FIELD PROJECT DEMONSTRATION

a collaborative effort with University of Nevada, Reno and the NCHRP 9-58 research team, the Washoe County of Northern Nevada implemented a major rehabilitation project on Matterhorn Blvd (PWP-WA-2015-179) in September 2015 to study the influence of rejuvenators on hot mix asphalt (HMA) with high recycled asphalt pavement (RAP) materials. Information regarding the project details including the mix design and construction is presented in Appendix A. The author was responsible for the binder experiment in which the optimum dosage for the employed rejuvenating agents (RA) has been determined. Also, UTSST mixture testing were conducted on the Reheated Plant Mix Lab Compacted (RPMLC) as well as the Plant Mix Field Compacted (PMFC) samples discussed later in this chapter.

7.1 Material

Five different test sections were constructed in Matterhorn Blvd and the description of the RAs and binder blend in each section are presented in Table 7. 1 and Table 7. 2, respectively. Section 1 contains just the original binder and will be further used in the NCHRP 09-58 project to assess the effect of polymer modification by comparing to the other on-going field projects. Section 2 is used as a control section for section 3 and 4 to evaluate the possible benefits comes from the rejuvenating agents. It should be mentioned that since the maximum allowable RAP binder ratio and the actual state of the practice for

recycled material in Nevada is 0.15 RBR for both local and state agencies, one more control sections containing 0.15 RBR had been considered in this project.

Table 7. 1. NV Field Project Rejuvenating Agents Properties

Category	Description	Name	ID
Aromatic Extracts	Refined crude oil products with polar aromatic oil components	Reclamite	A2
Tall Oil	Same chemical family as liquid antistrip agents and emulsifiers	Evoflex	T2

Table 7. 2. Description of Nevada Field Project Test Sections

Section Number	Binder ID	Base Binder Type	RAP (RBR)	RA (Application Method)	Dosage by Replacement (%)
1	Base (64-28P)	NV 64-28P	—	—	—
2	Recycled (64-28P / 0.30 NV RAP)		NV (0.30)	—	—
3	Recycled w/T2 @ OPT (64-28P / 2% / 0.30 NV RAP)		NV (0.30)	T2 (Replacement)	2.0^{OPT}
4	Recycled w/A2 @ OPT (64-28P / 2% / 0.30 NV RAP)		NV (0.30)	A2 (addition)	2.0^{OPT}
5	Recycled* (64-28P / 0.15 NV RAP)		NV (0.15)	—	—

^{OPT} at Optimum dosage (it will be addressed in the "RA Dosage Selection" section)

7.2 RA Dosage Selection

The methodology utilized in the selection of the optimum RA dosage as described in Chapter 3 was employed to determine the A2 and T2 optimum dosages for the recycled blends in the NV field project. At least three different dosages were selected for each RA with respect to manufacturers' recommendations. Then, the binder PG grading tests were conducted on each recycled blend at the selected dosages which are presented in detail in Table 7. 3. Following the methodology, the PG grading test results were plotted as a function of RA dosages for the respective blends, Figure 7. 1 and Figure 7. 2. Following the dosage selection steps specified before in bullet points, the optimum dosage selected for the recycled blends with T2 and A2 came to be 2.60 and 2.40, respectively.

Table 7. 3. Binder PG Grade Results

Binder Blend	RA Type	RA Dosage (%)	High-Temperature Continuous PG Grade (°C)		Intermediate-Temperature Continuous PG Grade (°C)	Low-Temperature Continuous PG Grade (°C)		ΔTc	Final Continuous Grade
			Original	RTFO		S-controlled	m-controlled		
Base (64-28P)		0.0	67	65.6	13.4	-34.3	-30.7	-3.6	65.6-30.7
Recycled w/A2 (64-28P / 0.30 NV RAP)	A2	1.5	72.5	70.6	17.5	-31.6	-29.2	-2.4	70.6-29.2
		2.0	71.9	68.7	16.9	-32.2	-29.8	-2.4	68.7-29.8
Recycled w/T2 (64-28P / 0.30 NV RAP)	T2	1.0	71.2	69.1	17.0	-31.5	-27.7	-3.8	69.1-27.7
		3.0	66.1	65.1	15.0	-33.1	-31.4	-1.7	65.1-31.4
		5.0	61.7	59.2	11.5	-35.3	-34.8	-0.5	59.2-34.8

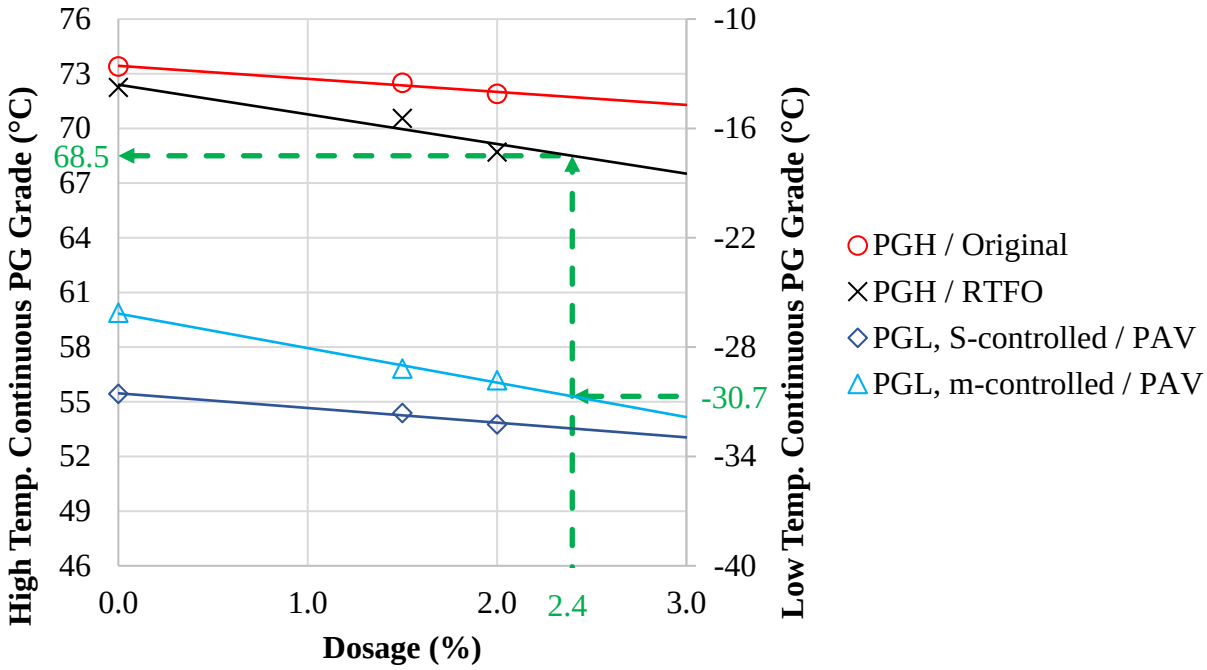

Figure 7. 1. RA Dosage selection for Recycled w/A2 (64-28P / 0.30 NV RAP) in NV Field Project

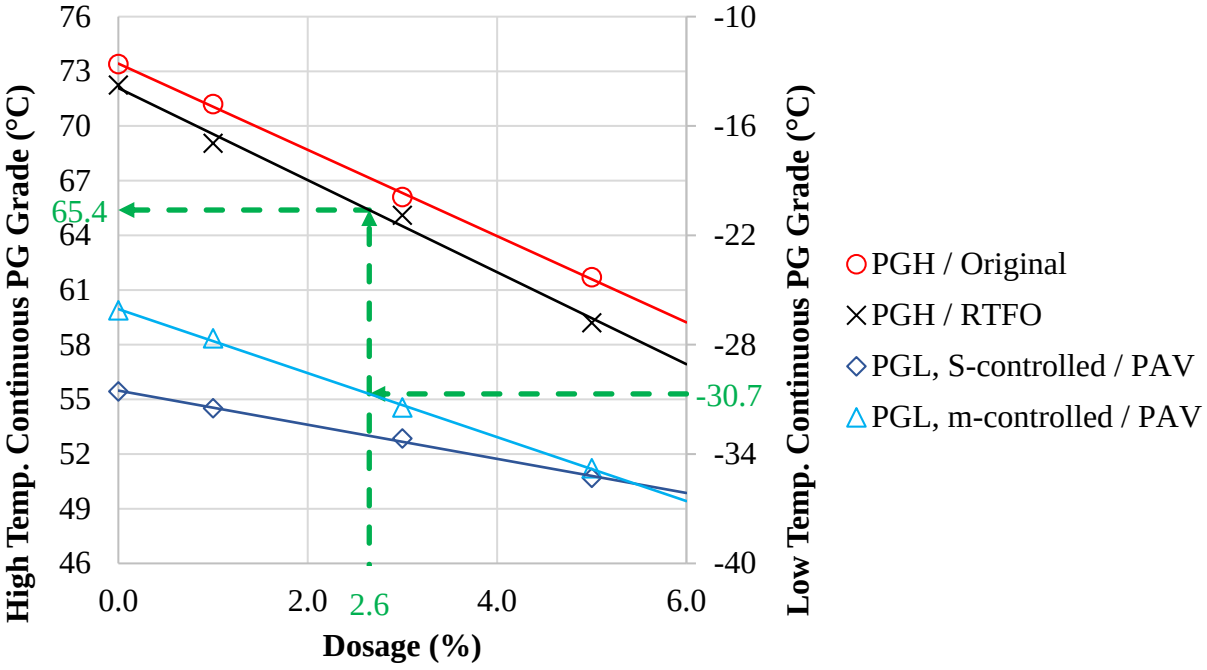

Figure 7. 2. RA Dosage selection for Recycled w/T2 (64-28P / 0.30 NV RAP) in NV Field Project

However, it should be mentioned that no specific methodology had been proposed at the time of the NV field project material preparation; therefore, the optimum dosages were determined based on another methodology developed in University of Nevada, Reno as described in the following:

- Plot original PGH, RTFO PGH, S-controlled PGL, and m-controlled PGL values versus RA dosage
- Establish linear regression equations for each value versus RA dosage
- Select initial RA dosage rate to restore target binder PGL using the limiting (warmer) PGL regression line
- Select initial RA dosage rate to restore target binder PGH using warmer PGH regression line
- Select a balanced dosage rate from the two previously selected dosage range that restores both PGH and PGL to a value close to the target PG continuous grades of control or base binder
- Check the selected dosage to be in the range of the manufacturer's recommendation
- Round the selected dosage to a practically used dosage in the actual field projects

The two methodologies showed quite similar results; however, the NV field project was constructed using 2% as a practical optimum dosage for both A2 and T2 in the recycled blends.

7.3 Binder Blending Results

The binder grading procedure was conducted on the NV field project binder blends according to AASHTO M320 Standard Specification. Corresponding results are presented

in Figure 7. 3 which clearly visualizes influences of the addition recycled material and/or RAs in PG grading results for the binder blends described in Table 7. 2. Apparently, the addition of the NV RAP to the 64-28P base binder at 0.15 RBR increased the high PG grade by almost 3°C, highlighting the stiffening impact of the NV recycled material. Expectedly, it was more pronounced when the RBR of the NV RAP increased to the higher value of 0.30 and as a result, the high PG grade increased by almost a full PG grade, i.e. 6°C. However, the addition of the rejuvenating agents, either A2 or T2, to the 0.30 RBR recycled blend at the optimum dosage of 2% effectively restored the PG high continuous grades. It was also observed that the restoration effect of the A2 at the specified dosage was more pronounced compared to T2 for this particular base binder.

Considering the low temperature trends in Table 7. 2, the recycled blend with 0.15 RAP binder ratio did not show a significant change in the continuous grade compared to the base binder, either in m-controlled or S-controlled continuous grades. The addition of 0.30 RBR to the 64-28P base binder, did negatively affected the low temperature continuous grade of the base binder noting that the influence of the recycled material was more significant on the m-controlled compared to the S-controlled continuous grades. Similar to what had been observed in high temperature continuous grade, the T2 and A2 RAs were able to efficiently restore the low temperature continuous grades in both m-controlled and S-controlled grades. However, a slightly higher efficiency was observed with T2 in the m-controlled continuous PG grade, the critical low temperature grade in this particular base binder.

The ΔTc parameter, which is the difference in continuous grade temperatures where binders reach their respective limits of 300 MPa stiffness (S) and 0.30 m-value, has been

suggested by Anderson et al. (2011) and Hanson et al. (2013) to assess the susceptibility of the binder to aging at low temperatures. A negative value of ΔTc (TS-Tm) indicates the controlling role of the relaxation properties of binder at low temperatures while the positive value represents that the binder stiffening is a more influential factor for tested binder compared to ductility in low temperatures. Anderson et al. (2011) verified the satisfactory correlation of ΔTc with ductility and DSRFn (reference) in several laboratory and field investigation and also proposed -2.5°C and -5°C as the correlation of ΔTc to the same cracking thresholds, i.e. onset and significant cracking, discussed in Glover-Rowe (G-R) (reference) parameter beforehand, i.e. crack warning and crack limit, respectively.

ΔTc results corresponding to the NV field project binder blends are presented in Figure 7. 4. The 64-28P base binder showed a negative ΔTc indicating the m-controlled behavior in low temperature properties. As expected, the addition of the 0.15 RBR of the NV RAP to the base binder had a negative influence on the base binder relaxation properties. However, increasing the RBR to 0.30 did not adversely affect the low temperature properties of the recycled blend, surprisingly. On the other hand, the addition of the RAs not only restored the ΔTc but also improved the controlling role of the relaxation properties, i.e. m-value, of binder at low temperatures. Similar to the low temperature continuous grades, T2 was observed to have a slightly better restoration effect compared to A2.

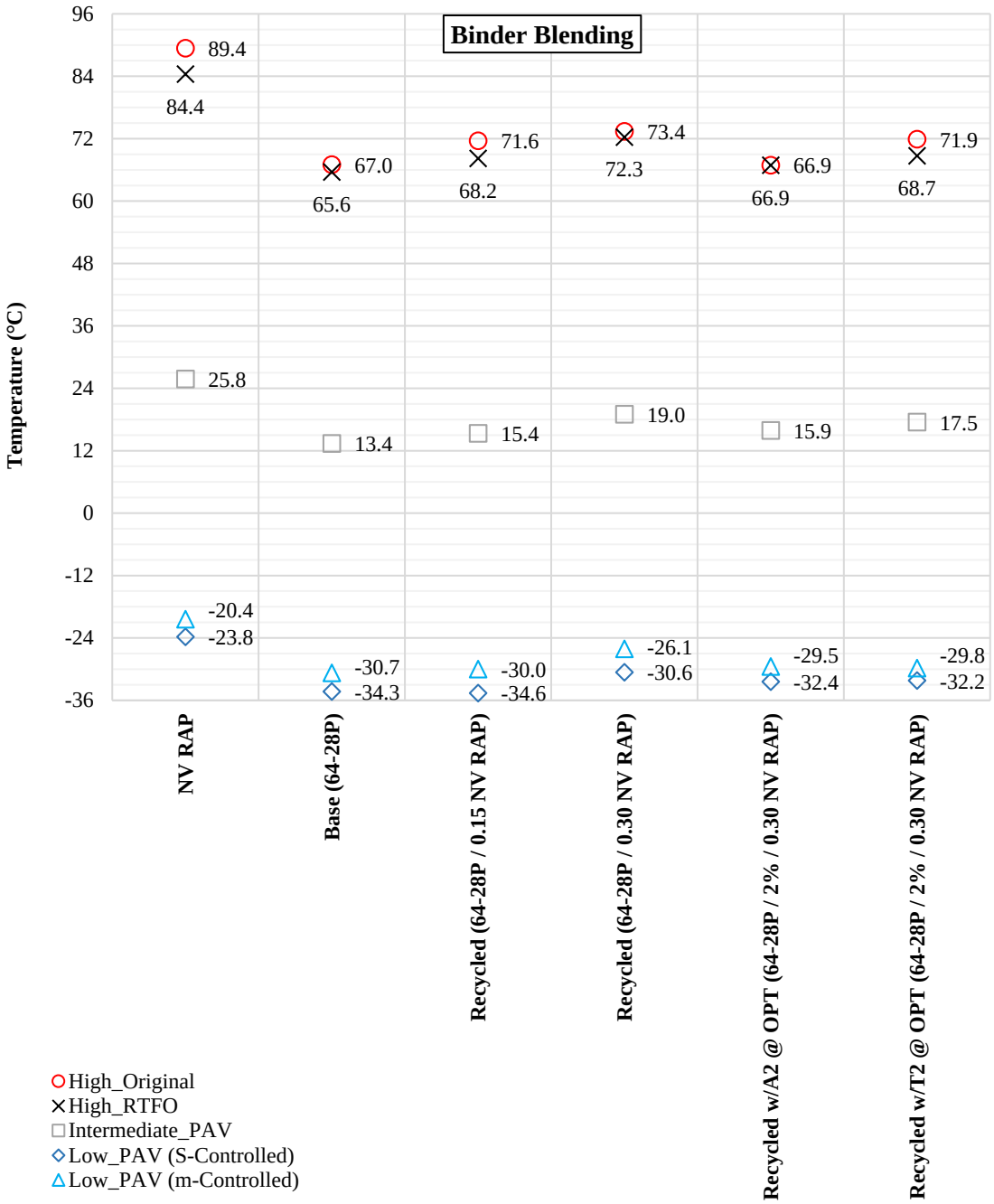

Figure 7. 3. Effect of Recycling and RA on Continuous Grades Based on Binder Blending Test Results for NV Field Materials

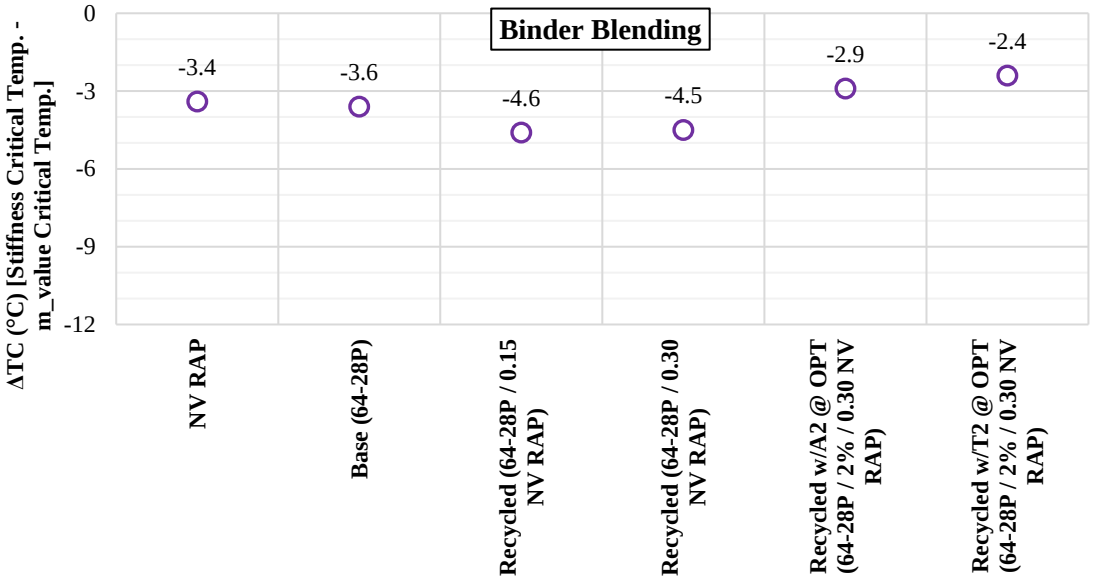

Figure 7. 4. Effect of Recycling and RA on Asphalt Binder Critical Temperature Difference Based on Binder Blending Test Results for NV Field Materials

7.4 Mortar Testing Results

The influences resulting from the addition of recycled materials and/or RAs to the base binder continuous grades were evaluated using PG grading test results in the previous section. Mortar testing was also utilized in this study to explore the effective PG grades of the investigated binders. The mortar testing methodology has been comprehensively outlined previously in Chapter 2. In this study, 12.4 was determined as the maximum RAP percentage keeping the recycled binder blend workable enough for testing at all grading temperatures. Noting that the mortar grades are determined as an offset to the binder blend PG grades (Mortar, 2012), the grade change rates due to the addition of pre-determined quantity of recycled material and RAs at respective ratios and dosages to the 64-28P base binder were determined from the laboratory testing. Table 7. 4 summarizes the grade

change rates for the investigated recycled blends, including each of the high, intermediate, and low temperatures.

Table 7. 4. Effect of Recycling and RA on Asphalt Binder Grade Change Rate for NV Field Materials (Mortar Test Results)

Asphalt Binder	RAP Binder Ratio[1] (%)	RA Type	Grade Change Rate (°C/%Recycled Binder Ratio)				
			High Temperature		Intermediate Temperature	Low Temperature	
			Original	RTFO		S-Controlled	m-Controlled
64-28P	12.4	—	0.07	0.15	0.12	0.09	0.32
	12.4	A2[2]	0.09	NA[4]	0.26	0.02	0.19
	12.4	T2[3]	0.09	0.30	0.13	0.07	0.23

[1] NV RAP binder ratio used during mortar testing experiment
[2] Binder addition of 2.0% by total weight of binder
[3] Binder replacement of 2.0% by total weight of binder
[4] Not available

Considering the determined grade change rates in recycled blends from Table 7. 4, high, intermediate and low temperature continuous grades were calculated at the corresponding RBR and RA dosages consistent with the ones used in the NV field project. The results are shown in Table 7. 5.

Table 7. 5. Mortar Process Continuous PG Grade Results

Binder ID	High-Temperature PG Grade (°C)		Intermediate PG Grade (°C)	Low-Temperature PG Grade (°C)		ΔTc	Final PG Grade
	Original	RTFO		S-controlled	m-controlled		
Recycled @ OPT (64-28P / 0.15 NV RAP)	68.0	67.9	15.1	-32.9	-25.9	-7.0	67.9-25.9
Recycled @ OPT (64-28P / 0.30 NV RAP)	69.0	70.2	17.0	-31.6	-21.1	-10.5	69-21.1
Recycled w/A2 @ OPT (64-28P / 2% / 0.30 NV RAP)	64.3	69.8	17.0	-33.7	-27.9	-5.8	64.3-27.9
Recycled w/T2 @ OPT (64-28P / 2% / 0.30 NV RAP)	69.2	60.5	19.1	-34.2	-27.1	-7.1	60.5-27.1

For the sake of comparison among the investigated binder blends, the mortar test results are visualized in Figure 7. 5. Similar to what was observed in the binder blending test results, the addition of NV RAP material to the 64-28P base binder showed an apparent stiffening effect on the continuous high PG grade, and the higher levels of RAP material used the higher the continuous high PG grade. Note that the increase in the high continuous PG grade from 0 to 0.15 RBR is the same as from 0.15 to 0.30 RBR as a result of linear relationship conducted for the grade change rate in the mortar testing methodology. It is noteworthy to mention that in contrast to the general expectations from the binder blending procedure, the original binder did not indicate a higher temperature continuous grade in all

binder blends, especially with blend containing the A2. As observed, the addition of the RAs to the recycled blend did restore the overall high continuous PG grade to that of the base binder, even a lower grade relatively. However, in case of recycled blend with T2, this restoration caused the continuous PG grade to fall one grade below the base binder, i.e. 58°C instead of 64°C. This phenomenon might be caused by two possible reasons, first, overestimating the A2 dosage in the recycled blend, or second, possible issues with mortar testing. The dosage selection procedure is highly dependent to the binder grading results. Any minor variation in the determination of the continuous PG grade will significantly affect the trend line slopes in Figure 7. 1 and Figure 7. 2 which relatively changes the optimum selected dosage. Besides, rounding the determined dosages from the aforementioned figures to practical dosages might be another external influence that resulted in overestimating or underestimating the respective dosages. The second reason, however, seems more realistic to the author since conducting PG grading tests on an assumed homogenous combination of mortar aggregate and binder (with or without RAs) without increasing the test variability does present certain difficulties, even with an experienced operator.

The continuous low-temperature PG grade trends in Figure 7. 5 indicates that the influence of recycled material was more significant on the m-value controlled temperature in comparison with the respective stiffness-controlled temperature. In this regard, the 64-28P base binder relaxation properties significantly decreased due to the addition of NV recycled material, i.e. RAP. This loss of relaxation negatively increased the low-temperature PG grade of the recycled blends by one and two grades for 0.15 and 0.30 RBR blends, respectively. However, the addition of the RAs, both A2 and T2, restored and even

improved the low continuous PG grade to the target PG grade of -28°C with a slightly better performance with A2. The A2 higher effectiveness and restoration was also captured and even pronounced in the ΔTc results depicted in Figure 7. 6. The figure also indicates an overall reduction in the ΔTc values due to the addition of the recycled material, which was partially restored with RAs at their respective dosages.

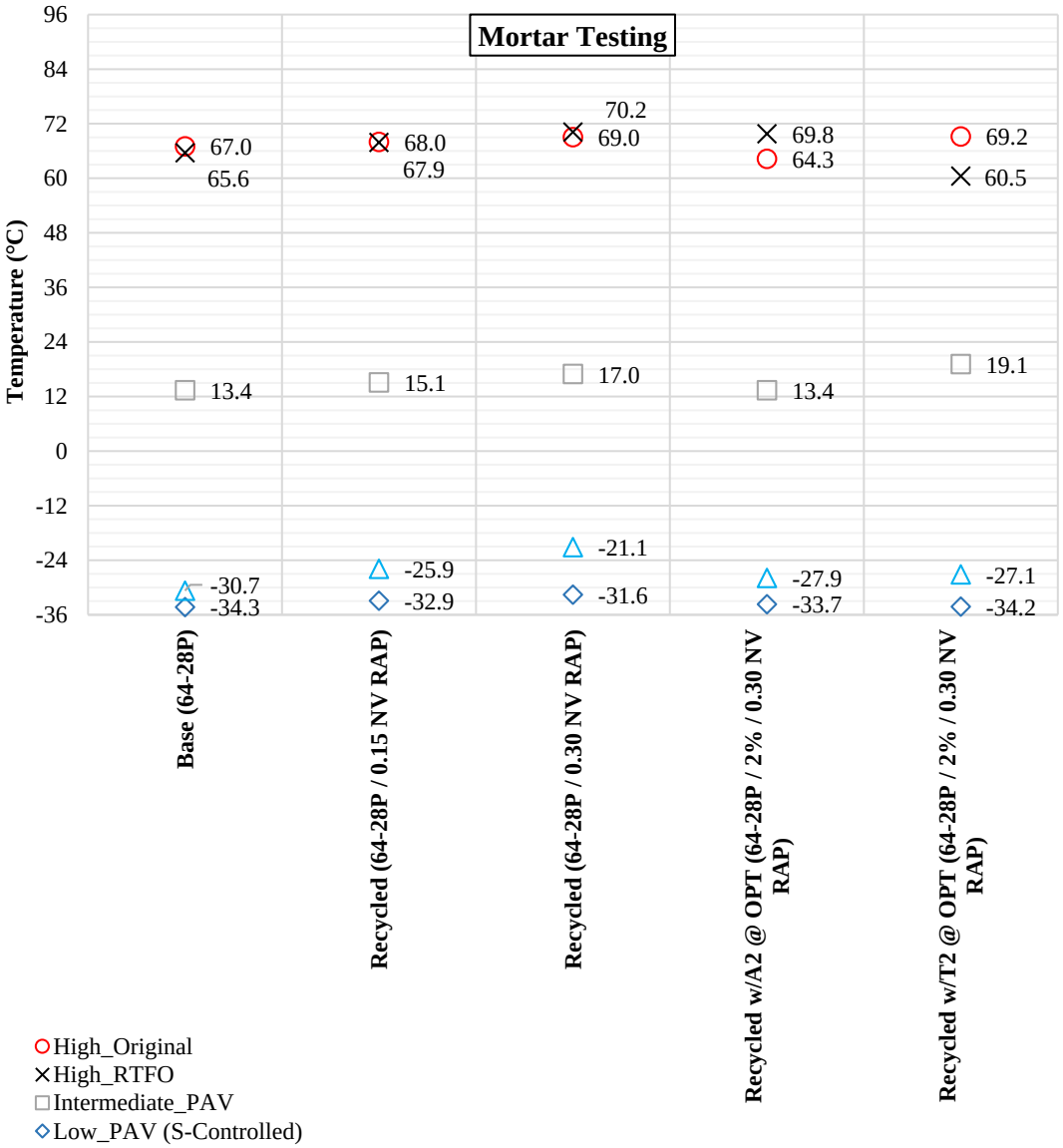

Figure 7. 5. Effect of Recycling and RA on Continuous Grades Based on Mortar Test Results for NV Field Materials

Figure 7. 6. Effect of Recycling and RA on Asphalt Binder Critical Temperature Difference Based on Mortar Test Results for NV Field Materials

7.5 Binder Blending and Mortar Testing Results Comparison

In the previous sections of this chapter, detailed analysis regarding the binder and mortar testing on NV field project material have been discussed. Within each respective test, an increase in stiffness and brittle behavior with the addition of recycled materials were generally indicated. This finding was subsequently followed by a partial restoration of the softness and flexibility with the addition of the RAs at the selected dosages. Both procedures provide consistent direction for the influence of the evaluation materials, i.e. NV RAP and RAs, and are generally in agreement.

However, a more comprehensive comparison of the relative influences of the respective procedures reveal the influence of the differences in the material preparations, i.e. full

compared to partial blending in the binder blending and mortar procedures, respectively. To conduct a clear comparison, Figure 7. 7 present the high-temperature PG grade of the evaluated binders according to the two methodologies.

Figure 7. 7 represents the high-temperature PG grade determinations for both the blended binder and mortar processes. In general, the blended binders exhibit nearly the same or slightly higher PG grades compared to the mortar results. This is most commonly understood to be the result of the complete blending of the base and recycled binders in the binder test results. As outlined previously, the mortar protocol does not require the full blending of all the recycled binder; as a result, some portions of the recycled binder act as black rock and the base binder happens to experience a lower degree of blending and subsequent stiffening. Therefore, the mortar testing results reveal lower values of continuous high-temperature PG grades compared to binder blending.

As observed, the increased recycled content when added to the 64-28P base binder tended to increase to the difference between the two methodologies, which helps support the concept of partial blending as a potential influence. However, inconsistent offsets were noted with the inclusion of the RAs in the two PG grades.

In the case of binder blend results for the 0.30 RAP binder ratio, the use of A2 or T2 at the selected respective dosage resulted in a blend binder that met the target high temperature performance grade of 64°C. The influence of T2 RA was, however, more significant on the high critical temperature (i.e., resulted in a softer high critical temperature) when compared to A2. Conversely, the mortar test results showed that A2 was more significant on the high RTFO critical temperature when compared to T2. While the use of T2 at the

selected respective dosage was effective in restoring the high temperature performance grade, the use of A2 resulted in a high-performance grade lower than the target of 64°C.

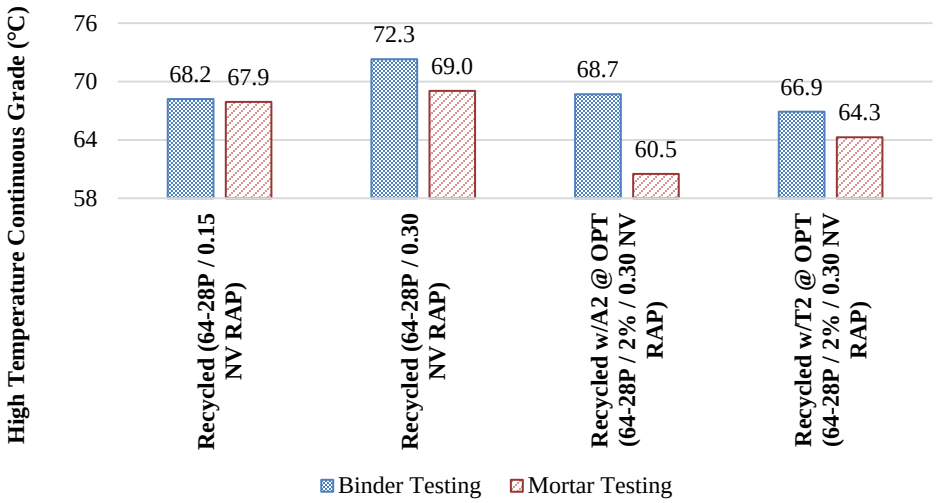

Figure 7. 7. High-Temperature Continuous Grade Comparison in Binder Blending and Mortar Testing

Additional consideration of these two testing methodologies are presented in Figure 7. 8. a and b presenting the continuous low-temperature PG grade determinations. Similar to the relative comparisons regarding the high temperature grade, Figure 7. 8 revealed a consistent shift toward warmer temperatures with the mortar procedure. This finding again supports the concept of full blending for the binder tests and partial blending with the mortar process. Specific to the full blending, the softer base binder is completely blended into the stiffer recycled materials and softened it. To the contrary in the mortar testing, the partial blending prevented the softer binder from fully interacting with the recycled materials. Therefore, during the actual testing duration the increased stiffness and subsequently reduced relaxation potential of the unblended portion of the mortar influenced the final continuous low-temperature grade of the mortar. This finding is additionally

supported by the fact that all the binder blends were m-controlled in the continuous low-temperature grades, indicating that the relaxation or flexibility is the limiting factor as opposed to overly stiff material blends.

Similar to the high-temperature grade, the increased recycled content increased the differential between the two methodologies. However, the addition of the RA to in these measures helped to reduce the method-specific discrepancy with the m-controlled low temperatures of the investigated binder blends.

The PG 64-28P binder results for low temperature showed that, the use of A2 or T2 at the selected respective dosage was effective in restoring the low temperature grade of the blend binder to the target performance grade of -28°C when 0.30 RBR was used. The influence of A2 and T2 was more significant on the m-value low critical temperature in comparison to the respective stiffness low critical temperature. However, the mortar test results were relatively different compared to the binder blending test results. The RAs were not able to fully restore the m-value low critical temperature especially when using A2 at the selected respective dosage. As noted before, the A2 yet showed a relatively low value for the high-performance grade.

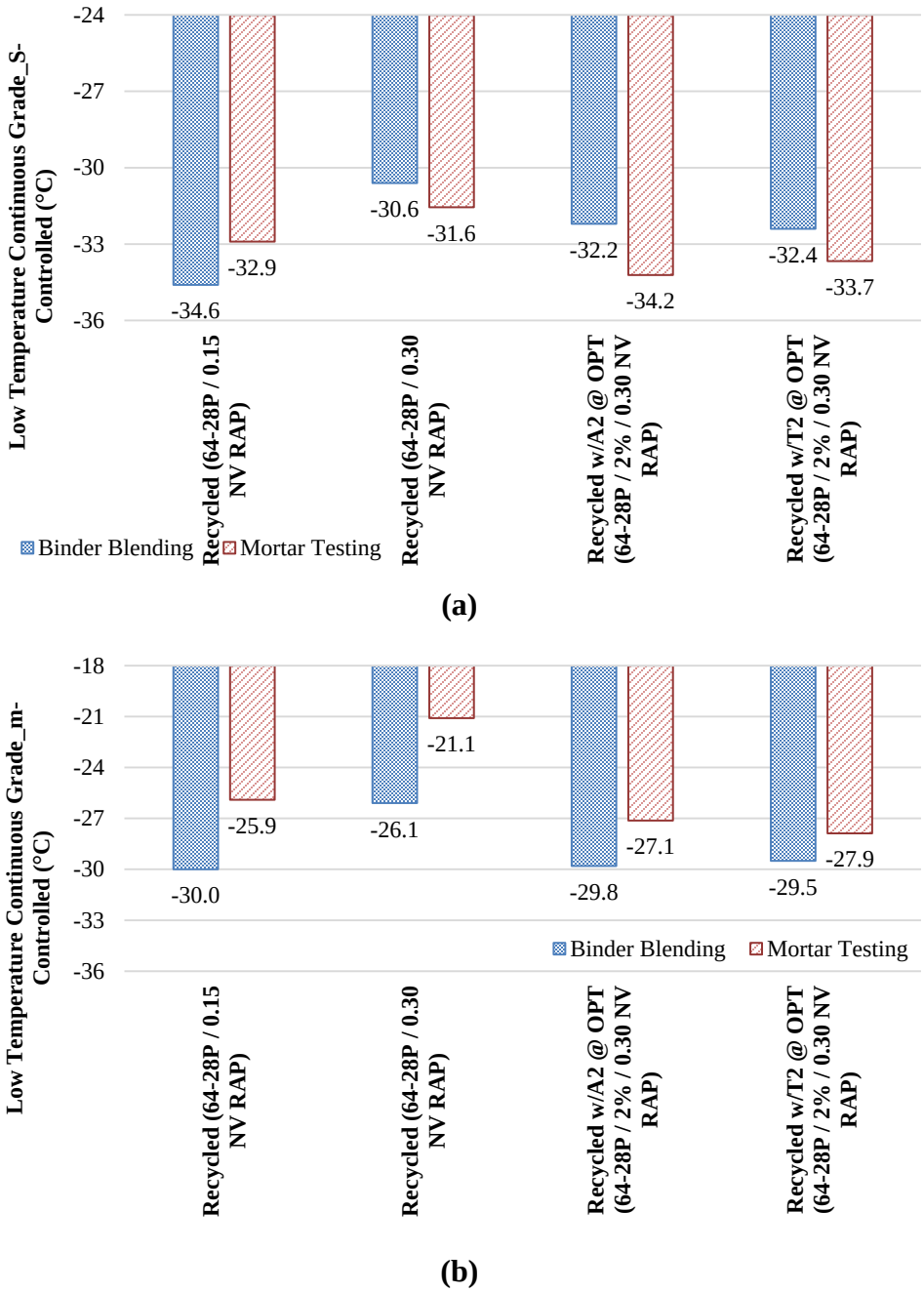

Figure 7. 8. Low-Temperature Continuous Grades Comparison in Binder Blending and Mortar Testing (a) S-Controlled, (b) m-Controlled

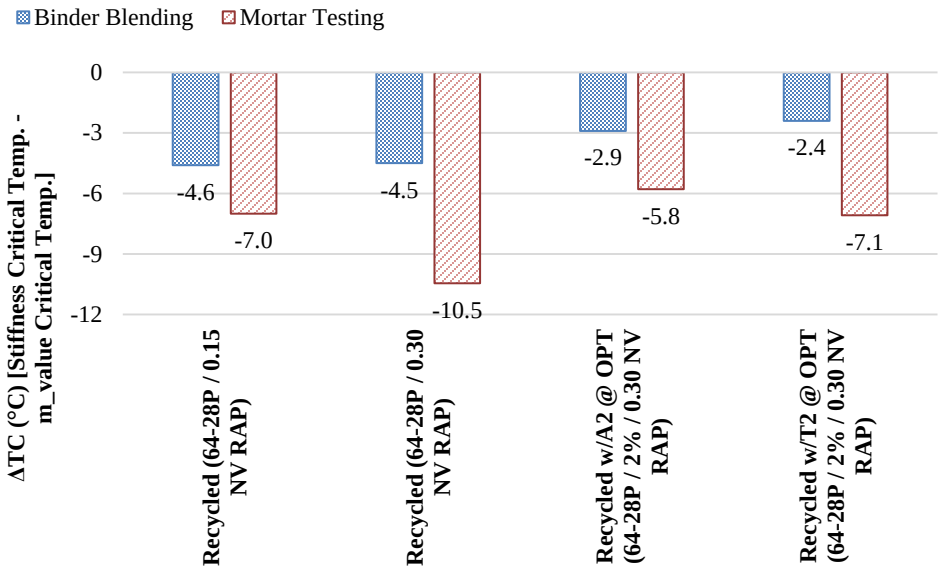

Figure 7. 9. ΔTc Comparison in Binder Blending and Mortar Testing

In conjunction with the typically warmer low-temperature PG grades noted with the mortar process, Figure 7. 9 indicates a typically larger value for the ΔTc parameter compared to the blended binder process. This finding is somewhat contrary to those of the low temperature continuous grade comparisons noted previously. It might suggest this is additional indication of the partial blending aspect. If the partial blending influence is acknowledged in conjunction with the low-temp grade of the all blends were m-controlled, the larger ΔTc would make sense. As observed in Figure 7. 8 the partial blending has a large influence on the relaxation parameter, i.e. m-value, but not as much on the overall stiffness, thus it causes the ΔTc to be higher in the mortar procedure. It also supports the softer grades in high temperature for mortar process suggesting that the high continuous PG grades were largely dictated by the softer unblended portions of the base binder. With this in mind, it is expected to have the same occurrence on the low temperature side meaning that the unblended binders control the stiffness to the RBR levels tested. However,

the increased levels of recycled materials did tend to reduce the relaxation capacity, i.e. m-value, subsequently increasing the difference between the two, represented as ΔTc.

In addition to the increased discrepancy for the recycled blends in ΔTc measurements, they also fall below the ΔTc limit of -5°C for the binder measures, but exceed it for the mortar analysis. Interpretation of these results generally presents two options: The first is that perhaps the proposed -5°C limit is specific to fully blended binder considerations and may not be applicable to mortar analyses. In this case, the mortar procedure would then potentially require a recalibration effort to determine what the appropriate level would be for the methodology. The second possible interpretation highlights the previously mentioned difference in the level of blending with the two processes. In the fully blended binder process, the recycled materials are fully combined and softened by the virgin binder, which logically should produce a smaller ΔTc value. The mortar procedure on the other hand, does not force the blending of the materials and subsequently may potentially produce more representative results of the field produced mixtures and thus more meaningful results.

To sum up, in the 64-28P target binder, the high critical temperature from the mortar procedure was, except in one case, lower (i.e., colder and ranging from 2.1 to 8.2°C) than the respective temperature determined using the binder blending procedure. On the other hand, different trends were observed between the S-controlled and m-controlled low critical temperature. The S-controlled low critical temperature from the mortar procedure was colder (ranging from 1.0°C to 2.0°C) than the respective temperature determined using the binder blending procedure. Conversely, the m-controlled low critical temperature from

the mortar procedure was warmer (ranging from 1.6°C to 5.0°C) than the respective temperature determined using the binder blending procedure.

The estimated PGH and PGL values based on the mortar procedure as compared to those from the binder blending results can be compared in **Error! Reference source not found.** and **Error! Reference source not found.** for the TX and NV field materials. In all cases, the effect of the RA indicated a reduction in both the PGH and PGL. In general, the complete blending from the binder tests resulted in over-estimation of the PGH (warmer by 3-8 °C for NV and 6-7 °C for TX) and the PGL (colder by 2-5 °C for NV and 2-3 °C for TX).

Considering all the aforementioned conclusions, the mortar procedure was capable of characterizing the effects of RAP and RA materials on virgin binder without the use of chemical extraction, acknowledging that there are some inconsistencies between the two procedure results. It also should be mentioned that the test variability was relatively higher for some cases in the mortar testing, which necessitated the testing of additional replicates and selecting the most repeatable results.

For the sake of additional investigation on the binder blending and mortar testing comparison results, Figure 7. 10 to Figure 7. 13 represent the correlation between the two testing methodologies. On the high temperature side, while Figure 7. 10 does not present a perfect correlation between the two systems, it does highlight the fact that the mortar testing procedure generally yields a lower high-temperature PG grade compared to the fully blended binder. Additionally, the increased recycled content tended to increase to the

difference between the two methodologies. However, inconsistent offsets were noted with the inclusion of the RAs across both base binders.

Similar to the high-temperature grade, the increased recycled content increased the differential between the two methodologies in the low temperature continuous grades as plotted in Figure 7. 11. In contrast however, the addition of the RA to in these measures helped to reduce the method-specific discrepancy. Comparing the low-temperature grades determined from the respective test methods indicates a rather consistent increase or warming of the low-temperature PG grades with the mortar testing. In actuality, since all the measures in this case were m-controlled grades, this figure would be the same for that case. Therefore, Figure 7. 12 presents the S-controlled PG grades from both the blended binder and mortar procedures. The figure also indicates the close agreement for all the blends, generally within one or two degrees for all the evaluated binders. It is noteworthy to mention that the temperatures associated with the limiting stiffness values are substantially colder than the actual low-temperature PG grades dictated by the m-value measures. Combining the stiffness and relaxation criteria in the format of ΔTc resulted in Figure 7. 13 which clearly presents the relative discrepancies between the two methodologies particularly with the addition of the recycled material.

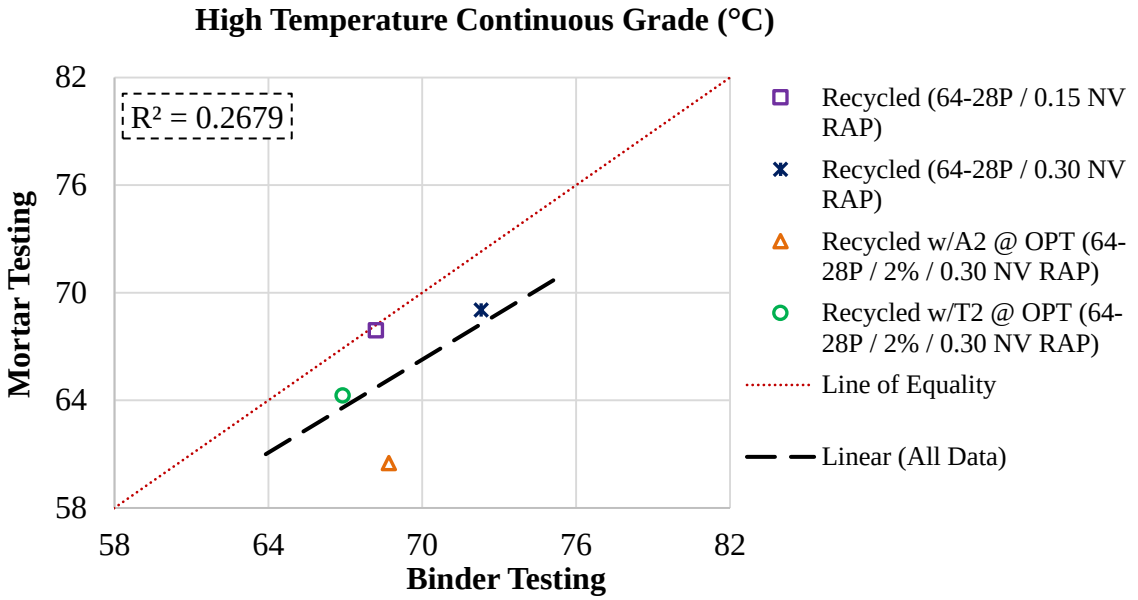

Figure 7. 10. Correlation between Binder Blending and Mortar Testing High Temperature Continuous Grade (°C)

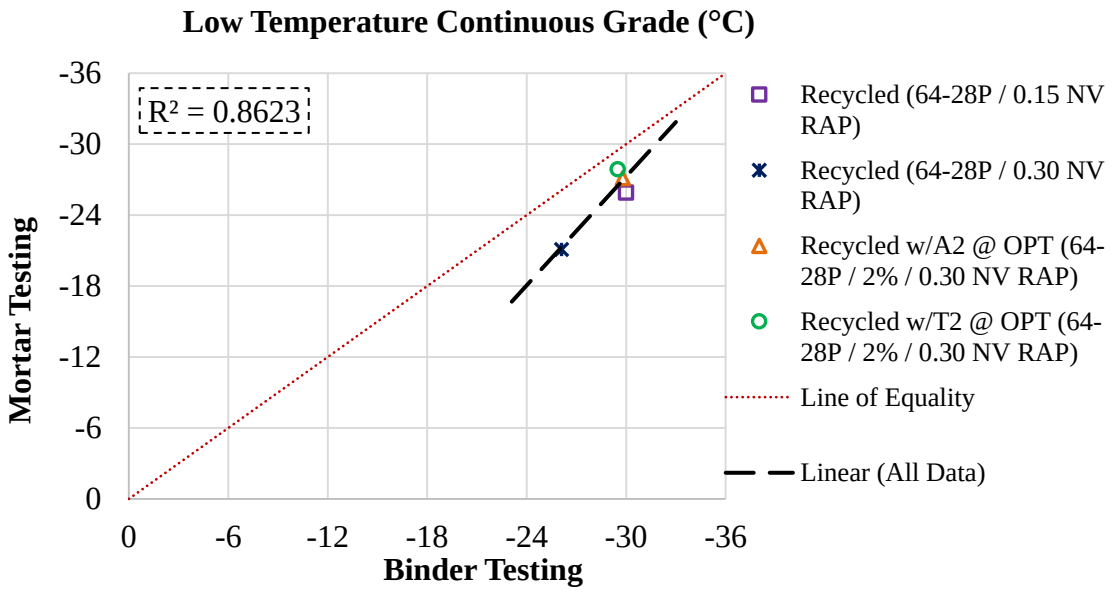

Figure 7. 11. Correlation between Binder Blending and Mortar Testing Low Temperature Continuous Grade (°C)

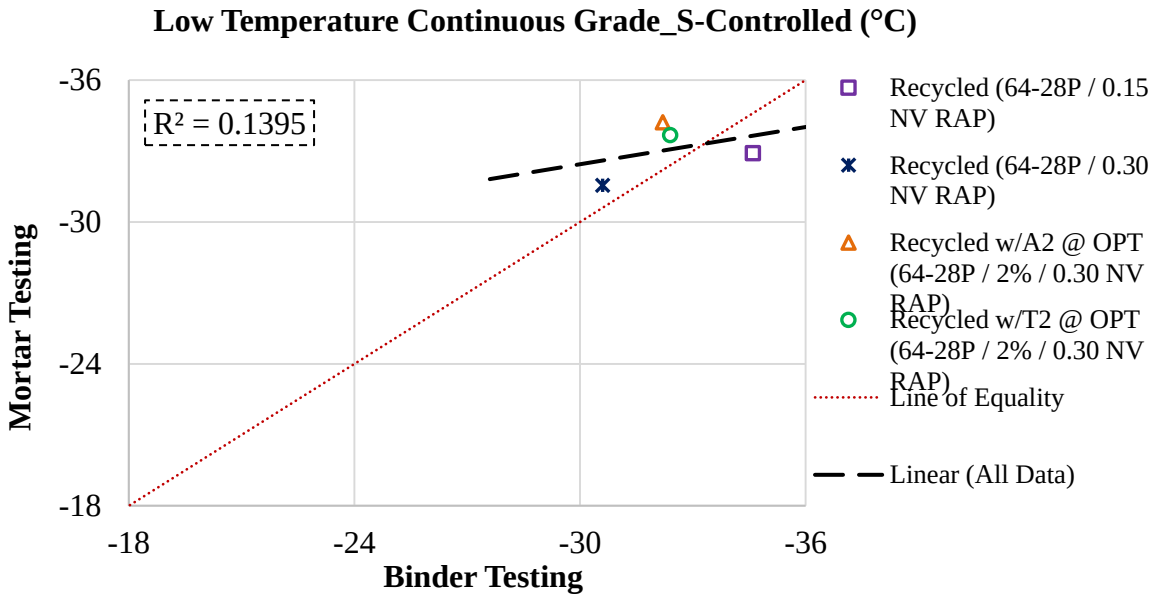

Figure 7. 12. Correlation between Binder Blending and Mortar Testing S-Controlled Continuous Grade (°C)

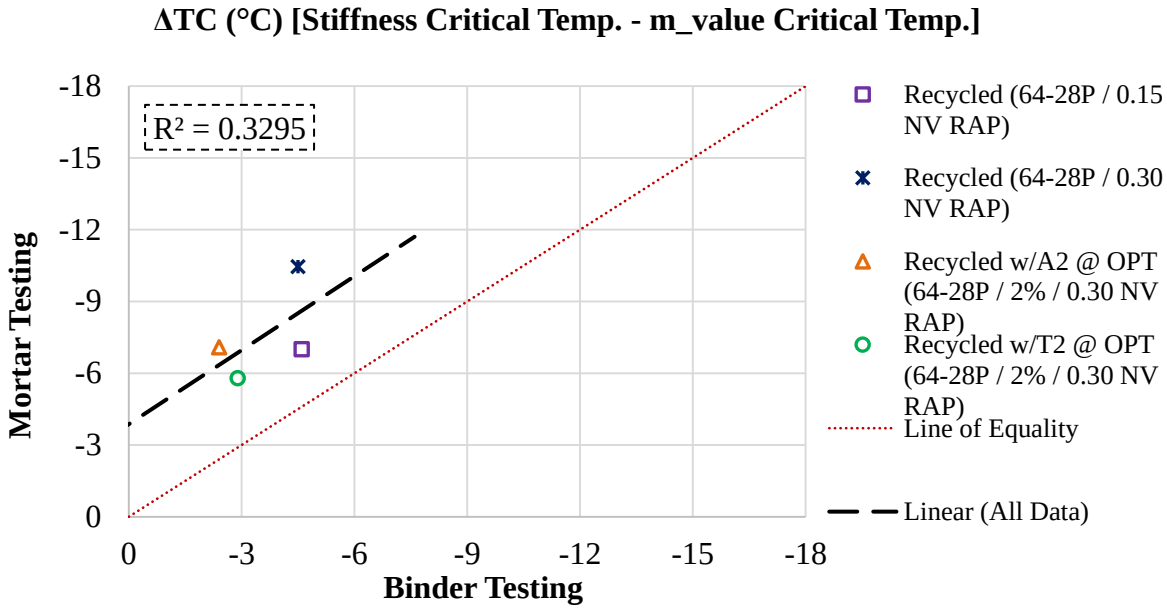

Figure 7. 13. Correlation between Binder Blending and Mortar ΔTc (°C)

7.6 Mixture Testing – Uniaxial Thermal Stress and Strain Test (UTSST)

The characterization of the low-temperature behavior of the asphalt mixtures was determined through the Uniaxial Thermal Stress and Strain Test. The development of the UTSST methodologies has permitted the determination of thermo-volumetric (i.e., coefficient of thermal contraction, CTC), thermo-viscoelastic (i.e., stiffness-temperature relationship), crack initiation, and fracture properties of asphalt mixtures using thermal stress and strain measurements (ASTM 2016).

7.6.1 UTSST Test Results

The UTSST was utilized to evaluate the performance of each of the Nevada field project mixtures previously described in Table 7. 2. Five different test sections were constructed to evaluate the effect of RAP materials in two different RBR levels as well as two different types of RAs, previously defined as A2 and T2. Detailed information regarding the NV field sections were presented in Table 7. 2.

Two different types of the specimen were prepared for this field project as follows:

1. Right after the construction, field cores or Plant Mix Field Compacted (PMFC) mixtures were collected from each specific section, and subjected to laboratory aging in the forced draft oven at 85°C for 5 days per AASHTO R 30.
2. The Reheated Plant Mixed Lab Compacted (RPMLC) specimens were prepared by reheating the loose mixtures from the plant to the required compaction temperature, and compacted as soon as the compaction temperature was reached. The RPMLC specimens were similarly oven aged in the forced draft oven for 5 days at 85°C per AASHTO R 30.

It is noteworthy to mention that the 5 days at 85°C were selected since a similar estimated level of aging was noted between the laboratory aging of 5 days at 85°C and an approximate range of 1.5 to 2.5 years in-service aging for certain example materials and locations in Texas (Glover and Cui, 2013, Glover et al. 2014, Alavi, 2014). After aging the specimens at this particular aging level to the UTSST protocol was conducted producing the results presented in the following section.

7.6.1.1 Plant Mixed Field Compacted (PMFC) Mixtures

As outlined formerly, the UTSST evaluation measures the developed stress and strain of the mixture under constant rate thermal loading. The measured stresses and strains were readily combined into the UTSST modulus in the temperature domain for PMFC mixtures as presented in Figure 7. 14. The overall observations of the figure suggest a stiffening, i.e. increased modulus values, with higher levels of recycled materials. However, this increase is not always consistent throughout the whole curve inasmuch as a lower modulus is observed at the peak of the recycled mixture with 0.30 RBR compared to the lower RBR of 0.15. A clear reduction in the crack initiation and fracture temperatures was also observed as the recycled materials ratio increased, which was shown to be at least partially alleviated with the addition of the RAs to some extent.

As defined earlier, the highest peak of the modulus-temperature curve corresponds to the start of the substantial micro cracking and damage. The recycled mixture with 0.15 RBR showed a higher crack initiation modulus than the base mixture. However, the cracking was initiated at a warmer temperature as well as lower stress levels compared to the base mixture as observed in Figure 7. 16 and Figure 7. 18, respectively. Such observations

suggested a brittle behavior as the mixture lost the ability to relax and tolerate the induced thermal stresses. This behavior was observed to a greater extent with the higher RBR PMFC mixtures where a lower stress level and warmer temperature in the crack initiation point was observed. However, it was noted that increasing the RBR from 0.15 to 0.30 caused the crack initiation modulus to be significantly reduced due to the apparent increase in brittle behavior. This reduction has been observed previously and was linked to observations of reduced UTSST modulus values either being due to lower stiffness, i.e. softer materials, or that of a damaged and subsequently lower modulus (Alavi *et al.*, 2015). These findings denoted the complex interaction between the induced stress from the thermally applied loading and the corresponding ability of the mixture to relax. Considering both of these factors leads to better understanding of the true material behavior. In general, the evaluation indicated that not only did the specimens incur more damage as they included more recycled material and became more brittle, but the observed brittleness and damaged behavior occurred at warmer temperatures.

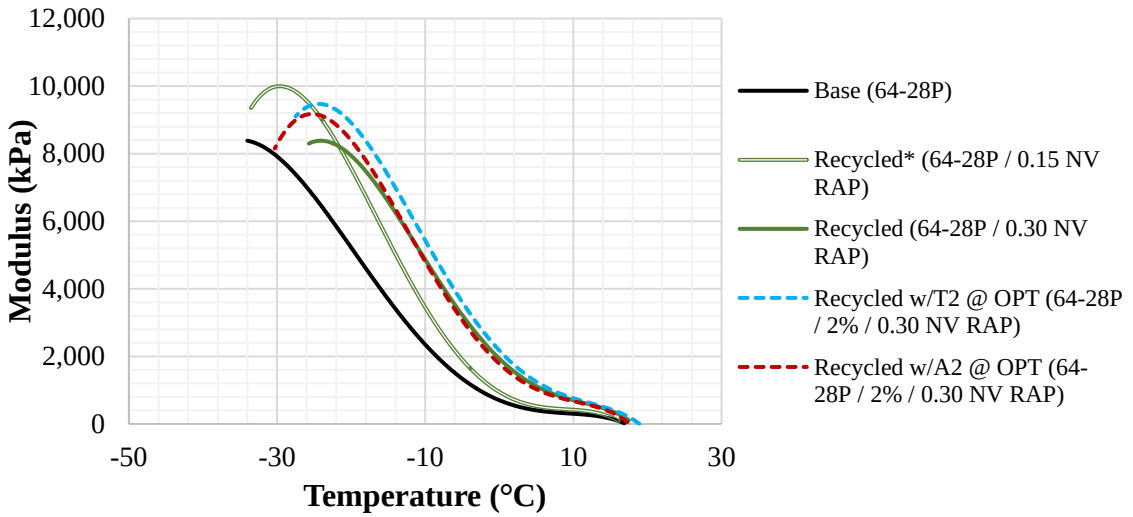

Figure 7. 14. UTSST Modulus Curves for Nevada Field Sections (PMFC)

7.6.1.2 Reheated Plant Mixed Laboratory Compacted (RPMLC) Mixtures

Similar to the field cores, i.e. PMFC mixtures, the UTSST was also implemented to evaluate the low temperature cracking resistance of the RPMLC mixtures from the Nevada field project test sections. The UTSST modulus curve in the temperature domain for the respective Nevada test sections are presented in **Error! Reference source not found.**.

General observations of the **Error! Reference source not found.** identify an overall increase in the modulus values with the addition of the 0.15 RBR recycled materials to the base binder. This was previously observed with the PMFC mixtures due to the stiffening effect of the recycled material. However, the increasing the recycled material ratio up to 0.30 RBR caused the modulus values to be significantly reduced, even lower than the base mixture before the fracture. A similar trend was also observed in the PMFC mixtures as a result of either a lower stiffness or substantial damage in the specimen with a higher RBR levels. As observed, the high RBR of 0.30 made the fracture at relatively warmer temperatures even without presenting a clear crack initiation point. Although the addition of the RAs to the recycled mixtures indicated to some extent a restoration of the modulus with slightly better performance noted with T2. The crack initiation and fracture events were observed to occur in significantly warmer temperatures compared to the base and 0.15 RBR mixture. Further discussions regarding the influences of the recycled materials and RAs are presented in the following section.

It is also important to note that the RPMLC specimens may have some residual effect due to the reheating process, e.g. potential aging, etc. Detailed information will be presented in the following sections.

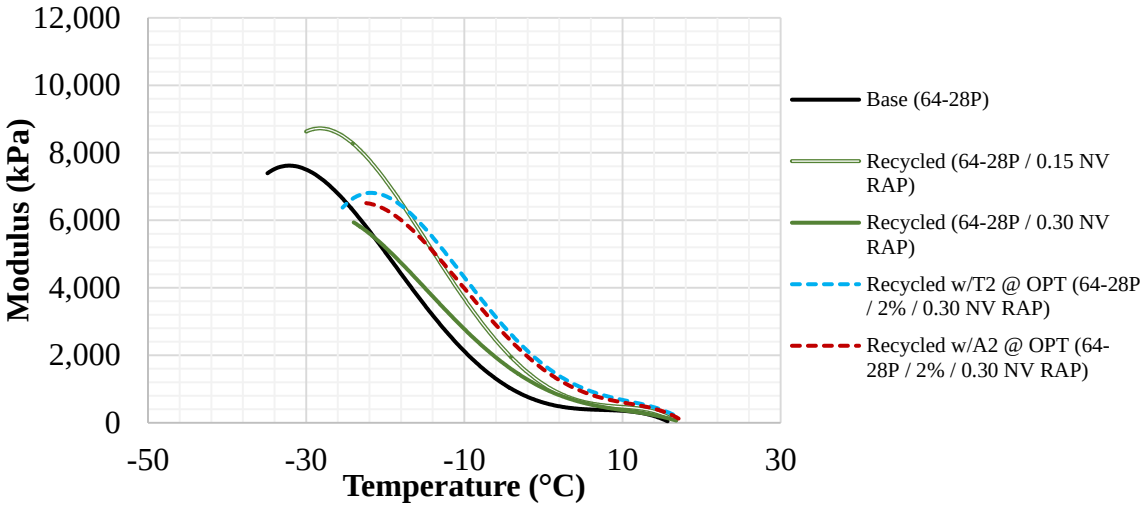

Figure 7. 15. UTSST Modulus Curves for Nevada Field Sections (RPMLC)

7.6.1.3 Thermo Viscoelastic Properties (TVEP)

To quantify the impacts of the RAs on the recycled mixtures property restoration, all the thermo viscoelastic properties of the PMFC and RPMLC specimens are presented in Figure 7. 16 through Figure 7. 20. As previously observed, both RAs, i.e. A2 and T2 provided an overall restoration of the low-temperature properties within the critical points. However, the RA effectiveness was not consistent throughout various properties. Although the RA dosages were at the optimum level, they were not able to reduce the crack initiation temperature to that of the base mixture, as observed in Figure 7. 16. This is even more prevalent with the RPMLC mixtures, where the RAs could not restore the temperature at critical points to that of the base mixture but also to the level of recycled mixtures as indicated by the warmer temperatures for the respective TVEP. However, the reheating process and resulting chemical changes might have some significant effects on the lack of improvement with the RAs when comparing the recycled mixture with and without the RAs.

Similar results were observed with the glassy hardening stage, where the mixture behavior is mostly glassy without significant flexibility contributions from the viscous or relaxation properties. Not only did the glassy hardening temperature occur at warmer temperatures with the addition of the recycled materials, but the mixtures also showed a higher modulus and stiffening effect in the 0.15 RBR recycled mixture. Also, the increase in the portion of recycled material from 0.15 up to 0.30 RBR increased the brittleness further, causing the modulus to be reduced in the higher RBR mixture. The addition of the RAs to the mixtures could not restore the glassy hardening temperature to that of the base mixture. However, the RAs seemed to be more effective in restoring the modulus rather than the temperature, to the level of the 0.15 RBR mixture. These restored mixtures were observed to have a higher stiffness but increased levels of brittle behavior compared to the base mixture when progressing to the glassy phase. It is also noteworthy to mention that the stress level did not significantly change among the five mixtures, acknowledging the base mixture exhibiting the highest stress capacity before fracture.

Prior to reaching the glassy hardening stage, another phase transformation called viscous-glassy transition occurs in the mixture in which the mixture shows a significant brittle behavior while retaining portions of the relaxation properties. The interpretation of the Figure 7. 16 through Figure 7. 19 represent the aforementioned general trend with the thermo viscoelastic properties in this behavioral phase, noting a less remarkable differences among the mixtures thermal stresses and moduli. It was highlighted in the viscous softening properties, where the initial build-up of the thermally induced stresses began and the mixtures were not capable of fully relaxing the induced thermal stress.

Consideration of the fracture temperatures led to the previous interpretations as were noted with the crack initiation properties. However, comparing the general trend of the thermally induced stress within the fracture and crack initiation stages revealed dissimilar behaviors, as presented in Figure 7. 18. All the mixtures tolerated greater stresses after the crack initiation for at least a 4°C temperature reduction except for the virgin mix. It suggests that the addition of the recycled material might have an effect on alleviating the brittle fracture after crack initiation in the mixtures. However, the initiation of the crack happens earlier with the recycled mixture as discussed previously. Also, noting that both crack initiation and fracture for the virgin mix happened at a colder temperature compared to the recycled blends, the higher difference between the crack initiation and fracture could be also related to partial blending of the recycled materials. In other words, the unblended RAP binder might crack in warmer temperatures while the virgin binder attempted to delay the fracture, however, not as cold as the virgin mix due to the discontinuity from the RAP fracture. Aging, the anomalies observed with the RPMLC mixtures could be related to the unknown chemical reactions in the reheating procedure.

As an additional thermo-volumetric property of the asphalt mixtures, Figure 7. 20 represents the liquid coefficient of thermal contraction of the RPMLC and PMFC mixtures. Given the regionally similar source of the virgin binder and the RAP material, the CTC_l did not significantly change among the various mixtures even with increasing RAP contents. This similarity was previously noted by Morian (2014) and Alavi (2014) as the lack of systematic transition of CTC_l with increased levels of oxidation. However, it is noteworthy to mention that such a similarity might subject to change upon the addition of RAS materials due to the previous observations in Chapter 5, i.e. the significant deviation

of the aging path form the virgin binder in HS plots and black space diagram with the RAS modified binder blends compared to the RAP only modified blends.

7.6.1.4 Resistance Index (RI)

The resistance index value, RI, previously defined in Chapter 3, evaluates the overall mixture resistance to the low temperature stresses and strains. Figure 7. 21 shows the RI results for the mixtures in the NV field project, which is a single parameter used to quantify the various contributions of the previously discussed TVEP indicators. A clear reduction in the RI was observed due to the addition of the recycled materials, and as resulted before, the more the recycled material the lower the low temperature resistance index. The addition of the RAs, either T2 or A2, increased the RI values, indicating some levels of the low temperature properties restoration. However, none of them were able to completely restore the mixture properties to those of the control mixtures.

Similar trends in the RI values were also noted with the RPMLC mixtures with a better restoration effect with A2 compared to T2. However, an anomaly was observed when comparing the RI of the recycled mixture w/0.15 RBR to that of the virgin mixture, implying a higher cracking resistance upon the addition of the limited quantity of recycled material. Before making any solid conclusions or labeling the recycled mixture result an outlier, additional investigations are required to confirm this measurement noting the lack of precision and bias for the test procedure. Further, the discrepancy could be related to some residual effect due to the reheating process, as previously stated.

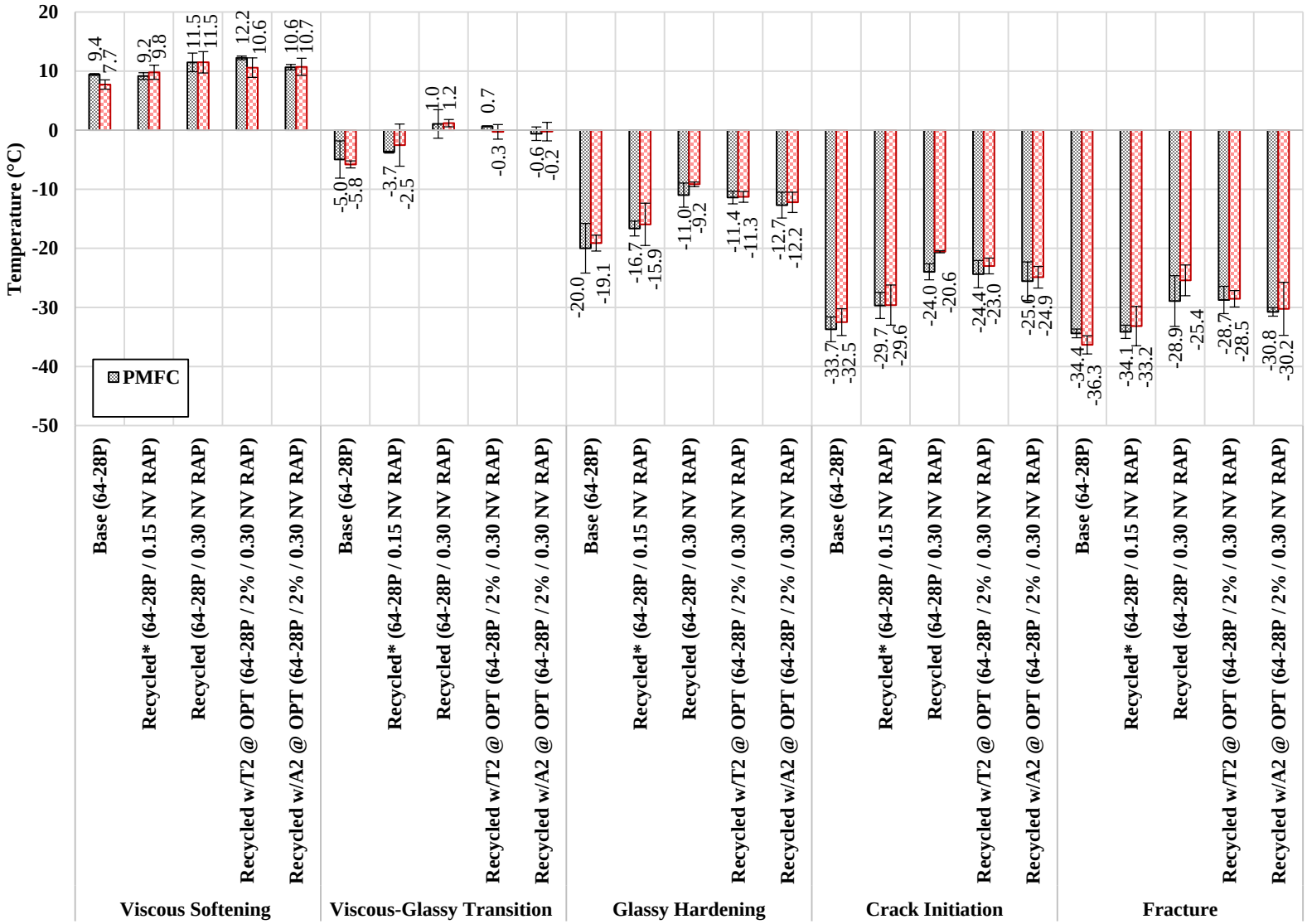

Figure 7. 16. UTSST Critical Temperature Measures for Nevada Field Sections, PMFC and RPMLC

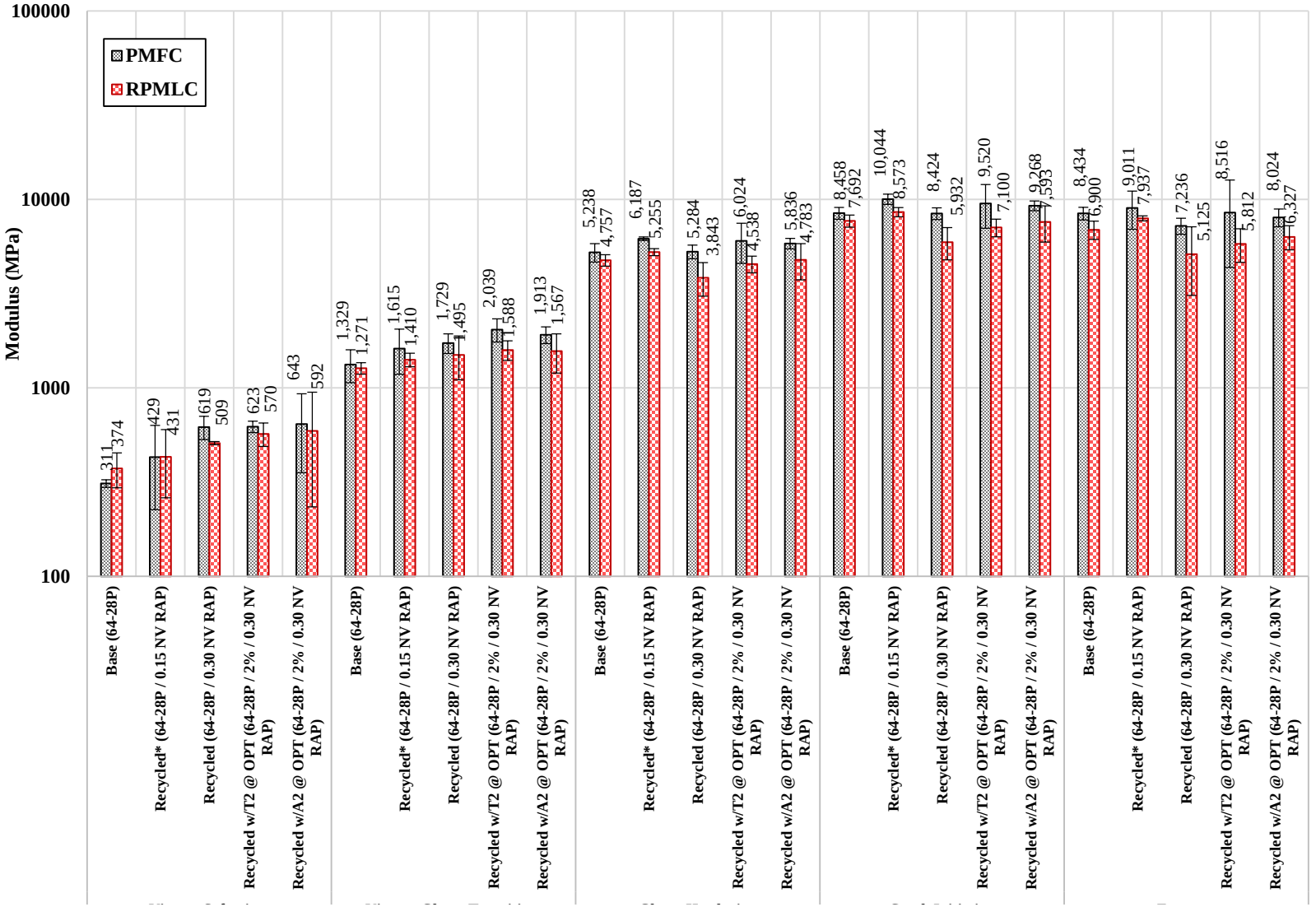

Figure 7. 17. UTSST Modulus for Nevada Field Sections, PMFC and RPMLC

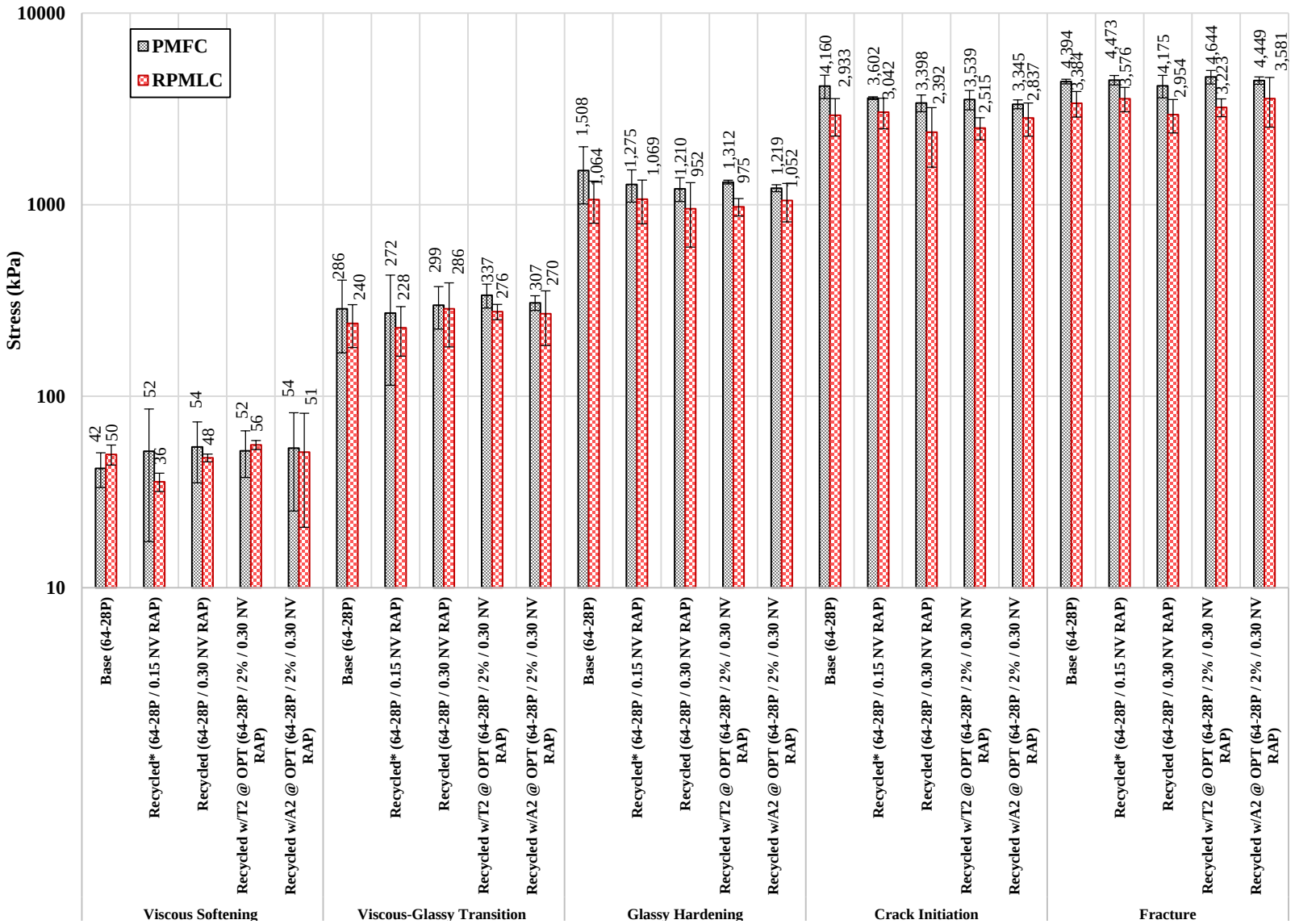

Figure 7. 18. UTSST Stress Measures for Nevada Field Sections, PMFC and RPMLC

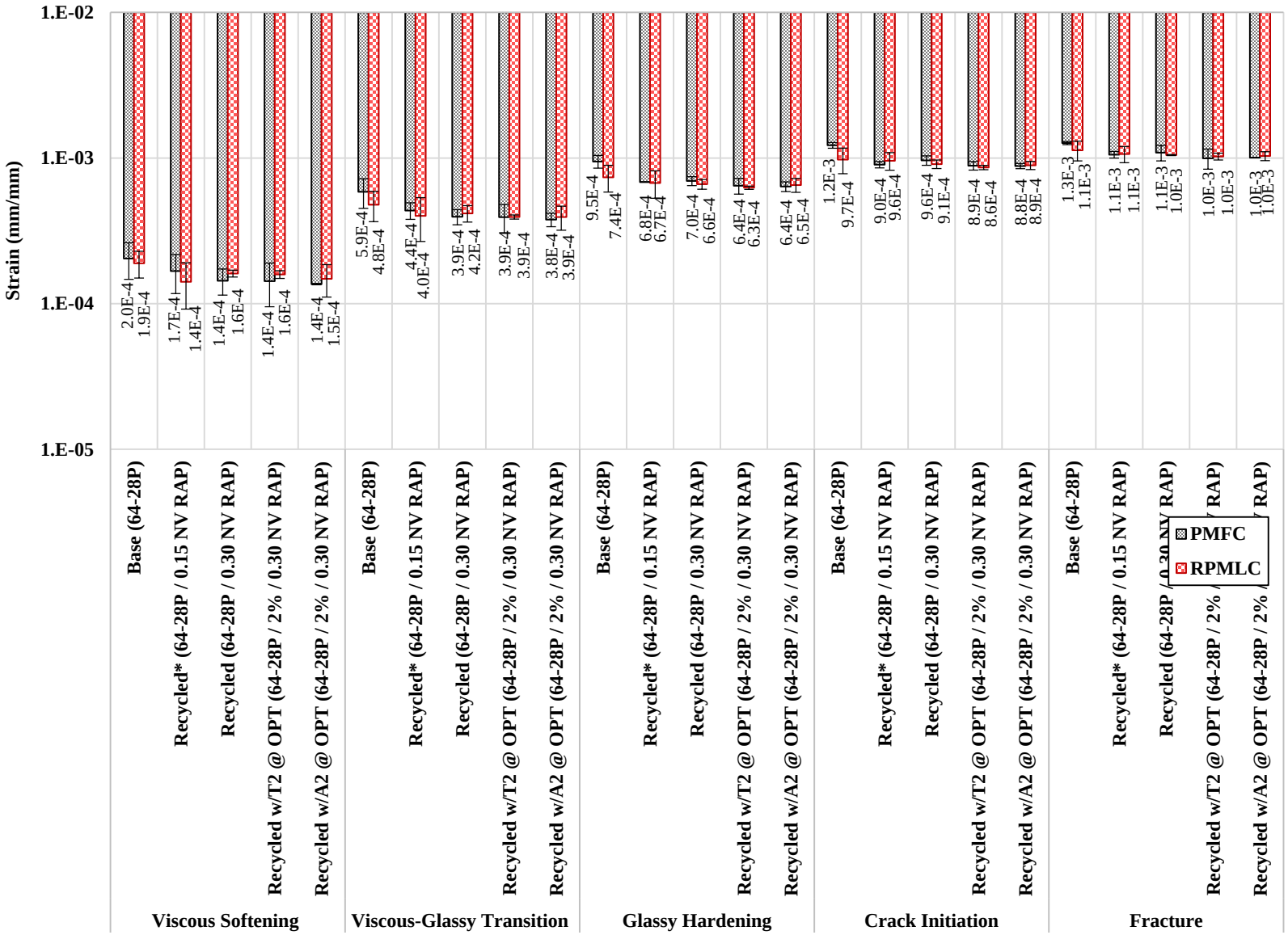

Figure 7. 19. UTSST Strain Measures for Nevada Field Sections, PMFC and RPMLC

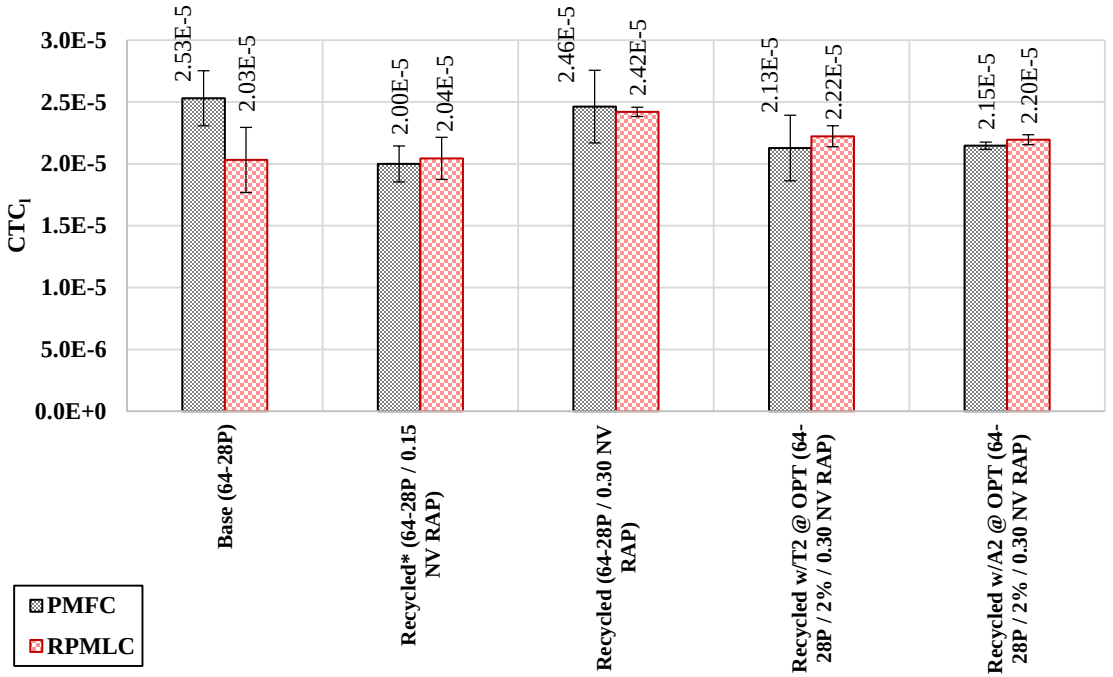

Figure 7. 20. Coefficient of Thermal Contraction for Measures for Nevada Field Sections, PMFC and

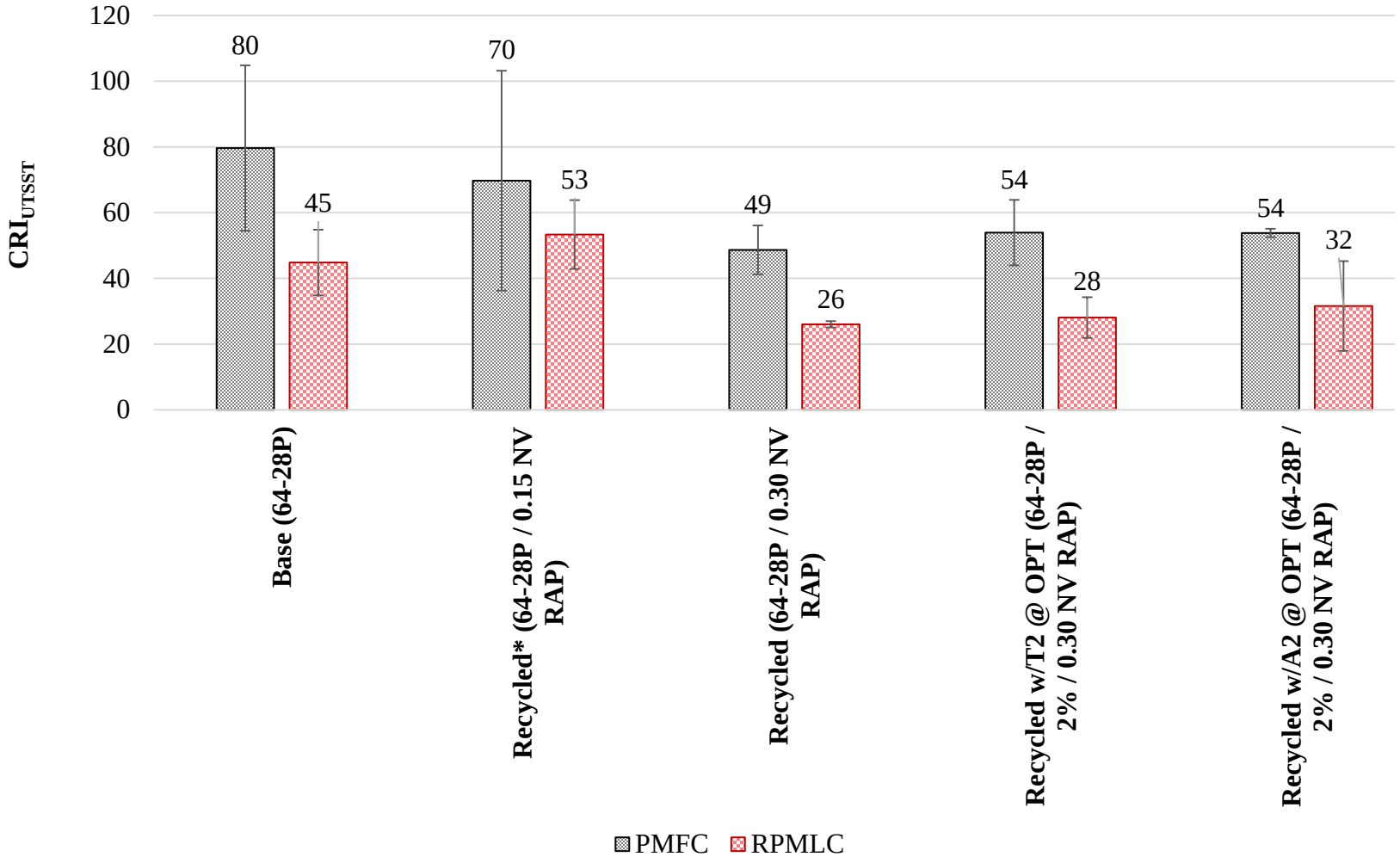

Figure 7. 21. CRI_{UTSST} for Nevada Field Sections, PMFC and RPMLC

7.6.1.5 Comparison between PMFC and RPMLC Specimens

As an initial comparison between two mixture types, Table 7. 6 represents the average bulk specific gravity and the air void content of the RPMLC and PMFC mixtures in the NV field project. Apparently the RPMLC specimens have relatively higher air voids and lower densities compared to the PMFC specimens. Currently, there is limited consistency in identifying correlations between the PMFC and RPMLC mixture properties. However, the reheating process and respective chemical reactions as well as the different compaction methods are the potential reasons of the properties difference in these two specimen categories.

In general, the compaction effort and more specifically the final aggregate orientation can potentially be different in the compaction methods of RPMLC and PMFC specimens. It should be noted that the field cores experience a confining pressure in addition to the compaction effort while the reheated specimens are compacted with Superpave Gyratory Compactor (SGC). In an image processing study conducted by Masad et. al. (1998), a clear difference was observed in the internal structure of the field cores compared to the ones compacted with SGC. It was also noted that the gyratory specimens reached the initial aggregate orientation of the field cores at higher number of gyrations while reached the cores percent air void at lower number of gyrations. Therefore, the method of compaction and the resulting internal structure, i.e. aggregate orientation and segregation, can play a major role in the physical properties of the specimen (Khan et. al., 1998; Button et. al., 1994; Masad et. al., 1998).

Additionally, the absorption and hardening or stiffening of the asphalt binder in the reheated samples during the reheating process could also be introduced as the potential cause of the difference in the specimen properties. However, the results from the NCHRP Report 818 indicated that the process-based factors, including return of baghouse fines, delay in specimen fabrication, aggregate absorption, aggregate hardness, and stockpile moisture content, did not have a significant effect on the differences of mechanical properties among the LMLC (lab mixed – lab compacted) and PMFC or RPMLC; Instead, the difference between the various types of the specimens was attributed to differences in compaction effort and confinement conditions between the two compaction processes (laboratory and field).

Table 7. 6. Air Void and Bulk Specific Gravity for Nevada Field Sections

Mixture ID	% Air Void		Bulk Specific Gravity	
	PMFC	RPMLC	PMFC	RPMLC
Base (64-28P)	3.99	6.15	2.365	2.31
Recycled* (64-28P / 0.15 NV RAP)	3.07	6.77	2.393	2.30
Recycled (64-28P / 0.30 NV RAP)	5.08	6.59	2.360	2.32
Recycled w/T2 @ OPT (64-28P / 2% / 0.30 NV RAP)	4.92	6.68	2.349	2.31
Recycled w/A2 @ OPT (64-28P / 2% / 0.30 NV RAP)	3.51	7.11	2.384	2.30

To statistically compare the air void and bulk specific gravity of the two categories, a Two-Sample assuming unequal variances t-Test was conducted on each of the properties. Results showed a statistically significant difference between the air void and bulk specific gravity levels of the PMFC and RPMLC specimens. Detailed results are provided in Table 7. 7 and Table 7. 8.

Table 7. 7. Results of the t-Test: Two-Sample Assuming Unequal Variances, Air Voids (%)

	PMFC	RPMLC
Mean	4.1119	6.659
Variance	0.76274	0.11996
Observations	5	5
Hypothesized Mean Difference	0	
df	5	
t Stat	-6.0621	
P(T<=t) one-tail	0.00088	
t Critical one-tail	2.01505	
P(T<=t) two-tail	0.00176	
t Critical two-tail	2.57058	

Table 7. 8. Results of the t-Test: Two-Sample Assuming Unequal Variances, Bulk Specific Gravity

	PMFC	RPMLC
Mean	2.37032	2.30738
Variance	0.00032	0.0001
Observations	5	5
Hypothesized Mean Difference	0	
df	6	
t Stat	6.80269	
P(T<=t) one-tail	0.00025	
t Critical one-tail	1.94318	
P(T<=t) two-tail	0.00049	
t Critical two-tail	2.44691	

The TVEP properties of the PMFC and RPMLC specimens in the critical points were also compared to each other in the correlation plots presented in Figure 7. 22 through Figure 7. 26. A reasonable correlation could be observed with an R-squared greater than 0.95 in all cases. However, a slight deviation from the line of equality was observed with the strain measurements as the temperature decreased or became closer to fracture point; a key region in the low-temperature behavior of asphalt mixture performance investigations.

Similar comparisons of the UTSST modulus was also showed a decent correlation but a slight deviation from the line of equality again particularly evident in in the lower temperatures in Figure 7. 25. Thus, implying higher moduli for the PMFC specimens. The higher levels of air void along with unknown chemical reactions in the reheating process, previously noted with the RPMLC specimens, could cause the RPMLC specimens to be more brittle, resulting a lower modulus compared to the PMFC specimens.

Observation of the CRI_{UTSST} correlation between the PMFC and RPMLC specimens in Figure 7. 26, did not show as strong of coefficient of determination compared to the other properties previously discussed. It could result from combination of all variations noted between the TVEP properties. Additionally, the PMFC mixtures showed a higher CRI_{UTSST} which aging could be related to discrepancies resulting from the laboratory compaction, reheating procedure, and compacted aggregate structure observations discussed previously.

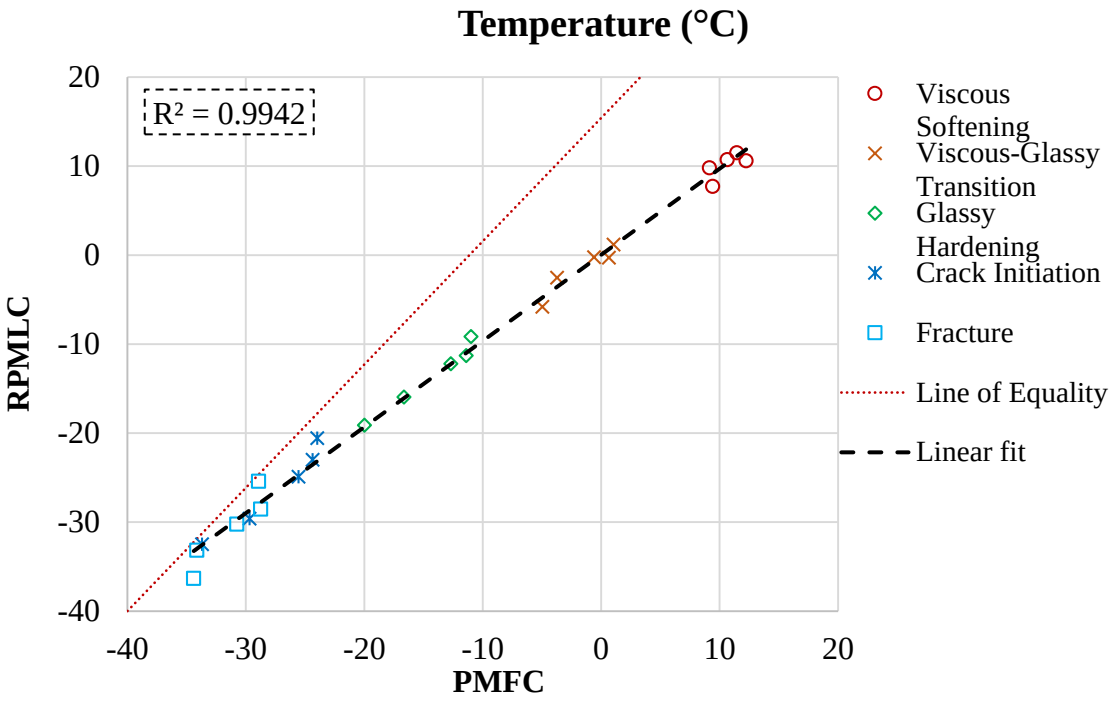

Figure 7. 22. UTSST Temperature Measures Comparison Between the PMFC and RPMLC Specimens

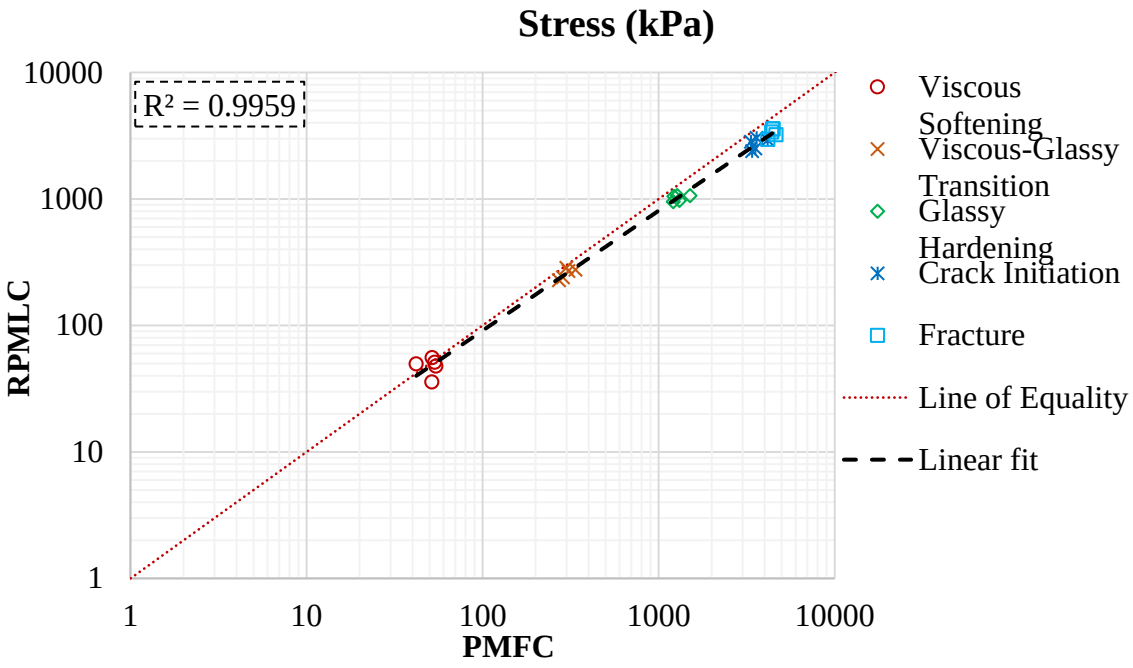

Figure 7. 23. UTSST Stress Measures Comparison Between the PMFC and RPMLC Specimens

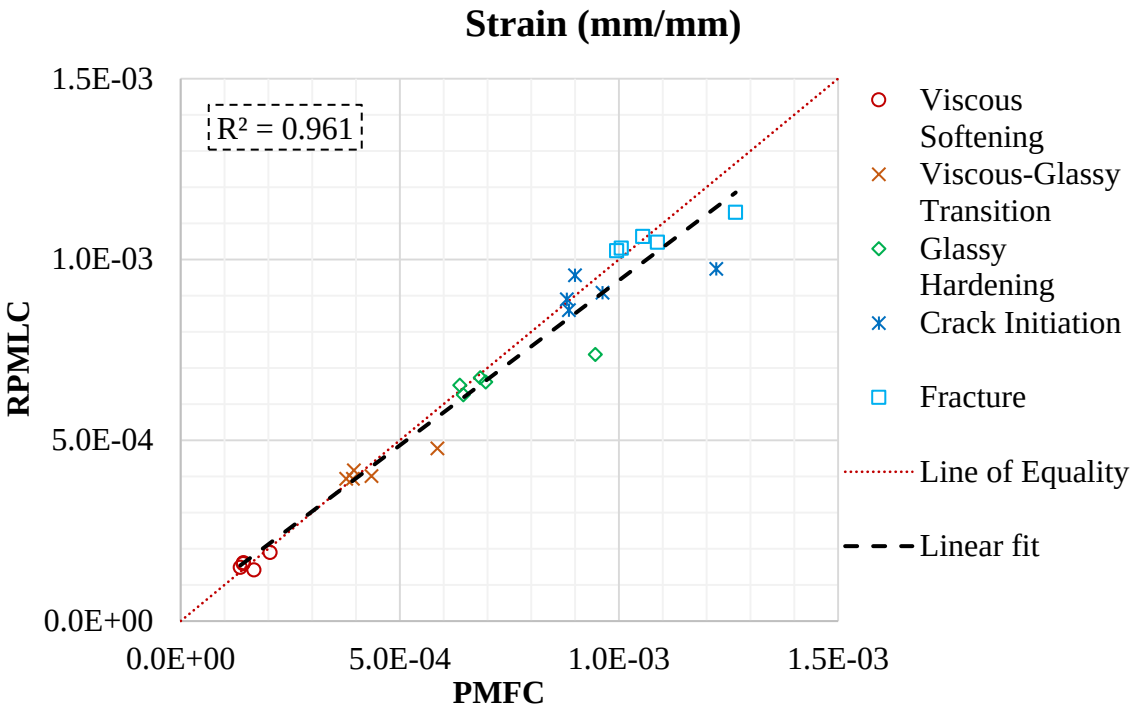

Figure 7. 24. UTSST Strain Measures Comparison Between the PMFC and RPMLC Specimens

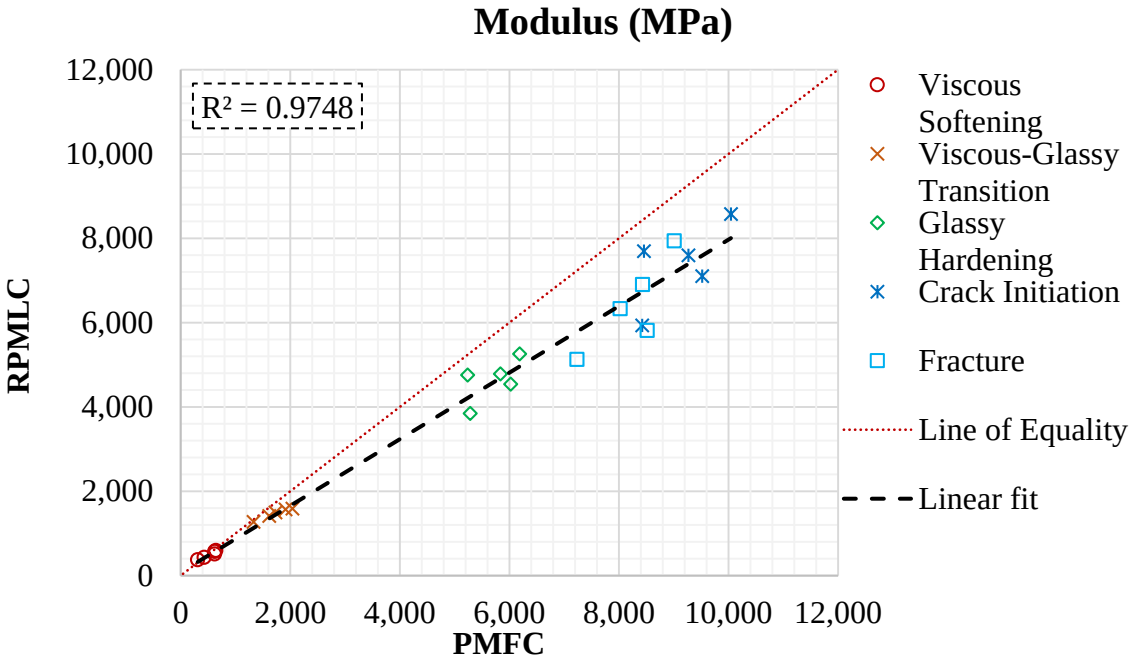

Figure 7. 25. UTSST Modulus Comparison Between the PMFC and RPMLC Specimens

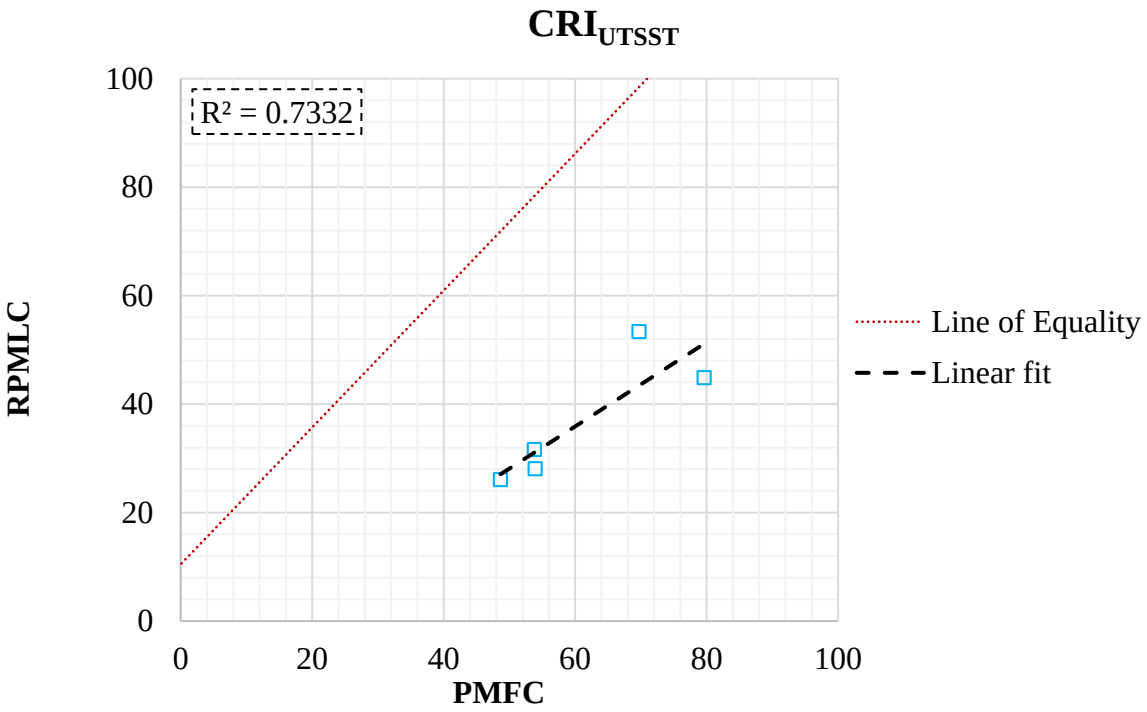

Figure 7. 26. CRI_{UTSST} Comparison Between the PMFC and RPMLC Specimens

7.7 Summary of the Chapter

The initial sections of this chapter focus on the influences of the recycled material and RAs on the 64-28P base binder through the binder PG grading and mortar testing. The material came from the Nevada field project utilizing the PG 64-28P base binder, NV RAP and two different RAs at respective optimum dosages. Within each respective test, an increase in stiffness and brittle behavior with the addition of recycled materials were generally indicated. This finding was subsequently followed by a partial restoration of the flexibility with the addition of the RAs at the selected optimum dosages. Both procedures provide consistent direction for the influence of the evaluation materials, i.e. NV RAP and RAs, and are generally in agreement.

The results also suggested that the mortar procedure was capable of characterizing the effects of RAP and RA materials on virgin binder without the use of chemical extraction, acknowledging that there are some inconsistencies between the PG grading and mortar procedure results. It also should be mentioned that the test variability was relatively higher for some cases in the mortar testing, which necessitated the testing of additional replicates and selecting the most repeatable results.

In addition, the PMFC and RPMLC specimens of five different test sections in the NV field project were subjected to the Uniaxial Thermal Stress and Strain Test (UTSST) after laboratory aging for 5 days at 85°C. The findings of the PG grading and mortar testing regarding the influence of the recycled material and RAs were also verified with this mixture testing.

Generally, most of the thermo-viscoelastic properties were observed to occur at warmer temperatures with increased levels of recycled material within the evaluated mixtures. Thus, the general findings were understood to indicate a general stiffening of the mixtures at the warmer temperatures where the viscous properties were prevalent. Further, the low temperature portion of the test indicated a clear increase in the brittle behavior of the mixtures with increased recycled material levels. Although the addition of the RAs to the recycled mixtures indicated some extent of modulus restoration, crack initiation and fracture were observed to occur in significantly warmer temperatures compared to the virgin and recycled mixture.

These findings were also supported with CRI_{UTSST} where the addition of the RAs did increase the RI values, indicating some levels of the low temperature properties restoration;

however, none of them were able to completely restore the mixture properties to those of the control mixtures.

The air void level of the mixtures was observed to have a substantial difference between the PMFC and RPMLC mixtures which mainly caused by the difference between the compaction methods. However, both mixture types were found to have a similar direction of behavior upon the addition of the RAs and/or recycled materials.

CHAPTER 8 SUMMARY, CONCLUSIONS AND RECOMMENDATIONS

This study has been conducted as a part of NCHRP 09-58 project entitled with "The Effects of Recycling Agents on Asphalt Mixtures with High RAS and RAP Binder Ratios." The objectives of this research are to evaluate the effectiveness of recycling agents (RAs) in HMA and WMA mixtures with high RAS, RAP, or combined RAS/RAP binder ratios through a coordinated program of laboratory and field experiments. The University of Nevada, Reno is responsible for the laboratory oxidative aging of the material cluster defined in this project as well as conducting a field project in Reno, Nevada. The detailed methodology implemented in this study following by the respective outcomes and data analysis were elaborately discussed in previous chapters. An overall summary of the effort undertaken as part of this thesis is presented in this chapter.

8.1 Summary and Conclusions

The information of the three different types of base binders and their corresponding blends of recycled material and RAs were previously defined in Chapter 4. Implementing the proposed methodologies defined in Chapter 3, the laboratory forced-draft oven aging and accelerated aging (PAV at 20, 40, and 60 hours) were conducted according to the experimental plan. The FT-IR tests and the DSR isothermal frequency sweep tests were conducted on the aged binders to analyze the resulting oxidation kinetics and rheological properties. Then, in Chapter 5, the rheological parameters, i.e. G*, phase angle, LSV, G-R (at 15°C and 0.005 rad/sec) were implemented along with the CA measurements to provide

the HS plots for evaluating the oxidative aging and the different modifier's effect. The kinetic results indicated that the oxidative aging rate are influenced by the aging temperature, duration, base binder type, and the utilized asphalt modifier, i.e. recycled materials and RAs. It was also concluded that both RAs reduced the overall stiffness in the investigated stages of oxidation. However, differential aging rates or HS were observed between the RA and RAP/RAS additions to each of the three base binders form the forced-draft oven aging. In fact, the base binder aging properties due to the addition of the recycled material was highly influenced by the RA dosages within each blend. This finding highlights the importance and effect of the dosage selection on the binder aging behavior. Further, the noted differences were not consistent with the type of RAS, i.e. MWAS or TOAS. In general, the differences in the base binders and the type of RAS potentially led to the difference in the interaction of all the blended materials, resulting in the overall difference in aging behavior.

Then the linear regression analysis was conducted on the LSV HS plots to explore the significance of variation of the modified binder blends aging path to that of the corresponding base binders. The results indicated that the addition of the RA only did not generally change the slope of the HS plots; also, a non-significant deviation from the base binder aging path were observed upon the addition of the recycled materials except for one of the binder blends. Therefore, additional investigations were recommended to confirm the validity of the statistical analysis measurement before making a real exception between the overall behaviors of the base binder with the modified-blends.

General observations of the HS plots showed that the two aging protocols were representing relatively similar results. However, caution must be taken in the selection of PAV aging protocol in which the aging pressure and temperature substantially deviates from actual field condition.

Additionally, the evaluation of the cracking potential of the PAV aged binders through ΔTc and G-R parameter did not indicate a strong correlation between the these cracking indicators, due to the different states of material evaluation at intermediate and low temperature, noting the constant temperature of 15°C and constant frequency of 0.005 rad/s for the G-R parameter. Further, the required PAV time duration for each of the respective binders to reach the G-R cracking limits were investigated at modified temperatures of 15°C, PG.mid and PG.low+43. The results yielded to some levels of discrepancy between the observations of the binder behaviors, highlighting the essence of further investigation on the actual in-place pavement mixture specimens to properly understand what happens in reality rather than just binder evaluations.

In the next step, the binder blend aging predictions conducted through combined kinetics and hardening susceptibility (HS) models driven by temperature estimation modeling (using TEMPS) within the binder specific geographic locations, i.e. TX, NH, and NV in Chapter 6. The use of this procedure permits the relative comparison of the evaluated binder blends in terms of an estimated time to reach the two predefined G-R limits (i.e., 180 kPa and 600 kPa) as a function of time in-service at their corresponding environments.

Overall, the recycling agents showed a beneficial effect on the base binder performance life; the larger the dosage resulted in a more substantial benefit of the recycling agent.

However, this consistent trend did not continue with the inclusion of the recycled material, which tends to counteract the RAs. The results indicated that using the recycled materials along with the recycling agents at the optimum dosage was able to restore the binder blend properties to the virgin binder. Thus, confirming the RA dosage selection methodology proposed in Chapter 3, which in general showed the need for a considerably higher optimum RA dosage to restore the PG of the base binder when compared to the low dosage used in the field.

The influences of the recycled material and RAs on the PG 64-28P base binder were also investigated through the binder PG grading and mortar testing in Chapter 7. Within each respective test, an increase in stiffness and brittle behavior with the addition of recycled materials were generally indicated. This finding was subsequently followed by a partial restoration of the flexibility (i.e., increase in phase angle) with the addition of the RAs at the selected optimum dosages. Both procedures provide consistent direction for the influence of the evaluation materials, i.e. NV RAP and RAs, and are generally in agreement.

The results also suggested that the mortar procedure was capable of characterizing the effects of RAP and RA materials on virgin binder without the use of chemical extraction, acknowledging that there are some inconsistencies between the PG and mortar procedure results. It also should be mentioned that the test variability was relatively higher for some cases in the mortar testing, which necessitated the testing of additional replicates and selecting the most repeatable results.

In addition, the PMFC and RPMLC specimens of five different test sections in the NV field project were subjected to the Uniaxial Thermal Stress and Strain Test (UTSST) after

laboratory aging for 5 days at 85°C. The findings of the PG and mortar testing regarding the influence of the recycled material and RAs were also verified with this mixture testing.

Generally, most of the thermo-viscoelastic properties were observed to occur at warmer temperatures with increased levels of recycled material within the evaluated mixtures. Thus, the general findings were understood to indicate a general stiffening of the mixtures at the warmer temperatures where the viscous properties were prevalent. Further, the low temperature portion of the test indicated a clear increase in the brittle behavior of the mixtures with increased recycled material levels. Although the addition of the RAs to the recycled mixtures indicated some extent of modulus restoration, crack initiation and fracture were observed to occur at significantly warmer temperatures compared to the virgin mixture.

These findings were also supported with CRI_{UTSST} where the addition of the RAs did increase the cracking resistance values, indicating some levels of the low temperature properties restoration. However, none of the RAs at the evaluated dosage were able to completely restore the mixture properties to those of the control mixtures.

The air void level of the mixtures was observed to have a substantial difference between the PMFC and RPMLC mixtures, which can be attributed to the difference between the laboratory and field compaction methods. However, both mixture types were found to have a similar direction of behavior upon the addition of the RAs and/or recycled materials.

8.2 Recommendations

This study covered several aspects of oxidative aging over a variety of base binders, recycled materials and RAs. The outcomes were generally reasonable, confirming the results of previous investigations that have been completed at the University of Nevada, Reno while initiating a number of follow-up research topics. The following are recommendations that can be implemented in future studies:

- Increasing the variety of the base binder types, recycled materials, RAs, as well as the variety of the binder blends including the recycled blends without RA, and the RAS only blends with and without RAs in the experimental plan would provide more insight into the potential influence of the RAs on the base binder and recycled materials.
- Additional related asphalt mixture testing and field pavement aging in various environment is required to investigate the correlation between the laboratory binder aging and the actual field oxidative aging of asphalt mixtures.
- Comprehensive cost analysis on the potential cost-savings for using recycled materials with RAs would motivate the industry to consider and implement the findings from this study.
- In general, additional evaluation efforts in laboratory and field are required considering the influence of various base binders, additives, and recycled materials to explore the potential benefits of the newly

proposed limits in ΔTc and crossover temperatures, as well as the possible correlation between the various cracking indicators.

REFERENCES

AASHTO, Standard Specifications for Transportation Materials and Methods of Sampling and Testing. American Association of State Highway and Transportation Officials, 31st Edition, Washington, D.C, 2010.

Airey, G.D. Rheological Properties of Styrene Butadiene Styrene Polymer Modified Road Bitumens, Fuel, Vol. 82, No. 14, pp. 1709–1719, 2003.

Alavi, M. Z. Comprehensive Methodologies for Analysis of Thermal Cracking in Asphalt Concrete Pavements. Ph.D. Dissertation, Pavements/Materials Program, Civil Engineering Department, University of Nevada, Reno, UMI Number: 3638109, ProQuest UMI Dissertation Publishing, Ann Arbor, MI, August 2014.

Alavi, M. Z., and Hajj, E. Y. Effect of Cooling Rate on the Thermo-Volumetric, Thermo-Viscoelastic, and Fracture Properties of Asphalt Mixtures. Asphalt Pavements, Tylor and Francis Group, London, 2014, pp. 405-416.

Alavi, M. Z., E. Y. Hajj, and P. E. Sebaaly. A Comprehensive Model for Prediction Thermal Cracking Events in Asphalt Pavements. International Journal of Pavement Engineering, Taylor & Francis, 2015.

Alavi, M. Z., Hajj, E.Y., Morian, N., and Sebaaly, P.E., Low Temperature Characterization of Asphalt Mixtures by Measuring Visco-Elastic Properties under Thermal Loading. ISCORD 2013: Proceeding of International Symposium on Cold Regions Development, American Society of Civil Engineering, 2013, pp. 404-415.

Alavi, M.Z., Morian, N., Hajj, E.Y., Sebaaly, P.E., "Influence of Asphalt Binder Oxidative Aging on Critical Thermal Cracking Characteristics of Asphalt Mixtures," Journal of the Association of Asphalt Paving Technologists, Vol 84, 2015, pp. 115-142.

Anderson, R. M., G. N. King, D. I. Hanson, and P.B. Blankenship. Evaluation of the Relationship between Asphalt Binder Properties and Non-Load Related Cracking. Journal of the Association of Asphalt Paving Technologists, Vol. 80, 2011, pp. 615-649.

Asli, H., E. Ahmadinia, M. Zargar, and M. R. Karim. Investigation on Physical Properties of Waste Cooking Oil—Rejuvenated Bitumen Binder. Construction and Building Materials, Vol. 37, 2012, pp. 398-405.

Asphalt Institute. Asphalt Hot-Mix Recycling. The Asphalt Institute Manual, Series No. 20 (MS-20), Second Edition, 1986, 46 p.

ASTM, 2016. American Society for Testing and Materials, ASTM International, West Conshohocken, New Jersey.

Bahia, H. Low-Temperature Isothermal Physical Hardening of Asphalt Cements. Ph.D. Dissertation, Pennsylvania State University, 1991.

Booshehrian, A., W.S. Mogawer, and R. Bonaquist. How to Construct an Asphalt Binder Master Curve and Assess the Degree of Blending between RAP and Virgin Binders. Journal of Materials in Civil Engineering, Vol. 25, No. 12, 2013, pp. 1813-1821.

Coffey, S., E. Dubois, Y. Mehta, and C. Purdy. Determining Impact of Degree of Blending Between Virgin and Reclaimed Asphalt Binder on Predicted Pavement Performance Using Mechanistic-Empirical Pavement Design Guide. 92nd Annual Meeting of the Transportation Research Board, Washington, DC, Proceedings, 2013.

Copeland, A. Reclaimed Asphalt Pavement in Asphalt Mixtures: State of the Practice, Report No. FHWA-HRT-11-021, Federal Highway Administration, Washington, DC, 2011.

Epps Martin, M., E. Arambula, F. Kaseer, F. Yin, E. Hajj, J. Daniel, C. Glover, N. Morian, S. Pournoman. The Effect of Recycling Agents on Asphalt Mictures with High RAS and RAP Binder Ratios, Phase IIB Interim Report. Transportation Research Board, Washington, D.C., 2017.

Epps Martin, M., F. Zhou, E. Arambula, E. S. Park, A. Chowdhury, F. Kaseer, J. C. Munoz, E. Hajj, J. Daniel, C. Glover. The Effect of Recycling Agents on Asphalt Mictures with High RAS and RAP Binder Ratios, Phase I Interim Report. Transportation Research Board, Washington, D.C., 2015, http://onlinepubs.trb.org/onlinepubs/nchrp/docs/NCHRP09-58_PhI_InterimReport.pdf.

Epps Martin, M., F. Zhou, E. Arambula, E. S. Park, A. Chowdhury, F. Kaseer, J. C. Munoz, E. Hajj, A. Rose, J. Daniel, C. Glover. The Effect of Recycling Agents on Asphalt Mictures with High RAS and RAP Binder Ratios, Phase II Interim Report. Transportation Research Board, Washington, D.C., 2016, http://onlinepubs.trb.org/onlinepubs/nchrp/docs/NCHRP09-58_PhII_DraftInterimReport.pdf.

Epps, J.A., D.N. Little, R.J. Holmgreen, and R.L. Terrel. Guidelines for Recycling Pavement Materials, NCHRP Report 224, National Cooperative Highway Research Program, Washington, DC, 1980.

Epps, J.A., D.N. Little, R.J. Holmgreen, and R.L. Terrel. Guidelines for Recycling Pavement Materials, NCHRP Report 224, National Cooperative Highway Research Program, Washington, DC, 1980.

Epps, J.A., D.N. Little, R.J. Holmgreen, and R.L. Terrel. Guidelines for Recycling Pavement Materials, NCHRP Report 224, National Cooperative Highway Research Program, Washington, DC, 1980.

Glover, C. G., and Y. Cui. Exploring the Combined Effects of Asphalt Oxidation Kinetics, Hardening Susceptibility, Oxygen Diffusivity, Pavement Characteristics and Climate on Pavement Durability, presentation at the 50th Annual Petersen Asphalt Research Conference, July 16, 2013, Laramie, Wyoming.

Glover, C.J., R. Han, X. Jin, N. Prapaitrakul, Y. Cui, A. Rose, JJ. Lawrence, M. Padigala, E. Arambula, E. Sug Park, A. Epps Martin. Evaluation of Binder Aging and Its Influence in Aging of Hot Mix Asphalt Concrete: Technical Report, Report No. FHWA/TX-14/0-6009-2, Texas A&M Transportation Institute, College Station, TX, January 2014.

Glover, J.C., R.R. Davison, C.H. Domke, Y. Ruan, P. Juristyarini, D.B. Knorr, and S.H. Jung. Development of a New Method for Assessing Asphalt Binder Durability with Field Evaluation. Report No. FHWA/TX/05-1872-2, Texas Transportation Institute, College Station, TX, 2005, 334 pp.

Hajj, E. Y., Alavi , M. Z., Morian, N. E., and Sebaaly, P. E., Effect of Select Warm-Mix Additives on Thermo-Viscoelastic Properties of Asphalt Mixtures. Journal of Road Material and Pavement Design, Vol. 14, Special Issue: EATA 2013, 2013, pp. 175-186.

Hajj, E. Y., N. Morian, P. E. Sebaaly, H. Nabizadeh, and S. Pournoman. Evaluation of Adaptive Glover-Rowe Parameter on Aging of Select Modified Binders. Presented at 95th Annual Meeting of the Transportation Research Board, Washington, D.C., 2016.

Hajj, E.Y., P.E. Sebaaly, and R. Shresta. Laboratory Evaluation of Mixes Containing Recycled Asphalt Pavement (RAP). International Journal of Road Materials and Pavements Design, Vol. 10, No. 3, 2009.

Han, R. Improvement to a Transport Model of Asphalt Binder Oxidation in Pavements: Pavement Temperature Modeling, Oxition Diffusivity in Asphalt Binders and Mastics, and Pavement Air Void Charactrization. Ph.D. Dissertation, Texas A&M University, 2011.

Han, R., Jin, X., and C. J., Glover (2013), Oxygen Diffusivity in Asphalts and Mastics, Petroleum Science and Technology, Vol. 31, Issue 15.

Hanson, D. I., P. B. Blankenship, G. N. King, and R. M. Anderson. Techniques for Prevention and Remediation of Non-Load-Related Distresses on HMA Airport Pavements – Phase II, Final Report, Airfield Asphalt Pavement Technology Program, Project 06-01, 2010.

Hussain, A., and Q. Yanjun. Evaluation of Asphalt Mixes Containing Reclaimed Asphalt Pavement for Wearing Courses. International Conference on Traffic and Transportation Engineering (ICTTE 2012), 2012, pp. 43-48.

Im, S., F. Zhou, R. Lee, and T. Scullion. Impacts of Rejuvenators on Performance and Engineering Properties of Asphalt Mixtures Containing Recycled Materials. Construction and Building Materials, Vol. 53, 2014, pp. 596-603.

Kandhal, P.S. ASTM STP 628: Low-Temperature Properties of Bituminous Materials and Compacted Bituminous Paving Mixtures. C.R. Marek (Ed.), American Society for Testing and Materials, Philadelphia, PA, 1977.

Kandhal, P.S., and R.B. Mallick. Pavement Recycling Guidelines for State and Local Governments—Participant's Reference Book. Report No. FHWA-SA-97, Chapter 7: Hot Mix Asphalt Recycling (Materials and Mix Design), National Center for Asphalt Technology, Auburn, AL, 1997.

Kari, W.J., N.E. Andersen, D.D. Davidson, H.L. Davis, R.N. Doty, S.J. Escobar, D.L. Kline, and T.K. Stone. Prototype Specifications for RAs Used in Hot-Mix Recycling. Journal of the Association of Asphalt Paving Technologists, Vol. 49, 1980, pp. 177-192.

King, G. WRI Pavement Preservation Symposium, July 2013. http://www.petersenasphaltconference.org/download/2013/2013P3Symposium_files/AM%20no%202%20King.pdf. Accessed July 31, 2015.

King, G., M. Anderson, D. Hanson, and P. Blankenship. Using Black Space Diagrams to Predict Age-Induced Cracking. 7th RILEM International Conference on Cracking in Pavements, Vol. 4, pp. 453-463, Delft, Netherlands, 2012.

Kriz, P., D.L. Grant, B.A. Veloza, M.J. Gale, A.G. Blahey, J.H. Brownie, R.D. Shirts, and S. Maccarrone. Blending and Diffusion of Reclaimed Asphalt Pavement and Virgin Asphalt Binders. Journal of the Road Materials and Pavement Design, Vol. 15, No. S1, 2014, pp. 78-112.

Lee, T., R.L. Terrel, and J.P. Mahoney. Test for Efficiency of Mixing of Recycled Asphalt Paving Mixtures. Transportation Research Record No. 911, Transportation Research Board, National Research Council, Washington, DC, 1983, pp. 51-60.

Li, X., M.O. Marasteanu, R.C. Williams, and T.R. Clyne. Effect of RAP (Proportion and Type) and Binder Grade on the Properties of Asphalt Mixtures. Transportation Research Record No. 2051, Transportation Research Board, National Research Council, Washington, DC, 2008, pp. 90-97.

Lin, J., J. Hong, C. Huang, J. Liu, and S. Wu. Effectiveness of Rejuvenator Seal Materials on Performance of Asphalt Pavement. Construction and Building Materials, Vol. 55, 2014, pp. 63-68.

Lin, P., T.L. Wu, C. Chang, and B. Chou. Effects of RAs on Aged Asphalt Binders and Reclaimed Asphalt Concrete. Materials and Structures, Vol. 44, No. 5, 2011, pp. 911-921.

Little, D.N., R.J. Holmgreen, and J.A. Epps. Effect of RAs on the Structural Performance of Recycled Asphalt Concrete Materials. Journal of the Association of Asphalt Paving Technologists, Vol. 50, 1981, pp. 32-63.

Lu, X., and U. Isacsson. Chemical and Rheological Characteristics of Styrene-Butadiene Styrene Polymer-Modified Bitumens, In Transportation Research Record: Journal of the Transportation Research Board, No. 1661, Transportation Research Board of the National Academies, Washington, D.C., 1999, pp. 83–92.

M. Liu, M.A. Ferry, Richard R. Davison, Charles J. Glover, and Jerry A. Bullin, Oxygen Uptake as Correlated to Carbonyl Growth in Aged Asphalts and Asphalt Corbett Fractions, Industrial & Engineering Chemistry Product Research and Development, Vol. 37.

McDaniel, R. S., and H. U. Bahia. Field Evaluation of Asphalt Additives to Control Rutting and Cracking, In Transportation Research Record: Journal of the Transportation Research Board, No. 1829, Transportation Research Board of the National Academies, Washington, D.C., pp. 47–54, 2003.

Mogawer, W. S., A. J. Austerman, R. Kluttz, S. Puchalski. Using Polymer Modification and Rejuvenators to Improve the Performance of High Reclaimed Asphalt Pavement Mixtures, in Transportation Research Record No. 2575, Transportation Research Board, Washington, D.C, pp. 10-18, 2016.

Mogawer, W., A. Austerman, L. Mohammad, and M.E. Kutay. Evaluation of High RAPWMA Asphalt Rubber Mixtures. Road Materials and Pavement Design, Vol. 14, 2013, 2013, pp. 129-147.

Mogawer, W., T. Bennert, J. Daniel, R. Bonaquist, A. J. Austerman, and A. Booshehrian. Performance Characteristics of Plant Produced High RAP Mixtures. Journal of the Road Materials and Pavement Design, Vol. 13, 2012, pp. 183-208.

Mogawer, W.S., A. Booshehrian, S. Vahidi, and A.J. Austerman. Evaluating the Effect of Rejuvenators on the Degree of Blending and Performance of High RAP, RAS, and RAP/ RAS Mixtures. Journal of the Road Materials and Pavement Design, Vol. 14, Supplement 2, 2013, pp. 193-213.

Mogawer, W.S., A. Booshehrian, S. Vahidi, and A.J. Austerman. Evaluating the Effect of Rejuvenators on the Degree of Blending and Performance of High RAP, RAS, and RAP/ RAS Mixtures. Journal of the Road Materials and Pavement Design, Vol. 14, Supplement 2, 2013, pp. 193-213.

Mohammad, L. N., M. A. Elseifi, S. B. Cooper, III, C. S. Hughes, C. S., J. W. Button, E. L. Dukatz, Jr. NCHRP Report 818: Comparing the Volumetric Mechanical Properties of Laboratory and Fiels Specimens of Asphalt Concrete. Transportation Research Board, Washington, D.C., 2016. http://www.trb.org/Main/Blurbs/173797.aspx

Mohammad, L. N., M. A. Elseifi, S. B. Cooper, III, C. S. Hughes, C. S., J. W. Button, E. L. Dukatz, Jr. NCHRP Report 818: Comparing the Volumetric Mechanical Properties of Laboratory and Fiels Specimens of Asphalt Concrete. Transportation Research Board, Washington, D.C., 2016. http://www.trb.org/Main/Blurbs/173797.aspx

Morian, N. E. Evaluation of Thermal Oxidative Aging Effect on the Rheological Performance of Modified Asphalt Binders, Master Thesis, University of Nevada, Reno, 2015.

Morian, N. E. Influence of Mixture Characteristics on the Oxidative Aging of Asphalt Binders, PhD dissertation, University of Nevada, Reno, 2014.

Morian, N., S. Pournoman, E. Y. Hajj, and P. E. Sebaaly. Assessment of Asphalt Binder Cracking Indicators: A Pilot Study. Presented at 96th Annual Meeting of the Transportation Research Board, Washington, D.C., 2017.

Morian, N., Zhu, C. and E.Y., Hajj. "Rheological Indices: Phenomenological Aspects of Asphalt Binder Aging Evaluations," Transportation Research Record: Journal of the Transportation Research Board, Issue No. 2505, Transportation Research Board of the National Academies, Washington, D.C., 2015, pp. 32-40.

NCAT. Hot-Mix Asphalt Materials, Mixture Design and Construction. NAPA Research and Education Foundation, Lanham, MD, 2009, 720 pp.

Newcomb, D.E., and J.A. Epps. Asphalt Recycling Technology: Literature Review and Research Plan. Report No. ESL-TR-81-42, Air Force Engineering and Services Center, Florida, 1981.

Newcomb, D.E., B.J. Nusser, B.M. Kiggundu, and D.M. Zallen. Laboratory Study of the Effects of Recycling Modifiers on Aged Asphalt Cement. Transportation Research Record No. 968, Transportation Research Board, National Research Council, Washington, DC, 1984, pp. 66-77.

Pucci et al. T. Pucci, A. G. Dumont, and Herve Di Benedetto. Thermomechanical and Mechanical Behavior of Asphalt Mixtures at Cold Temperature, Road Materials and Pavement Design, Vol. 5, No.1, Taylor & Francis, 2004.

RHEA. Rhea, Rheology Analysis Software, version 1.2.1 Abatech, Inc., Blooming Glen, PA, 2011.

Rostler, F.S., and R.M. White. Influence of Chemical Composition of Asphalts on Performance, Particularly Durability. American Society of Testing and Materials, Special Technical Publication, 1959.

Rowe, G. M. Prepared Discussion for the AAPT Paper by Anderson et al.: Evaluation of the Relationship between Asphalt Binder Properties and Non-Load Related Cracking. Journal of the Association of Asphalt Paving Technologists, Vol. 80, 2011, pp. 649-662.

Ruan, Y., R. R. Davison, and C. J. Glover. An Investigation of Asphalt Durability: Relationships between Ductility and Rheological Properties for Unmodified Asphalts. Petroleum Science and Technology, Vol. 21, 2003, pp. 231-254.

Ruan, Y., R.R. Davison, and C.J. Glover. An Investigation of Asphalt Durability: Relationships between Ductility and Rheological Properties for Unmodified Asphalts. Petroleum Science and Technology, Vol. 21, pp. 231-254, 2003.

Sebaaly, P.E., A. Lake, and J. Epps. Evaluation of Low-Temperature Properties of HMA Mixtures, Journal of Transportation Engineering, Vol. 128, No. 6, pp. 578-586, 2002.

Shah, A., R.S. McDaniel, G.A. Huber, and V.L. Gallivan. Investigation of Properties of Plant-Produced Reclaimed Asphalt Pavement Mixtures. Transportation Research Record No. 1998, Transportation Research Board, National Research Council, Washington, DC, 2007, pp. 103-111.

Shen, J., and Y. Ohne. Determining Rejuvenator Content for Recycling Reclaimed Asphalt Pavement by SHRP Binder Specifications. The International Journal of Pavement Engineering, Vol. 3, No. 4, 2002, pp. 261-268.

Shen, J., S. Amirkhanian, and J.A. Miller. Effects of Rejuvenating Agents on Superpave Mixtures Containing Reclaimed Asphalt Pavement. Journal of Materials in Civil Engineering, Vol. 19, No. 5, 2007, pp. 376-384.

Shen, J., S. Amirkhanian, and S. Lee. The Effects of Rejuvenating Agents on Recycled Aged CRM Binders. The International Journal of Pavement Engineering, Vol. 6, No. 4, 2005, pp. 273-279.

Smith. Brian C. Smith, Fundamentals of Fourier Transform Infrared Spectroscopy, Second Edition, CRC Press, Taylor & Francis Group, Boca Raton, Florida, 2011.

The Minitab Blog. “How to Compare Regression Slopes”. Jim Frost. www.blog.minitab.com. Accessed April. 29, 2017.

Tran, N.H., A. Taylor, and R. Willis. Effect of Rejuvenator on Performance Properties of HMA Mixtures with High RAP and RAS Contents. NCAT Report 12-05, National Center for Asphalt Technology, Auburn, AL, 2012, 70 pp.

Tran, N.H., A. Taylor, and R. Willis. Effect of Rejuvenator on Performance Properties of HMA Mixtures with High RAP and RAS Contents. NCAT Report 12-05, National Center for Asphalt Technology, Auburn, AL, 2012, 70 pp.

Valdés, G., F. Pérez-Jiménez, R. Miró, A. Martínez, R. Lee, and R. Botella. Experimental Study of Recycled Asphalt Mixtures with High Percentages of Reclaimed Asphalt Pavement (RAP). Construction and Building Materials, Vol. 25, (March), 2011, pp. 1289-1297.

West, R., A. Kvasnak, N. Tran, B. Powell, and P. Turner. Testing of Moderate and High RAP Content Mixes: Laboratory and Accelerated Field Performance at the National Center for Asphalt Technology Test Track. Transportation Research Record No. 2126, Transportation Research Board, National Research Council, Washington, DC, 2009, pp. 100-108.

West, R., Willis, J.R., and M. Marasteanu. NCHRP 9-46: Improved Mix Design, Evaluation, and Materials Management Practices for Hot Mix Asphalt with High

Reclaimed Asphalt Pavement Content, NCHRP Report 752, Transportation Research Board, National Research Council, Washington, DC, 2013.

Woo, W. J., A. Chowdhury, and C. J. Glover. Field Aging of Unmodified Asphalt Binder in Three Texas Long-Term Performance Pavements. In Transportation Research Record: Journal of the Transportation Research Board, No. 2051, Transportation Research Board of the National Academies, Washington D.C., 2008, pp. 15-22.

Woo, W. J., E. Ofori-Abebresse, A. Chowdhury, J. M. Hilbrich, Z. Kraus, A. E. Martin, and C. J. Glover. Polymer Modified Asphalt Durability in Pavements, Report No. FHWA/TX-07/0-4688-1, Texas Transportation Institute, College Station, Texas, 2007a.

Woo, W. J., J. M. Hilbrich, and C. J. Glover. Loss of Polymer-Modified Binder Durability with Oxidative Aging, in Transportation Research Record No. 1998, Transportation Research Board, Washington, D.C, 2007b.

Yan, J., Z. Zhang, H. Zhu, F. Li, and Q. Liu. Experimental Study of Hot Recycled Asphalt Mixtures with High Percentages of Reclaimed Asphalt Pavement and Different RAs. ASTM Journal of Testing and Evaluation, Vol. 42, No. 5, 2014.

Yu, X., M. Zaumanis, S. Santos, L.D. Poulikakos. Rheological, Microscopic, and Chemical Characterization of the Rejuvenating Effect on Asphalt Binders. Fuel, Vol. 135, 2014, pp. 162-171.

Zaumanis, M., R. Mallick, and R. Frank. Determining Optimum Rejuvenator Dose for Asphalt Recycling Based on Superpave Performance Grade Specifications. Construction and Building Materials, Vol. 69, 2014a, pp. 159-166.

Zaumanis, M., R. Mallick, and R. Frank. Evaluation of Different RAs for Restoring Aged Asphalt Binder and Performance of 100 % Recycled Asphalt. Materials and Structures, 2014b, 4 p.

Zaumanis, M., R. Mallick, and R. Frank. Evaluation of Rejuvenator's Effectiveness with Conventional Mix Testing for 100% Reclaimed Asphalt Pavement Mixtures. Transportation Research Record No. 2370, Transportation Research Board, National Research Council, Washington, DC, 2013, pp. 17-25.

Zhu, C. Evaluation of Thermal Oxidative Aging Effect on the Rheological Performance of Modified Asphalt Binders, M.S. thesis, University of Nevada, Reno, 2015.

Zhou, F., J.W. Button, and J.A. Epps. Best Practice for Using RAS in HMA. Report No. FHWA/TX-12/0-6614-1, Texas Transportation Institute, College Station, TX, 2012, pp. 72.

APPENDIX A

NEVADA FIELD PROJECT REPORT

A.1 Introduction

In a collaborative effort with University of Nevada, Reno and its NCHRP 9-58 research team, the Washoe County of Northern Nevada implemented a major rehabilitation project on Matterhorn Blvd (PWP-WA-2015-179) to study the influence of rejuvenators on hot mix asphalt (HMA) with high recycled asphalt pavement (RAP) materials. The Matterhorn Blvd is a low volume road with a single lane in each direction located 17 miles north of Reno, Nevada. The existing pavement before rehabilitation had 3.5 to 5.0 inches of hot mix asphalt on top of the aggregate base and it was severely damaged by thermal cracking. The old asphalt pavement layer was constructed using lightweight Allite aggregates with a water absorption of the aggregate being around 5.3%. The rehabilitation project consisted of pulverization and compaction of the existing asphalt pavement and base to the depth of 6 inches and placing a new 3-inch-thick overlay on top. Granite Construction Company was the contractor and Summit Engineering was the consultant for this project.

Five different test sections were constructed in September 2015 and the description of each section is given in Table 9. 1. The test sections were laid out on Matterhorn Blvd as shown in Figure 9. 1. Each section spreads to about 24 feet in width and 2000 feet in length.

Table 9. 1. Description of Nevada Test Sections

Sections	Description
Section 1 (Virgin section)	PG64-28NV/ No RAP / No Recycling Agent (RA)
Section 2 (Control section with 0.3RBR)	PG64-28NV/ 0.30 RAP Binder Ratio (RBR)/ No RA
Section 3 (Tall oil section)	PG64-28NV/ 0.30 RBR / Evoflex
Section 4 (Aromatic extract section)	PG64-28NV/ 0.30 RBR / Reclamite

Section 5 (Control section with 0.15RBR)	PG64-28NV/ 0.15 RBR / No RA

Figure 9. 1. Nevada Test Sections Layout

A.2 Materials and Hot Mix Asphalt Production

The aggregates and RAP materials were obtained from Granite pit at Lockwood and the asphalt binder (PG64-28NV polymer-modified) was supplied by Paramount Nevada Asphalt Company at Fernley. The RAP material was a mixture of plant rejects and locally obtained old pavement materials processed to meet the ½" RAP specification of the Orange Book Standard Specifications for Public Work Construction (SSPWC) from Washoe County. The Evoflex and Reclamite recycling agents were supplied by MWV Specialty Chemicals and Tricor Refining, LLC, respectively. The job mix formula (JMF) was obtained by combining five different aggregate stockpiles: ¾" crushed aggregates (17%), ½" crushed aggregates (10%), 3/8" crushed aggregates (15%), #4 crusher fines (14%), and #4 Natural fines (10%); all the percentages are by total weight of mixture. Summary of the aggregate consensus properties, asphalt binder properties, and rejuvenator properties are given in A.5 .1. Granite Construction Company conducted the Marshall mix designs (50 blows) for Type 2 hot mix asphalt mixes according to the Orange Book (SSPWC). The volumetric properties of the designed mixes are summarized in Table 9. 2 and the detailed mix design reports are attached in A.5 .1. Figure 9. 2 shows the pictures of raw materials at the mixing plant. The coarse and fine aggregates were marinated with 1% hydrated lime and stored in separate stockpiles prior to mixing.

The marinated aggregates were mixed with asphalt in a continuous mixing drum (Figure 9. 3b) at 335°F. The rejuvenators were at 120°F and injected to the asphalt line during mixing as recommended by the manufacturer. Mixed hot mix asphalt mixtures were transferred to the silos for storage. The silo time (storage time) varied between 30 minutes and 3 hours

throughout the production. The average temperature of hot mix asphalt when discharged from the silo into the hauling truck was 320°F. The construction site was located at about 23 miles from the mixing plant and the average hauling time was around 30 minutes. Figure 9. 3 shows the pictures of the mixing plant of Granite Construction Company at Lockwood facility.

Table 9. 2: Summary of the Nevada Test Sections Mix Designs

	Section 1	**Section 2**	**Section 3**	**Section 4**	**Section 5**
RAP, %	0	33	33	33	15
RA type, %	-	-	T2[1], 2.0%	A2[1], 2.0%	-
RAP Binder Ratio (RBR)	0	0.324	0.332	0.324	0.144
Optimum total binder content, %TWM[2]	5.37	4.60	4.50	4.60	5.04
Virgin binder content, %TWM[2]	5.37	3.11	3.01	3.11	4.32
VMA, %	13.3	13.7	13.9	14.0	13.3
VFA, %	69.8	71.1	71.2	71.8	69.8

[1] T2-Evoflex, A2-Reclamite

[2] TWM denotes "Total Weight of Mix"

(a) (b)

(c)

Figure 9. 2. Picture of (a) Aggregate Stockpiles; (b) Processed RAP Stockpile; and (c) Marinated Aggregate Stockpile Along with Asphalt Binder Tanks at Granite Construction Hot Plant Facility

(a)

(b)

(c)

Figure 9. 3. Picture of (a) Array of Aggregate Bins; (b) Continuous Mixing Drum; and (c) Storage Silos at Granite Construction Hot Plant Facility

A.3 Construction of Nevada test sections

The pulverization and compaction of the existing asphalt pavement and base were completed couple of days prior to the construction of the new asphalt pavement layer. The pulverized and compacted base layer was wetted and levelled by a motor grader before placing the hot mix asphalt. The air temperature varied between 77 and 84°F and the wind speed varied between 5 and 15 mph during construction. The hot mix asphalt was transported to the construction site using belly dump trucks with the capacity of 40 ton. The hot mix asphalt was placed in a windrow on top of the compacted base. Figure 9. 4 shows the belly dump truck and the hot mix asphalt material placed in a windrow. A Weiler E650 windrow elevator picked up the hot mix asphalt and transferred it into the paver hopper. A Caterpillar AP-1055D model paver (Figure 9. 5) laid down the hot mix asphalt on top of the base. The hot mix asphalt layer was placed in one lift since the target thickness of the layer was 3 inches. One lane (12 feet) was paved at a time and the other lane was kept open to the traffic. The paved hot mix asphalt mixtures were compacted using three types of rollers; CAT CB64 vibratory roller, Volvo DD38 vibratory roller, and CAT CC34 pneumatic rollers. The breakdown roller (CAT CB64) did four vibratory passes and one static pass followed by two static passes by the pneumatic roller. The Volvo DD38 was used to compact the joints properly and finish the compaction with two static passes. A pass here is defined as both wheels of the compactor rolling over a specific point on the mat. Figure 9. 6 shows the fleet of compactors and the break down compactor behind the paver. A summary of the windrow temperature and beginning and end station marks of each test section are given in Table 9. 3. There was not any physical or functional differences observed between rejuvenator added mixtures and regular hot mix asphalt

mixes during the mixing and compaction process in the field. Figure 9. 7 shows the pictures of pavement surfaces of the test sections. The mat densities were measured after the completion of compaction using nuclear density gauges by both contractor and consultant.

(a)

(b)

Figure 9. 4. Picture of (a) Belly Dump Truck; and (b) Hot Mix Asphalt Placed in a Windrow

Figure 9. 5. Picture of the Windrow Lifter and Paver

(a)

(b)

Figure 9. 6. Picture of (a) Fleet of Compactors; and (b) Breakdown Roller Behind the Paver

(a) (b) (c)

(d) (e)

Figure 9. 7. Picture of Compacted Pavement Surface of (a) Section 1-Virgin; (b) Section 2-Control with 0.3 RBR; (c) Section 3-0.3 RBR with Tall Oil; (d) Section 4-0.3 RBR with Aromatic Extract; and (e) Section 5-Control with 0.15 RBR.

Table 9. 3. Summary of the Windrow Temperature and Station Locations

Construction Date	Section number	RBR	RA	Lane	Start station	Stop station	Windrow HMA Temp. (°F)
10-Sept. 2015	4	0.30	Aromatic Extract	SB	279	304	305
				NB	279	304	290-310
	1	0.00	None	SB	252+70	279	295-305
				NB	252+70	279	295-305
11-Sept. 2015	3	0.30	Tall Oil	SB	226	252+70	310-320
				NB	232+50	252+70	302
	2	0.30	None	SB	198+50	226	290-305
				NB	197+55	232+50	310-320
16 and 17-Sept. 2015	5	0.15	None	SB	102	198+50	300-310
				NB	102	197+55	300-310

A.4 Quality control tests

The quality control (QC) and quality assurance (QA) samples were taken from each lot during the construction by Summit Engineering and Granite Construction, respectively. Each section had at least two lots. The test sections and associated lot numbers are summarized in Table 9. 4. The QC samples were tested for asphalt mixture properties such as gradation, asphalt content, theoretical maximum specific gravity, Marshall Stability, etc. Three cores were taken from each lot for thickness and density measurements after the construction. The summary of sieve analysis (AASHTO T27), asphalt binder content (AASHTO T308), and Marshall Stability and flow (AASHTO T245) of QC samples are shown in Figure 9. 8 to 9. A summary of core densities (AASHTO T166) and percent of compaction (AASHTO T269) are shown in Figure 9. 11 to 12. A detailed report of the QC test results is attached in A.6 .

Table 9. 4. Summary of Lot Numbers Associated with Each of the NV Test Sections

NV Test Section	Lot Numbers
1	12 and 14
2	15 and 17
3	16 and 18
4	11 and 13
5	9 and 10

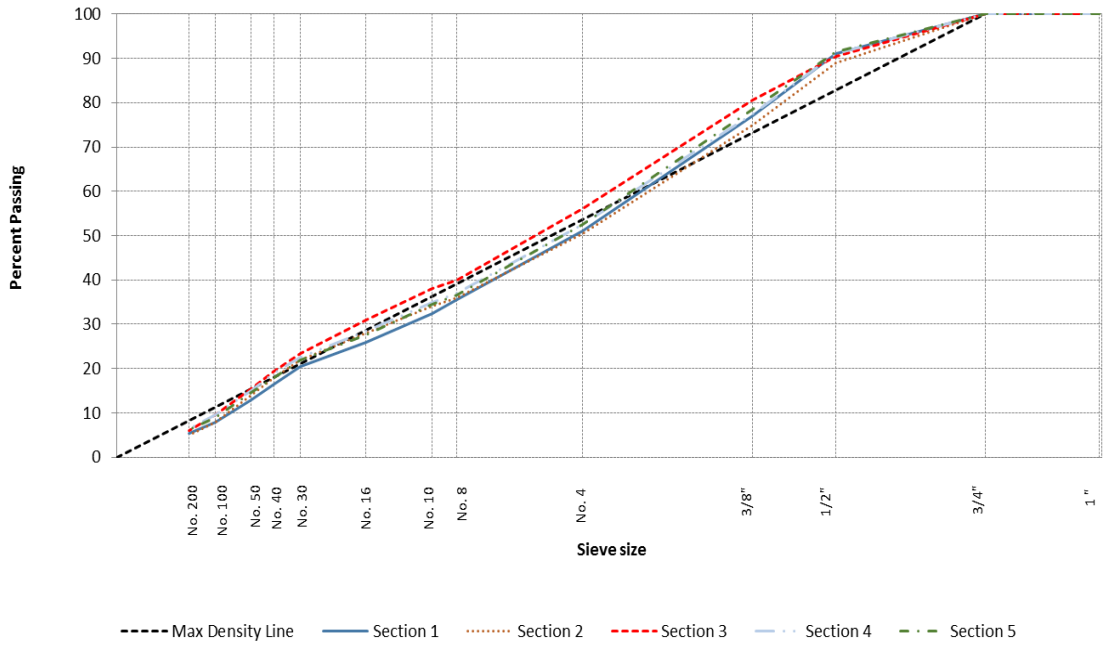

Figure 9. 8. Hot Mix Asphalt Aggregate Gradation from QC Samples

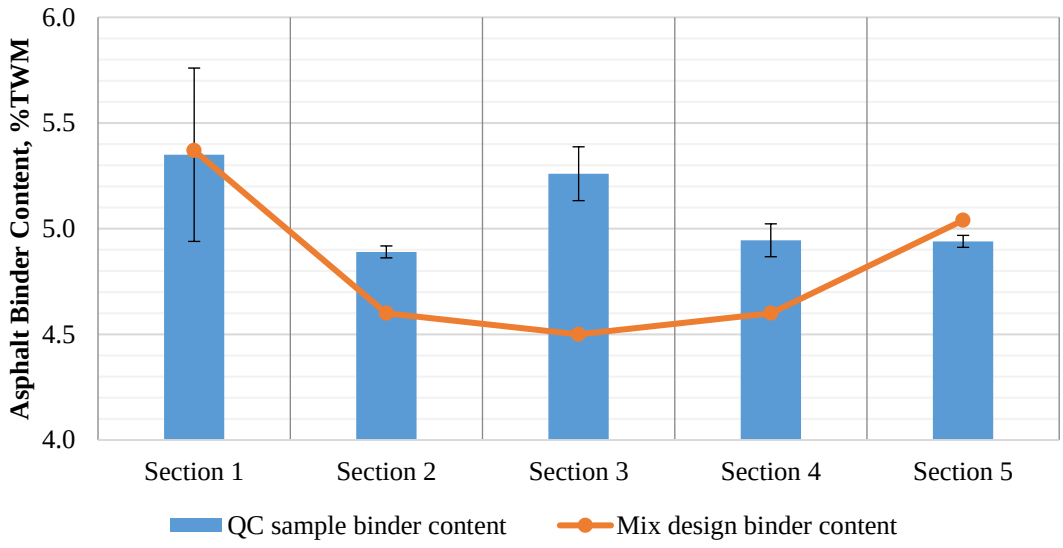

Figure 9. 9. Asphalt Binder Contents of QC Samples from Each Section

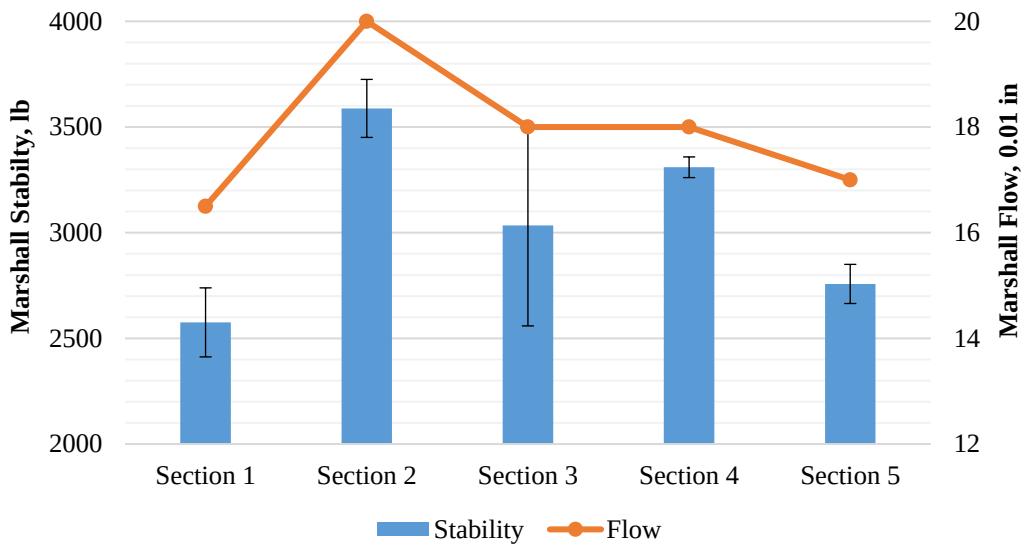

Figure 9. 10. Marshall Stability and Flow of QC Samples from Each Section

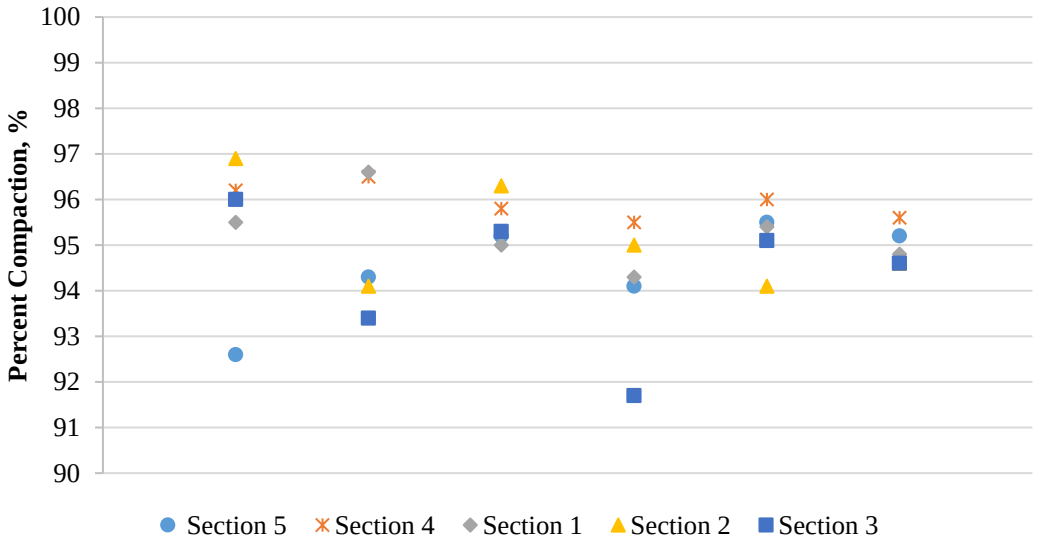

Figure 9. 11. Percent Compaction of Asphalt Layers from Cores

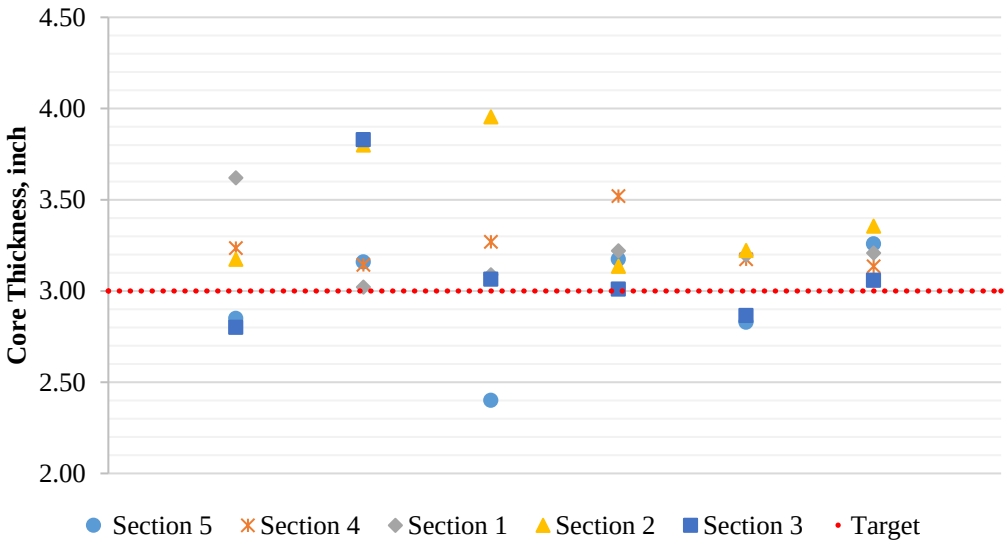

Figure 9. 12. Asphalt Layer Thickness of Each Section from Cores

A.5 Marshall Mix Design Report

GRANITE™ AAR

July 14, 2015

Asphalt Concrete Mix Design: TY2 PG64-28NV 4V50B w/LIME
Asphalt Concrete Mix Design ID: 1511 – 3/4" HMA64-28NV 4V50BLM
Asphalt Source: Paramount - Nevada
Aggregate Source: Lockwood / Wade
Design Criteria: Orange Book (SSPWC) / Asphalt Institute (MS-2)

Attached is an asphalt mix submittal report including laboratory testing and mix design criteria for a Type 2 hot mix asphalt concrete. All material and mix design procedures were performed in our AMRL accredited Lockwood Materials Laboratory by NAQTC qualified technicians in accordance with the above referenced standard specifications, the Asphalt Institute Manual Series 2 (MS-2), and the project special technical specifications for the Matterhorn Boulevard Improvement Project.

Aggregate lime treatment is prepared using the NDOT "Marination Method" as per section 401.03.08 of the Standard Specifications for Public Works Construction (Silver Book).

During production of this material, process control testing will be conducted to determine if mix properties meet acceptance criteria. Past experience has shown that differences in mix properties may exist between laboratory generated specimen for mix design purposes, and actual plant produced material. Adjustments to plant bin percentages and asphalt set point may be necessary during production to achieve job mix formula targets and / or in-place specifications requirements.

Attached are the laboratory's test results of the hot mix asphalt design.

Respectfully Submitted,
Granite Construction Company

PROFESSIONAL ENGINEER STATE OF NEVADA
DOUGLAS E. BROWN
Exp: 12-31-16
CIVIL
No. 19129
7-14-15

Teilhard Benkovich, CET
QC Operations Supervisor

Douglas "Bucky" Brown, P.E.
Quality Control Manager

GRANITE

Lockwood HMA Plant
10600 Canyon Way
Lockwood, NV 89431
775-352-2933

Asphalt Mix Submittal Report

Submittal Information

Submittal Name 2015 - Mix Design (JMF)
Producer Granite Construction Incorporated
Plant Lockwood HMA Plant
Contact Bucky Brown
Email bucky.brown@gcinc.com
Phone 775-352-2927
Prepared By Bucky Brown
Date Prepared 7/14/2015
Submitted By Bucky Brown
Date Submitted 7/14/2015

Mix Information

Mix ID 1511
Mix Name 3/4"HMA64-28NV 4V50BLM
Design Criteria SSPWC / MS-2 / STS Matterhorn Blvd
Design Method Marshall
Mix Category Orange Book Type 2
Aggregate Nominal Size 3/4" (19mm)
Mixing Temperature 330 °F
Compaction Temperature 309 °F
Compaction Effort 50

Notes
TMM% = Total Weight of Mixture
TMA% = Dry Weight of Aggregate
Aggregates prepared in accordance with the NDOT "Marination Method" as per 401.03.08 of the Silver Book

Mix Properties

	TMA %	TMM %
AC Total	5.37	5.1
AC Virgin	5.37	5.1
AC Recycled	0	0

Aggregate	Type	Name	Supplier	%	TMM %	Specific Gravity	Grade
Aggregate	Coarse Aggregate	3/4" AGG CRUSHED	Lockwood	16.50		2.643	
	Coarse Aggregate	1/2" AGG CRUSHED	Lockwood	10.00		2.631	
	Coarse Aggregate	3/8" AGG CRUSHED	Lockwood	25.00		2.644	
	Fine Aggregate	#4 - CRUSHER FINES	Lockwood	35.00		2.522	
	Fine Aggregate	#4 - NATURAL FINES	Wade	12.00		2.528	
	Lime	HYDRATED LIME	Lhoist North America	1.50		2.256	
Binder	Performance Grade	PNAC PG 64-28NV	Paramount - Nevada	5.37	5.10	1.018	

GRANITE

Lockwood HMA Plant
10600 Canyon Way
Lockwood, NV 89431
775-352-2933

Mix Properties

Mix 1511-3/4"HMA64-28NV 4V50BLM
Specification 1511-2015 JMF Submittal

Mix Properties			
Property	Unit	Design	Specification
AC Content (Pb)	%TMM	5.1	4.9-5.8
AC Content (Effective,Pbe)	%	4	
AC Content (Absorbed,Pba)	%	1.16	
Air Voids (Va)	%	4	3-5
VMA	%	13.3	>13
VFA	%	69.8	65-78
Stability	lbf	3300	>1800
Plastic Flow	.01in	17	8-20
Unit Wt (Compacted)	lb/ft3	146.7	
Unit Wt (Max)	lb/ft3	152.7	
SPGR (Compacted,Gmb)		2.356	
SPGR (Max,Gmm)		2.454	
SPGR (Dry,Gsb)		2.578	
SPGR (SSD)		2.651	
SPGR (Apparent)		2.768	
Spgr (Effective,Gse)		2.656	
Absorption (Coarse)	%	2	
Absorption (Blend)	%	2.6	
Absorption (Fine)	%	3.3	
Fractured Faces (>1)	%	100	>50
Fractured Faces (>2)	%	100	
Liquid Limit		<35	<35
Plasticity Index	%	0	<8
LA Abrasion	%	14.7	<37
Soundness (Na2SO4) Coarse	%	2.2	<12
Soundness (Na2SO4) Fine	%	3.1	<15
TSR (Freeze/Thaw)	%	86	
Tensile Strength (Dry)	psi	93	

Gradation		
Sieve	% Passing	Specification
1" (25mm)	100.0	100-100
3/4" (19mm)	100.0	93-100
1/2" (12.5mm)	89.8	
3/8" (9.5mm)	79.0	72-86
#4 (4.75mm)	52.6	46-60
#8 (2.36mm)	38.6	
#10 (2mm)	36.1	32-40
#16 (1.18mm)	29.0	
#30 (0.6mm)	21.4	
#40 (0.425mm)	17.7	14-22
#50 (0.3mm)	13.6	
#100 (0.15mm)	8.7	
#200 (75um)	6.3	4.3-8.3

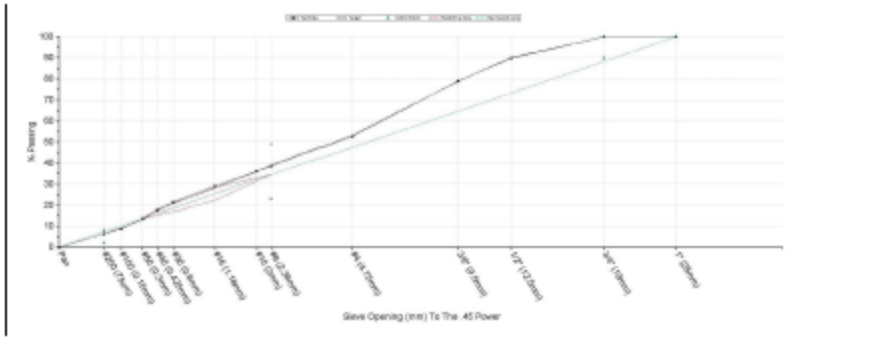

GRANITE™

Lockwood HMA Plant
10600 Canyon Way
Lockwood, NV 89431
775-952-2693

Mix Blend

Mix 1511-3/4"HMA64-28NV 4V50BLM

Sieve/Test	Spec	Result	Dust	3/4" AGG CRUSHED	1/2" AGG CRUSHED	3/8" AGG CRUSHED	#4 - CRUSHER FINES	#4 - NATURAL FINES	HYDRATED LIME
Type				Coarse Aggregate	Coarse Aggregate	Coarse Aggregate	Fine Aggregate	Fine Aggregate	Lime
Include				Yes	Yes	Yes	Yes	Yes	Yes
%				16.5	10	25	35	12	1.5
1" (25mm) %	100-100	100.0		100.0	100	100	100.0	100.0	100.0
3/4" (19mm) %	90-100	100.0		100.0	100	100	100.0	100.0	100.0
1/2" (12.5mm) %		89.8		38.1	100	100	100.0	100.0	100.0
3/8" (9.5mm) %	83-85	79.0		4.0	48.6	100	100.0	100.0	100.0
#4 (4.75mm) %	45-85	52.6		0.4	0.7	19.8	97.6	99.2	100.0
#8 (2.36mm) %		38.6		0.4	0.6	0.9	71.4	97.7	100.0
#10 (2mm) %	30-44	36.1		0.4	0.6	0.8	64.5	97.3	100.0
#16 (1.18mm) %		29.0		0.3	0.5	0.7	45.5	94.2	100.0
#30 (0.6mm) %		21.4		0.3	0.4	0.6	29.8	77.3	99.8
#40 (0.425mm) %	12-22	17.7		0.3	0.4	0.6	25.3	59.0	99.8
#50 (0.3mm) %		13.6		0.3	0.4	0.6	21.5	36.0	99.8
#100 (0.15mm) %		8.7		0.3	0.4	0.5	16.6	9.7	99.8
#200 (75um) %	3-8	6.3		0.2	0.3	0.5	12.9	2.8	86.80

GRANITE

Lockwood HMA Plant
10600 Canyon Way
Lockwood, NV 89431
775-352-2933

Volumetric Charts

Mix: 1511-3/4"HMA64-28NV 4V50BLM

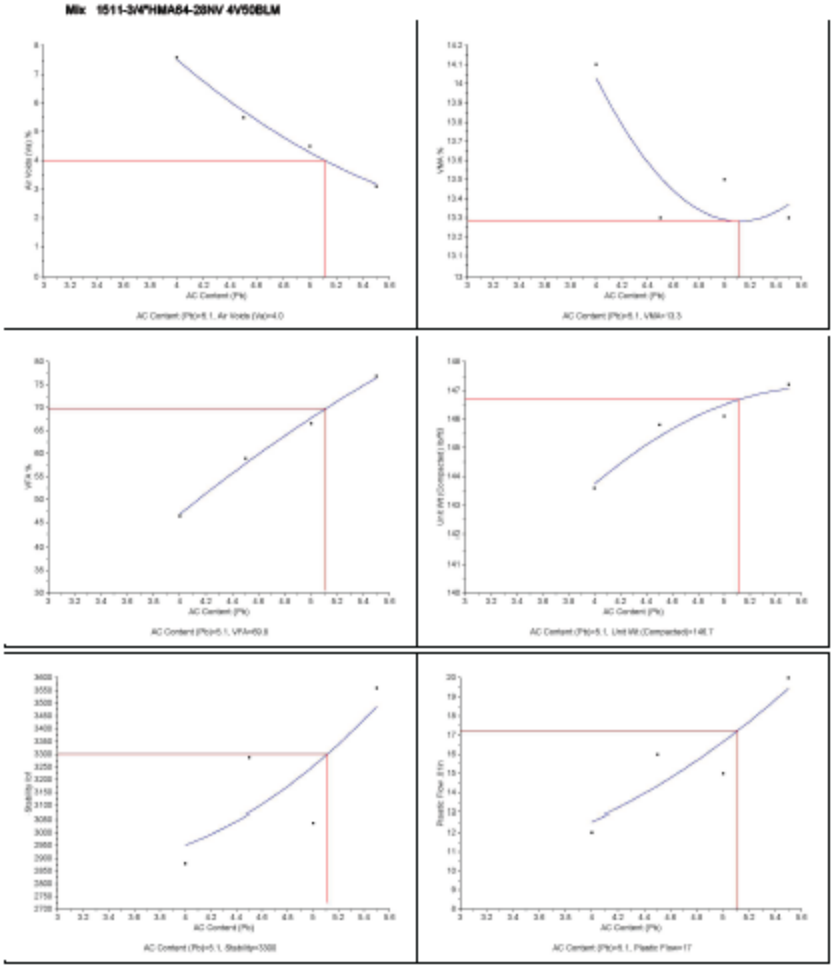

GRANITE

Lockwood HMA Plant
10600 Canyon Way
Lockwood, NV 89431
775-352-2933

Batch Test Summary

Mix 1511-3/4"HMA64-28NV 4V50BLM

Test	Sample 1	Sample 2	Sample 3	Sample 4
AC Content (Pb)	4.0	4.5	5.0	5.5
AC Content (Absorbed,Pba) %	1.15	1.15	1.16	1.16
AC Content (Effective,Pbe) %	2.9	3.4	3.9	4.4
Air Voids (Va) %	7.6	5.5	4.5	3.1
VMA %	14.1	13.3	13.5	13.3
VFA %	46.4	58.9	66.6	76.9
SPGR (Compacted,Gmb)	2.306	2.341	2.347	2.365
Unit Wt (Compacted) lb/ft3	143.8	145.8	146.1	147.2
SPGR (Max,Gmm)	2.495	2.476	2.458	2.440
Unit Wt (Max) lb/ft3	155.3	154.1	153.0	151.9
Stability lbf	2879	3288	3038	3560
Plastic Flow .01in	12	16	15	20

StonemontQC 07/14/2015

GRANITE

Lockwood HMA Plant
10600 Canyon Way
Lockwood, NV 89431
775-352-2933

Asphalt Mix Submittal Report

Submittal Information

Submittal Name	2015 Mix Design (JMF)
Producer	Granite Construction Incorporated
Plant	Lockwood / Sparks HMA Plants
Contact	Bucky Brown
Email	bucky.brown@gcinc.com
Phone	775-352-2927
Prepared By	Bucky Brown
Date Prepared	3/31/2015
Submitted By	Bucky Brown
Date Submitted	4/1/2015

Mix Information

Mix ID	2041
Mix Name	3/4"HMA64-28NV 4V50BR15LM
Design Criteria	MS-2 / SSPWC
Design Method	Marshall
Mix Category	Orange Book Type 2
Aggregate Nominal Size	3/4" (19mm)
Mixing Temperature	330 °F
Compaction Temperature	311 °F
Compaction Effort	50-Blow

Notes

TMM% = Total Weight of Mixture
TMA% = Dry Weight of Aggregate
1-1/2% Lime added by dry weight of virgin aggregate using the "Marination Method". TSR Done with no Lime added.

Mix Properties

	TMA %	TMM %
AC Total	5.04	4.8
AC Virgin	4.32	4.11
AC Recycled	0.72	0.69

Aggregate	Type	Name	Supplier	%	TMM %	Specific Gravity	Grade
Aggregate	Coarse Aggregate	**3/4" AGG CRUSHED**	Lockwood	16.70			
	Coarse Aggregate	**1/2" AGG CRUSHED**	Lockwood	10.00			
	Coarse Aggregate	**3/8" AGG CRUSHED**	Lockwood	19.00			
	Fine Aggregate	**#4 - CRUSHER FINES**	Lockwood	24.00			
	Fine Aggregate	**#4 - NATURAL FINES**	Wade	14.00			
	Lime	**HYDRATED LIME**	Lhoist North America	1.30			
RAP	Fine RAP	**1/2" Lockwood RAP**	Lockwood	15.00			
Binder	Performance Grade	**Paramount PG 64-28NV**	Paramount	4.32	4.11	1.019	PG 64-28NV

GRANITE

Lockwood HMA Plant
10600 Canyon Way
Lockwood, NV 89431
775-352-2933

Mix Properties

Mix 2041-3/4"HMA64-28NV 4V50BR15LM
Specification 2015 JMF Submittal

Mix Properties			
Property	**Unit**	**Design**	**Specification**
AC Content (Pb)	%TMM	4.8	4.3-5.3
Air Voids (Va)	%	4	3-5
VMA	%	13.3	>13
VFA	%	69.8	65-78
Stability	lbf	4285	>1800
Plastic Flow	.01in	16	8-20
TSR (Freeze-Thaw)	%	72	>70
Unit Wt (Compacted)	lb/ft3	147.5	
Unit Wt (Max)	lb/ft3	153.7	
SPGR (Compacted,Gmb)		2.389	
SPGR (Max,Gmm)		2.469	
SPGR (Dry,Gsb)		2.602	
SPGR (SSD)		2.652	
SPGR (Apparent)		2.767	
Absorption (Fine)	%	3.2	
Absorption (Blend)	%	2.5	
Absorption (Coarse)	%	2.0	
Tensile Strength (Dry)	psi	130	>65
Fractured Faces (>1)	%	100	>50
Fractured Faces (>2) Liquid	%	100	
Limit		<35	<35
Plasticity Index	%	0	<8
LA Abrasion	%	14.5	<37
Soundness (Na2SO4) Coarse	%	2.2	<12
Soundness (Na2SO4) Fine	%	3.0	<15

Gradation		
Sieve	**% Passing**	**Specification**
1" (25mm)	100	100-100
3/4" (19mm)	100	93-100
1/2" (12.5mm)	90	
3/8" (9.5mm)	78	71-85
#4 (4.75mm)	53	46-60
#8 (2.36mm)	40	
#10 (2mm)	37	33-41
#16 (1.18mm)	31	
#30 (0.6mm)	24	
#40 (0.425mm)	20	16-24
#50 (0.3mm)	15	
#100 (0.15mm)	9	
#200 (75um)	6.3	4.3-8

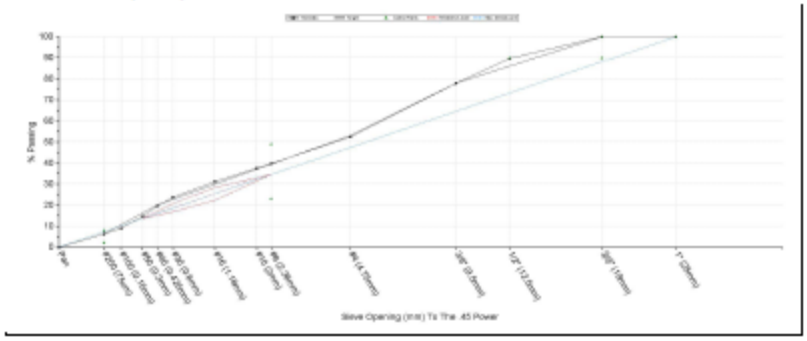

GRANITE

Lockwood HMA Plant
10600 Canyon Way
Lockwood, NV 89431
775-352-2933

Mix Blend

Mix 2041 - 3/4"HMA64-28NV 4V50BR15LM

Sieve/Test	Spec	Result	Dust	3/4" AGG CRUSHED	1/2" AGG CRUSHED	3/8" AGG CRUSHED	#4 - CRUSHER FINES	#4 - NATURAL FINES	HYDRATED LIME	1/2" Lockwood RAP
Type				Coarse Aggregate	Coarse Aggregate	Coarse Aggregate	Fine Aggregate	Fine Aggregate	Lime	Fine RAP
Include				Yes	Yes	Yes	Yes	Yes	Yes	Yes
%				16.7	10	19	24	14	1.3	15
1" (25mm) %	100-100	100.0		100.0	100.0	100.0	100.0	100.0	100.0	100.0
3/4" (19mm) %	90-100	100.0		100.0	100.0	100.0	100.0	100.0	100.0	100.0
1/2" (12.5mm) %		89.6		38.1	100.0	100.0	100.0	100.0	100.0	100.0
3/8" (9.5mm) %	63-85	77.9		4.0	48.6	100.0	100.0	100.0	100.0	94.7
#4 (4.75mm) %	45-65	52.5		0.4	0.7	19.8	97.6	99.2	100.0	67.4
#8 (2.36mm) %		39.7		0.4	0.6	0.9	71.4	97.7	100.0	48.8
#10 (2mm) %	30-44	37.4		0.4	0.6	0.8	64.5	97.3	100.0	45.2
#16 (1.18mm) %		31.1		0.3	0.5	0.7	45.5	94.2	100.0	36.9
#30 (0.6mm) %		23.7		0.3	0.4	0.6	29.8	77.3	99.8	28.5
#40 (0.425mm) %	12-22	19.5		0.3	0.4	0.6	25.3	59.0	99.8	24.4
#50 (0.3mm) %		14.7		0.3	0.4	0.6	21.5	36.0	99.8	20.3
#100 (0.15mm) %		8.9		0.3	0.4	0.5	16.6	9.7	99.8	14.4
#200 (75um) %	3-8	6.3		0.2	0.3	0.5	12.9	2.8	86.80	10.7

GRANITE

Lockwood HMA Plant
10600 Canyon Way
Lockwood, NV 89431
775-352-2933

Volumetric Charts

Mix 2041-3/4"HMA64-28NV 4V50BR15LM

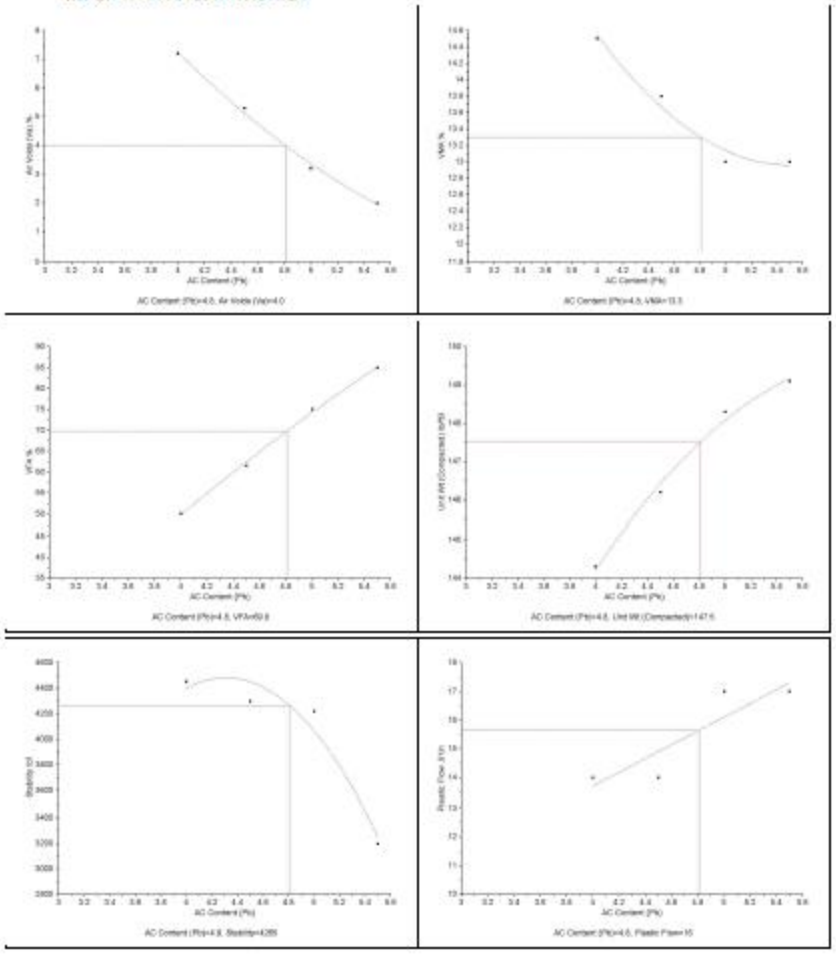

GRANITE

Lockwood HMA Plant
10600 Canyon Way
Lockwood, NV 89431
775-952-2633

Batch Test Summary

Mix 2041-3/4"HMA64-28NV 4V50BR15LM

Test	Sample 1	Sample 2	Sample 3	Sample 4
AC Content (Pb)	4.0	4.5	5.0	5.5
AC Content (Absorbed,Pba) %	0.85	0.85	0.86	0.86
AC Content (Effective,Pbe) %	3.2	3.7	4.2	4.7
Air Voids (Va) %	7.2	5.3	3.2	2.0
VMA %	14.5	13.8	13.0	13.0
VFA %	50.0	61.5	75.1	84.9
SPGR (Compacted,Gmb)	2.318	2.348	2.382	2.396
Unit Wt (Compacted) lb/ft3	144.3	146.2	148.3	149.1
SPGR (Max,Gmm)	2.499	2.480	2.462	2.444
Unit Wt (Max) lb/ft3	155.5	154.4	153.2	152.1
Stability lbf	4452	4298	4220	3195
Plastic Flow .01in	14	14	17	17

Stonemont/QC 04/01/2015

GRANITE

Lockwood HMA Plant
10600 Canyon Way
Lockwood, NV 89431
775-352-2933

Asphalt Mix Submittal Report

Submittal Information

Submittal Name	Type 2 HMA - Section 2: Control Section
Producer	Granite Construction Incorporated
Plant	Lockwood HMA Plant
Contact	Bucky Brown
Email	bucky.brown@gcinc.com
Phone	775-352-2927
Project Name	Matterhorn Blvd. Improvement Project
Contractor	Granite Construction Incorporated
Prepared By	Bucky Brown
Date Prepared	8/3/2015
Submitted By	Bucky Brown
Date Submitted	8/3/2015

Mix Information

Mix ID	3546
Mix Name	3/4" HMA64-28NV 4V50BR30LM
Design Criteria	SSPWC / MS-2 / Matterhorn Blvd
Design Method	Marshall
Mix Class	
Mix Category	Orange Book Type 2
Intended Use	Section 2: Control Section
Traffic Designation	
Aggregate Nominal Size	3/4" (19mm)
Mixing Temperature	330 °F
Compaction Temperature	309 °F
Compaction Effort	50-Blow

Notes

TMM% = Total Weight of Mixure
TMA% = Dry Weight of Aggregate
Aggregates prepared in accordance with the NDOT "Marination Method" as per 401.03.08 of the Silver Book

Mix Properties

	TMA %	TMM %
AC Total	4.83	4.6
AC Virgin	3.26	3.11
AC Recycled	1.57	1.49
Rap Binder Ratio (RBR)	0.325	0.324

Aggregate	Type	Name	Supplier	%	TMM %	Specific Gravity	Grade
Aggregate	Coarse Aggregate	**3/4" AGG CRUSHED**	Lockwood	17.00		2.643	
	Coarse Aggregate	**1/2" AGG CRUSHED**	Lockwood	10.00		2.631	
	Coarse Aggregate	**3/8" AGG CRUSHED**	Lockwood	15.00		2.644	
	Fine Aggregate	#4 - CRUSHER FINES	Lockwood	14.00		2.522	
	Fine Aggregate	#4 - NATURAL FINES	Wade	10.00		2.528	
	Lime	HYDRATED LIME	Lhoist North America	1.00		2.35	
RAP	Fine RAP	1/2" Lockwood RAP	Lockwood	33.00		2.735	
Binder	Performance Grade	PNAC PG 64-28NV	Paramount	3.26	3.11	1.018	

GRANITE

Lockwood HMA Plant
10800 Canyon Way
Lockwood, NV 89431
775-352-2933

Mix Properties

Mix 3546-3/4" HMA64-28NV 4V50BR30LM
Specification 3546-2015 JMF Submittal

Mix Properties				Gradation			
Property	Unit	Design	Specification	Sieve	% Passing	Specification	
AC Content (Pb)	%TMM	4.6	4.4-5.3 (TV -0.2 +0.7)	1" (25mm)	100.0	100-100	
AC Content (Absorbed,Pba)	%	0.41		3/4" (19mm)	100.0	+/-7	93-100
Air Voids (Va)	%	4	3-5	1/2" (12.5mm)	89.3		
VMA	%	13.7	>13	3/8" (9.5mm)	76.8	+/-7	70-84
VFA	%	71.1	65-78	#4 (4.75mm)	49.7	+/-7	43-57
Stability	lbf	4031	>1800	#8 (2.36mm)	36.7		
Plastic Flow	.01in	16	8-20	#10 (2mm)	34.5	+/-4	31-39
Unit Wt (Compacted)	lb/ft3	148.4		#16 (1.18mm)	28.6		
Unit Wt (Max)	lb/ft3	154.5		#30 (0.6mm)	21.8		
SPGR (Compacted,Gmb)		2.383		#40 (0.425mm)	18.1	+/-4	14-22
SPGR (Max,Gmm)		2.482		#50 (0.3mm)	13.9		
SPGR (Dry,Gsb)		2.637		#100 (0.15mm)	8.9		
SPGR (SSD)		2.66		#200 (75µm)	6.4	+/-2	4.4-8.4
SPGR (Apperent)		2.77					
Spgr (Effective,Gse)		2.666					
Absorption (Coarse)	%	2					
Absorption (Blend)	%	2.3					
Absorption (Fine)	%	3.2					
Fractured Faces (>1)	%	100	>50				
Fractured Faces (>2)	%	100					
Liquid Limit	%	<35	<35				
Plasticity Index	%	0	<6				
LA Abrasion	%	14.2	<37				
Soundness (Na2SO4) Coarse	%	2.2	<12				
Soundness (Na2SO4) Fine	%	3.1	<15				

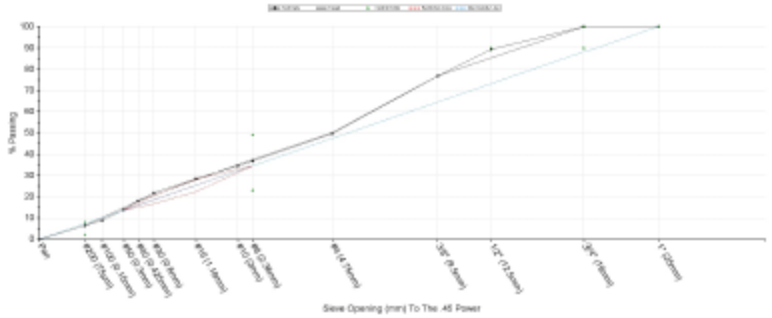

GRANITE

Lockwood HMA Plant
10600 Canyon Way
Lockwood, NV 89431
775-352-2933

Mix Blend

Mix 3548-3/4" HMA64-28NV 4V50BR30LM

Sieve/Test	Spec	Result	Dust	3/4" AGG CRUSHED	1/2" AGG CRUSHED	3/8" AGG CRUSHED	#4 - CRUSHER FINES	#4 - NATURAL FINES	HYDRATED LIME	1/2" Lockwood RAP
Type				Coarse Aggregate	Coarse Aggregate	Coarse Aggregate	Fine Aggregate	Fine Aggregate	Lime	Fine RAP
Include				Yes	Yes	Yes	Yes	Yes	Yes	Yes
%				17	10	15	14	10	1	33
1" (25mm) %	100-100	100.0		100.0	100	100	100.0	100.0	100.0	100.0
3/4" (19mm) %	90-100	100.0		100.0	100	100	100.0	100.0	100.0	100.0
1/2" (12.5mm) %		89.3		38.1	100	100	100.0	100.0	100.0	99.9
3/8" (9.5mm) %	63-85	76.8		4.0	48.6	100	100.0	100.0	100.0	95.6
#4 (4.75mm) %	45-65	49.7		0.4	0.7	19.8	97.6	99.2	100.0	67.6
#8 (2.36mm) %		36.7		0.4	0.6	0.9	71.4	97.7	100.0	47.9
#10 (2mm) %	30-44	34.5		0.4	0.6	0.8	64.5	97.3	100.0	44.4
#16 (1.18mm) %		28.6		0.3	0.5	0.7	45.5	94.2	100.0	35.4
#30 (0.6mm) %		21.8		0.3	0.4	0.6	29.8	77.3	99.8	26.6
#40 (0.425mm) %	12-22	18.1		0.3	0.4	0.6	25.3	59.0	99.8	22.8
#50 (0.3mm) %		13.9		0.3	0.4	0.6	21.5	38.0	99.8	18.8
#100 (0.15mm) %		8.9		0.3	0.4	0.5	16.6	9.7	99.8	13.6
#200 (75µm) %	3-8	6.4		0.2	0.3	0.5	12.9	2.8	86.80	10.2

GRANITE

Lockwood HMA Plant
10800 Canyon Way
Lockwood, NV 89431
775-352-2933

Volumetric Charts

Mix 3546-3/4" HMA64-28NV 4V50BR30LM

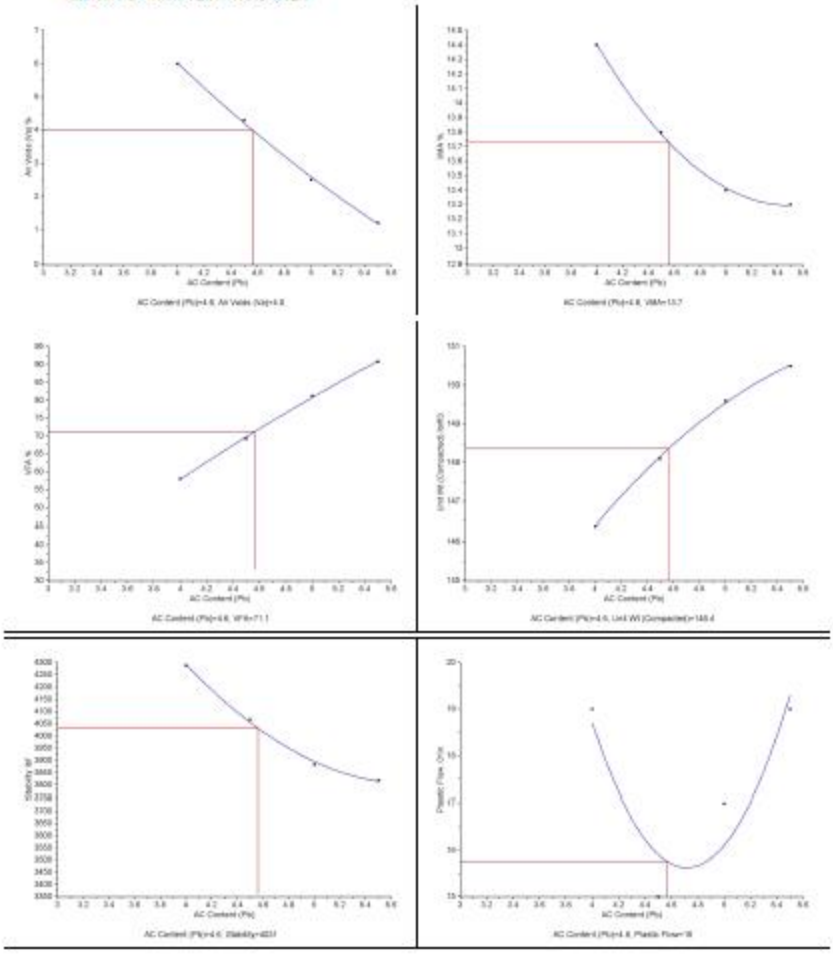

GRANITE

Lockwood HMA Plant
10600 Canyon Way
Lockwood, NV 89431
775-352-2933

Batch Test Summary

Mix 3548-3/4" HMA64-28NV 4V50BR30LM

Test	Sample 1	Sample 2	Sample 3	Sample 4
AC Content (Pb)	4.0	4.5	5.0	5.5
AC Content (Absorbed,Pba) %	0.41	0.42	0.41	0.42
AC Content (Effective,Pbe) %	3.6	4.1	4.6	5.1
Air Voids (Va) %	6.0	4.3	2.5	1.2
VMA %	14.4	13.8	13.4	13.3
VFA %	58.0	69.2	81.2	90.8
SPGR (Compacted,Gmb)	2.352	2.379	2.404	2.418
Unit Wt (Compacted) lb/ft3	146.4	148.1	149.6	150.5
SPGR (Max,Gmm)	2.503	2.485	2.466	2.448
Unit Wt (Max) lb/ft3	155.8	154.7	153.5	152.4
Stability lbf	4289	4068	3882	3818
Plastic Flow .01in	19	15	17	19

StonemontQC 08/03/2015

GRANITE
Quality Management

Guidance Document

Asphalt Binder Blending Chart

Mix		
% Total Asphalt Binder Content of Mix	4.82 %DWA	4.60 %TWM

RAP		
RAP Asphalt Binder Content	4.63	%TWM
% RAP in Mix (Aggregate + Asphalt)	33.0	%
% RAP Asphalt Binder in Mix	1.53	%TWM
% of RAP Asphalt Binder to Total Asphalt Binder	33.30	%

Virgin Asphalt Binder Supplier: *Paramount*
Grade: *64-28NV*
Desired Final Binder Grade: *PG 64-28*
Plant: *Lockwood*
Mix Identification: *3546 - 3/4"HMA64-28NV4V50BR30LM*

Temperature	Property	Performance Grade								Test Method
		Target		Virgin Binder		RAP Binder		Blend		
		Value	Criteria	Value	Plot	Value	Plot	Value	Plot	
High	Original Asphalt Binder, DSR, °C	64	Min	67.9	67.4	85.1	83.2	73.6	72.7	D7125
	RTFO Aged Asphalt Binder, DSR, °C	64	Min	67.4		83.2		72.7		D7125
Intermediate	PAV Aged Asphalt Binder, DSR, °C	22	Max	12.5	12.5	24.4	24.4	16.5	16.5	D7125
Low	PAV Aged Asphalt Binder, BBR, Creep Stiffness, °C	-28	Max	-35.5	-33.6	-25.1	-24.1	-32.0	-30.4	D6816
	PAV Aged Asphalt Binder, BBR, m-value, °C	-28	Max	-33.6		-24.1		-30.4		D6816

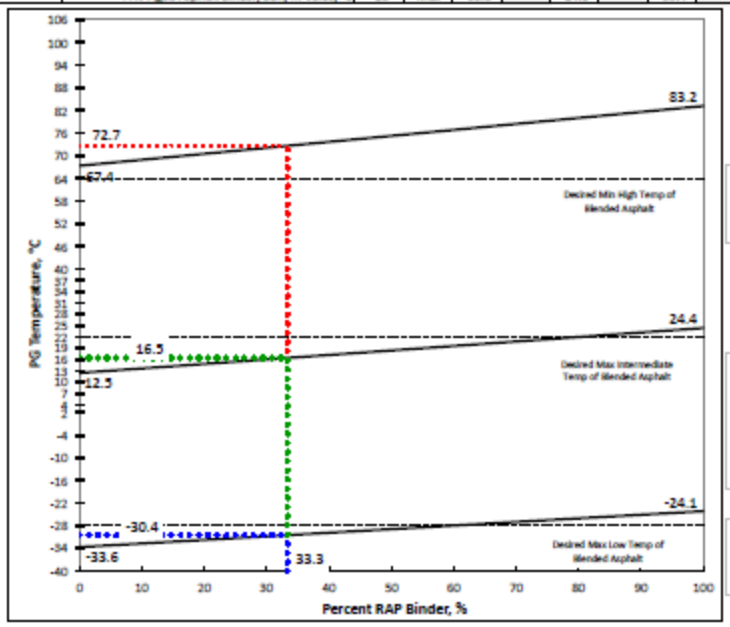

GRANITE

Lockwood HMA Plant
10600 I-80 Exit 22
Lockwood, NV 89434
775-352-2927

Asphalt Mix Submittal Report

Submittal Information

Submittal Name Type 2 HMA - Section 3: 0.30 RBR / Evoflex
Producer Granite Construction Incorporated
Plant Lockwood HMA Plant
Contact Bucky Brown
Email bucky.brown@gcinc.com
Phone 775-352-2927
Project Name Matterhorn Blvd. Improvement Project
Contractor Granite Construction Company
Prepared By Bucky Brown
Date Prepared 8/14/2015
Submitted By Bucky Brown
Date Submitted 8/21/2015

Mix Information

Mix ID 3584
Mix Name 3/4" HMA64-28NV 4V50BR30LM EVO
Design Criteria SSPWC / MS-2 / STS Matterhorn Blvd
Design Method Marshall
Mix Category Orange Book Type 2
Intended Use Section 3: Evoflex - Tall Oil
Aggregate Nominal Size 3/4" (19mm)
Mixing Temperature 330 °F
Compaction Temperature 309 °F
Compaction Effort 50-Blow

Notes

TMM% = Total Weight of Mixture
TMA% = Dry Weight of Aggregate
Aggregates prepared in accordance with NDOT "Marination Method" as per 401.03.08 of the Silver Book

Mix Properties

	TMA %	TMM %
AC Total	4.72	4.5
AC Virgin	3.15	3.01
AC Recycled	1.57	1.49
Rap Binder Ratio (RBR)	0.333	0.332

Aggregate	Type	Name	Supplier	%	TMM %	Specific Gravity	Grade
Aggregate	Coarse Aggregate	**3/4" AGG CRUSHED**	Lockwood	17.00		2.643	
	Coarse Aggregate	**1/2" AGG CRUSHED**	Lockwood	10.00		2.631	
	Coarse Aggregate	**3/8" AGG CRUSHED**	Lockwood	15.00		2.644	
	Fine Aggregate	**#4 - CRUSHER FINES**	Lockwood	14.00		2.522	
	Fine Aggregate	**#4 - NATURAL FINES**	Wade	10.00		2.528	
	Lime	**HYDRATED LIME**	Lhoist North America	1.00		2.35	
RAP	Fine RAP	**1/2" Lockwood RAP**	Lockwood	33.00		2.735	
Binder	Performance Grade	**PNAC PG 64-28NV (Matterhorn)**	Paramount	3.15	3.01	1.018	
Additive	Binder Additive	**Evoflex**	MeadWestvaco Corporation	2 % New AC			

GRANITE

Lockwood HMA Plant
10600 I-80 Exit 22
Lockwood, NV 89434
775-352-2927

Mix Properties

Mix 3564-3/4" HMA64-28NV 4V50BR30LM (Evoflex)

Specification 3564-2015 JMF Submittal

Mix Properties				Gradation		
Property	Unit	Design	Specification	Sieve	% Passing	Specification
AC Content (Pb)	%TMM	4.5	4.3-5.2	1" (25mm)	100.0	100-100
AC Content (Effective,Pbe)	%	4.2		3/4" (19mm)	100.0	93-100
AC Content (Absorbed,Pba)	%	0.26		1/2" (12.5mm)	89.3	
Air Voids (Va)	%	4	3-5	3/8" (9.5mm)	76.8	70-84
VMA	%	13.9	>13	#4 (4.75mm)	49.7	43-57
VFA	%	71.2	65-78	#8 (2.36mm)	36.7	
Stability	lbf	4316	>1800	#10 (2mm)	34.5	31-39
Plastic Flow	.01in	17	8-20	#16 (1.18mm)	28.6	
Unit Wt (Compacted)	lb/ft3	148		#30 (0.6mm)	21.8	
SPGR (Compacted,Gmb)		2.377		#40 (0.425mm)	18.1	14-22
SPGR (Max,Gmm)		2.477		#50 (0.3mm)	13.9	
SPGR (Dry,Gsb)		2.637		#100 (0.15mm)	8.9	
SPGR (SSD)		2.66		#200 (75µm)	6.4	4.4-8
SPGR (Apparent)		2.77				
Absorption (Coarse)		2				
Absorption	%	2.3				
Absorption (Fine)		3.2				
Fractured Faces (>1)	%	100	>50			
Fractured Faces (>2)	%	100				
Liquid Limit	%	<35	<35			
Plasticity Index	%	0	<6			
LA Abrasion		14.2	<37			
Soundness (Na2SO4) Coarse	%	2.2	<12			
Soundness (Na2SO4) Fine	%	3.1	<15			

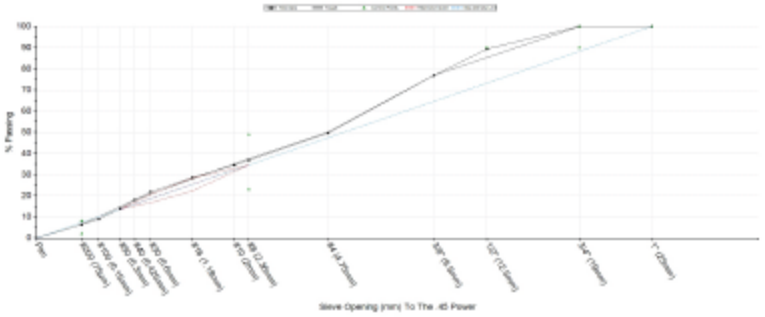

GRANITE

Lockwood HMA Plant
10600 I-80 Exit 22
Lockwood, NV 89434
775-352-2927

Mix Blend

Mix 3564-3/4" HMA64-28NV 4V50BR30LM (Evoflex)

Sieve/Test	Spec	Result	Dust	3/4" AGG CRUSHED	1/2" AGG CRUSHED	3/8" AGG CRUSHED	#4 - CRUSHER FINES	#4 - NATURAL FINES	HYDRATED LIME	1/2" Lockwood RAP
Type				Coarse Aggregate	Coarse Aggregate	Coarse Aggregate	Fine Aggregate	Fine Aggregate	Lime	Fine RAP
Include				Yes	Yes	Yes	Yes	Yes	Yes	Yes
%				17	10	15	14	10	1	33
1" (25mm) %	100-100	100.0		100.0	100.0	100.0	100.0	100.0	100.0	100.0
3/4" (19mm) %	90-100	100.0		100.0	100.0	100.0	100.0	100.0	100.0	100.0
1/2" (12.5mm) %		89.3		38.1	100.0	100.0	100.0	100.0	100.0	99.9
3/8" (9.5mm) %	63-85	76.8		4.0	48.6	100.0	100.0	100.0	100.0	95.6
#4 (4.75mm) %	45-65	49.7		0.4	0.7	19.8	97.6	99.2	100.0	67.6
#8 (2.36mm) %		36.7		0.4	0.6	0.9	71.4	97.7	100.0	47.9
#10 (2mm) %	30-44	34.5		0.4	0.6	0.8	64.5	97.3	100.0	44.4
#16 (1.18mm) %		26.6		0.3	0.5	0.7	45.5	94.2	100.0	35.4
#30 (0.6mm) %		21.8		0.3	0.4	0.6	29.8	77.3	99.8	26.6
#40 (0.425mm) %	12-22	18.1		0.3	0.4	0.6	25.3	59.0	99.8	22.8
#50 (0.3mm) %		13.9		0.3	0.4	0.6	21.5	36.0	99.8	18.8
#100 (0.15mm) %		8.9		0.3	0.4	0.5	16.6	9.7	99.8	13.6
#200 (75µm) %	3-8	6.4		0.2	0.3	0.5	12.9	2.8	86.8	10.2

GRANITE

Lockwood HMA Plant
10600 I-80 Exit 22
Lockwood, NV 89434
775-352-2927

Volumetric Charts

Mix: 3564-3/4" HMA64-28NV 4V50BR30LM (Evotlex)

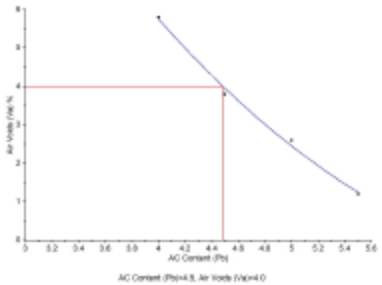

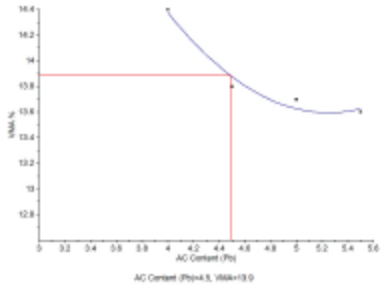

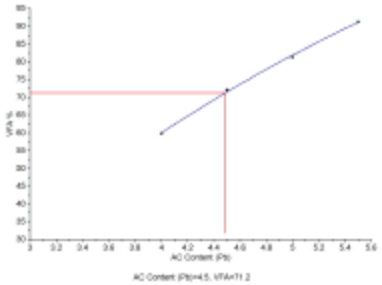

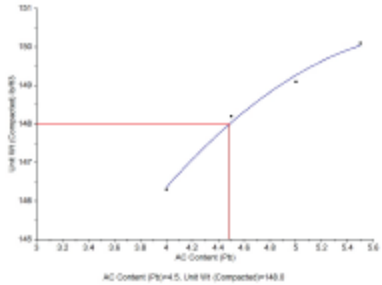

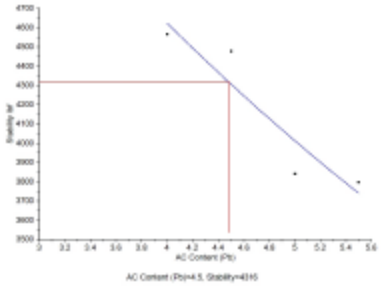

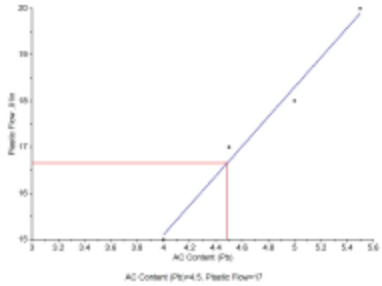

GRANITE

Lockwood HMA Plant
10600 I-80 Exit 22
Lockwood, NV 89434
775-352-2927

Batch Test Summary

Mix 3584-3/4" HMA64-28NV 4V50BR30LM (Evoflex)

Test	Sample 1	Sample 2	Sample 3	Sample 4
AC Content (Pb)	4.0	4.5	5.0	5.5
AC Content (Absorbed,Pba) %	0.27	0.26	0.27	0.28
AC Content (Effective,Pbe) %	3.7	4.2	4.7	5.2
Air Voids (Va) %	5.9	3.8	2.6	1.2
VMA %	14.8	13.8	13.7	13.8
VFA %	59.3	72.1	81.3	91.3
SPGR (Compacted,Gmb)	2.347	2.381	2.395	2.411
Unit Wt (Compacted) lb/ft3	146.1	148.2	149.1	150.1
SPGR (Max,Gmm)	2.495	2.476	2.458	2.440
Unit Wt (Max) lb/ft3	155.3	154.1	153.0	151.9
Stability lbf	4587	4478	3842	3797
Plastic Flow .01in	15	17	18	20

StonemontQC 08/14/2015

GRANITE
Quality Management

Guidance Document
Asphalt Binder Blending Chart

Mix		
% Total Asphalt Binder Content of Mix	4.71 %DWA	4.50 %TWM

RAP		
RAP Asphalt Binder Content	4.63	%TWM
% RAP in Mix (Aggregate + Asphalt)	33.0	%
% RAP Asphalt Binder in Mix	1.53	%TWM
% of RAP Asphalt Binder to Total Asphalt Binder	34.00	%

Virgin Asphalt Binder Supplier: *Paramount*
Grade: *64-28NV*
Desired Final Binder Grade: *PG 64-28*
Plant: *Lockwood*
Mix Identification: *3564 - 3/4"HMA64-28NV4V50BR30LM EVO*

Temperature	Property	Performance Grade: Target Value	Target Criteria	Virgin Binder Value	Virgin Binder Plot	RAP Binder Value	RAP Binder Plot	Blend Value	Blend Plot	Test Method
High	Original Asphalt Binder, DSR, °C	64	Min	67.9	67.4	85.1	83.2	73.7	72.8	D7125
	RTFO Aged Asphalt Binder, DSR, °C	64	Min	67.4		83.2		72.8		D7125
Intermediate	PAV Aged Asphalt Binder, DSR, °C	22	Max	12.5	12.5	24.4	24.4	16.5	16.5	D7125
Low	PAV Aged Asphalt Binder, BBR, Creep Stiffness, °C	-28	Max	-35.5	-33.6	-25.1	-24.1	-32.0	-30.4	D6816
	PAV Aged Asphalt Binder, BBR, m-value, °C	-28	Max	-33.6		-24.1		-30.4		D6816

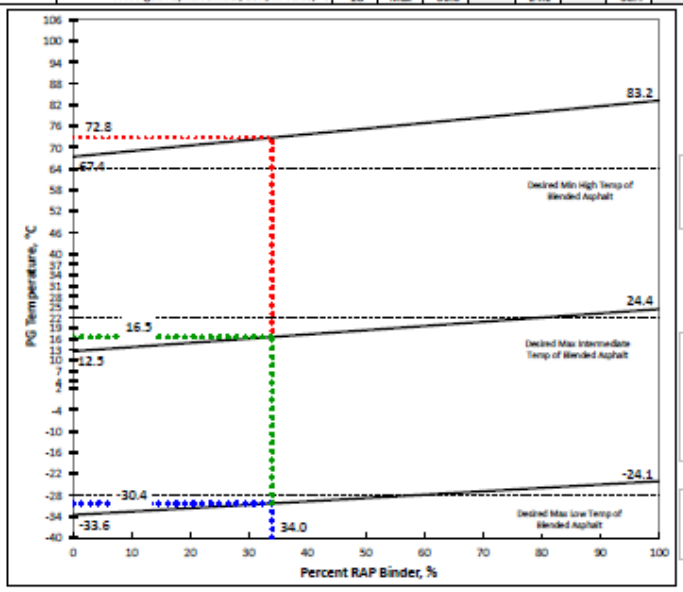

A.6 Quality Control Test Results

PAVEMENT RESULTS
FOR
MATTERHORN BLVD. IMPROVEMENT PROJECT
NEVADA PUBLIC WORKS PROJECT NO. PWP-WA-2015-179

SUMMIT ENGINEERING CORPORATION ™

SUMMIT ENGINEERING CORPORATION

CONTENTS:

SUMMIT ENGINEERING CORPORATION

SECTION 1:

Asphaltic Concrete Hot Mix Analysis

SUMMIT ENGINEERING CORPORATION

SUMMIT ENGINEERING CORPORATION
An AASHTO Accredited Testing Facility

ASPHALTIC CONCRETE HOT MIX ANALYSIS

Project Name: Matterhorn Blvd. **Lab No.** 1515-1520

Project No: 30096 **Tested by:** KH **Date:** 10/1/15

Sample Locations and Temperatures:

1515	Lot 1: Sta 390+00 Rt., Temp=305 ℉, Tonnage=198.88, Section 5
1516	Lot 2: Sta. 378+00 Rt., Temp=295 ℉ Tonnage=733.44, Section 5
1517	Lot 3: Sta. 357+00 Rt., Temp=300 ℉, Tonnage=1,233.45, Section 5
1518	Lot 4: Sta. 342+00 Lt., Temp=305 ℉, Tonnage=1,659.76, Section 5
1519	Lot 5: Sta. 360+50 Lt., Temp=305 ℉, Tonnage=2,231.82, Section 5
1520	Lot 6: Sts. 344+00, Temp=301 ℉, Tonnage=2,621.52, Section 5

Paving Date	**9-8-15**	**9-8-15**	**9-8-15**	**9-8-15**	**9-8-15**	**9-8-15**
Lot No.	**1**	**2**	**3**	**4**	**5**	**6**
Sample Number	**1515**	**1516**	**1517**	**1518**	**1519**	**1520**
% Bitumen by Total Weight of Mix (ASTM D 6307)	**4.66**	**4.80**	**4.60**	**4.83**	**5.20**	**5.44**
Rice Specific Gravity (ASTM D-2041)	**2.475**	**2.325**	**2.484**	**2.476**	**2.466**	**2.465**
Marshall Unit Weight (ASTM D-2726)	**145.16**	**144.73**	**145.89**	**145.16**	**145.62**	**147.10**
% Voids (ASTM D3203)	**5.76**	**5.82**	**5.63**	**5.81**	**5.13**	**4.12**
Marshall Stability (Lbs.) and Flow (1/100 in.) (ASTM D 6927)	**2937 / 21**	**2312 / 23**	**3297 / 21**	**2698 / 19**	**2267 / 23**	**2780 / 17**

REMARKS:

Section 1 Design: AC Content: 5.1%, Air Voids: 4.0%, Unit Wt. (Compacted): 146.7 pcf, SPGR (Max):2.454
Section 2 Design: AC Content: 4.6%, Air Voids: 4.0%, Unit Wt. (Compacted): 148.4 pcf, SPGR (Max):2.482
Section 3 Design: AC Content: 4.5%, Air Voids: 4.0%, Unit Wt. (Compacted): 148.0 pcf, SPGR (Max):2.477
Section 4 Design: AC Content: 4.6%, Air Voids: 4.0%, Unit Wt. (Compacted): 147.9 pcf, SPGR (Max):2.474
Section 5 Design: AC Content: 4.8%, Air Voids: 4.0%, Unit Wt. (Compacted): 147.5 pcf, SPGR (Max):2.469

*Note: Design Specifications from Granite Construction.

SUMMIT ENGINEERING CORPORATION

SUMMIT ENGINEERING CORPORATION
An AASHTO Accredited Testing Facility

ASPHALTIC CONCRETE HOT MIX ANALYSIS

Project Name: Matterhorn Blvd. **Lab No.** 1521-1526

Project No: 30096 **Tested by:** KH **Date:** 10/1/15

Sample Locations and Temperatures:

1521	Lot 7: Sta. 377+00 Rt., Temp=310°F, Tonnage=197.57, Section 5
1522	Lot 8: Sta. 315+00 Rt., Temp=300°F, Tonnage=695.39, Section 5
1523	Lot 9: Sta. 332+00 Lt., Temp=305°F, Tonnage=1,111.82, Section 5
1524	Lot 10: Sta. 309+50 Lt., Temp=300°F, Tonnage=1,650.55, Section 5
1525	Lot 11: Sta. 297+50 Rt., Temp=305°F, Tonnage=196.47, Section 4
1526	Lot 12: Sta. 276+00 Rt., Temp=303°F, Tonnage=150.25, Section 1

Paving Date	9-9-15	9-9-15	9-9-15	9-9-15	9-10-15	9-10-15
Lot No.	7	8	9	10	11	12
Sample Number	1521	1522	1523	1524	1525	1526
% Bitumen by Total Weight of Mix (ASTM D 6307)	5.09	5.09	4.92	4.96	4.89	5.06
Rice Specific Gravity (ASTM D-2041)	2.467	2.465	2.473	2.461	2.455	2.465
Marshall Unit Weight (ASTM D-2726)	146.54	145.95	145.08	146.34	146.36	146.91
% Voids (ASTM D3203)	4.56	4.87	5.74	4.46	4.21	4.25
Marshall Stability (Lbs.) and Flow (1/100 in.) (ASTM D 6927)	3190/20	2633/18	2692/18	2823/16	3344/19	2691/16

REMARKS:

Section 1 Design: AC Content: 5.1%, Air Voids: 4.0%, Unit Wt. (Compacted): 146.7 pcf, SPGR (Max):2.454
Section 2 Design: AC Content: 4.6%, Air Voids: 4.0%, Unit Wt. (Compacted): 148.4 pcf, SPGR (Max):2.482
Section 3 Design: AC Content: 4.5%, Air Voids: 4.0%, Unit Wt. (Compacted): 148.0 pcf, SPGR (Max):2.477
Section 4 Design: AC Content: 4.6%, Air Voids: 4.0%, Unit Wt. (Compacted): 147.9 pcf, SPGR (Max):2.474
Section 5 Design: AC Content: 4.8%, Air Voids: 4.0%, Unit Wt. (Compacted): 147.5 pcf, SPGR (Max):2.469

*Note: Design Specifications from Granite Construction.

SUMMIT ENGINEERING CORPORATION

SUMMIT ENGINEERING CORPORATION
An AASHTO Accredited Testing Facility

ASPHALTIC CONCRETE HOT MIX ANALYSIS

Project Name: Matterhorn Blvd. **Lab No.** 1527-1532

Project No: 30096 **Tested by:** KH **Date:** 10/1/15

Sample Locations and Temperatures:

1527	Lot 13: Sta.297+00 Lt., Temp=300°F, Tonnage=782.48, Section 4
1528	Lot 14: Sta.271+00 Lt., Temp=295°F, Tonnage=785.71, Section 1
1529	Lot 15: Sta.244+50 Rt., Temp=300°F, Tonnage=195.81, Section 2
1530	Lot 16: Sta.218+00 Rt., Temp=305°F, Tonnage=191.23, Section 3
1531	Lot 17: Sta. 246+00 Lt., Temp=300°F, Tonnage=733.08, Section 2
1532	Lot 18: Sta.221+00 Lt., Temp=285°F, Tonnage=868.22, , Section 3

Paving Date	9-10-15	9-10-15	9-11-15	9-11-15	9-11-15	9-11-15
Lot No.	13	14	15	16	17	18
Sample Number	1527	1528	1529	1530	1531	1532
% Bitumen by Total Weight of Mix (ASTM D 6307)	5.00	5.64	4.91	5.35	4.87	5.17
Rice Specific Gravity (ASTM D-2041)	2.454	2.460	2.449	2.445	2.461	2.453
Marshall Unit Weight (ASTM D-2726)	146.33	145.96	147.10	147.83	146.39	146.39
% Voids (ASTM D3203)	4.19	4.67	3.50	2.85	4.43	4.12
Marshall Stability (Lbs.) and Flow (1/100 in.) (ASTM D 6927)	$\frac{3275}{17}$	$\frac{2460}{17}$	$\frac{3685}{19}$	$\frac{2698}{19}$	$\frac{3491}{21}$	$\frac{3370}{17}$

REMARKS:

Section 1 Design: AC Content: 5.1%, Air Voids: 4.0%, Unit Wt. (Compacted): 146.7 pcf, SPGR (Max):2.454
Section 2 Design: AC Content: 4.6%, Air Voids: 4.0%, Unit Wt. (Compacted): 148.4 pcf, SPGR (Max):2.482
Section 3 Design: AC Content: 4.5%, Air Voids: 4.0%, Unit Wt. (Compacted): 148.0 pcf, SPGR (Max):2.477
Section 4 Design: AC Content: 4.6%, Air Voids: 4.0%, Unit Wt. (Compacted): 147.9 pcf, SPGR (Max):2.474
Section 5 Design: AC Content: 4.8%, Air Voids: 4.0%, Unit Wt. (Compacted): 147.5 pcf, SPGR (Max):2.469

*Note: Design Specifications from Granite Construction.

SUMMIT ENGINEERING CORPORATION

SUMMIT ENGINEERING CORPORATION
An AASHTO Accredited Testing Facility

ASPHALTIC CONCRETE HOT MIX ANALYSIS

Project Name: Matterhorn Blvd. **Lab No.** 1535-1540

Project No: 30096 **Tested by:** KH **Date:** 10/1/15

Sample Locations and Temperatures:

1535	Lot 19: Sta. 191+00 Rt., Temp=300°F, Tonnage=197.37, Section 5
1536	Lot 20: Sta.167+00 Rt., Temp=305°F, Tonnage=765.53, Section 5
1537	Lot 21 Sta.147+00 Rt., Temp=305°F, Tonnage=1,202.22, Section 5
1538	Lot 22: Sta.178+50 Lt., Temp=305°F, Tonnage=1,706.82, Section 5
1539	Lot 23: Sta.154+50 Lt., Temp=300°F, Tonnage=2,245.51, Section 5
1540	Lot 24: Sta.133+00 Lt., Temp=300°F, Tonnage=196.07, Section 5

Paving Date	**9-16-15**	**9-16-15**	**9-16-15**	**9-16-15**	**9-16-15**	**9-17-15**
Lot No.	**19**	**20**	**21**	**22**	**23**	**24**
Sample Number	**1535**	**1536**	**1537**	**1538**	**1539**	**1540**
% Bitumen by Total Weight of Mix (ASTM D 6307)	**4.90**	**5.11**	**5.68**	**5.26**	**5.08**	**5.03**
Rice Specific Gravity (ASTM D-2041)	**2.478**	**2.465**	**2.441**	**2.451**	**2.472**	**2.475**
Marshall Unit Weight (ASTM D-2726)	**146.09**	**146.60**	**146.51**	**146.33**	**146.07**	**147.15**
% Voids (ASTM D3203)	**5.28**	**4.44**	**3.56**	**4.08**	**5.06**	**4.47**
Marshall Stability (Lbs.) and Flow (1/100 in.) (ASTM D 6927)	**3026 / 20**	**3237 / 17**	**2664 / 19**	**2145 / 19**	**2864 / 19**	**3099 / 16**

REMARKS:

Section 1 Design: AC Content: 5.1%, Air Voids: 4.0%, Unit Wt. (Compacted): 146.7 pcf, SPGR (Max):2.454
Section 2 Design: AC Content: 4.6%, Air Voids: 4.0%, Unit Wt. (Compacted): 148.4 pcf, SPGR (Max):2.482
Section 3 Design: AC Content: 4.5%, Air Voids: 4.0%, Unit Wt. (Compacted): 148.0 pcf, SPGR (Max):2.477
Section 4 Design: AC Content: 4.6%, Air Voids: 4.0%, Unit Wt. (Compacted): 147.9 pcf, SPGR (Max):2.474
Section 5 Design: AC Content: 4.8%, Air Voids: 4.0%, Unit Wt. (Compacted): 147.5 pcf, SPGR (Max):2.469

*Note: Design Specifications from Granite Construction.

SUMMIT ENGINEERING CORPORATION

SUMMIT ENGINEERING CORPORATION
An AASHTO Accredited Testing Facility

ASPHALTIC CONCRETE HOT MIX ANALYSIS

Project Name: Matterhorn Blvd. **Lab No.** 1541-1543

Project No: 30096 **Tested by:** KH **Date:** 10/1/15

Sample Locations and Temperatures:

1541	Lot 25: Sta. 112+00 Lt., Temp=295 F, Tonnage=695.86, Section 5
1542	Lot 26: Sta.136+00 Rt., Temp=295 F, Tonnage=1,199.35, Section 5
1543	Lot 27: Sta.115+00 Rt., Temp=295 F, Tonnage=1,676.05, Section 5

Paving Date	9-17-15	9-17-15	9-17-15			
Lot No.	25	26	27			
Sample Number	1541	1542	1543			
% Bitumen by Total Weight of Mix (ASTM D 6307)	5.29	5.49	5.19			
Rice Specific Gravity (ASTM D-2041)	2.466	2.448	2.462			
Marshall Unit Weight (ASTM D-2726)	147.97	147.58	147.17			
% Voids (ASTM D3203)	3.59	3.14	3.96			
Marshall Stability (Lbs.) and Flow (1/100 in.) (ASTM D 6927)	$\frac{2947}{18}$	$\frac{2771}{17}$	$\frac{2657}{19}$			

REMARKS:

Section 1 Design: AC Content: 5.1%, Air Voids: 4.0%, Unit Wt. (Compacted): 146.7 pcf, SPGR (Max):2.454
Section 2 Design: AC Content: 4.6%, Air Voids: 4.0%, Unit Wt. (Compacted): 148.4 pcf, SPGR (Max):2.482
Section 3 Design: AC Content: 4.5%, Air Voids: 4.0%, Unit Wt. (Compacted): 148.0 pcf, SPGR (Max):2.477
Section 4 Design: AC Content: 4.6%, Air Voids: 4.0%, Unit Wt. (Compacted): 147.9 pcf, SPGR (Max):2.474
Section 5 Design: AC Content: 4.8%, Air Voids: 4.0%, Unit Wt. (Compacted): 147.5 pcf, SPGR (Max):2.469

*Note: Design Specifications from Granite Construction.

SUMMIT ENGINEERING CORPORATION

SECTION 2:

Asphaltic Concrete Hot Mix Sample Gradation Report

SUMMIT ENGINEERING CORPORATION

SUMMIT ENGINEERING CORPORATION
SIEVE ANALYSIS
(ASTM C 136)

Job Name	Matterhorn Blvd	**Lab No.**	1515-1520
Job No.	30096	**Date**	10-1-2015
Sample Description	TYPE 2 AC	**Technician**	KH/GM
Material Source	GRANITE LOCKWOOD HOT PLANT		

Sieve Size	SAMPLE NUMBER: COMBINED % PASSING						Specifications
	1515	1516	1517	1518	1519	1520	
3"							
2"							
1½"							
1"	100	100	100	100	100	100	100
¾"	100	100	100	100	100	100	90-100
½"	87	89	89	91	90	94	
3/8"	74	75	75	78	78	81	63-85
#4	50	48	47	53	51	54	45-65
#8	34	33	33	36	36	37	
#10	32	31	31	34	33	34	30-44
#16	25	25	25	27	27	28	
#30	20	20	20	21	21	22	
#40	17	17	17	17	18	18	12-22
#50	13	13	13	14	14	15	
#100	8	8	8	9	9	9	
#200	5.8	6.0	6.0	6.0	6.1	6.1	3-8

REMARKS:

SUMMIT ENGINEERING CORPORATION

SUMMIT ENGINEERING CORPORATION
SIEVE ANALYSIS
(ASTM C 136)

Job Name	Matterhorn Blvd	**Lab No.**	1521-1526
Job No.	30096	**Date**	10-1-2015
Sample Description	TYPE 2 AC	**Technician**	KH/GM
Material Source	GRANITE LOCKWOOD HOT PLANT		

Sieve Size	SAMPLE NUMBER: COMBINED % PASSING						Specifications
	1521	1522	1523	1524	1525	1526	
3"							
2"							
1½"							
1"	100	100	100	100	100	100	100
¾"	100	100	100	100	100	100	90-100
½"	90	88	92	91	91	90	
3/8"	79	76	79	78	76	75	63-85
#4	54	51	54	51	51	49	45-65
#8	37	37	38	35	36	34	
#10	34	34	36	33	34	31	30-44
#16	27	28	29	26	28	25	
#30	21	21	23	21	22	20	
#40	18	18	19	17	19	16	12-22
#50	14	14	15	14	15	13	
#100	9	9	9	9	9	8	
#200	6.1	6.0	6.5	6.0	6.3	5.3	3-8

REMARKS:

SUMMIT ENGINEERING CORPORATION

SUMMIT ENGINEERING CORPORATION
SIEVE ANALYSIS
(ASTM C 136)

Job Name	Matterhorn Blvd	**Lab No.**	1527-1532
Job No.	30096	**Date**	10-1-2015
Sample Description	TYPE 2 AC	**Technician**	KH/GM
Material Source	GRANITE LOCKWOOD HOT PLANT		

Sieve Size	SAMPLE NUMBER: COMBINED % PASSING						Specifications
	1527	1528	1529	1530	1531	1532	
3"							
2"							
1½"							
1"	100	100	100	100	100	100	100
¾"	100	100	100	100	100	100	90-100
½"	91	92	89	91	89	90	
3/8"	79	79	75	82	75	79	63-85
#4	54	53	50	57	51	55	45-65
#8	38	37	36	41	36	39	
#10	36	34	34	39	34	37	30-44
#16	29	27	28	32	28	30	
#30	23	21	22	24	22	23	
#40	19	17	18	20	18	19	12-22
#50	15	13	14	16	14	15	
#100	10	8	8	9	8	10	
#200	6.7	5.3	5.0	5.2	4.9	6.9	3-8

REMARKS:

SUMMIT ENGINEERING CORPORATION

SUMMIT ENGINEERING CORPORATION
SIEVE ANALYSIS
(ASTM C 136)

Job Name	Matterhorn Blvd	**Lab No.**	1535-1540
Job No.	30096	**Date**	10-1-2015
Sample Description	TYPE 2 AC	**Technician**	KH/GM
Material Source	GRANITE LOCKWOOD HOT PLANT		

Sieve Size	SAMPLE NUMBER: COMBINED % PASSING						Specifications
	1535	1536	1537	1538	1539	1540	
3"							
2"							
1½"							
1"	100	100	100	100	100	100	100
¾"	100	100	100	100	100	100	90-100
½"	86	89	91	88	91	90	
3/8"	73	76	78	78	75	77	63-85
#4	47	50	54	54	50	49	45-65
#8	33	35	38	38	35	33	
#10	31	33	35	35	32	31	30-44
#16	25	27	28	28	26	25	
#30	19	21	21	22	20	20	
#40	16	22	17	18	17	17	12-22
#50	13	14	13	14	14	13	
#100	8	9	8	9	9	9	
#200	5.5	6.1	5.8	6.3	5.9	6.4	3-8

REMARKS:

SUMMIT ENGINEERING CORPORATION

SUMMIT ENGINEERING CORPORATION
SIEVE ANALYSIS
(ASTM C 136)

Job Name	Matterhorn Blvd	**Lab No.**	1541-1543
Job No.	30096	**Date**	10-1-2015
Sample Description	TYPE 2 AC	**Technician**	KH/GM
Material Source	GRANITE LOCKWOOD HOT PLANT		

Sieve Size	SAMPLE NUMBER: COMBINED % PASSING						Specifications
	1541	1542	1543				
3"							
2"							
1½"							
1"	100	100	100				100
¾"	100	100	100				90-100
½"	91	94	93				
3/8"	78	82	81				63-85
#4	52	56	55				45-65
#8	35	39	38				
#10	33	36	35				30-44
#16	27	29	28				
#30	21	22	21				
#40	17	18	18				12-22
#50	14	15	14				
#100	9	9	9				
#200	6.3	6.4	6.4				3-8

REMARKS:

SUMMIT ENGINEERING CORPORATION

SECTION 3:

Mat and Joint Core Relative Compaction Report

SUMMIT ENGINEERING CORPORATION

SUMMIT ENGINEERING CORPORATION
An AASHTO Accredited Testing Facility

RELATIVE COMPACTION ASPHALTIC CONCRETE CORE SAMPLES (ASTM D-2041, D-2726)

Project Name	MATTERHORN BLVD.	**Date**	10-19-15
Project Number	30096	**Lab No.**	1535
Location	See below	**Tested By**	KH

Lot Number	1	1	1	2	2	2
Sample Number	A	B	C	A	B	C
Thickness (in.) Total	3.179	3.222	3.405	3.492	3.467	3.033
Lift Top						
Lift Bottom						
Specific Gravity	2.349	2.352	2.298	2.335	2.342	2.358
Average Rice Specific Gravity	2.475	2.475	2.475	2.469	2.469	2.469
% Compaction (Rice)	94.9	95.0	92.8	94.6	94.9	95.5
Average Marshall Unit Weight (PCF)	145.16	145.16	145.16	144.73	144.73	144.73
% Compaction (Marshall)	100.7	100.8	98.5	100.4	100.7	101.4

Lot 1 Average % Rice Compaction = 94.2 **% Marshall Compaction = 100.0**
Lot 2 Average % Rice Compaction = 95.0 **% Marshall Compaction = 100.8**

1A West Bound Tupelo St. @ Sta. 392+00
1B West Bound Tupelo St. @ Sta. 388+00
1C East Bound Tupelo St. @ Sta. 391+00

2A East Bound Tupelo St. @ Sta. 285+00
2B South Bound Matterhorn Blvd. @ Sta. 378+00
2C South Bound Matterhorn Blvd. @ Sta. 371+00

SUMMIT ENGINEERING CORPORATION

SUMMIT ENGINEERING CORPORATION
An AASHTO Accredited Testing Facility

RELATIVE COMPACTION ASPHALTIC CONCRETE CORE SAMPLES (ASTM D-2041, D-2726)

Project Name	MATTERHORN BLVD.	**Date**	10-19-15
Project Number	30096	**Lab No.**	1535
Location	See below	**Tested By**	KH

Lot Number	3	3	3	4	4	4
Sample Number	A	B	C	A	B	C
Thickness (in.) Total	3.245	3.560	3.684	3.149	3.140	3.400
Lift Top						
Lift Bottom						
Specific Gravity	2.341	2.346	2.329	2.341	2.325	2.299
Average Rice Specific Gravity	2.484	2.484	2.484	2.476	2.476	2.476
% Compaction (Rice)	94.2	94.4	94.8	94.5	93.9	92.9
Average Marshall Unit Weight (PCF)	145.89	145.89	145.89	145.16	145.16	145.16
% Compaction (Marshall)	99.9	100.1	99.4	100.4	99.7	98.6

Lot 3 Average % Rice Compaction = 94.5 **% Marshall Compaction = 99.8**
Lot 4 Average % Rice Compaction = 93.8 **% Marshall Compaction = 99.6**

3A South Bound Matterhorn Blvd. @ Sta. 366+00
3B South Bound Matterhorn Blvd. @ Sta. 358+00
3C South Bound Matterhorn Blvd. @ Sta. 351+00

4A South Bound Matterhorn Blvd. @ Sta. 346+00
4B North Bound Matterhorn Blvd. @ Sta. 381+00
4C North Bound Matterhorn Blvd. @ Sta. 373+00

SUMMIT ENGINEERING CORPORATION

SUMMIT ENGINEERING CORPORATION
An AASHTO Accredited Testing Facility

RELATIVE COMPACTION ASPHALTIC CONCRETE CORE SAMPLES (ASTM D-2041, D-2726)

Project Name	MATTERHORN BLVD.	**Date**	10-19-15
Project Number	30096	**Lab No.**	1535
Location	See below	**Tested By**	KH

Lot Number	5	5	5	6	6	6
Sample Number	A	B	C	A	B	C
Thickness (in.) **Total**	3.421	3.540	3.890	3.293	3.508	3.432
Lift Top						
Lift Bottom						
Specific Gravity	2.304	2.322	2.312	2.329	2.298	2.349
Average Rice Specific Gravity	2.466	2.466	2.466	2.465	2.465	2.465
% Compaction (Rice)	93.4	94.1	93.8	94.5	93.2	95.3
Average Marshall Unit Weight (PCF)	145.62	145.62	145.62	147.10	147.10	147.10
% Compaction (Marshall)	98.5	99.2	98.8	98.5	97.2	99.4

Lot 5 Average % Rice Compaction = 93.7 **% Marshall Compaction = 98.8**
Lot 6 Average % Rice Compaction = 94.3 **% Marshall Compaction = 98.4**

5A North Bound Matterhorn Blvd. @ Sta. 365+00
5B North Bound Matterhorn Blvd. @ Sta. 360+00
5C North Bound Matterhorn Blvd. @ Sta. 355+00

6A North Bound Matterhorn Blvd. @ Sta. 351+00
6B North Bound Matterhorn Blvd. @ Sta. 348+00
6C North Bound Matterhorn Blvd. @ Sta. 345+00

SUMMIT ENGINEERING CORPORATION

SUMMIT ENGINEERING CORPORATION
An AASHTO Accredited Testing Facility

RELATIVE COMPACTION ASPHALTIC CONCRETE CORE SAMPLES (ASTM D-2041, D-2726)

Project Name	MATTERHORN BLVD.	**Date**	10-19-15
Project Number	30096	**Lab No.**	1535
Location	See below	**Tested By**	KH

Lot Number	7	7	7	8	8	8
Sample Number	A	B	C	A	B	C
Thickness (in.) Total	3.915	3.078	3.131	3.266	3.336	3.283
Lift Top						
Lift Bottom						
Specific Gravity	2.371	2.386	2.394	2.383	2.386	2.354
Average Rice Specific Gravity	2.467	2.467	2.467	2.465	2.465	2.465
% Compaction (Rice)	96.1	96.7	97.0	96.7	96.8	95.5
Average Marshall Unit Weight (PCF)	146.54	146.54	146.54	145.95	145.95	145.95
% Compaction (Marshall)	100.7	101.3	101.7	101.6	101.8	100.0

Lot 7 Average % Rice Compaction = 96.6 **% Marshall Compaction = 101.2**
Lot 8 Average % Rice Compaction = 96.3 **% Marshall Compaction = 101.1**

7A South Bound Matterhorn Blvd. @ Sta. 338+00
7B South Bound Matterhorn Blvd. @ Sta. 333+00
7C South Bound Matterhorn Blvd. @ Sta. 328+00

8A South Bound Matterhorn Blvd. @ Sta. 318+00
8B South Bound Matterhorn Blvd. @ Sta. 313+00
8C South Bound Matterhorn Blvd. @ Sta. 308+00

SUMMIT ENGINEERING CORPORATION

SUMMIT ENGINEERING CORPORATION
An AASHTO Accredited Testing Facility

RELATIVE COMPACTION ASPHALTIC CONCRETE CORE SAMPLES (ASTM D-2041, D-2726)

Project Name	MATTERHORN BLVD.	**Date**	10-19-15
Project Number	30096	**Lab No.**	1535
Location	See below	**Tested By**	KH

Lot Number	9	9	9	10	10	10
Sample Number	A	B	C	A	B	C
Thickness (in.) **Total**	2.849	3.159	2.400	3.174	2.828	3.258
Lift Top						
Lift Bottom						
Specific Gravity	2.291	2.332	2.354	2.316	2.351	2.343
Average Rice Specific Gravity	2.473	2.473	2.473	2.461	2.461	2.461
% Compaction (Rice)	92.6	94.3	95.2	94.1	95.5	95.2
Average Marshall Unit Weight (PCF)	145.08	145.08	145.08	146.34	146.34	146.34
% Compaction (Marshall)	98.3	100.0	100.1	98.5	100.0	99.7

Lot 9 Average % Rice Compaction = 94.0 **% Marshall Compaction = 99.5**
Lot 10 Average % Rice Compaction = 94.9 **% Marshall Compaction = 99.4**

9A North Bound Matterhorn Blvd. @ Sta. 338+00
9B North Bound Matterhorn Blvd. @ Sta. 328+00
9C North Bound Matterhorn Blvd. @ Sta. 318+00

10A North Bound Matterhorn Blvd. @ Sta. 313+00
10B North Bound Matterhorn Blvd. @ Sta. 310+00
10C North Bound Matterhorn Blvd. @ Sta. 307+00

SUMMIT ENGINEERING CORPORATION

SUMMIT ENGINEERING CORPORATION
An AASHTO Accredited Testing Facility

RELATIVE COMPACTION ASPHALTIC CONCRETE CORE SAMPLES (ASTM D-2041, D-2726)

Project Name	MATTERHORN BLVD.	**Date**	10-19-15
Project Number	30096	**Lab No.**	1535
Location	See below	**Tested By**	KH

Lot Number	11	11	11	12	12	12
Sample Number	A	B	C	A	B	C
Thickness (in.) **Total**	2.234	3.143	3.269	3.620	3.021	3.089
Lift Top						
Lift Bottom						
Specific Gravity	2.362	2.370	2.353	2.354	2.380	2.342
Average Rice Specific Gravity	2.455	2.455	2.455	2.465	2.465	2.465
% Compaction (Rice)	96.2	96.5	95.8	95.5	96.6	95.0
Average Marshall Unit Weight (PCF)	146.36	146.36	146.36	146.91	146.91	146.91
% Compaction (Marshall)	100.4	100.8	100.0	99.7	100.8	99.2

Lot 11 Average % Rice Compaction = 96.2 **% Marshall Compaction = 100.4**
Lot 12 Average % Rice Compaction = 95.7 **% Marshall Compaction = 99.9**

11A South Bound Matterhorn Blvd. @ Sta. 300+00
11B South Bound Matterhorn Blvd. @ Sta. 292+00
11C South Bound Matterhorn Blvd. @ Sta. 284+00

12A South Bound Matterhorn Blvd. @ Sta. 273+00
12B South Bound Matterhorn Blvd. @ Sta. 265+00
12C South Bound Matterhorn Blvd. @ Sta. 257+00

SUMMIT ENGINEERING CORPORATION

SUMMIT ENGINEERING CORPORATION
An AASHTO Accredited Testing Facility

RELATIVE COMPACTION ASPHALTIC CONCRETE CORE SAMPLES (ASTM D-2041, D-2726)

Project Name	MATTERHORN BLVD.	**Date**	10-19-15
Project Number	30096	**Lab No.**	1535
Location	See below	**Tested By**	KH

Lot Number	13	13	13	14	14	14
Sample Number	A	B	C	A	B	C
Thickness (in.) **Total**	3.520	3.174	3.135	3.220	3.197	3.208
Lift Top						
Lift Bottom						
Specific Gravity	2.343	2.356	2.347	2.320	2.348	2.332
Average Rice Specific Gravity	2.454	2.454	2.454	2.460	2.460	2.460
% Compaction (Rice)	95.5	96.0	95.6	94.3	95.4	94.8
Average Marshall Unit Weight (PCF)	146.33	146.33	146.33	145.96	145.96	145.96
% Compaction (Marshall)	99.7	100.2	99.8	98.9	100.1	99.4

Lot 13 Average % Rice Compaction = 95.7 **% Marshall Compaction = 99.9**
Lot 14 Average % Rice Compaction = 94.8 **% Marshall Compaction = 99.5**

13A North Bound Matterhorn Blvd. @ Sta. 300+00
13B North Bound Matterhorn Blvd. @ Sta. 292+00
13C North Bound Matterhorn Blvd. @ Sta. 284+00

14A North Bound Matterhorn Blvd. @ Sta. 273+00
14B North Bound Matterhorn Blvd. @ Sta. 265+00
14C North Bound Matterhorn Blvd. @ Sta. 257+00

SUMMIT ENGINEERING CORPORATION

SUMMIT ENGINEERING CORPORATION
An AASHTO Accredited Testing Facility

RELATIVE COMPACTION ASPHALTIC CONCRETE CORE SAMPLES (ASTM D-2041, D-2726)

Project Name	MATTERHORN BLVD.	**Date**	10-19-15
Project Number	30096	**Lab No.**	1535
Location	See below	**Tested By**	KH

Lot Number	15	15	15	16	16	16
Sample Number	A	B	C	A	B	C
Thickness (in.) Total	3.174	3.800	2.954	2.800	3.892	3.064
Lift Top						
Lift Bottom						
Specific Gravity	2.374	2.305	2.360	2.347	2.284	2.331
Average Rice Specific Gravity	2.449	2.449	2.449	2.445	2.445	2.445
% Compaction (Rice)	96.9	94.1	96.3	96.0	93.4	95.3
Average Marshall Unit Weight (PCF)	147.10	147.10	147.10	147.83	147.83	147.83
% Compaction (Marshall)	100.4	97.5	99.9	98.8	96.2	98.1

Lot 15 Average % Rice Compaction = 95.8 **% Marshall Compaction = 99.3**
Lot 16 Average % Rice Compaction = 94.9 **% Marshall Compaction = 97.7**

15A South Bound Matterhorn Blvd. @ Sta. 248+00
15B South Bound Matterhorn Blvd. @ Sta. 238+00
15C South Bound Matterhorn Blvd. @ Sta. 228+00

16A South Bound Matterhorn Blvd. @ Sta. 222+00
16B South Bound Matterhorn Blvd. @ Sta. 212+00
16C South Bound Matterhorn Blvd. @ Sta. 202+00

SUMMIT ENGINEERING CORPORATION

SUMMIT ENGINEERING CORPORATION
An AASHTO Accredited Testing Facility

RELATIVE COMPACTION ASPHALTIC CONCRETE CORE SAMPLES (ASTM D-2041, D-2726)

Project Name	MATTERHORN BLVD.	**Date**	10-19-15
Project Number	30096	**Lab No.**	1535
Location	See below	**Tested By**	KH

Lot Number	17	17	17	18	18	18
Sample Number	A	B	C	A	B	C
Thickness (in.) Total	3.135	3.222	3.355	3.010	3.865	3.058
Lift Top						
Lift Bottom						
Specific Gravity	2.340	2.316	2.329	2.250	2.341	2.321
Average Rice Specific Gravity	2.461	2.461	2.461	2.453	2.453	2.453
% Compaction (Rice)	95.0	94.1	94.6	91.7	95.1	94.6
Average Marshall Unit Weight (PCF)	146.39	146.39	146.39	146.39	146.39	146.39
% Compaction (Marshall)	99.5	98.5	99.0	95.7	99.5	98.7

Lot 17 Average % Rice Compaction = 94.6 **% Marshall Compaction = 99.0**
Lot 18 Average % Rice Compaction = 93.8 **% Marshall Compaction = 98.0**

17A North Bound Matterhorn Blvd. @ Sta. 248+00
17B North Bound Matterhorn Blvd. @ Sta. 241+00
17C North Bound Matterhorn Blvd. @ Sta. 235+00

18A North Bound Matterhorn Blvd. @ Sta. 222+00
18B North Bound Matterhorn Blvd. @ Sta. 212+00
18C North Bound Matterhorn Blvd. @ Sta. 202+00

SUMMIT ENGINEERING CORPORATION

SUMMIT ENGINEERING CORPORATION
An AASHTO Accredited Testing Facility

RELATIVE COMPACTION ASPHALTIC CONCRETE CORE SAMPLES (ASTM D-2041, D-2726)

Project Name	MATTERHORN BLVD.	**Date**	10-19-15
Project Number	30096	**Lab No.**	1535
Location	See below	**Tested By**	KH

Lot Number	19	19	19	20	20	20
Sample Number	A	B	C	A	B	C
Thickness (in.) **Total**	3.277	3.297	3.150	3.240	3.507	3.384
Lift Top						
Lift Bottom						
Specific Gravity	2.357	2.343	2.344	2.345	2.324	2.334
Average Rice Specific Gravity	2.478	2.478	2.478	2.465	2.465	2.465
% Compaction (Rice)	95.1	94.6	94.6	95.1	94.2	94.7
Average Marshall Unit Weight (PCF)	146.09	146.09	146.09	146.60	146.60	146.60
% Compaction (Marshall)	100.4	99.8	99.9	99.6	98.7	99.1

Lot 19 Average % Rice Compaction = 94.8 **% Marshall Compaction = 100.0**
Lot 20 Average % Rice Compaction = 94.7 **% Marshall Compaction = 99.1**

19A South Bound Matterhorn Blvd. @ Sta. 194+00
19B South Bound Matterhorn Blvd. @ Sta. 198+00
19C South Bound Matterhorn Blvd. @ Sta. 182+00

20A South Bound Matterhorn Blvd. @ Sta. 174+00
20B South Bound Matterhorn Blvd. @ Sta. 168+00
20C South Bound Matterhorn Blvd. @ Sta. 158+00

SUMMIT ENGINEERING CORPORATION

SUMMIT ENGINEERING CORPORATION
An AASHTO Accredited Testing Facility

RELATIVE COMPACTION ASPHALTIC CONCRETE CORE SAMPLES (ASTM D-2041, D-2726)

Project Name	MATTERHORN BLVD.	**Date**	10-19-15
Project Number	30096	**Lab No.**	1535
Location	See below	**Tested By**	KH

Lot Number	21	21	21	22	22	22
Sample Number	A	B	C	A	B	C
Thickness (in.) **Total**	3.220	3.070	3.389	3.326	3.294	3.333
Lift Top						
Lift Bottom						
Specific Gravity	2.353	2.308	2.330	2.297	2.348	2.301
Average Rice Specific Gravity	2.441	2.441	2.441	2.451	2.451	2.451
% Compaction (Rice)	96.4	94.6	95.5	93.7	95.8	93.9
Average Marshall Unit Weight (PCF)	146.51	146.51	146.51	146.33	146.33	146.33
% Compaction (Marshall)	100.0	98.0	99.0	97.7	99.9	97.9

Lot 21 Average % Rice Compaction = 95.5 **% Marshall Compaction = 99.0**
Lot 22 Average % Rice Compaction = 94.5 **% Marshall Compaction = 98.5**

21A South Bound Matterhorn Blvd. @ Sta. 148+00
21B North Bound Matterhorn Blvd. @ Sta. 194+00
21C North Bound Matterhorn Blvd. @ Sta. 188+00

22A North Bound Matterhorn Blvd. @ Sta. 184+00
22B North Bound Matterhorn Blvd. @ Sta. 178+00
22C North Bound Matterhorn Blvd. @ Sta. 168+00

SUMMIT ENGINEERING CORPORATION

SUMMIT ENGINEERING CORPORATION
An AASHTO Accredited Testing Facility

RELATIVE COMPACTION ASPHALTIC CONCRETE CORE SAMPLES (ASTM D-2041, D-2726)

Project Name	MATTERHORN BLVD.	**Date**	10-19-15
Project Number	30096	**Lab No.**	1535
Location	See below	**Tested By**	KH

Lot Number	23	23	23	24	24	24
Sample Number	A	B	C	A	B	C
Thickness (in.) **Total**	3.177	3.274	3.312	3.272	2.993	3.740
Lift Top						
Lift Bottom						
Specific Gravity	2.324	2.347	2.288	2.295	2.360	2.329
Average Rice Specific Gravity	2.472	2.472	2.472	2.475	2.475	2.475
% Compaction (Rice)	94.0	94.9	92.6	92.7	95.4	94.1
Average Marshall Unit Weight (PCF)	146.07	146.07	146.07	147.15	147.15	147.15
% Compaction (Marshall)	99.0	100.0	97.5	97.1	99.8	98.5

Lot 23 Average % Rice Compaction = 93.8 **% Marshall Compaction = 98.8**
Lot 24 Average % Rice Compaction = 94.1 **% Marshall Compaction = 98.5**

23A North Bound Matterhorn Blvd. @ Sta. 158+00
23B North Bound Matterhorn Blvd. @ Sta. 154+00
23C North Bound Matterhorn Blvd. @ Sta. 148+00

24A North Bound Matterhorn Blvd. @ Sta. 128+00
24B North Bound Matterhorn Blvd. @ Sta. 132+00
24C North Bound Matterhorn Blvd. @ Sta. 138+00

SUMMIT ENGINEERING CORPORATION

SUMMIT ENGINEERING CORPORATION
An AASHTO Accredited Testing Facility

RELATIVE COMPACTION ASPHALTIC CONCRETE CORE SAMPLES (ASTM D-2041, D-2726)

Project Name	MATTERHORN BLVD.	**Date**	10-19-15
Project Number	30096	**Lab No.**	1535
Location	See below	**Tested By**	KH

Lot Number	25	25	25	26	26	26
Sample Number	A	B	C	A	B	C
Thickness (in.) **Total**	3.067	3.167	3.555	3.291	3.130	3.212
Lift Top						
Lift Bottom						
Specific Gravity	2.365	2.329	2.285	2.349	2.346	2.310
Average Rice Specific Gravity	2.466	2.466	2.466	2.448	2.448	2.448
% Compaction (Rice)	95.9	94.4	92.7	96.0	95.8	94.4
Average Marshall Unit Weight (PCF)	147.97	147.97	147.97	147.58	147.58	147.58
% Compaction (Marshall)	99.5	98.0	96.1	99.1	98.9	97.4

Lot 25 Average % Rice Compaction = 94.3 **% Marshall Compaction = 97.9**
Lot 26 Average % Rice Compaction = 95.4 **% Marshall Compaction = 98.5**

25A North Bound Matterhorn Blvd. @ Sta. 104+00
25B North Bound Matterhorn Blvd. @ Sta. 108+00
25C North Bound Matterhorn Blvd. @ Sta. 118+00

26A South Bound Matterhorn Blvd. @ Sta. 128+00
26B South Bound Matterhorn Blvd. @ Sta. 134+00
26C South Bound Matterhorn Blvd. @ Sta. 138+00

SUMMIT ENGINEERING CORPORATION

SUMMIT ENGINEERING CORPORATION
An AASHTO Accredited Testing Facility

RELATIVE COMPACTION ASPHALTIC CONCRETE CORE SAMPLES (ASTM D-2041, D-2726)

Project Name	MATTERHORN BLVD.	**Date**	10-19-15
Project Number	30096	**Lab No.**	1535
Location	See below	**Tested By**	KH

Lot Number	27	27	27			
Sample Number	A	B	C			
Thickness (in.) **Total**	3.110	3.430	3.185			
Lift Top						
Lift Bottom						
Specific Gravity	2.335	2.310	2.360			
Average Rice Specific Gravity	2.462	2.462	2.462			
% Compaction (Rice)	94.8	93.8	95.9			
Average Marshall Unit Weight (PCF)	147.17	147.17	147.17			
% Compaction (Marshall)	98.8	97.7	99.8			

Lot 27 Average % Rice Compaction = 94.8 **% Marshall Compaction = 98.8**

27A South Bound Matterhorn Blvd. @ Sta. 108+00
27B South Bound Matterhorn Blvd. @ Sta. 114+00
27C South Bound Matterhorn Blvd. @ Sta. 118+00

SUMMIT ENGINEERING CORPORATION

SUMMIT ENGINEERING CORPORATION
An AASHTO Accredited Testing Facility

RELATIVE COMPACTION ASPHALTIC CONCRETE CORE SAMPLES (ASTM D-2041, D-2726)

Project Name	MATTERHORN BLVD.	**Date**	10-19-15
Project Number	30096	**Lab No.**	1535
Location	See below	**Tested By**	KH

Lot Number	27	27	26	26	27	23
Sample Number	JC1	JC2	JC3	JC4	JC5	JC6
Thickness (in.) Total	2.892	2.930	3.108	3.330	2.934	3.240
Lift Top						
Lift Bottom						
Specific Gravity	2.249	2.214	2.206	2.283	2.204	2.232
Average Rice Specific Gravity	2.462	2.462	2.448	2.448	2.462	2.472
% Compaction (Rice)	91.3	89.9	90.1	93.3	89.5	90.3
Average Marshall Unit Weight (PCF)	147.17	147.17	147.58	147.58	147.17	146.07
% Compaction (Marshall)	95.1	93.6	93.0	96.3	93.2	99.0

JC1: % Voids = 8.7
JC2: % Voids = 10.1
JC3: % Voids = 9.9
JC4: % Voids = 6.7
JC5: % Voids = 10.5
JC6: % Voids = 9.7

LOCATIONS:

JC1 South Bound Matterhorn Blvd. @ Sta. 108+00
JC2 South Bound Matterhorn Blvd. @ Sta. 118+00
JC3 South Bound Matterhorn Blvd. @ Sta. 128+00
JC4 South Bound Matterhorn Blvd. @ Sta. 138+00
JC5 South Bound Matterhorn Blvd. @ Sta. 148+00
JC6 North Bound Matterhorn Blvd. @ Sta. 158+00

SUMMIT ENGINEERING CORPORATION

SUMMIT ENGINEERING CORPORATION
An AASHTO Accredited Testing Facility

RELATIVE COMPACTION ASPHALTIC CONCRETE CORE SAMPLES (ASTM D-2041, D-2726)

Project Name	MATTERHORN BLVD.	**Date**	10-19-15
Project Number	30096	**Lab No.**	1535
Location	See below	**Tested By**	KH

Lot Number	22	22	21	18	16	16
Sample Number	JC7	JC8	JC9	JC10	JC11	JC12
Thickness (in.) Total	2.996	3.084	3.270	2.745	3.105	2.929
Lift Top						
Lift Bottom						
Specific Gravity	2.236	2.251	2.271	2.337	2.265	2.292
Average Rice Specific Gravity	2.451	2.451	2.441	2.453	2.445	2.445
% Compaction (Rice)	91.2	91.8	93.0	95.3	92.6	93.7
Average Marshall Unit Weight (PCF)	146.33	146.33	146.51	146.39	147.83	147.83
% Compaction (Marshall)	95.1	95.7	96.5	99.4	95.4	96.5

JC7: % Voids = 8.8
JC8: % Voids = 8.2
JC9: % Voids = 7.0
JC10: % Voids = 4.7
JC11: % Voids = 7.4
JC12: % Voids = 6.3

LOCATIONS:

JC7	North Bound Matterhorn Blvd. @ Sta. 168+00
JC8	North Bound Matterhorn Blvd. @ Sta. 178+00
JC9	North Bound Matterhorn Blvd. @ Sta. 188+00
JC10	South Bound Matterhorn Blvd. @ Sta. 198+00
JC11	North Bound Matterhorn Blvd. @ Sta. 208+00
JC12	North Bound Matterhorn Blvd. @ Sta. 218+00

SUMMIT ENGINEERING CORPORATION

SUMMIT ENGINEERING CORPORATION
An AASHTO Accredited Testing Facility

RELATIVE COMPACTION ASPHALTIC CONCRETE CORE SAMPLES (ASTM D-2041, D-2726)

Project Name	MATTERHORN BLVD.	**Date**	10-19-15
Project Number	30096	**Lab No.**	1535
Location	See below	**Tested By**	KH

Lot Number	15	15	15	12	12	12
Sample Number	JC13	JC14	JC15	JC16	JC17	JC18
Thickness (in.) Total	2.870	2.886	2.905	2.844	2.905	2.253
Lift Top						
Lift Bottom						
Specific Gravity	2.213	2.258	2.327	2.301	2.311	2.334
Average Rice Specific Gravity	2.449	2.449	2.449	2.465	2.465	2.465
% Compaction (Rice)	90.4	92.2	95.0	93.3	93.8	94.7
Average Marshall Unit Weight (PCF)	147.10	147.10	147.10	146.91	146.91	146.91
% Compaction (Marshall)	93.6	95.5	98.5	97.5	94.9	98.9

JC13: % Voids = 9.6
JC14: % Voids = 7.8
JC15: % Voids = 5.0
JC16: % Voids = 6.7
JC17: % Voids = 6.2
JC18: % Voids = 5.3

LOCATIONS:

JC13 North Bound Matterhorn Blvd. @ Sta. 228+00
JC14 North Bound Matterhorn Blvd. @ Sta. 238+00
JC15 North Bound Matterhorn Blvd. @ Sta. 248+00
JC16 North Bound Matterhorn Blvd. @ Sta. 258+00
JC17 North Bound Matterhorn Blvd. @ Sta. 268+00
JC18 North Bound Matterhorn Blvd. @ Sta. 278+00

SUMMIT ENGINEERING CORPORATION

SUMMIT ENGINEERING CORPORATION
An AASHTO Accredited Testing Facility

RELATIVE COMPACTION ASPHALTIC CONCRETE CORE SAMPLES (ASTM D-2041, D-2726)

Project Name	MATTERHORN BLVD.	**Date**	10-19-15
Project Number	30096	**Lab No.**	1535
Location	See below	**Tested By**	KH

Lot Number	11	11	8	8	7	7
Sample Number	JC19	JC20	JC21	JC22	JC23	JC24
Thickness (in.) Total	3.130	2.089	3.133	2.895	2.712	2.712
Lift Top						
Lift Bottom						
Specific Gravity	2.260	2.288	2.306	2.330	2.323	2.331
Average Rice Specific Gravity	2.455	2.455	2.465	2.465	2.467	2.467
% Compaction (Rice)	92.1	93.2	93.5	94.5	94.2	94.5
Average Marshall Unit Weight (PCF)	146.36	146.36	145.95	145.95	146.54	146.54
% Compaction (Marshall)	96.1	97.3	98.3	99.4	98.7	99.0

JC19: % Voids = 7.9
JC20: % Voids = 6.8
JC21: % Voids = 6.5
JC22: % Voids = 5.5
JC23: % Voids = 5.8
JC24: % Voids = 5.5

LOCATIONS:

JC19 North Bound Matterhorn Blvd. @ Sta. 288+00
JC20 North Bound Matterhorn Blvd. @ Sta. 298+00
JC21 North Bound Matterhorn Blvd. @ Sta. 308+00
JC22 North Bound Matterhorn Blvd. @ Sta. 318+00
JC23 North Bound Matterhorn Blvd. @ Sta. 328+00
JC24 North Bound Matterhorn Blvd. @ Sta. 338+00

SUMMIT ENGINEERING CORPORATION

SUMMIT ENGINEERING CORPORATION
An AASHTO Accredited Testing Facility

RELATIVE COMPACTION ASPHALTIC CONCRETE CORE SAMPLES (ASTM D-2041, D-2726)

Project Name	MATTERHORN BLVD.	**Date**	10-19-15
Project Number	30096	**Lab No.**	1535
Location	See below	**Tested By**	KH

Lot Number	4	3	2	2	1	
Sample Number	JC25	JC26	JC27	JC28	JC29	
Thickness (in.) **Total**	3.150	2.270	3.150	2.940	3.375	
Lift Top						
Lift Bottom						
Specific Gravity	2.302	2.287	2.314	2.319	2.327	
Average Rice Specific Gravity	2.476	2.484	2.469	2.469	2.475	
% Compaction (Rice)	93.0	92.1	93.8	93.9	94.0	
Average Marshall Unit Weight (PCF)	145.16	145.89	144.73	144.73	145.16	
% Compaction (Marshall)	98.7	97.6	99.5	99.7	99.8	

JC25: % Voids = 7.0
JC26: % Voids = 7.9
JC27: % Voids = 6.3
JC28: % Voids = 6.1
JC29: % Voids = 6.0

LOCATIONS:

JC25 North Bound Matterhorn Blvd. @ Sta. 348+00
JC26 North Bound Matterhorn Blvd. @ Sta. 358+00
JC27 North Bound Matterhorn Blvd. @ Sta. 368+00
JC28 North Bound Matterhorn Blvd. @ Sta. 378+00
JC29 West Bound Matterhorn Blvd. @ Sta. 388+00

SUMMIT ENGINEERING CORPORATION

SECTION 4:

Asphaltic Concrete Core Thickness

SUMMIT ENGINEERING CORPORATION
Engineering The West Since 1978.
5405 Mae Anne Ave.
Reno, Nevada 89523
Phone (775)747-8550 Fax (775) 747-8559

Asphaltic Concrete Core Thickness

JOB NAME: Matterhorn Blvd. LAB NO.: 1534

JOB NUMBER: 30096 TESTED BY: KH DATE: 9/15/2015

LOT NUMBER	CORE A THICKNESS (IN)	CORE B THICKNESS (IN)	CORE C THICKNESS (IN)	JOINT CORE THICKNESS (1)		JOINT CORE THICKNESS (2)		JOINT CORE THICKNESS (3)		AVERAGE LOT THICKNESS (IN.)	
LOT 1	3.179	3.222	3.405	JC29	3.375					3.3	*
LOT 2	3.492	3.467	3.033	JC28	2.940	JC27	3.150			3.2	*
LOT 3	3.245	3.560	3.684	JC 26	3.270					3.4	
LOT 4	3.149	3.140	3.400	JC25	3.150					3.2	*
LOT 5	3.421	3.540	3.890							3.6	
LOT 6	3.293	3.508	3.432							3.4	
LOT 7	2.915	3.078	3.131	JC23	2.922	JC24	2.712			3.0	
LOT 8	3.266	3.336	3.283	JC21	3.133	JC22	2.895			3.2	
LOT 9	2.849	3.159	2.400							2.8	*
LOT 10	3.174	2.828	3.258							3.1	
LOT 11	3.235	3.143	3.269	JC20	3.089	JC19	3.130			3.2	
LOT 12	3.620	3.021	3.089	JC17	2.905	JC18	3.253	JC16	2.844	3.1	
LOT 13	3.520	3.174	3.135							3.3	
LOT 14	3.220	3.197	3.208							3.2	
LOT 15	3.174	3.800	3.954	JC14	2.886	JC15	2.905	JC13	2.87	3.3	
LOT 16	2.800	3.829	3.064	JC11	3.105	JC12	2.929			3.1	
LOT 17	3.135	3.222	3.355							3.2	
LOT 18	3.010	2.865	3.058	JC10	2.745					2.9	
LOT 19	3.277	3.297	3.150							3.2	
LOT 20	3.240	3.507	3.384							3.4	
LOT 21	3.220	3.070	3.389	JC9	3.270					3.2	
LOT 22	3.326	3.245	3.333	JC7	2.996	JC8	3.084			3.2	
LOT 23	3.177	3.274	3.312	JC6	3.24					3.3	
LOT 24	3.470	2.993	3.272							3.2	
LOT 25	3.067	3.167	3.355							3.2	
LOT 26	3.291	3.130	3.212	JC3	3.108	JC4	3.330			3.2	
LOT 27	3.110	3.430	3.185	JC1	2.892	JC2	2.930	JC5	2.934	3.1	

***Did not meet the required thickness. Mitigation will be required.**

SUMMIT ENGINEERING CORPORATION
Engineering The West Since 1978.

5405 Mae Anne Ave.
Reno, Nevada 89523
Phone (775)747-8550 Fax (775) 747-8559

Additional Asphaltic Concrete Core Thickness

JOB NAME: Matterhorn Blvd. LAB NO.: 1534

JOB NUMBER: 30096 TESTED BY: KH

DATE: 9/15/2015

CORE ID	CORE THICKNESS (IN)	REQUIRED THICKNESS (IN)
1V	3.4	3.5
1W	3.4	3.5
1X	3.5	3.5
1Y	3.3	3.5
1Z	3.4	3.5
2V	3.7	3.5
2W	3.8	3.5
2X	3.5	3.5
2Y	3.5	3.5
2Z	3.3	3.5
4V	3.4	3.5
4W	3.4	3.5
4X	3.6	3.5
4Y	3.6	3.5
4Z	3.6	3.5
9V	3.2	3.0
9W	3.1	3.0
9X	3.1	3.0
9Y	3.3	3.0
9Z	3.1	3.0

SUMMIT ENGINEERING CORPORATION

SECTION 5:

Longitudinal Joint – Data/Calculation Sheets

MATTERHORN BLVD. IMPROVEMENT PROJECT
Longitudinal Joint - Data/Calculation Sheet

Joint ID	Lot #	Joint Type (Hot/ Cold)	Nuclear Gauge Test			Mean Joint Density (MJD)		Core Location	Core Marshall Density (lb/cu.ft.)	In-Place Air Voids (%)	Individ. Factor F_I (%)
			Station	Left (L)	Right(R)	MJD-L	MJD-R				
			104+00	139.5	144.8						
			106+00	139.3	144.3						
JC-1	27	HOT	108+00	142.6	148.3	140.4	145.4	108+00 (L)	140.0	9%	0%
			110+00	139.8	142.8						
			112+00	141.0	147.0						
			114+00	140.8	150.6						
			116+00	142.8	150.4						
JC-2	27	HOT	118+00	138.4	150.4	140.6	150.3	118+00 (L)	137.8	10%	0%
			120+00	140.7	151.1						
			122+00	140.2	148.9						
			124+00	141.0	145.6						
			126+00	144.7	146.3						
JC-3	26	HOT	128+00	138.3	147.2	140.6	147.0	128+00 (L)	137.3	10%	0%
			130+00	137.7	146.6						
			132+00	141.3	149.3						
			134+00	139.3	145.5						
			136+00	140.6	148.8						
JC-4	26	HOT	138+00	138.6	148.0	138.9	147.9	138+00 (L)	142.1	7%	5%
			140+00	142.4	147.3						
			142+00	133.5	149.8						
			144+00	147.9	141.4						
			146+00	144.8	127.4						
JC-5	27	HOT	148+00	143.5	136.5	144.1	134.7	148+00 (R)	137.2	11%	-5%
			150+00	142.7	134.0						
			152+00	141.7	134.3						
			154+00	142.7	139.6						
			156+00	148.8	132.4						
JC-6	23	HOT	158+00	149.5	137.7	146.9	137.8	158+00 (R)	138.9	10%	5%
			160+00	144.9	140.6						
			162+00	148.4	138.5						
			164+00	145.7	135.2						
			166+00	141.8	136.6						
JC-7	22	HOT	168+00	147.4	38.6	144.8	117.2	168+00 (R)	139.2	9%	0%
			170+00	141.6	137.5						
			172+00	147.4	138.3						
			174+00	145.7	135.4						
			176+00	145.4	137.7						
JC-8	22	HOT	178+00	148.4	138.0	145.8	137.4	178+00 (R)	140.1	8%	0%
			180+00	147.6	138.8						
			182+00	142.0	137.1						
			184+00	145.2	139.1						
			186+00	143.8	138.3						
JC-9	21	HOT	188+00	143.8	137.7	144.0	138.4	188+00 (R)	141.3	7%	5%
			190+00	143.1	137.7						
			192+00	144.1	139.1						

J:\WPDATA\LAB\30095 - Matterhorn Road\Asphalt Results\SUMMARIES\30095 Matterhorn Blvd. - Longitudinal Joint Bond Sheet.xls Prepared : 09/11/08, 1/4

MATTERHORN BLVD. IMPROVEMENT PROJECT
Longitudinal Joint - Data/Calculation Sheet

Joint ID	Lot #	Joint Type (Hot/ Cold)	Nuclear Gauge Test			Mean Joint Density (MJD)		Core Location	Core Marshall Density (lb/cu.ft.)	In-Place Air Voids (%)	Individ. Factor F_i (%)
			Station	Left (L)	Right(R)	MJD-L	MJD-R				
			194+00	142.1	137.7						
			196+00	143.4	139.2						
JC-10	18	HOT	198+00	136.6	147.4	142.3	141.5	198+00 (R)	145.5	5%	5%
			200+00	144.2	138.3						
			202+00	145.4	144.7						
			204+00	144.4	140.1						
			206+00	143.5	138.6						
JC-11	16	HOT	208+00	145.6	140.5	145.2	139.5	208+00 (R)	141.0	7%	5%
			210+00	148.2	140.9						
			212+00	144.4	137.5						
			214+00	146.3	141.2						
			216+00	142.7	139.8						
JC-12	16	HOT	218+00	144.0	143.1	144.3	141.2	218+00 (R)	142.7	6%	5%
			220+00	143.2	141.4						
			222+00	145.5	140.3						
			224+00	143.3	138.2						
			226+00	140.6	139.6						
JC-13	15	HOT	228+00	142.8	136.6	142.8	138.5	228+00 (R)	137.70	10%	0%
			230+00	143.7	138.2						
			232+00	143.7	140.1						
			234+00	144.6	141.0						
			236+00	145.4	139.3						
JC-14	15	HOT	238+00	145.7	139.4	145.7	139.4	238+00 (R)	140.50	8%	0%
			240+00	146.7	139.8						
			242+00	146.1	137.5						
			244+00	145.9	138.2						
			246+00	146.8	138.3						
JC-15	15	HOT	248+00	141.6	143.2	145.0	141.1	248+00 (R)	144.80	5%	5%
			250+00	146.0	141.6						
			252+00	144.8	144.0						
			254+00	145.3	139.6						
			256+00	146.8	141.6						
JC-16	12	HOT	258+00	146.4	139.6	144.9	141.2	258+00 (R)	143.20	7%	5%
			260+00	143.8	142.8						
			262+00	142.4	142.3						
			264+00	143.7	138.3						
			266+00	146.6	140.8						
JC-17	12	HOT	268+00	145.5	138.8	145.4	140.2	268+00 (R)	143.80	6%	5%
			270+00	145.7	140.1						
			272+00	145.3	142.8						
			274+00	147.0	139.0						
			276+00	142.5	143.3						
JC-18	12	HOT	278+00	143.9	145.5	144.2	141.5	278+00 (R)	145.30	5%	5%
			280+00	146.8	139.8						
			282+00	140.7	139.9						

MATTERHORN BLVD. IMPROVEMENT PROJECT
Longitudinal Joint - Data/Calculation Sheet

Joint ID	Lot #	Joint Type (Hot/ Cold)	Nuclear Gauge Test			Mean Joint Density (MJD)		Core Location	Core Marshall Density (lb/cu.ft.)	In-Place Air Voids (%)	Individ. Factor F_i (%)
			Station	Left (L)	Right(R)	MJD-L	MJD-R				
			284+00	145.6	140.0						
			286+00	145.5	143.3						
JC-19	11	HOT	288+00	146.1	141.2	145.6	141.2	288+00 (R)	140.70	8%	0%
			290+00	142.8	137.8						
			292+00	147.9	143.7						
			294+00	144.4	141.7						
			296+00	141.3	140.6						
JC-20	11	HOT	298+00	144.0	142.0	144.4	141.0	298+00 (R)	142.40	7%	5%
			300+00	145.7	139.6						
			302+00	146.7	141.2						
			304+00	147.3	137.3						
			306+00	148.6	145.9						
JC-21	8	HOT	308+00	148.0	142.5	147.3	141.5	308+00 (R)	143.50	7%	5%
			310+00	145.9	138.3						
			312+00	146.7	143.7						
			314+00	147.7	138.8						
			316+00	148.3	140.7						
JC-22	8	HOT	318+00	147.4	143.6	147.9	142.8	318+00 (R)	145.95	6%	5%
			320+00	149.1	144.4						
			322+00	146.9	146.4						
			324+00	148.2	145.4						
			326+00	148.6	143.4						
JC-23	7	HOT	328+00	145.8	145.3	147.1	144.8	328+00 (R)	144.60	6%	5%
			330+00	149.6	145.6						
			332+00	143.1	144.2						
			334+00	140.7	137.3						
			336+00	147.8	142.6						
JC-24	7	HOT	338+00	149.8	141.9	145.1	142.2	338+00 (R)	145.10	6%	5%
			340+00	140.4	145.8						
			342+00	146.9	143.5						
			344+00	149.9	137.2	* Did not meet required AC thickness					
			346+00	148.8	139.5						
JC-25	4	HOT	348+00	149.8	141.8	148.4	140.8	348+00 (R)	143.30	7%	0%
			350+00	148.4	142.4						
			352+00	145.2	143.3						
			354+00	146.3	142.3						
			356+00	146.6	140.9						
JC-26	3	HOT	358+00	145.7	140.5	146.7	141.5	358+00 (R)	142.30	8%	0%
			360+00	148.7	140.4						
			362+00	146.4	143.4						
			364+00	146.2	139.1	* Did not meet required AC thickness					
			366+00	145.2	137.3						
JC-27	2	HOT	368+00	147.4	140.8	147.1	140.6	368+00 (R)	144.00	6%	0%
			370+00	149.2	144.0						
			372+00	147.6	142.0						

MATTERHORN BLVD. IMPROVEMENT PROJECT
Longitudinal Joint - Data/Calculation Sheet

Joint ID	Lot #	Joint Type (Hot/ Cold)	Nuclear Gauge Test			Mean Joint Density (MJD)		Core Location	Core Marshall Density (lb/cu.ft.)	In-Place Air Voids (%)	Individ. Factor F_i (%)
			Station	Left (L)	Right(R)	MJD-L	MJD-R				
			374+00	145.8	138.9	* Did not meet required AC thickness					
			376+00	148.8	140.7						
JC-28	2	HOT	378+00	146.7	139.5	146.1	140.0	378+00 (R)	144.30	6%	0%
			380+00	143.2	139.8						
			382+00	145.8	140.9						
			384+00	142.8	143.2	* Did not meet required AC thickness					
			386+00	142.1	143.4						
JC-29	1	HOT	388+00	143.6	144.0	143.7	143.9	388+00 (L)	144.80	6%	0%
			390+00	146.4	145.0						

Joints Passing		19
Joints Failing		1
Joints Not Qualified		4
Net Joints for Bonus		14
Total number of longitudinal joint segments, *N*		29
Project Bonus/Penalty Factor		48%
Unit Bid Price (Joint Bonus)		$ 37,610.10
Project Longitudinal Joints Bonus/Penalty		$ 18,156.55

APPENDIX B

OXIDATION KINETIC RESULTS

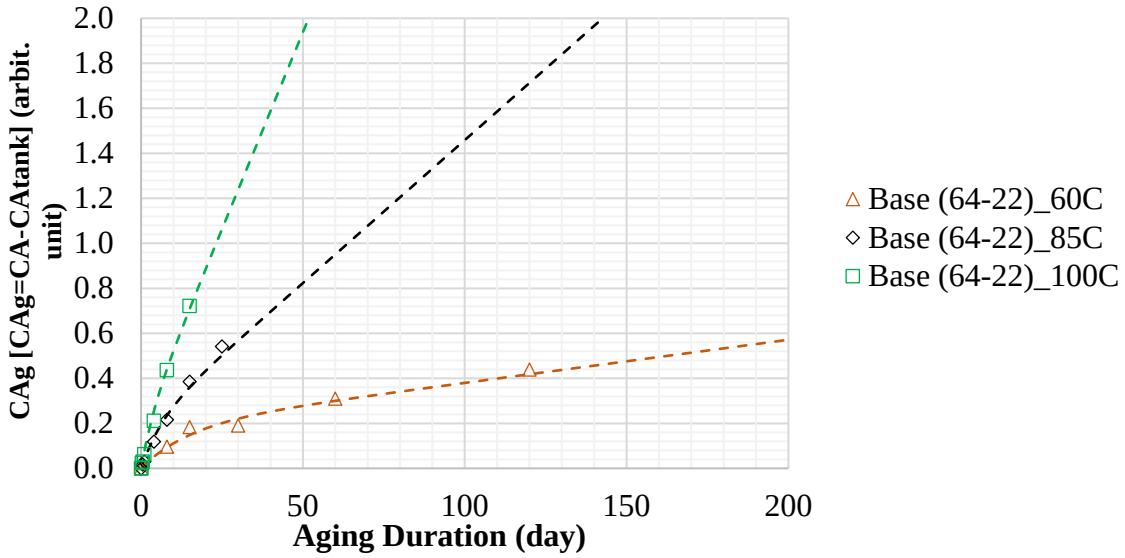

Figure 10. 1. Oxidation of Base 64-22 after 60, 85, and 100°C Oven Aging

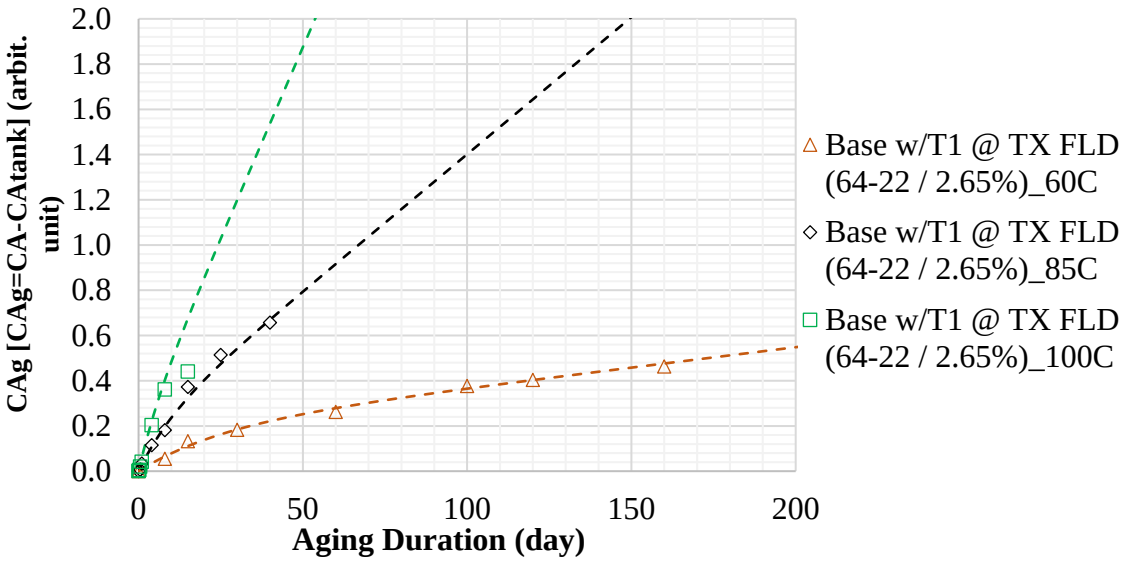

Figure 10. 2. Oxidation of Base 64-22 w/T1 @ TX FLD after 60, 85, and 100°C Oven Aging

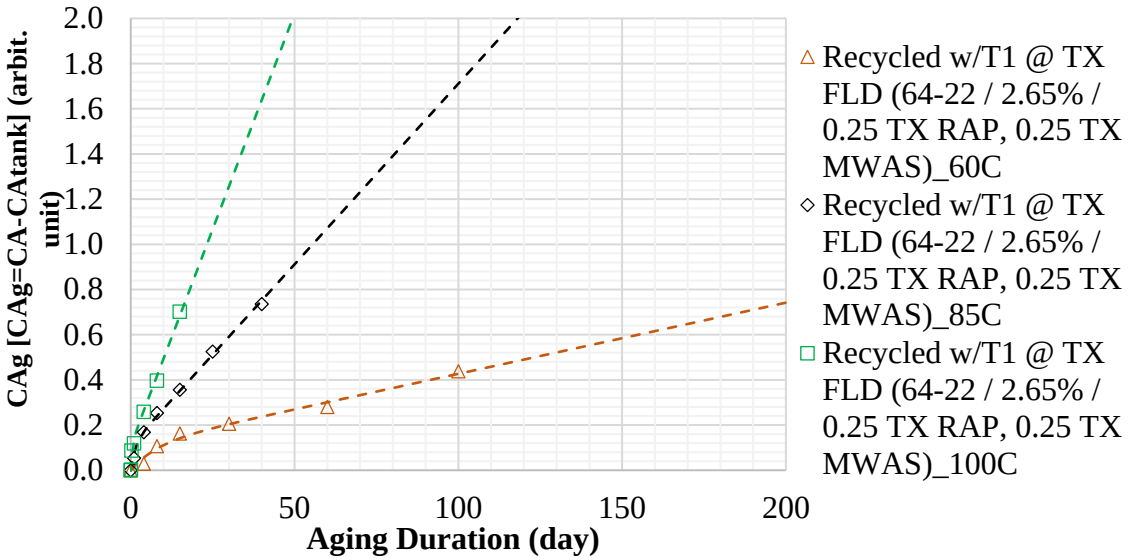

Figure 10. 3. Oxidation of Recycled w/T1 @ TX FLD (Base 64-22) after 60, 85, and 100°C Oven Aging

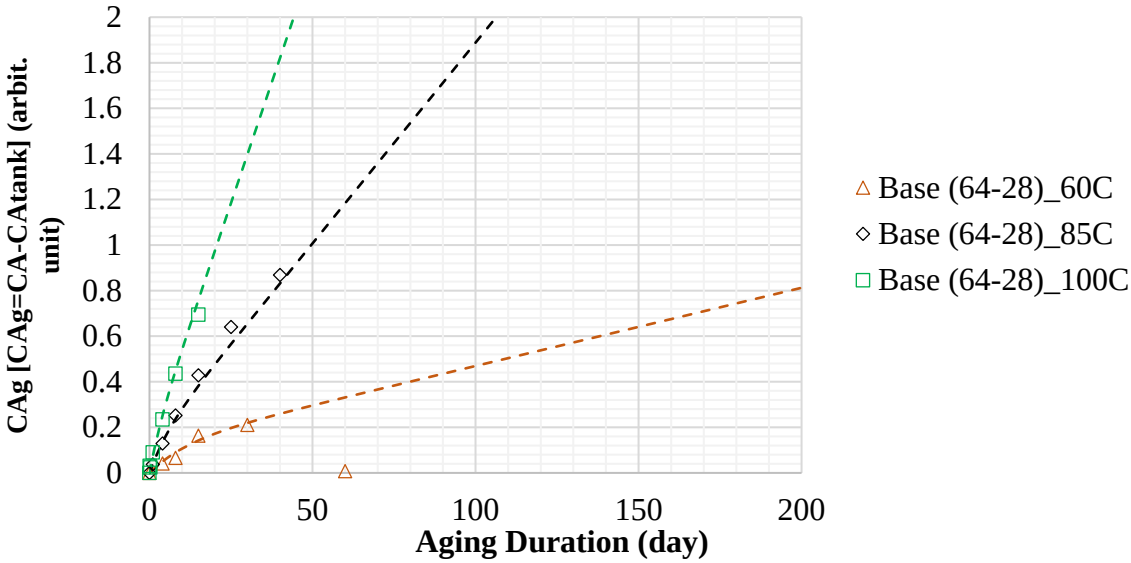

Figure 10. 4. Oxidation of Base 64-28 after 60, 85, and 100°C Oven Aging

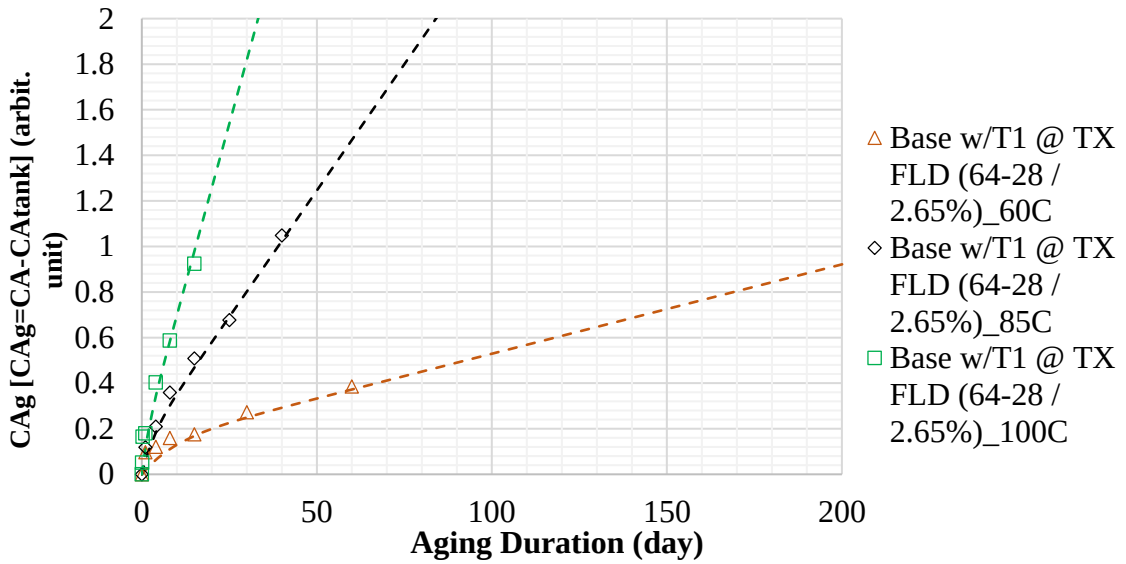

Figure 10. 5. Oxidation of Base 64-28 w/T1 @ TX FLD after 60, 85, and 100°C Oven Aging

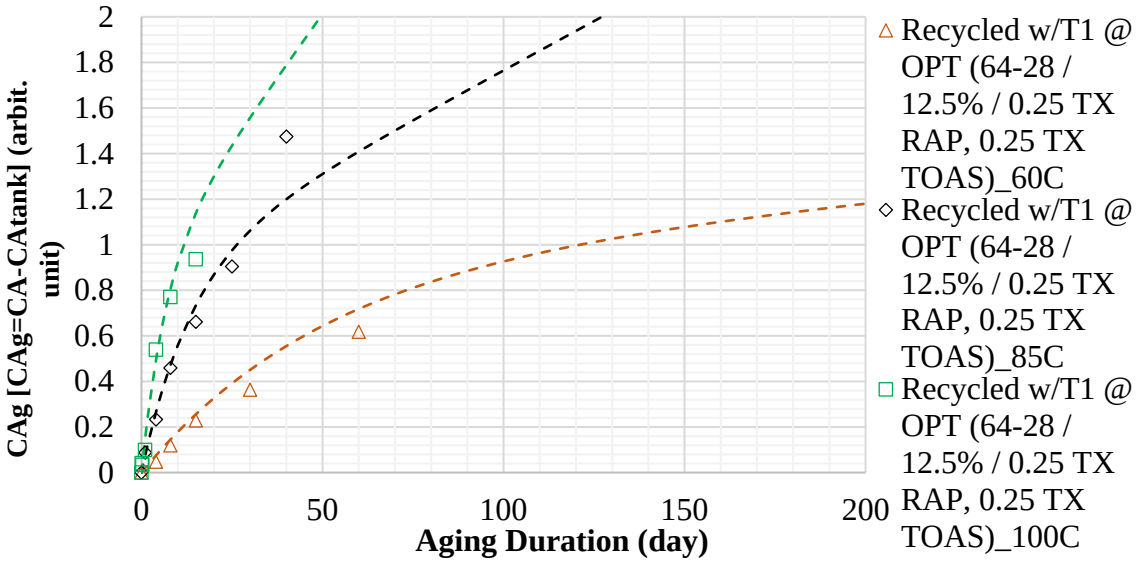

Figure 10. 6. Recycled w/T1 @ OPT (Base 64-28) after 60, 85, and 100°C Oven Aging

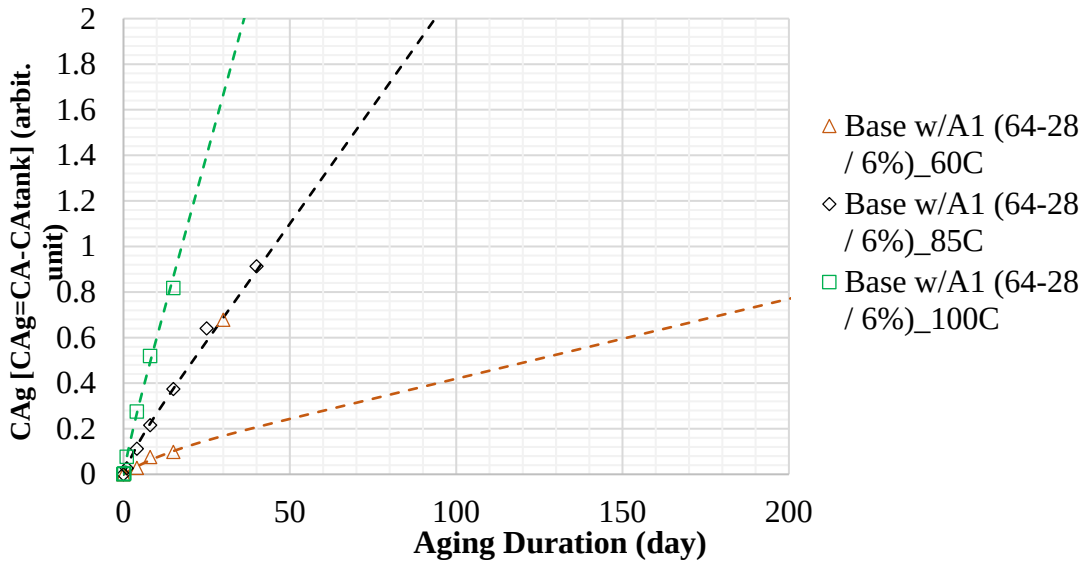

Figure 10. 7. Oxidation of Base 64-28 w/A1 @ OPT after 60, 85, and 100°C Oven Aging

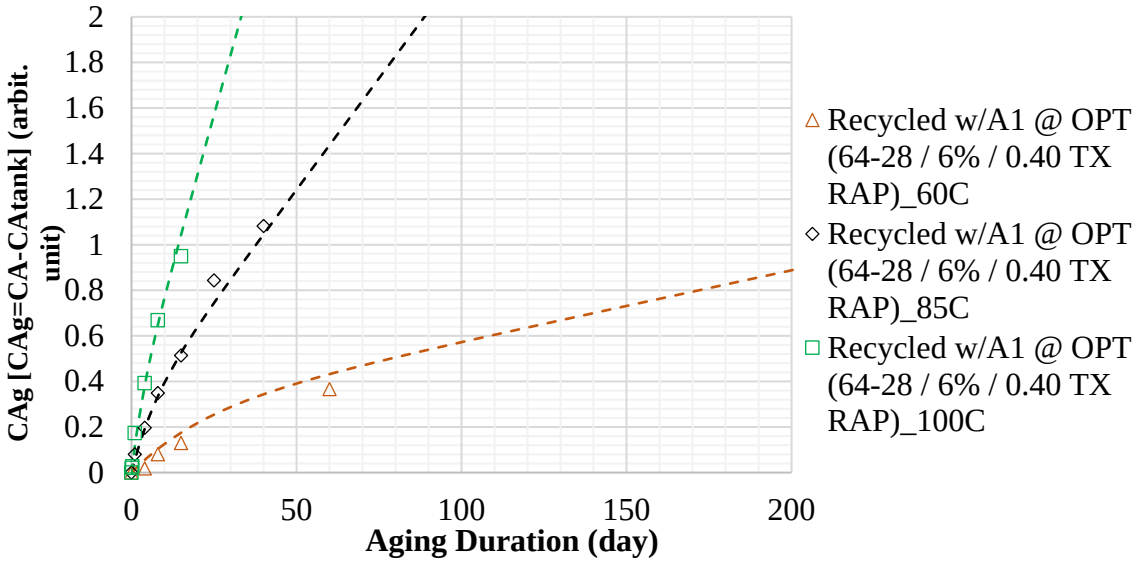

Figure 10. 8. Oxidation of Recycled w/A1 @ OPT (Base 64-28) after 60, 85, and 100°C Oven Aging

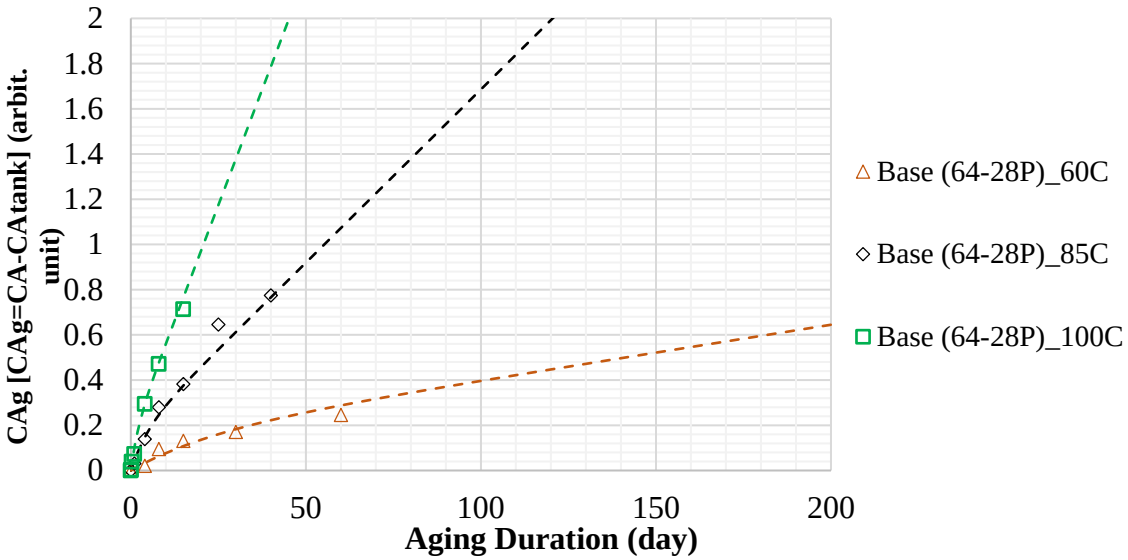

Figure 10. 9. Oxidation of Base 64-28P after 60, 85, and 100°C Oven Aging

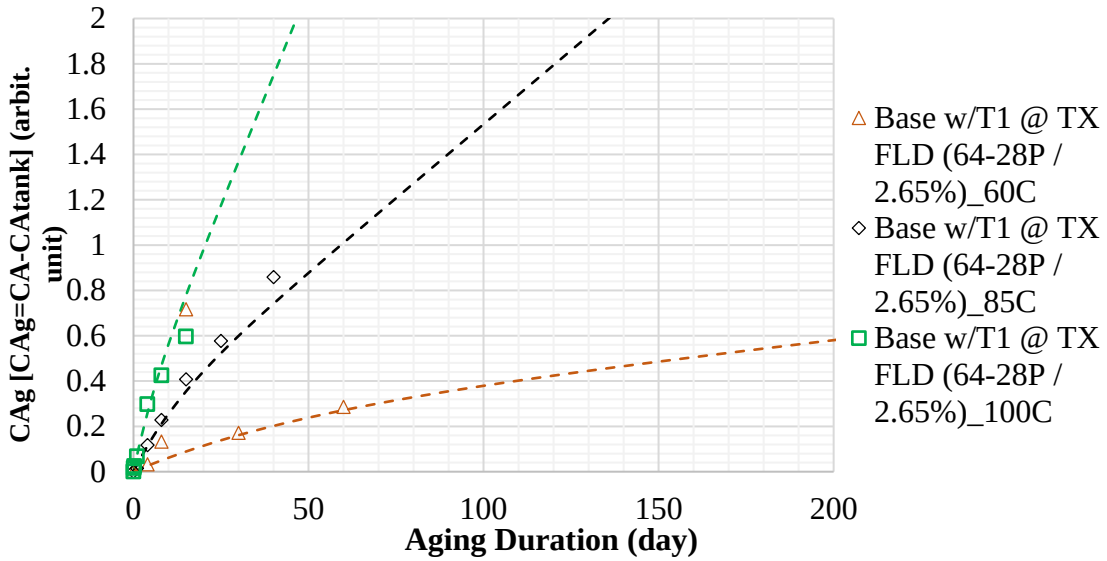

Figure 10. 10. Oxidation of Base 64-28P w/T1 @ TX FLD after 60, 85, and 100°C Oven Aging

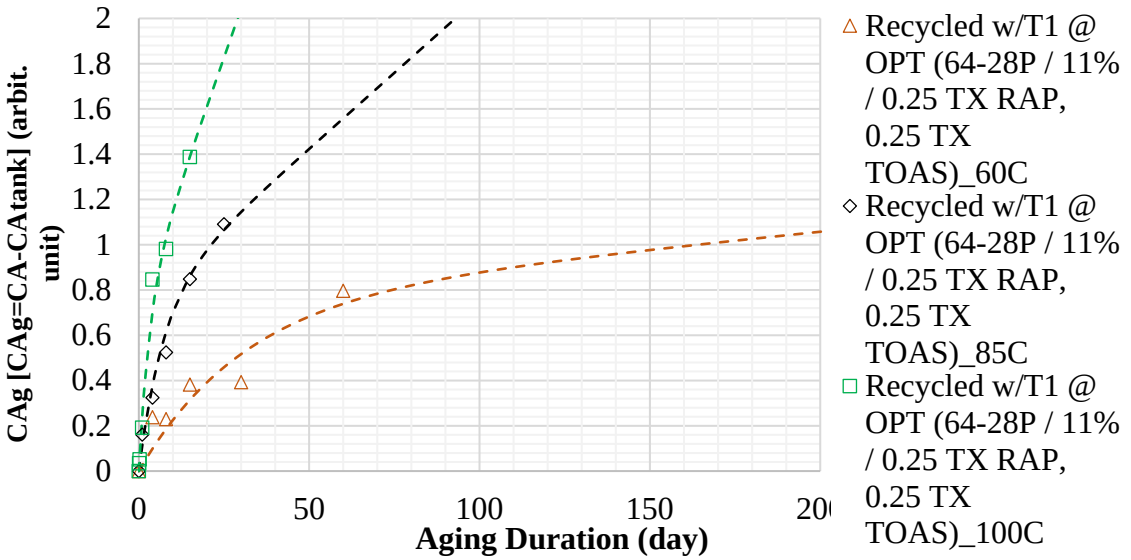

Figure 10. 11. Oxidation of Recycled w/T1 @ OPT (Base 64-28P) after 60, 85, and 100°C Oven Aging

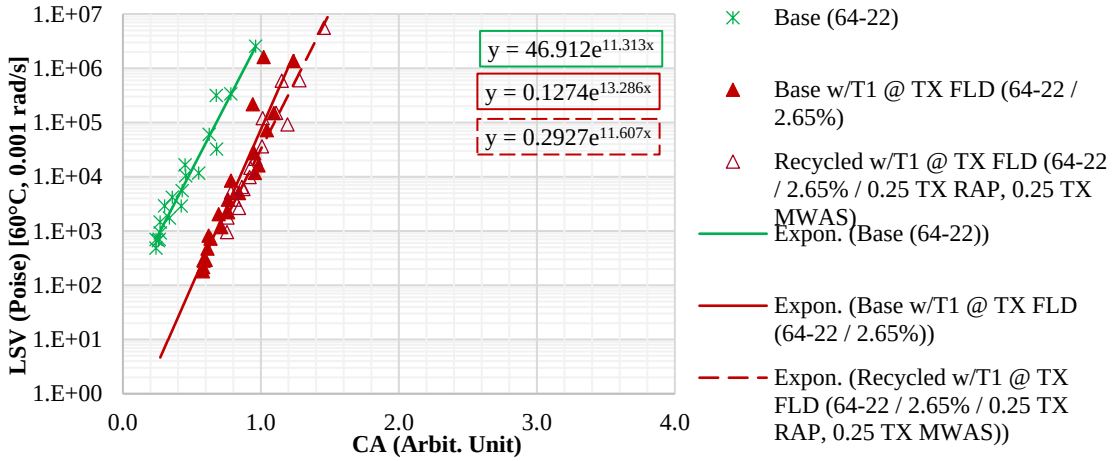

Figure 10. 12. Hardening Susceptibility – LSV at 60°C for PG 64-22 Base Binder

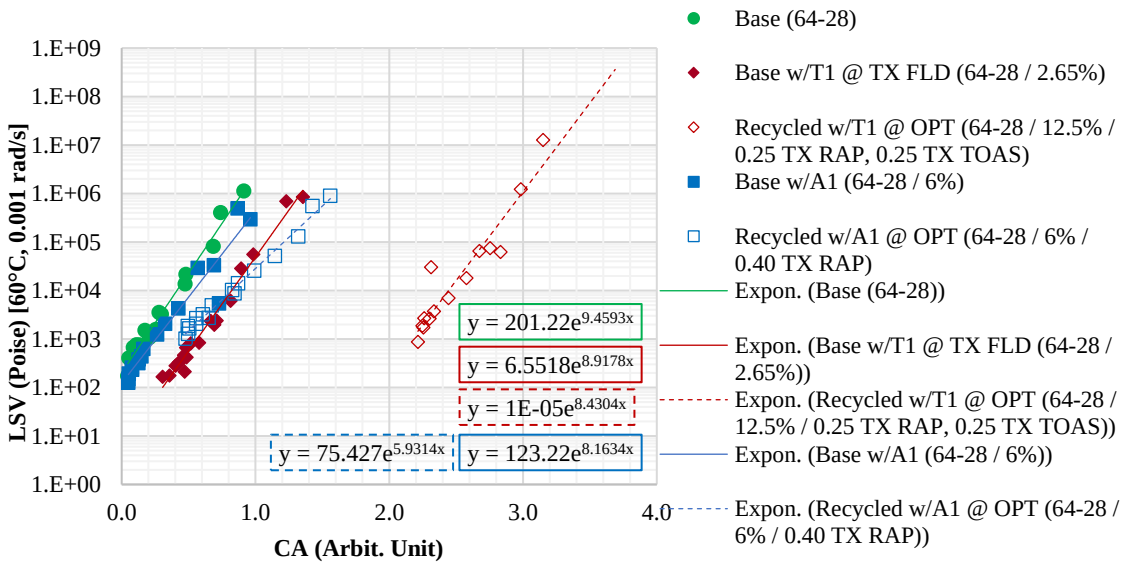

Figure 10. 13. Hardening Susceptibility – LSV at 60°C for PG 64-28 Base Binder

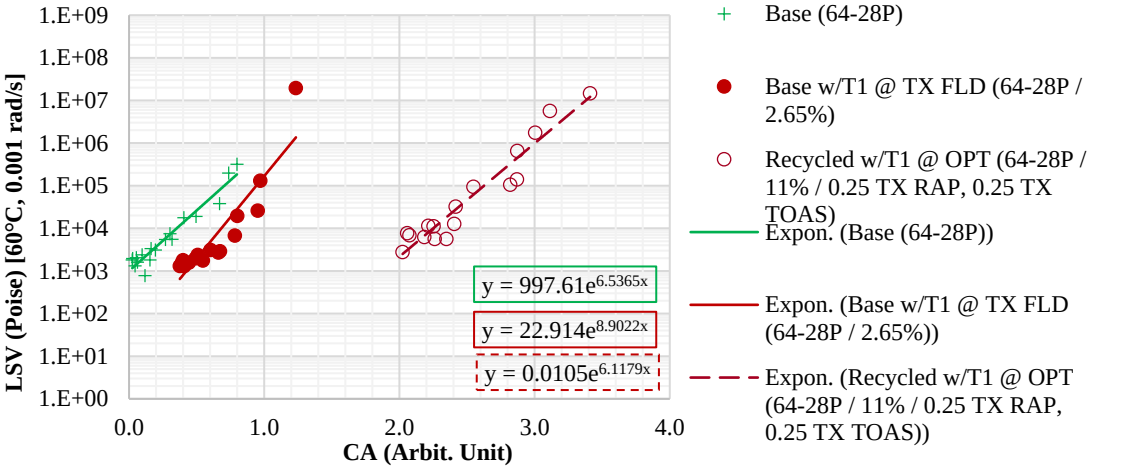

Figure 10. 14. Hardening Susceptibility – LSV at 60°C for PG 64-28P Base Binder

APPENDIX C

CA PREDICTION RESULTS

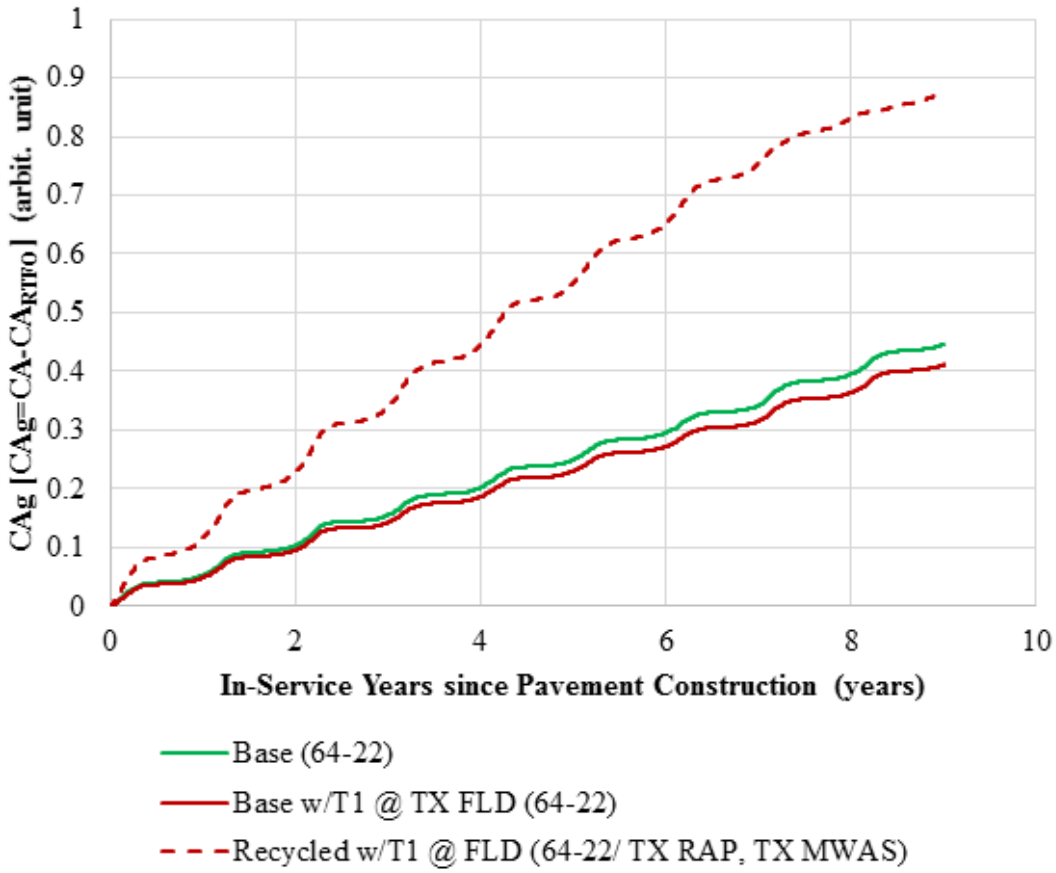

Figure 11. 1. Carbonyl Area Prediction in Asphalt Mixture Surface Layer for Base 64-22 Binder Blends in TX, Tyler

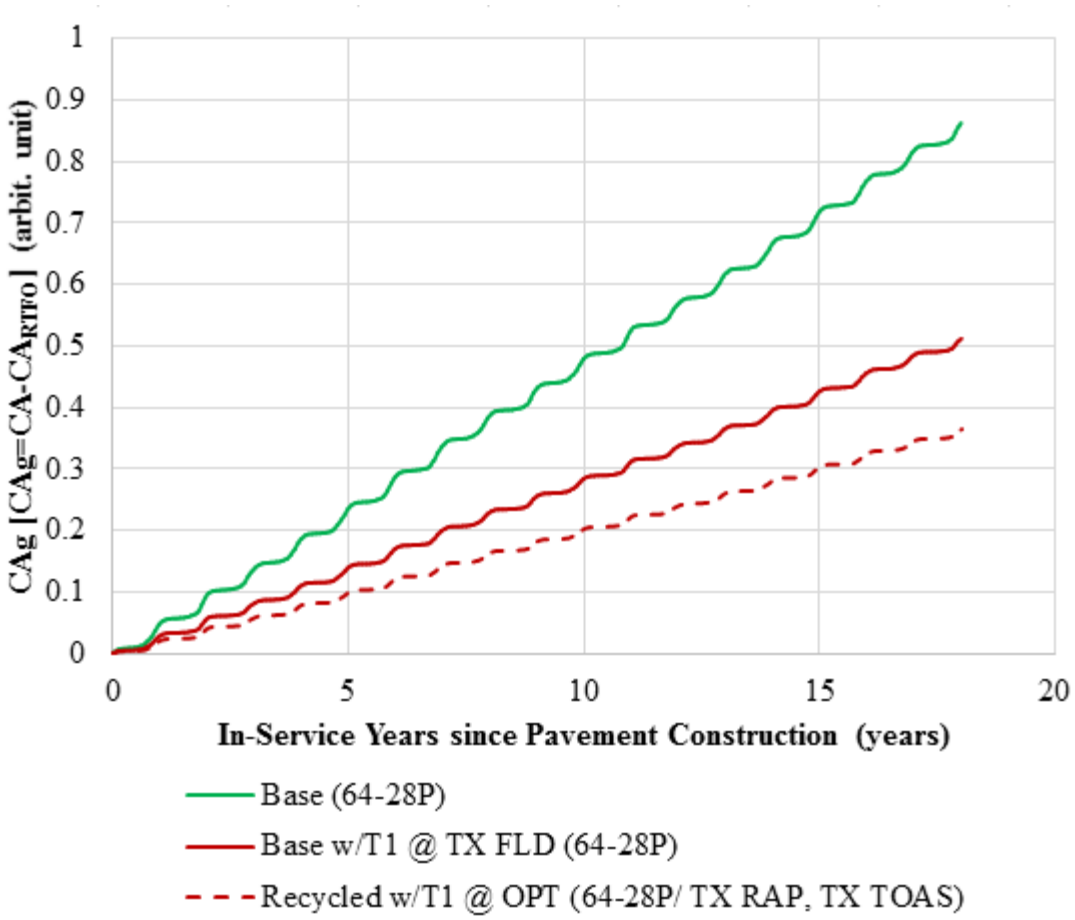

Figure 11. 2. Carbonyl Area Prediction in Asphalt Mixture Surface Layer for Base 64-28P Binder Blends in NV, Reno

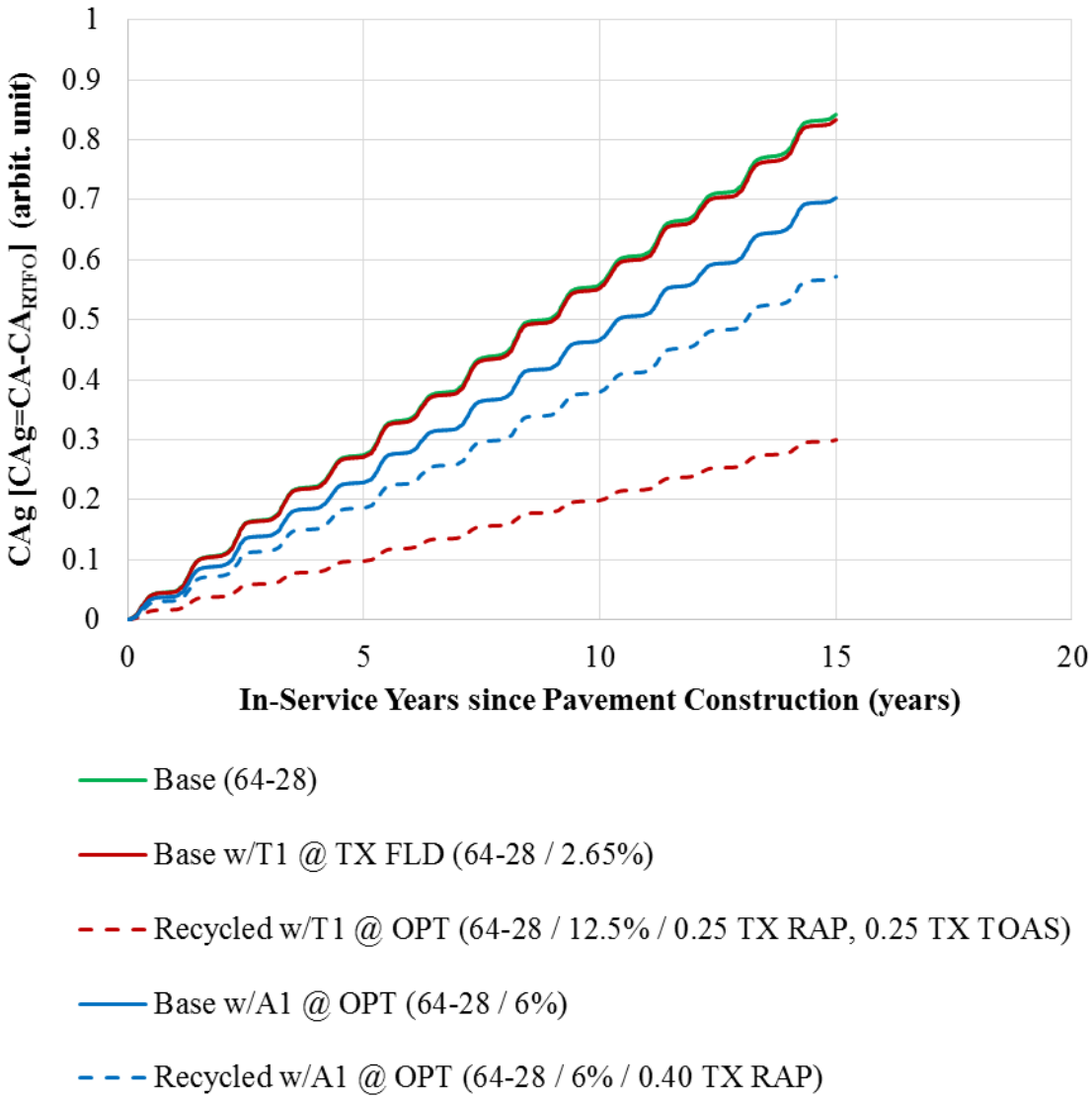

Figure 11. 3. Carbonyl Area Prediction in Asphalt Mixture Surface Layer for Base 64-28 Binder Blends in NH, Durham

APPENDIX D

STEP BY STEP PROCEDURE OF TEMPERATURE PROFILE PREDICTION USING TEMPS SOFTWARE

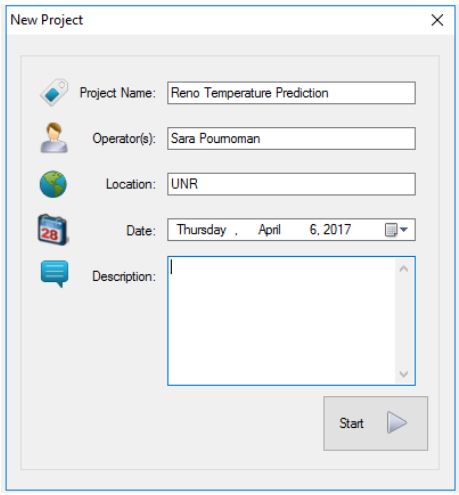

Figure 12. 1. Step (1) General Project Information

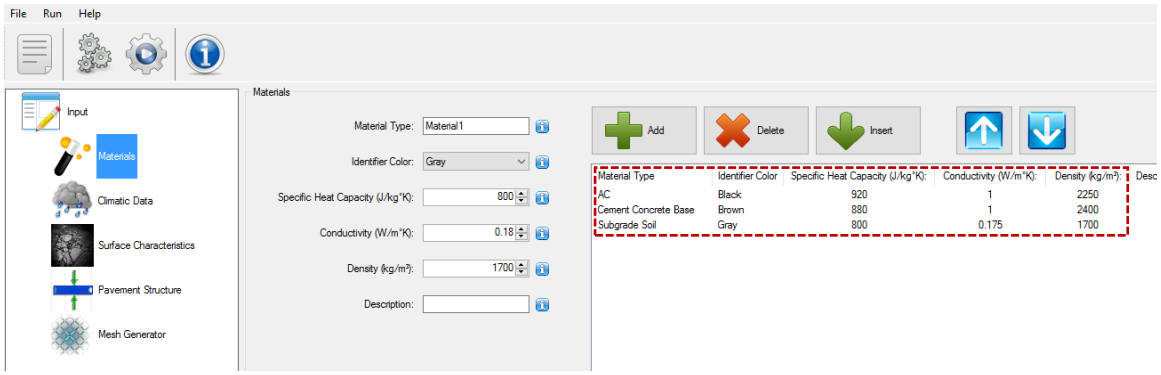

Figure 12. 2. Step (2) Material Properties Input

Figure 12. 3. Step (3) Historical Climatic Data Input

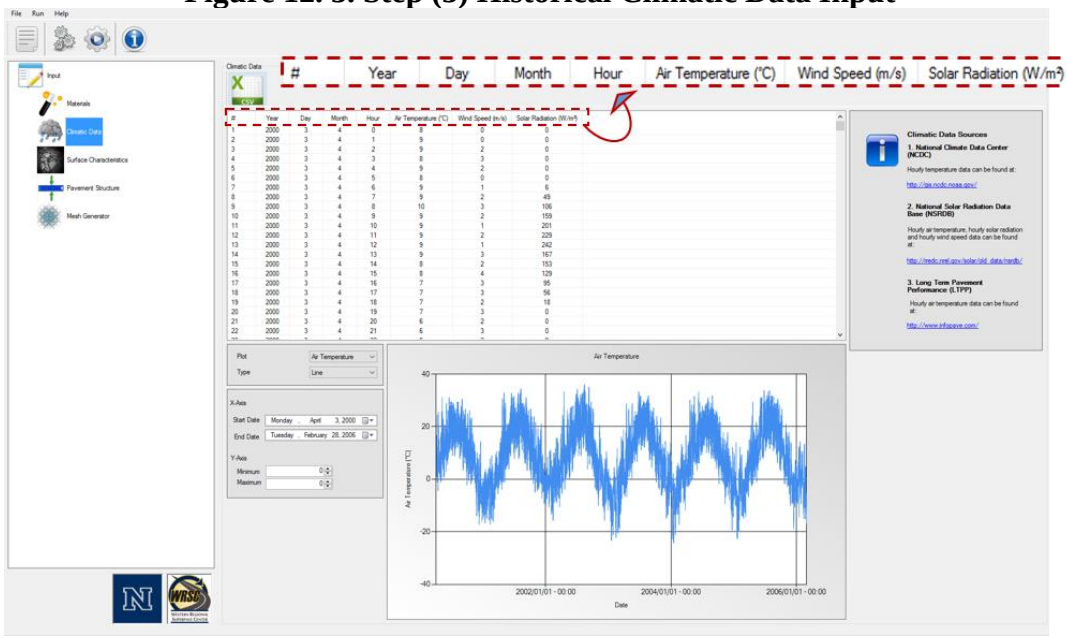

Figure 12. 4. Example of Historical Climatic Data Input

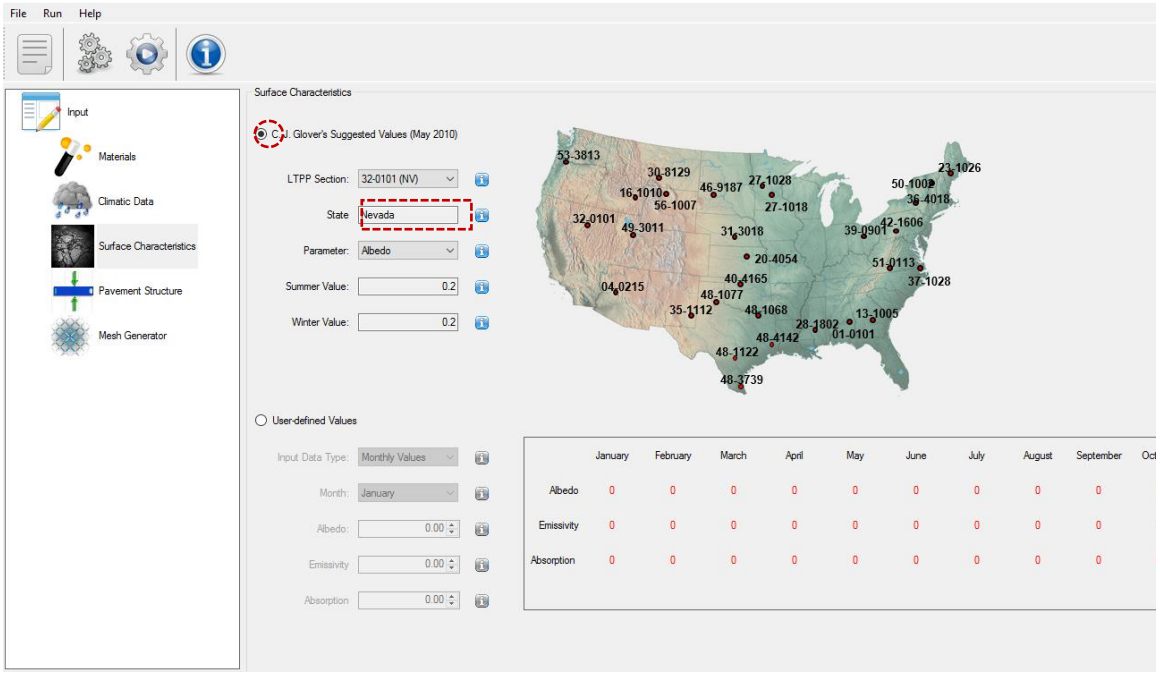

Figure 12. 5. Step (4) Surface Characteristic Input

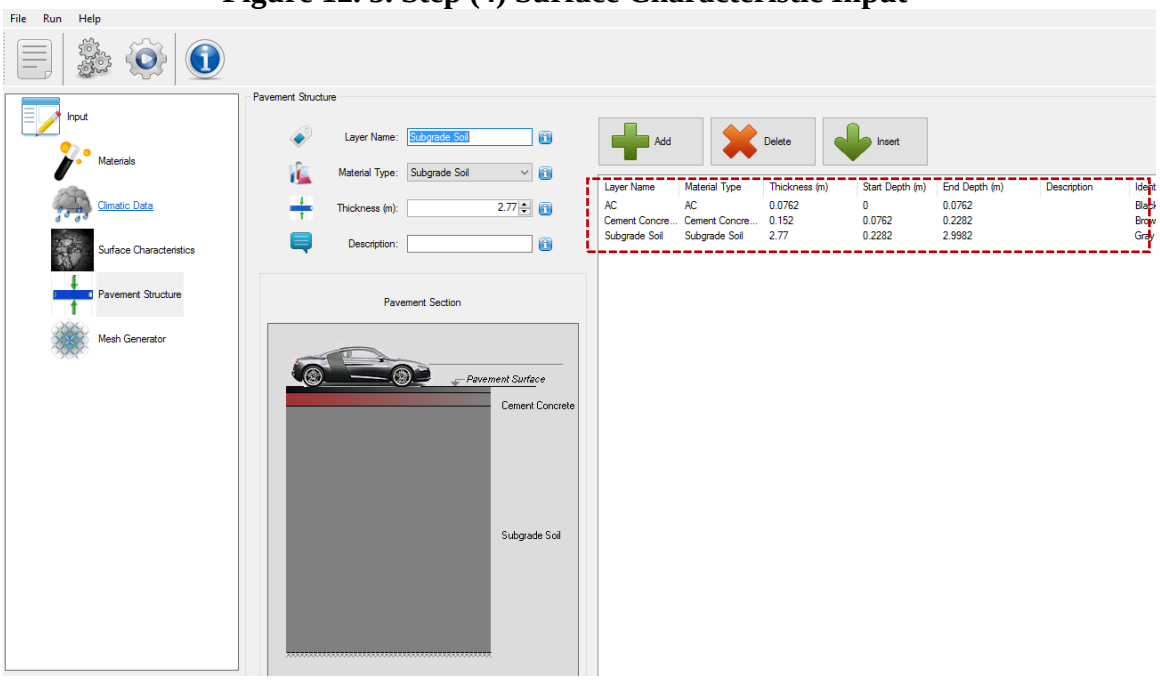

Figure 12. 6. Step (5) Pavement Structure Input

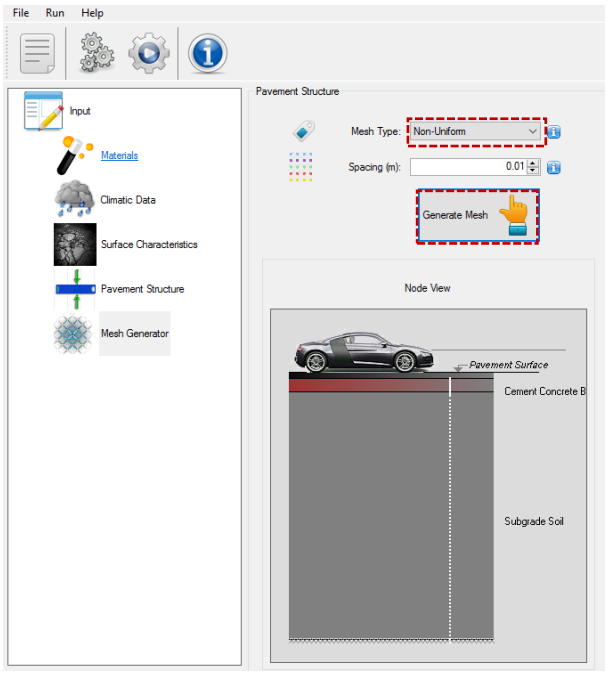

Figure 12. 7. Step (6) Mesh Generator Input

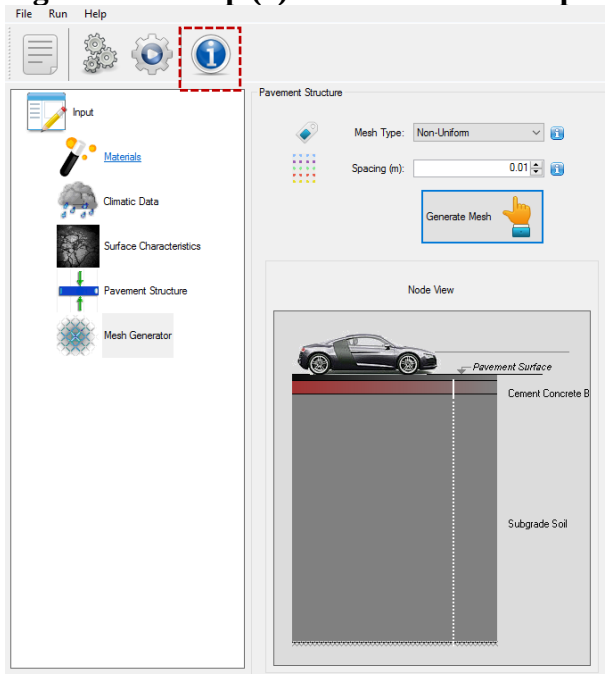

Figure 12. 8. Step (7) Running the Program

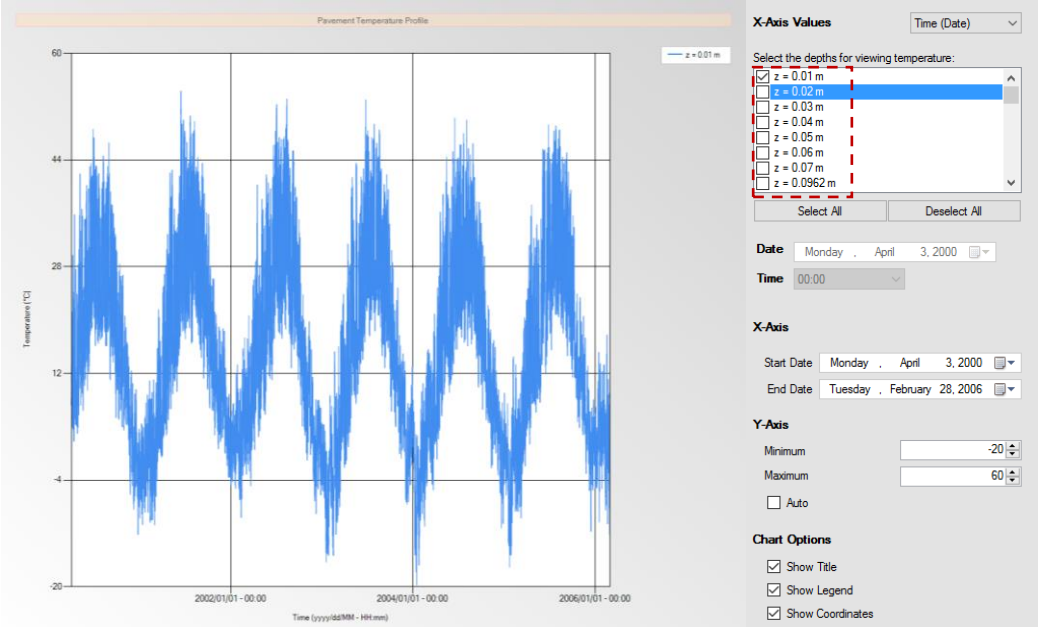

Figure 12. 9. Example Output for Hourly Pavement Temperature Prediction (Various depths could be added.)

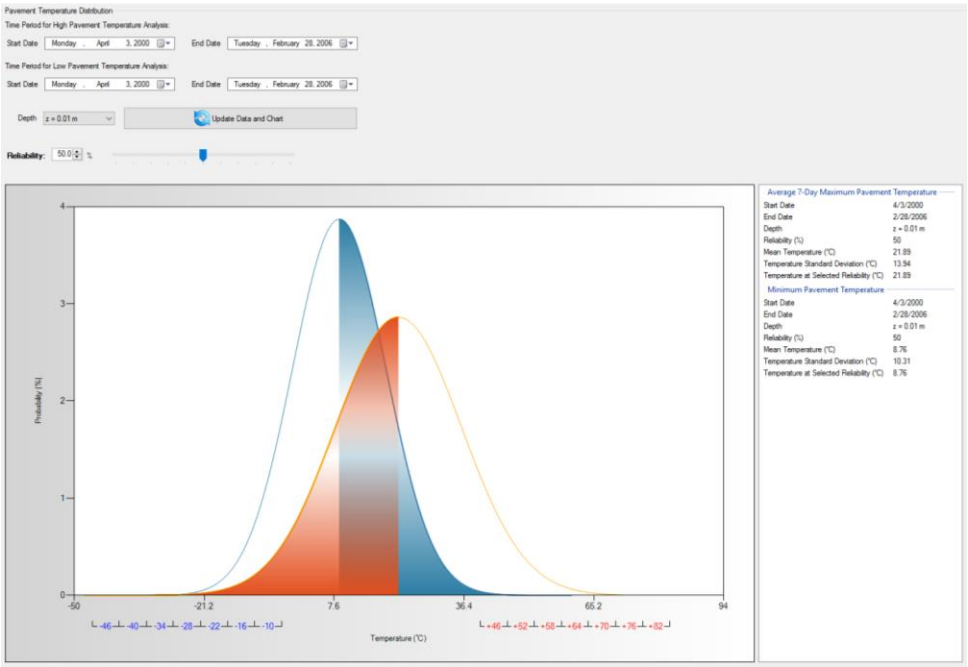

Figure 12. 10. Example Output for Hourly Pavement Temperature Prediction Statistical Analysis

	A	B	C	D	E	F	G	H	I	J	K
1	Date-Time	z = 0.01m	z = 0.02m	z = 0.03m	z = 0.04m	z = 0.05m	z = 0.06m	z = 0.07m	z = 0.1m	z = 0.12m	z = 0.14m
2	9/1/1996-0:00	10.53	10.46	10.39	10.33	10.26	10.19	10.12	9.94	9.8	9.66
3	9/1/1996-1:00	9.19	9.41	9.56	9.67	9.75	9.79	9.81	9.78	9.71	9.61
4	9/1/1996-2:00	8.39	8.65	8.87	9.05	9.19	9.3	9.38	9.5	9.52	9.49
5	9/1/1996-3:00	7.97	8.2	8.41	8.59	8.75	8.88	8.99	9.2	9.29	9.32
6	9/1/1996-4:00	7.49	7.74	7.97	8.16	8.34	8.49	8.62	8.89	9.04	9.12
7	9/1/1996-5:00	6.94	7.22	7.48	7.7	7.9	8.08	8.23	8.57	8.77	8.9
8	9/1/1996-6:00	6.6	6.86	7.11	7.33	7.54	7.72	7.88	8.26	8.5	8.68
9	9/1/1996-7:00	7.1	7.19	7.29	7.41	7.53	7.65	7.77	8.09	8.31	8.49
10	9/1/1996-8:00	9.53	9.12	8.81	8.6	8.45	8.36	8.31	8.31	8.38	8.47
11	9/1/1996-9:00	14.15	12.99	12.05	11.29	10.69	10.22	9.85	9.22	8.93	8.78
12	9/1/1996-10:00	19.93	18.06	16.48	15.15	14.04	13.12	12.38	10.88	10.06	9.54
13	9/1/1996-11:00	26.1	23.65	21.52	19.69	18.11	16.77	15.64	13.2	11.77	10.76
14	9/1/1996-12:00	31.42	28.71	26.29	24.14	22.25	20.6	19.17	15.92	13.88	12.37
15	9/1/1996-13:00	35.44	32.73	30.25	28	25.97	24.16	22.55	18.71	16.18	14.22
16	9/1/1996-14:00	38.16	35.62	33.25	31.05	29.02	27.17	25.49	21.34	18.45	16.15
17	9/1/1996-15:00	39	36.88	34.84	32.88	31.04	29.3	27.7	23.52	20.5	17.99
18	9/1/1996-16:00	38.64	36.97	35.31	33.68	32.09	30.56	29.11	25.17	22.17	19.6
19	9/1/1996-17:00	36.81	35.71	34.54	33.33	32.09	30.86	29.64	26.16	23.36	20.87
20	9/1/1996-18:00	33.72	33.24	32.62	31.88	31.07	30.2	29.28	26.45	24.01	21.74

Figure 12. 11. Exported Data from TEMPS